DNA 5216F-1

JOINT ELECTRON BEAM COMMONALITY EXPERIMENTS ON BLACKJACK 3 AND 3 PRIME

Part I — Machine Characterizations

D. V. Keller

A. J. Watts, et al

Ktech Corporation
901 Pennsylvania Ave., N.E.
Albuquerque, New Mexico 87110

31 December 1979

Final Report for Period 1 January 1979—31 December 1979

CONTRACT No. DNA 001-79-C-0127

THIS WORK SPONSORED BY THE DEFENSE NUCLEAR AGENCY
UNDER RDT&E RMSS CODE B342079464 N99QAXAG12301 H2590D.

Prepared for
Director
DEFENSE NUCLEAR AGENCY
Washington, D. C. 20305

Destroy this report when it is no longer needed. Do not return to sender.

PLEASE NOTIFY THE DEFENSE NUCLEAR AGENCY, ATTN: STTI, WASHINGTON, D.C. 20305, IF YOUR ADDRESS IS INCORRECT, IF YOU WISH TO BE DELETED FROM THE DISTRIBUTION LIST, OR IF THE ADDRESSEE IS NO LONGER EMPLOYED BY YOUR ORGANIZATION.

UNCLASSIFIED

SECURITY CLASSIFICATION OF THIS PAGE *(When Data Entered)*

(19) REPORT DOCUMENTATION PAGE	READ INSTRUCTIONS BEFORE COMPLETING FORM
(18) 1. REPORT NUMBER: DNA 5216F-1	2. GOVT ACCESSION NO.: AD-A090 740	3. RECIPIENT'S CATALOG NUMBER
(6) 4. TITLE *(and Subtitle)*: JOINT ELECTRON BEAM COMMONALITY EXPERIMENTS ON BLACKJACK 3 AND 3 PRIME. Part I - Machine Characterizations.	(9) 5. TYPE OF REPORT & PERIOD COVERED: Final Report for Period 1 Jan 79 - 31 Dec 79
	6. PERFORMING ORG. REPORT NUMBER: TR79-11
(10) 7. AUTHOR(s): Donald V. Keller, D. A. Rice, Alan J. Watts, J. J. Powe	(15) 8. CONTRACT OR GRANT NUMBER(s): DNA 001-79-C-0127 NEW
9. PERFORMING ORGANIZATION NAME AND ADDRESS: Ktech Corporation, 901 Pennsylvania Ave., N.E., Albuquerque, New Mexico 87110	(16) 10. PROGRAM ELEMENT, PROJECT, TASK AREA & WORK UNIT NUMBERS: Subtask N99QAXAG123-01
11. CONTROLLING OFFICE NAME AND ADDRESS: Director, Defense Nuclear Agency, Washington, D.C. 20305 (17) G123	(11) 12. REPORT DATE: 31 December 1979
	13. NUMBER OF PAGES: 242
(12) 240 14. MONITORING AGENCY NAME & ADDRESS *(if different from Controlling Office)*: (14) KTECH-TR-79-24-PT-1	15. SECURITY CLASS *(of this report)*: UNCLASSIFIED
	15a. DECLASSIFICATION/DOWNGRADING SCHEDULE

PE 62704H

16. DISTRIBUTION STATEMENT *(of this Report)*

Approved for public release; distribution unlimited.

17. DISTRIBUTION STATEMENT *(of the abstract entered in Block 20, if different from Report)*

18. SUPPLEMENTARY NOTES

This work sponsored by the Defense Nuclear Agency under RDT&E RMSS Code B342079464 N99QAXAG12301 H2590D.

19. KEY WORDS *(Continue on reverse side if necessary and identify by block number)*

Stress-Time Profiles	Thermo Mechanical Stress
Electron Energy Deposition	Stress Relief
Deposition-Time Dependence	Tantalum
Vapor Tail	Aluminum
Stress Generation	Electron Beam Materials Testing

20. ABSTRACT *(Continue on reverse side if necessary and identify by block number)*

As part of the DNA Commonality program, material stress generation experiments were performed using the pulsed relativistic electron beam from the Maxwell Laboratories' Blackjack-3 and -3 Prime electron beam machines. Materials used were solid aluminum and tantalum, each of sufficient thickness to be opaque to the beams. The induced stress histories were monitored using X-cut quartz gauges, carbon gauges, and laser velocity interferometry. Fluence levels of up to 150 cal/cm^2 were used, giving deposition of up to 750 cal/g, and the →(over)

DD FORM 1 JAN 73 1473 EDITION OF 1 NOV 65 IS OBSOLETE

UNCLASSIFIED

SECURITY CLASSIFICATION OF THIS PAGE *(When Data Entered)*

sq cm

408270

20. ABSTRACT (Continued)

deposition time was varied from 30 to 55 ns. The electron beam characterization included measurement of fluences as a function of axial and radial positions relative to the anodes, analysis of machine performance (voltage, current) to give electron energy spectra, and establishment of mean electron angles of incidence by comparison of Monte Carlo computations with experimental dose-depth measurements. The observed stresses and electron beam parameters are to be analyzed by SRI for comparison with their wave propagation codes. The stress pulse shapes and amplitudes agree well with nominal predictions, except that a high amplitude stress tail was observed on the high dose experiments that produced Ta vapor.

SUMMARY

Material stress generation experiments were performed using the pulsed relativistic electron beams from the Maxwell Laboratories' Blackjack-3 and -3 Prime electron beam machines. Materials used were solid aluminum and tantalum, each sufficiently thick to be opaque to the beams. The induced stress histories were monitored using X-cut quartz gauges, carbon gauges, and laser velocity interferometry. Energy depositions of up to 750 cal/g were used, with deposition times varying from 30 to 55 ns.

The electron beam characterization included measurement of fluences as a function of axial and radial positions relative to the anode, using total beam stopping calorimeters; analysis of machine performance (voltage, current versus time) to give electron energy spectra, using fast digital recording and processing by computer; and establishment of mean electron angles of incidence by comparison of Monte Carlo computations with experimental dose-depth measurements, using thin carbon foil stacks.

The observed stress pulse shapes and amplitudes agree well with nominal predictions, and will be analyzed in detail by SRI using their wave propagation codes. However, at high deposition levels in tantalum, where considerable vaporization occurred, a high amplitude stress tail was observed. This was not predicted by the PUFF hydrocode. PUFF does not contain a three-phase equation of state of materials, whereas the CHART D code does. It is recommended that further work be done using the CHART D code to assess such vapor situations.

PREFACE

This work was sponsored by the Defense Nuclear Agency; the contracting officer was Mr. Donald J. Kohler, DNA/SPAS.

The experimental work was performed at Maxwell Laboratories, San Diego, under the overall supervision of Mr. J. Menglesdorf, and with excellent support from the Blackjack operating crew, under the direction of Mr. J. Devlin.

Grateful acknowledgement is given to Messrs. G. Hansen, M. Ruebish, and J. Romine, of Division 1126 Sandia Laboratories, Albuquerque, for their use and operation of the Sandia 7912/PDP 11 Data Acquisition System.

Thanks are also due to Messrs. C. D. Newlander and J. Brewer of the Air Force Weapons Laboratory, Kirtland AFB, NM, for providing the special ELTRAN II pack and useful information relevant to ELTRAN and PUFF, facilitating the computational work performed by Ktech staff.

The authors are also grateful to Dr. R. E. Tokheim, of Stanford Research Institute, Menlo Park, CA, for his supply of valuable pre-test stress computations which facilitated easier initial set-up of the experiments.

TABLE OF CONTENTS

LIST OF ILLUSTRATIONS

LIST OF ILLUSTRATIONS (Continued)

LIST OF TABLES

SECTION 1

OBJECTIVES

The commonality program for the Defense Nuclear Agency (DNA) is intended to obtain "common" valid electron beam data on material response from different electron beam facilities by different experimenters. The validity of the data, and comparison of experimenters' results taken on identical materials but with possibly different measurement techniques and beam diagnostics, will be determined through computer correlations with the best material equation-of-state (EOS) model. Both a well understood test material and a complex practical shielding material are included.

The commonality program is being carried out in three phases, although they may not be separate in time. The first part uses a simple, well known material, aluminum, in a few tests to run through each of the various procedures, experiments and correlations. The second phase uses a high density material, tantalum, to study stresses that are affected by deposition time, and several different machines with differing deposition times will be used. The third phase characterizes various screening materials and their constituents, including porosity effects.

This specific contract concerns work done using the Blackjack 3 and 3 Prime machines, and involving the first two phases mentioned above. In particular, Ktech Corporation accomplished the following specific tasks:

1. Development and characterization of the new "short pulse" Blackjack 3 Prime accelerator at Maxwell Laboratories, Inc., San Diego, to obtain an electron beam suitable for commonality experiments. The electron beam was to have the following measured characteristics:

- 30 ns pulse width (FWHM)
- 800 keV mean energy
- 100 cal/cm^2 over 3 to 5 cm^2

2. Design and conduct experiments for commonality Al and Ta tests on Blackjack 3 and 3 Prime at several dose levels up to about 750 cal/g. The measurements included beam diagnostics (voltage, current, depth-dose and fluence) and specimen response (laser velocity interferometry, quartz stress gauges, and carbon stress gauges).

3. Coordination with other DNA commonality contractors as requested by DNA for the purposes of planning, coordinating, and correlating materials, tests and test results. In particular, furnish all relevant data from Task 2 to Stanford Research Institute (SRI), who have responsibility for overall validation of results by comparison with their computational models and wave propagation codes.

SECTION 2

INTRODUCTION

The principal objective of the commonality work is to fully investigate the ability of various electron beam machines to give suitable, well understood energy deposition in selected materials, together with the ability to use proven experimental techniques to measure the resulting material stress waves. The energy deposition and resultant stress wave propagation are compared with the available electron energy deposition codes and hydrodynamic wave propagation codes.

The choice of available electron beam machines was dependent upon the need to address the sensitivity of the energy deposition and stress generation to various parameters. These parameters include the specific energy loading (cal/g), the deposition range (cm), the time of deposition (Full Width Half Maximum [FWHM], ns), and the degree of stress attenuation due to propagation characteristics of the materials.

Table 1 indicates the electron beam machines chosen by the various commonality experimenters and gives the salient features of the machine characteristics.

The general properties of electron energy deposition are that the peak energy loading (cal/g) is only weakly coupled to the Z number of any sample (varying only by a factor of 2 over the Z range of 6 to 90). Likewise, the range of deposition is only weakly coupled to the Z number, if measured in areal mass (g/cm^2). The higher the mean energy of the electrons the greater the range of deposition, and the lower the normalized specific energy loading (cal/g per incident cal/cm^2). However, high Z materials in general have high densities, and thus the electron ranges are significantly less in high Z materials than in low Z ones, when measured in cms. In addition, high Z materials differ from low Z ones in their ability to scatter electrons and produce Bremsstrahlung.

Table 1. Electron beam machines for commonality experiments.

Machine	Mean Energy (MeV)	Deposition Time (ns)	Peak Dose* (cal/gm)	Experimenter
Blackjack 3 Prime	1	30	1000	Ktech
Blackjack 3	1	60	1000	Ktech
REHYD	1	100	1000	SLA/Ktech
OWL-2	1	120	1000	SRI/PI
PI-1150	4	60	200	SRI/PI
Hermes 2	10	100	250	SLA/Ktech
Aurora	8	160	200	HDL

* To be used in this program.

Specific energy loading, energy scatter and deposition range are all related to the incident angle of the electron beam to a sample. The ability to measure the result of these effects, such as the deposition profile using dose-depth calorimetry stacks (see Section 3-3), provides a thorough test of experimental techniques, and can be compared with energy deposition code predictions.

A parameter of great importance is the deposition time of the electron beam. During energy deposition the induced stresses start to propagate along the beam direction, and this has the effect of reducing the peak stress generated. The total beam energy is distributed over a larger volume of material during deposition than that due solely to the electron deposition range, owing to this wave propagation. This "stress relaxation" occurs from both ends of the deposition profile, and its magnitude is dependent on the ratio of the distance propagated by a relief wave during the deposition time (CT) where C is release speed, T deposition time, and the width of the deposition profile (R_E). The parameter (R_E/CT) is referred to as "swiftness," and is a function of electron beam machine and sample. A "swift" situation is one in which the degree of wave propagation during deposition is small compared to the deposition range. This gives only a small degree of stress relief during deposition (see Section 3-6).

Two suitable materials to investigate these effects are aluminum and tantalum. Aluminum has a low Z, and a large electron range in cms, and is a well understood material with a known equation-of-state (EOS) and hydrodynamic behavior. The degree of stress relief due to swiftness is relatively small. Conversely, tantalum has a high Z, and a small electron range in cms, but still is well understood. The degree of stress relief due to swiftness is significant for all but very short deposition times, or wide deposition ranges.

Table 2 itemizes the electron ranges and the relief thicknesses for these two materials when used with the machines listed in Table 1. The large differences in "swiftness" values can be seen in this table.

Depositions of interest involve energy loadings of up to about 750 cals/g, at which level only incipient vaporization may be produced in aluminum, whereas significant vaporization is produced in tantalum.

This report discusses only the Ktech tests on the Blackjack 3 and 3 Prime machines. These machines give deposition ranges which are less than the chosen Commonality sample thicknesses for both aluminum and tantalum. Measurement techniques included the use of X-cut quartz gauges for low fluence shots and carbon gauge and Laser Velocity Interferometry (LVI) for the higher fluence shots. Details are given in Section 3-4. Great attention was given to consideration of one-dimensionality to ensure that the measured stress waves could be correlated with the one-dimensionality codes to be utilized by SRI, who have the overall responsibility for validation of results (see Section 3-5).

Table 2. Electron range compared to stress relief depth.

Machine	Relief Thickness ($2C_o\tau$ - cm)		Electron Range R_e (cm)		$R_e/(2C_o\tau)$	
	Al	Ta	Al	Ta	Al	Ta
Blackjack 3 Prime	0.039	0.025	0.15	0.024	3.8	1.00
Blackjack 3	0.077	0.050	0.15	0.024	1.9	0.50
REHYD	0.128	0.083	0.15	0.024	1.2	0.30
OWL-2	0.154	0.100	0.15	0.024	1.0	0.24
PI-1150	0.077	0.050	1.10	0.180	14.0	3.60
Hermes 2	0.128	0.083	2.40	0.390	19.0	4.70
Aurora	0.205	0.133	1.80	0.300	9.0	2.30

SECTION 3

EXPERIMENTAL TECHNIQUES AND PREDICTIONS

3-1 GENERAL DESCRIPTION

Figure 1 gives a schematic view of the diode, drift tube and experimental shots on both Blackjack 3 and 3 Prime (BJ3 and BJ3'). BJ3 and BJ3' have several features in common. Both machines use a common Marx generator charged to 65 kV. Both use the same stainless steel drift tube of 15 cm I.D., and both use the same solenoidal magnetic field pulsed to 7 kV about 6 ms before beam generation and giving a peak field strength of 25 kilogauss at beam propagation time. The same anode and cathode are used. The anode is of 6.35 μm aluminized Mylar, while the cathode is of ATJ graphite of 6.03-cm diameter with a radiused circumference yielding a central flat region of 5.08-cm diameter.

BJ3 utilizes an anode-cathode gap of 5.6 mm and is designed to hold off to 1 MV, while BJ3' uses a gap of 8.8 mm and can hold off to 2 MV. The inductance of BJ3 is 30 nH; that of BJ3' is 45 nH. An overview of the general characteristics of BJ3 and BJ3' is given in reference 1.

It can be seen that electrons leaving the diode enter a compressive magnetic field which adiabatically heats and constrains the electrons to follow the field lines along the drift tube. Toward the experimental stations, beyond the peak magnetic field, the field lines gradually diverge and beam expansion and adiabatic cooling of the beam occurs. Figure 2 illustrates the magnetic field strength as a function of axial distance from the anode.

3-2 SPATIAL FLUENCE CALORIMETRY

The spatial fluence measurements were made using standard total beam stopping carbon calorimetry techniques. The majority of calorimeters used were of ATJ graphite, density 1.7 g/cm^3, and of various diameters ranging from

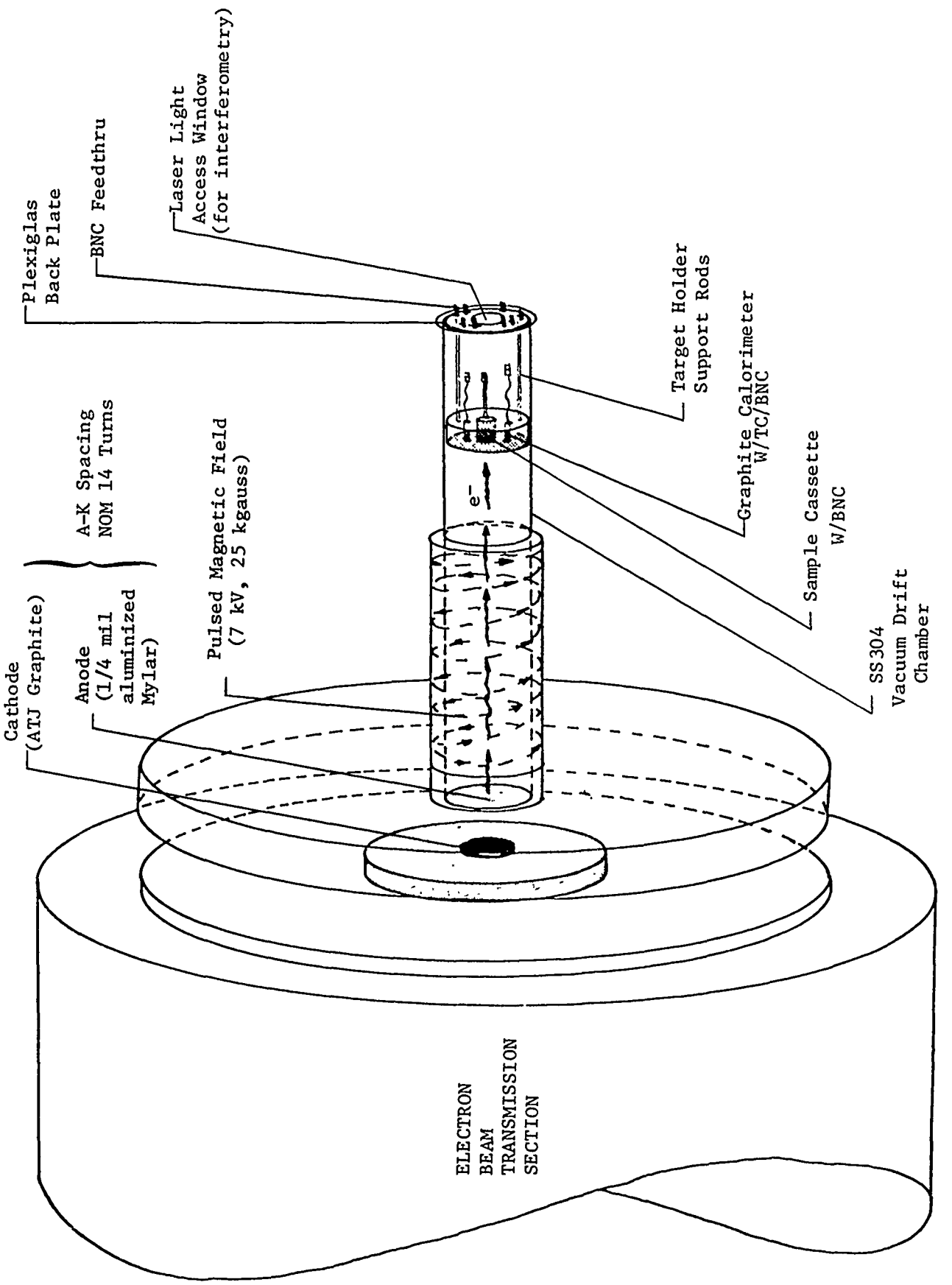

Figure 1. Overall schematic of beam environment.

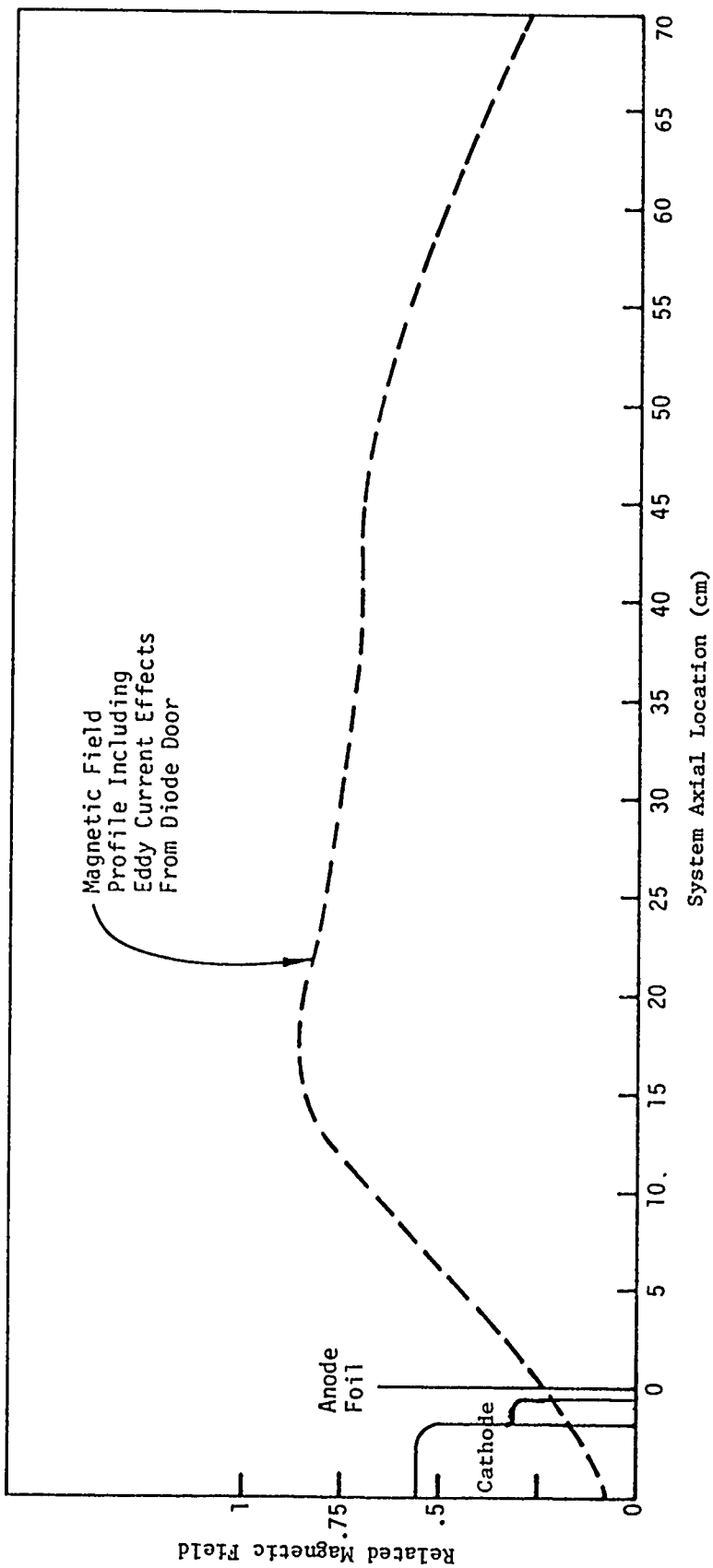

Figure 2. Blackjack 3 magnetic field profile used for materials testing.

0.635 to 2.24 cm depending on requirements. The most commonly used calorimeter elements were 0.635 or 0.762 cm in diameter and 1.29 cm long. They had a conically recessed front surface to help mitigate possible front surface fracture by rapidly dispersing induced shocks. A small steel screw was screwed into the rear of the calorimeters and a Chromel/Alumel thermocouple was soldered to the screw.

For spatial mapping purposes nine calorimeter elements were usually used. These consisted of a central element and two rings of four calorimeters each at radii of 2 cm and 3 cm. All these calorimeters were mounted in, but insulated from, a carbon equilibrator block. The latter ensured that the beam was essentially entering a common block of material and that mutual cross scattering within yielded typical beam fluences at the calorimeters.

The thermocouples were monitored using standard techniques, yielding visicorder traces of voltage versus time. The use of calibration steps allowed direct measurements of voltage, while use of the known calibration curve for the thermocouples yielded temperatures, and the carbon enthalpy data gave absorbed energy. The beam energy initially resides near the front surface of the calorimeters (away from the thermocouples); thereafter, the energy diffuses throughout the calorimeter.

For the carbon calcrimeters and the energy loadings and profile widths obtained using BJ3 and BJ3', the energy lost by blackbody radiation for the temperatures induced in these experiments ($\approx$2000°C max.) is only a small fraction, and has been ignored; e.g., for a fluence of about 150 cal/cm^2 the radiated loss is <4 percent, while for 75 cal/cm^2 it is <1 percent. The energy loss by conduction through the holder is more significant but it is possible to

correct for the leakage by extrapolating the observed temperature-time trace back to deposition time.

Conversion from temperature to fluence involves use of quoted enthalpies for the ATJ graphite and the steel screw, together with knowledge of the geometry of the calorimeter (total thermal mass and cross sectional area presented to the electron beam). Thus, if the fluence is ϕ cal/cm^2, the cross sectional area, A (cm^2), the masses of carbon and steel, m_c and m_s (gram), and the enthalpies, H_c and H_s (cal/g) respectively, we have

$$\phi = (m_c H_c + m_s H_s)/A$$

where the enthalpies are those appropriate for the observed temperature increases. Figure 3 gives details of the thermal properties of ATJ graphite assumed in this work.

Due to shot-to-shot variability, it is necessary to determine the fluence pertaining to the specific material experiment. This creates difficulties, particularly at high fluences where the beam narrows in cross section and the sample prevents use of a central calorimeter. For calorimetry performed simultaneously with stress measurements, different calorimeter arrangements were used. For outboard measurements a ring of four standard calorimeters was used, either at a radius of 3.0 or 3.18, depending on the equilibrator block. The inner ring of calorimeters was replaced by two "ring" designs. For some initial shots a ring of ATJ graphite with a mean radius of 0.92 cm was employed as a single calorimeter, giving a sample shine radius of 0.635 cm. This gave a good measurement of fluence, but was dropped in favor of a newer ring design with mean radius of about 1.9 cms. The latter design allowed a larger shine area on the sample of 0.89-cm radius, thereby ensuring longer one-dimensional stress gauge read times. This design was also monitored using four thermocouples at 90-degree spacing. The aspect ratio of the geometry was such as to allow the ring to behave

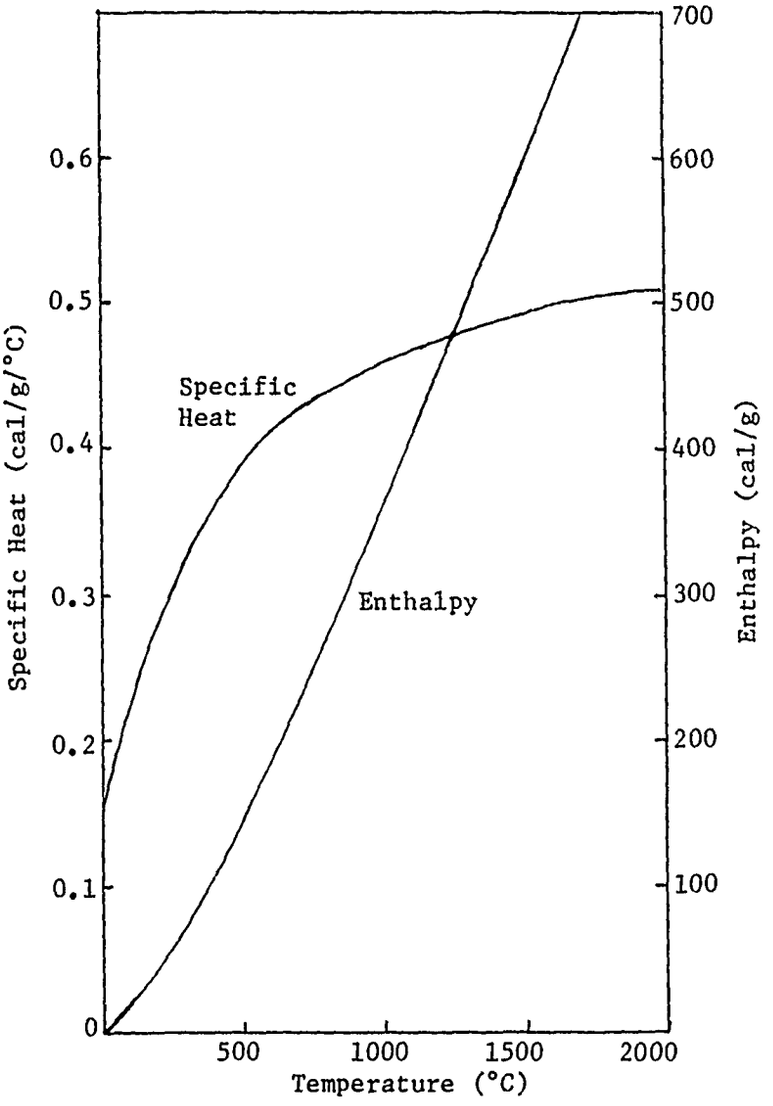

$$C_p = 0.15 + 7.82 \times 10^{-4}T - 7.51 \times 10^{-7}T^2 + 2.78 \times 10^{-10}T^3$$

Figure 3. Thermal properties of ATJ graphite.

essentially as four independent calorimeters. Overlap of thermal energy only occurred at late times, well beyond the peak thermal readings. Use of this ring calorimeter in conjunction with the (spatially wider) BJ3 sample irradiations permitted good one-dimensional recording times and simultaneous fluence measurements next to the sample. This design involved the use of chamfered edges to prevent beam "shine through," and due allowance was given to account for the partial transparency of this system to the electron beam (see Figure 5).

The majority of the stress measurements used this latter ring calorimeter, as did several of the spatial calorimetry shots in which the sample was replaced by a single large carbon calorimeter. Figures 4 and 5 illustrate the various calorimeters.

3-3 DOSE-DEPTH CALORIMETRY

The electron beam deposition profiles in carbon were measured using a stack of nine ATJ carbon foils having a thickness of 0.066 g/cm^2 each. The ATJ foils were mounted in holders in such a way as to minimize shock loading to allow limited movement (due to thermal effects) and to provide spacing between adjacent foils.

The dose-depth stack foils were placed inside the same large ring calorimeter described above (Figure 5) at the point of beam entry. This acted as part of the equilibrator/aperture system and also allowed additional total fluence calorimetry measurement. Thus both dose-depth and total stopping calorimetry were performed simultaneously.

Thermocouples were attached to the graphite foils outside the shine area and near the edge of the foils, and the data was recorded and reduced as described for the total stopping calorimeters.

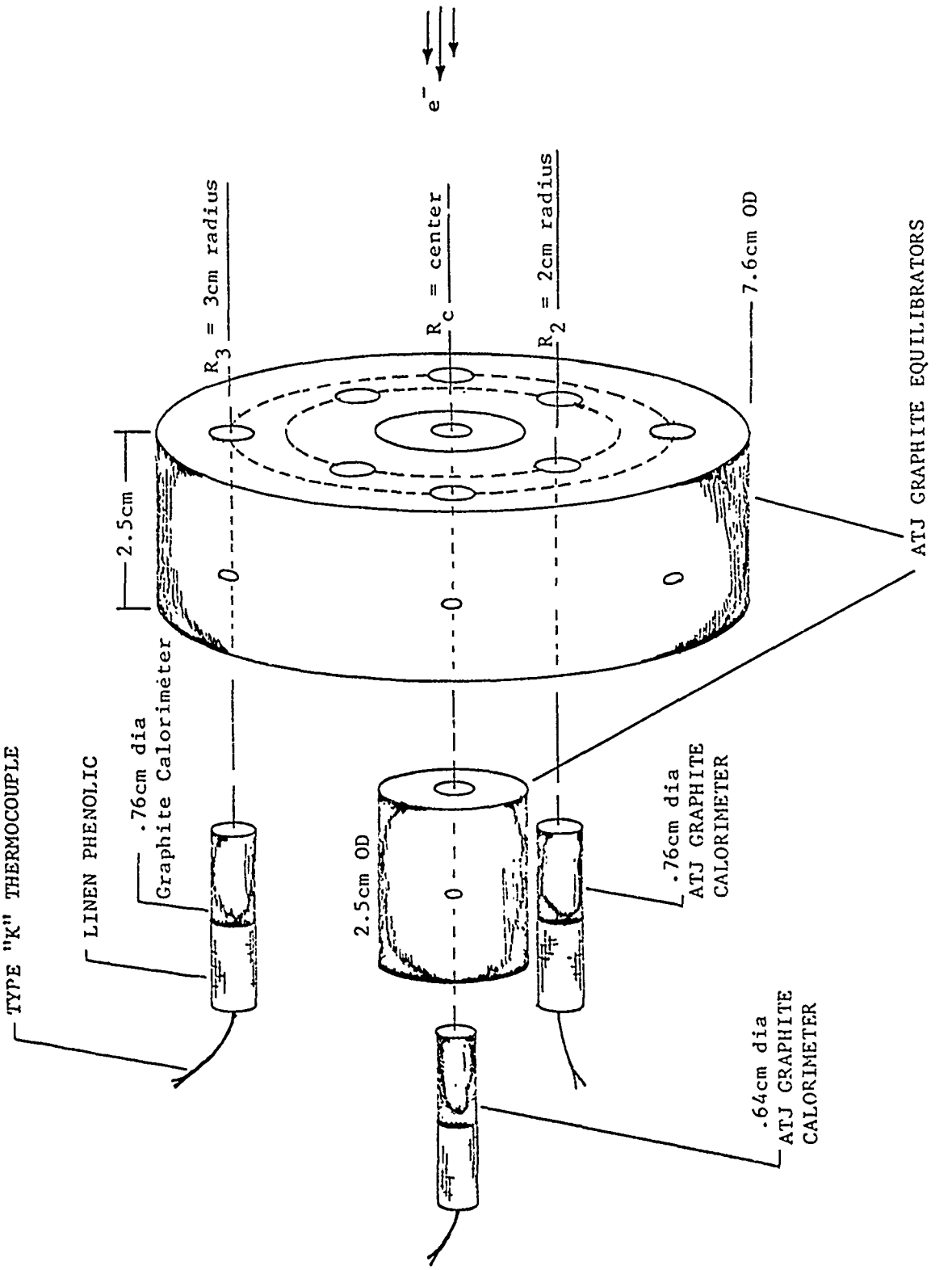

Figure 4. Spatial fluence monitor.

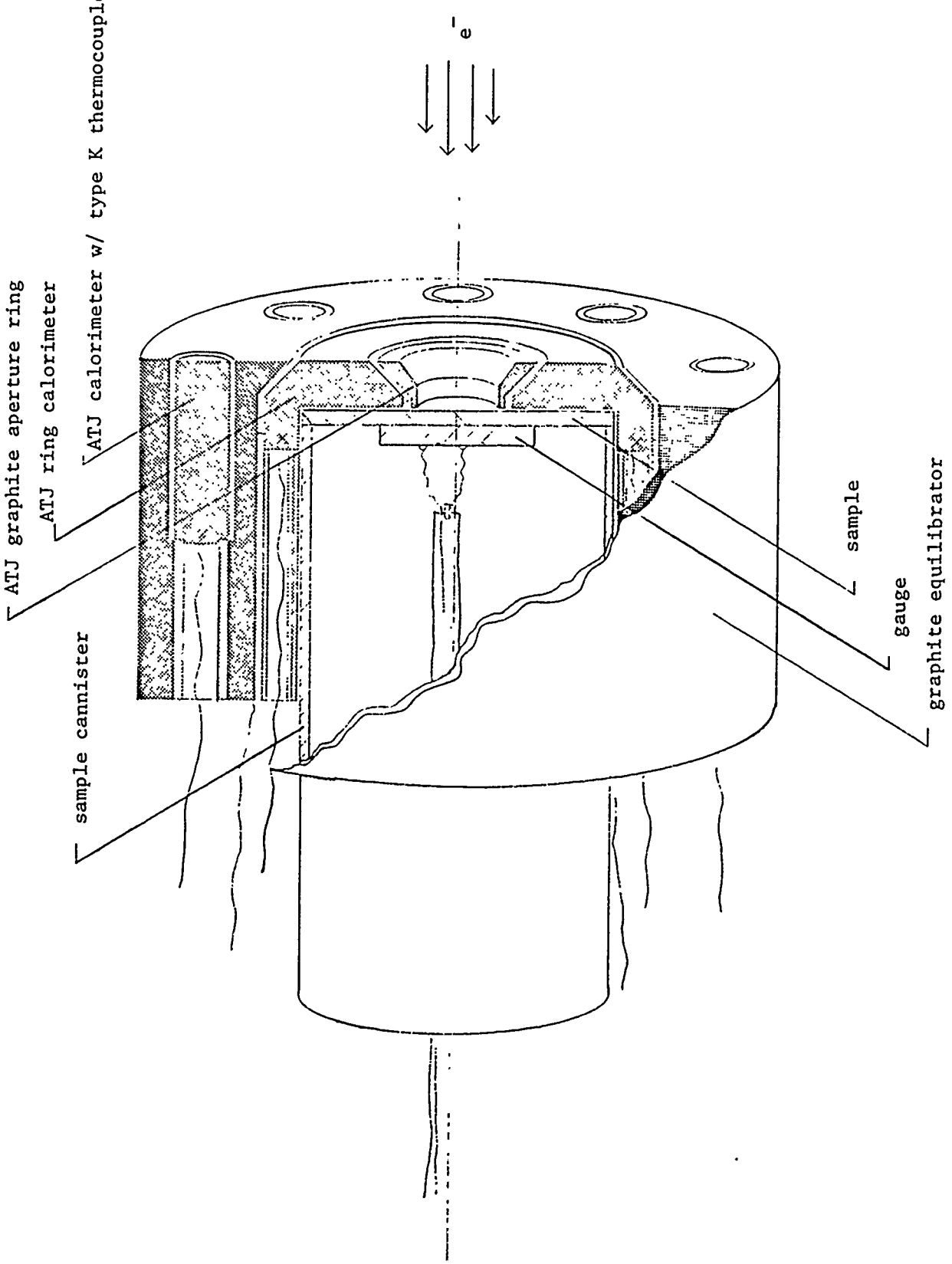

Figure 5. Calorimetry during stress measurements.

3-4 STRESS MEASUREMENT TECHNIQUES

The stress measurements were made on samples of aluminum and tantalum which were each thicker than the electron deposition ranges. The aluminum samples were about 1.4x electron range, while the tantalum samples were about 3.5x electron range. In all irradiations, therefore, only the front portion of the samples was heated by the beams, and any melt and/or vapor region was confined to the front surface. This arrangement guaranteed that there was always a cold, solid rear portion to the samples, allowing either (a) direct bonding of a quartz gauge, or (b) bonding of PMMA containing a carbon gauge, or (c) use of the free rear surface for LVI measurements, or (d) bonding with fused silica containing a buried mirror for other LVI measurements. The sample irradiation areas were chosen to be compatible with a good uniform beam and the need to ensure one-dimensionality of stress measurements (see Section 3-5).

Three basic techniques were used to measure sample stress generation. These were (a) X-cut quartz gauges, (b) carbon stress gauges, and (c) laser velocity interferometry (LVI).

3-4.1 X-Cut Quartz Gauges

The X-cut quartz gauges were of the wrap-around design in order to give maximum noise suppression in the noisy electron beam machine environment. Three basic gauge thicknesses of 0.25, 0.51, and 0.64 cm were used, giving potential recording times for single-transit pulses of 0.42, 0.85, and 1.1 μs respectively. The active central electrode area was 0.952-cm in diameter in all cases. The gauges were bonded directly to the rear of the samples. The overall diameter of the gauges was 3.18 cm for thick, and 2.54 cm for thin gauges. Such quartz gauges are known to give reliable stress records for stresses (within the gauge) of up to about 25 kbar. Beyond 25 kbar, the response tends to be nonlinear.

These gauges were used primarily for measurements at low or intermediate fluences. Although the pressure-energy coupling for Ta is five times greater than for Al, Ta suffers a greater degree of stress relief during deposition than Al. In addition, there is a greater mechanical impedance mismatch between Ta and quartz than between Al and quartz. These factors allowed measurement of stresses for both Al and Ta at fluences of up to about 65 cal/cm^2 (for Al) and 90 cal/cm^2 (for Ta) without inducing undesirably high stresses in the quartz.

3-4.2 Carbon Stress Gauges

Carbon stress gauges were employed at the highest fluences for measurement of both Al and Ta stresses. The gauges were of Dynasen* manufacture, with dimensions of 0.127 x 0.254 x 0.0089 cm. They were potted into PMMA as the host matrix.

The initial intent had been to rely essentially on the LVI system for the high fluence measurements. However, the high narrow peak stresses generated in Ta at the highest doses precluded using the LVI system due to photomultiplier and oscilloscope bandwidth limitations. Thus the high fluence Ta stress measurements were mostly obtained with the carbon gauge.

Since carbon gauges already existed in a prepackaged form, these were used as available. This involved the use of gauges embedded in PMMA of 0.953-cm total thickness, and with an initial 0.3175-cm-thick (1/8 in) buffer between the sample and the gauge. The buffer was bonded to the rear of the samples.

3-4.3 Laser Velocity Interferometry (LVI)

The LVI measurements employed a HeNe laser operating at a wavelength of 6328 Å. Delay legs on the order of 45 and 104 cm were used as appropriate to give a convenient compromise of fringe count and fringe frequency to allow good interpretation without serious bandwidth limitations. The basic method is

* Dynasen Corporation, 20 Dean Arnold Place, Goleta, CA 93017.

described in reference 2. Particle velocity $u(t)$ is inferred from the fringe count $F(t)$ using the relationship

$$u(t) = \frac{\lambda}{2\tau} \frac{F(t)}{(1+\Delta\nu/\nu_o)}$$

where λ is the laser wavelength, τ is the delay leg transit time, ν_o is the standard refractive index of the medium through which the beam travels to and from the reflector (e.g., vacuum, PMMA or fused silica), and $\Delta\nu$ is the change in the refractive index caused by the propagating stress pulse within this medium.

Some LVI measurements were done directly off the rear free surface of the sample. For this situation the sample required an optically reflecting surface. Since this arrangement yields the highest possible mirror velocity, it was used only when consistent with bandwidth limitations.

To reduce the mirror velocity, or to overcome poor sample reflectivity, other experiments either loaded the sample rear surface with PMMA while still using the sample as the mirror, or else made use of a mirror surface embedded within fused silica. In the latter case the mirror was 0.635 cm (1/4 in) from the sample. The fused silica was bonded to the rear of the samples.

Limitations in time precluded the operation of the most sophisticated LVI technique, in which the signal is analyzed in quadrature (P and S polarization vectors) and in which the overall light intensities are individually monitored (ref. 3). This sophistication would have removed the few ambiguities in the LVI records and more readily allow identification of turnaround points (reversal of particle motion).

3-5 ONE-DIMENSIONALITY CONSIDERATIONS

To assure one-dimensionality of stress measurement it is necessary to ensure that no relief waves can reach the region being monitored before arrival of the required information. Such relief waves can be generated by the finite boundaries

of the sample or backing material, or by the existence of a steep stress gradient extending perpendicular (i.e., radially) to the main wave propagation. The extreme case of this, of course, is the gradient created at the edge of the electron beam irradiation area. This is generally the most significant "edge" to consider. Of similar nature, but less severe in effect, is the slowly varying gradient caused by a non-uniform beam across the irradiation area. Properly designed experiments employ beam widths where this gradient is kept small.

Since electron beam deposition involves a finite depth of influence, the shine edge likewise has a finite depth from which relief waves can be generated. Thus, to be conservative in evaluating the minimum read time for one-dimensionality, it is necessary to compare the times of arrival of the fastest relief wave from the deepest range of energy deposition at the edge of shine with the axial arrival time of the main compressive stress pulse.

To compute the above accurately requires exact knowledge of both the compressive and relief wave speeds, which are in general both stress dependent, together with knowledge of the electron deposition profile. Such facts cannot be precisely known in advance. Hence "mean" behavior was assumed in determining the probable one-dimensionality of a given experimental arrangement. A mean exponential depth of deposition was assumed based on prior ELTRAN code energy deposition predictions and the stress-dependent shock and release wave speeds were used. This is particularly important for the LVI and carbon gauge experiments, where the dispersive or shocking behavior of fused silica and PMMA can have significant effect for the dimensions involved. Figure 6 shows the overall methodology for computing the one-dimensional time region, while Figures 7 through 10 show the predicted times for differing experiments as a function of electron beam irradiation area.

In all cases, except one small area quartz measurement on Al, the stress waves were one-dimensional up to and beyond the observed peak stresses. The limit of one-dimensionality is indicated on each stress record shown in Section 4-3.

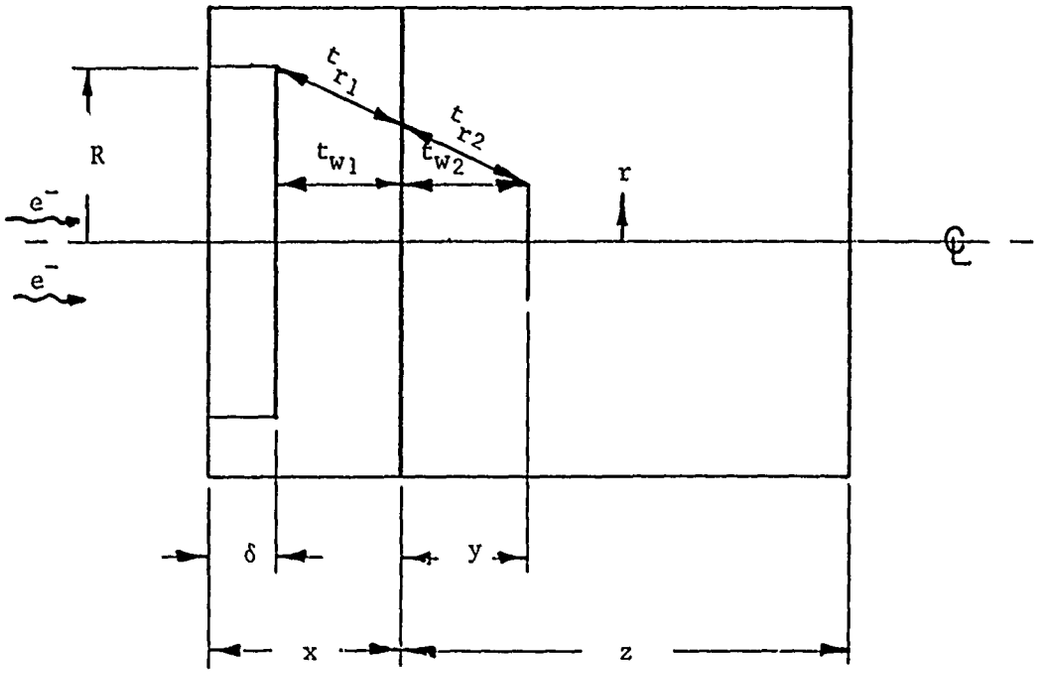

x = sample thickness

y = depth of monitoring point (carbon gauge, buried mirror)

z = thickness of backer (fused silica, PMMA, or quartz gauge)

R = irradiation radius

r = monitor area radius

δ = deposition depth

- Using standard geometry to establish path length, we define the one-dimensional read time at the monitor as

$$t_{1D} = (t_{r1} + t_{r2}) - (t_{w1} + t_{w2})$$

where

t_{r_1} = path/release speed in sample

t_{r_2} = path/release speed in backer

t_{w_1} = path/compressive wave speed in sample

t_{w_2} = path/compressive wave speed in backer.

For quartz gauges, $y = t_{r_2} = t_{w_2} = 0$.

Figure 6. One-dimensionality analysis.

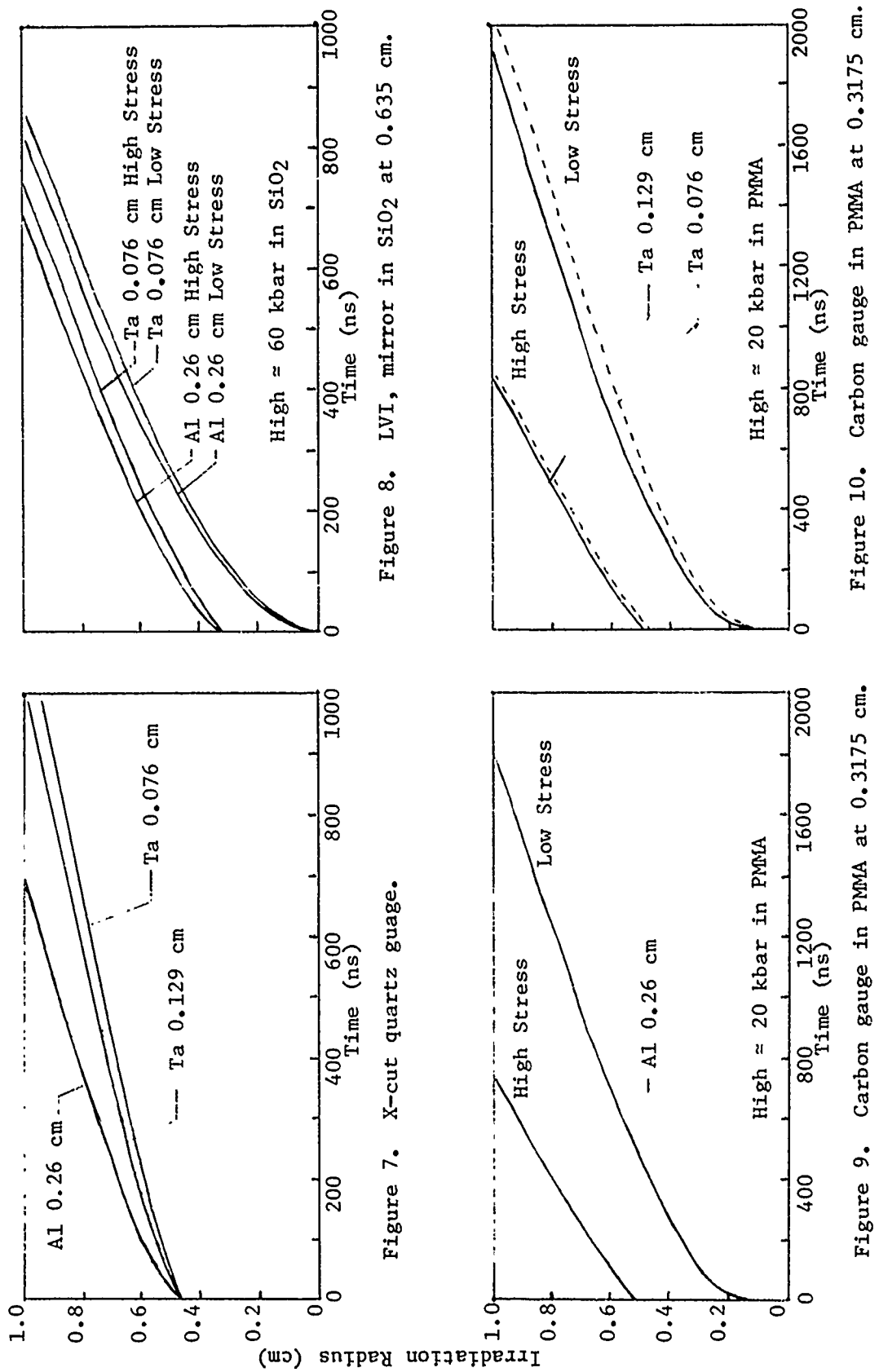

Figure 7. X-cut quartz guage.

Figure 8. LVI, mirror in SiO_2 at 0.635 cm.

Figure 9. Carbon gauge in PMMA at 0.3175 cm.

Figure 10. Carbon gauge in PMMA at 0.3175 cm.

Figures 7 through 10. One-dimensionality read times.

31

It is emphasized that this is a very conservative one-dimensional read time because of the method of calculation, and because time is "started" at the beginning of the stress pulse. Since the early release waves originate from weakly stressed regions of the material, the corresponding magnitude of release, and hence perturbation of true one-dimensional conditions, is also small. Thus the integrated effect of the release waves is small in general, only slowly increasing in magnitude as time progresses well beyond the stress readings of interest.

3-6 STRESS PREDICTIONS

The predictions for anticipated stress readings were primarily based on the application of the Gruneisen pressure-energy relationship, together with allowances for stress relief during finite deposition time and stress magnitude variation for transmitted waves across known impedance mismatches. Allowances were also made for attenuation of the stress waves during propagation through fused silica and PMMA, based on "typical" PUFF (ref. 4) computations.

Thus we have

$$\sigma_1 = \Gamma_s \rho_s E_s \tag{1}$$

as the stress generated for instantaneous deposition within the sample, where Γ_s = Gruneisen parameter, assumed constant, ρ_s = initial sample density, and E_s = specific energy loading in cal/g in sample.

Stress relief (see Section 2) during finite deposition time gives

$$\sigma_2 = \Gamma_s \rho_s E_s \cdot \alpha \tag{2}$$

where α is the relief factor and is given (approximately) by

$$\alpha = \frac{\delta}{2CT}\left(1-e^{-\frac{2CT}{\delta}}\right) \tag{3}$$

where δ is the pseudo-exponential dose profile e-folding width in cm, C is the relief wave speed in cm/sec, and T is the deposition time in seconds (power pulse measured at its full width-half maximum (FWHM). Figure 11 gives the stress relief factor, α, as a function of (CT/δ) according to equation (3). Also

$$\alpha = \frac{\delta}{2CT}\left(1-e^{-\frac{2CT}{\delta}}\right)$$

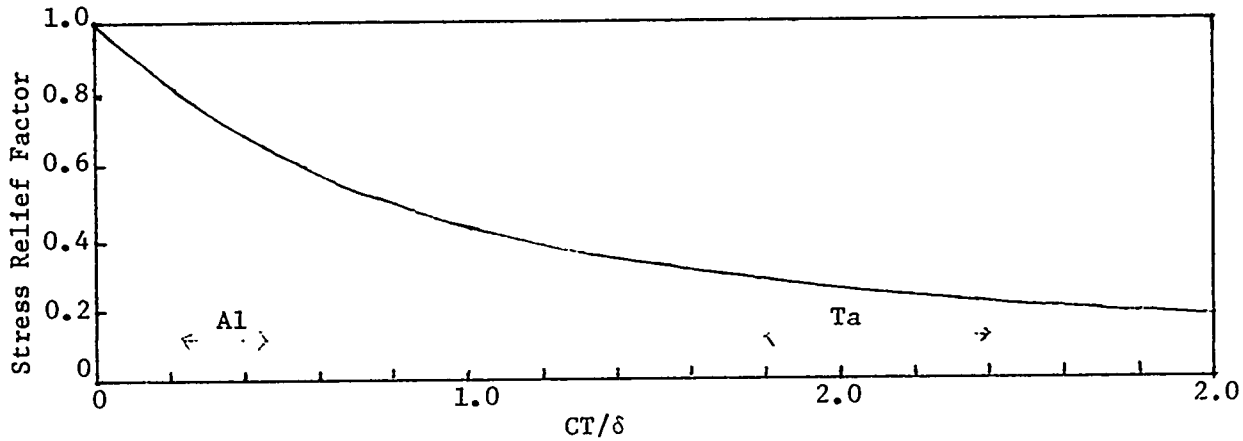

Plot of stress relief factor, α, as a function of CT/δ

α = relief factor

C = release wave speed

T = deposition time

δ = deposition width (e-folding value)

$\longleftrightarrow$ typical range of values for this work

Figure 11. Swiftness stress release factor.

indicated are typical ranges for Al and Ta relevant to this work. The relief for Al is typically small ($\alpha \simeq 0.75$), while for Ta it is very significant ($\alpha \simeq 0.25$).

After beam deposition the stress wave continues to propagate and proceeds to develop a compressive in-going wave followed by an out-going relaxation wave. The latter becomes a tensile in-going wave for low energy loadings, but can maintain a positive pressure during expansion for copious vapor production. This "splitting" of the initial stress profile produces a reduction in peak stress by a factor of the order of 2, yielding a propagating peak compressive stress given by

$$\sigma_3 = \Gamma_s \rho_s E_s \alpha/2 \tag{4}$$

after traveling a distance comparable to, or greater than, the deposition depth. Attenuation of the pulse can occur during propagation through the sample itself, yielding a further factor of β change in stress. If this stress reaches a free rear surface, it will induce a surface velocity given by

$$U_{FS} = \frac{2\sigma_3\beta}{\rho C} = \frac{\Gamma_s \rho_s E_s \alpha\beta}{\rho_s C} = \frac{\Gamma_s E_s \alpha\beta}{C} \tag{5}$$

where ρC is the sample acoustic impedance = Z.

If the stress propagates into another material (fused silica or PMMA), then the transmitted stress is given by

$$\sigma_4 = \sigma_3 \frac{2Z_{load}\,\beta}{(Z_{load} + Z_{sample})} \tag{6}$$

while the particle velocity (e.g., a buried mirror velocity) is given by

$$U_B = \frac{\sigma_4}{Z_{load}} = \frac{2\sigma_3\,\beta}{(Z_{load} + Z_{sample})} \tag{7}$$

Finally, if the expected attenuation of the stress pulse between the sample/backer interface and the monitoring point is γ, we may finally expect

$$\sigma_5 \text{ measured} = \frac{\Gamma_s \rho_s E_s \alpha \cdot Z_{load}}{(Z_{load} + Z_{sample})} \cdot \beta\gamma \qquad (8)$$

or the velocity

$$U_B \text{ measured} = \frac{\Gamma_s \rho_s E_s \alpha}{(Z_{load} + Z_{sample})} \cdot \beta\gamma \qquad (9)$$

3-7 ENERGY DEPOSITION CALCULATION - ELTRAN, AND BEAM CHARACTERISTICS

In order to compute the expected sample stresses, it is necessary to know the energy deposition within the sample. This can be computed using a Monte Carlo code such as ELTRAN (ref. 5), using as input the spectrum of electrons and the mean effective angle of beam incidence to the sample.

Throughout this work use was made of the Sandia Laboratories (Albuquerque) computerized analys_ of the Blackjack diode characteristics. This system uses a PDP-11 computer together with a Tektronix R7912 transient digital recorder, and accepts directly information from the voltage and current monitor probes of the machine. The system yields initial data for diode voltage and current versus time. It then applies the necessary correction to the voltage record due to inductive pickup, and also takes into account the known (measured from short circuit shots) time stagger between the voltage (V) and current (I) measurements. Thus it can compute the true power versus time behavior, determine the total beam energy, identify the true corrected peak voltage, and find the deposition time (FWHM). Of great importance is the fact that from the V and I data the system also computes the electron spectrum, giving relative numbers of electrons at each energy. This spectrum is given in histogram form by allocating the electrons into twenty "bins" of equal energy width between zero and peak voltage. This electron spectrum is used as input data for ELTRAN computations in conjunction with the floating parameter of incident beam angle to the sample.

Both BJ3 and 3' utilize a solenoidal magnetic field within the drift tube between the diode and the samples. This field is pulsed on about 6 ms before beam production and has a peak value of the order of 25 kilogauss. The purpose of this strong field is to guide the beam down the drift tube. The field counters any tendency for the beam to radially blow out (due to electrostatic repulsion) or pinch in (due to electromagnetic attraction) by inducing helical spiralling of the electrons about the field lines. In effect, the field produces a scattering matrix through which the electrons can only diffuse slowly in a direction perpendicular to the main beam axis.

The clear advantage of the magnetic field is the ability to propagate a well controlled beam over large flight paths of the order of 100 cm with only a slow variation in beam width (and hence fluence) as a function of axial position. This latter behavior is the one used to vary fluence.

The disadvantage of the field is that some electrons, particularly of low energy, can be reflected by the magnetic "mirror" as they enter the converging field. Thus the beam spectrum reaching the samples may vary from that generated at the diode, and there is an overall loss of total beam energy reaching the sample. In addition, the local trajectory of an electron is a complex function of mean motion of the beam due to overall divergence together with the helical motion induced about the magnetic field lines. Thus the mean angle of incidence is a complicated average of all such effects, and averages over all electron energies and time (see Figures 1 and 2).

These two effects, of possible spectrum change and gross averaging of incident angle, are primarily responsible for the usual inability to obtain perfect fits of ELTRAN computations with calorimetric measurements using the dose-depth calorimeter stack. Nevertheless, good fits are obtained by using the spectral information from the diode performance and chosing an appropriate mean angle for ELTRAN.

The majority of shots utilized a 0.025 g/cm^2 carbon cloth in the beam path. This was positioned in the maximum magnetic field a distance of 18 cms from the anode. Its purpose was to help produce a smoother beam (by removing any local hot spots), absorb very low energy electrons (which can produce dramatic variations in peak depositions in samples), and prevent anode debris from impacting the samples.

The cloth's effect on deposition was computed using ELTRAN in two distinct ways. The first approach, identified as ELTRAN I, treated the carbon cloth as a simple prescreen filter. Thus the beam is assumed totally one-dimensional and has a common definition of incident angle. This approach assumes that the large spacing between the cloth and sample (several 10's of cm) had no influence on beam behavior. Mutual scattering between the cloth and a sample are computed as though there were no gap.

The second approach, identified as ELTRAN II, computes for differing independent angles of incidence at both the cloth and a sample. One angle of incidence is chosen for beam entry to the cloth. The code computes the transmitted beam, and then an independent angle of incidence is chosen for this transmitted beam to enter the sample. This approach is physically more realistic since the beam is probably varying between the cloth and the sample and the electron angle is expected to vary with the magnetic field strength, and is thus not truly one-dimensional. However, this version of the code cannot correctly compute the mutual scattering between cloth and sample. The true advantage of this second approach, of course, is that it permits use of an additional free parameter with which to fit the predictions with measured deposition profiles.

SECTION 4

EXPERIMENTAL RESULTS

4-1 CALORIMETRY: BLACKJACK 3 PRIME

The first task was to develop and characterize the BJ3' beam for use, as appropriate, in commonality experiments. To do this involved spatial fluence measurements, yielding fluence as a function of axial position along the drift tube and as a function of radial spacing from beam axis. In addition, dose-depth calorimetry was used to establish typical deposition profiles from which mean angles of incidence could be established with the use of ELTRAN.

The fluence measurements were performed over the axial range of 35 to 80 cm from the diode anode. The overall averaged values are shown in Figures 12 to 19. It can be seen that the fluence rises from a value of the order of 15 cal/cm^2 at 80 cm axial position to around 180 cal/cm^2 at 35-cm axial position. There is a very rapid change of fluence in the 60- to 70-cm position. Note that all error bars represent ± 1 standard deviation on the data. Actual variations could be up to ± 3 deviations.

At the low fluence station the beam is essentially flat and occupies the majority of the drift tube (diameter of 15 cm). At the high fluence station the beam is much narrower, the half-max fluence occurring at a radius of about 1.5 cm. At intermediate stations it is observed that the beam is hollow, tending to peak at a radius of the order of 1.0 cm. This behavior corroborates earlier data taken on BJ3' (ref. 6).

The hollow beam poses difficulties for stress measurements since it makes interpretation of the central sample fluences more unreliable, even when supported by outboard calorimetry. Early shots on BJ3' utilized a small diameter ring calorimeter having a mean radius of 0.92 cm which was designed to measure fluence as close to center as possible. However, this produced a rather deep square-section

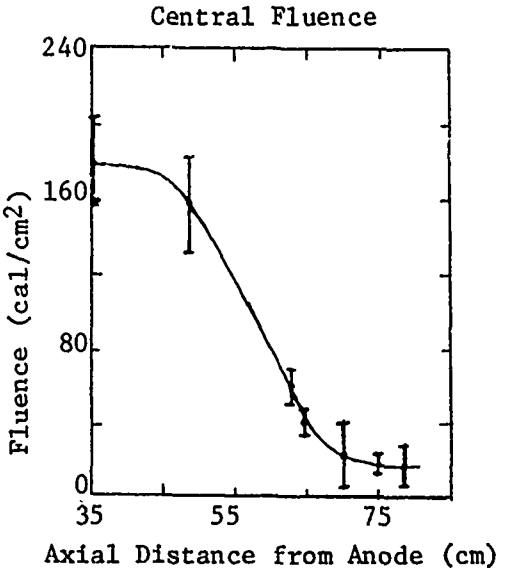

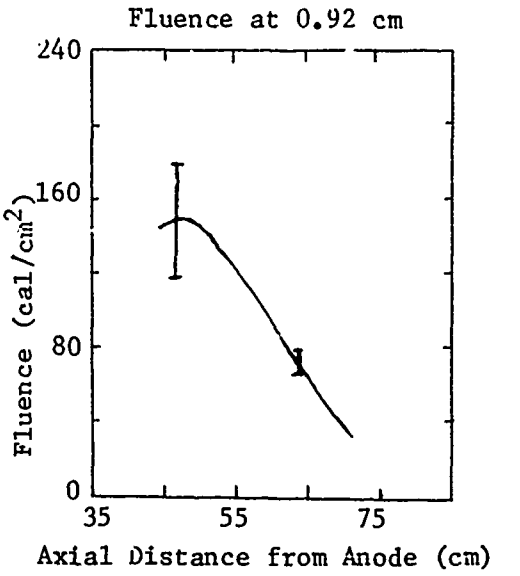

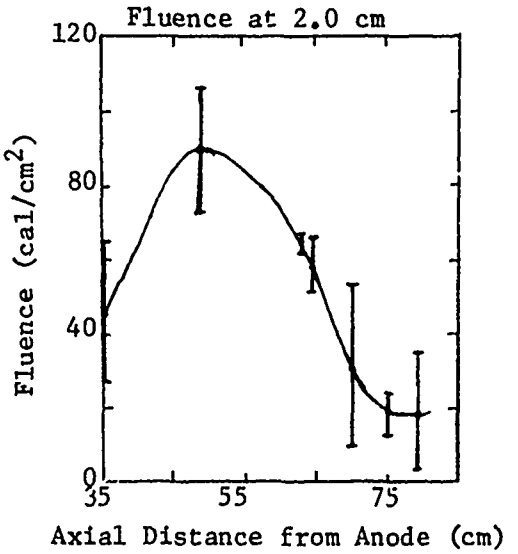

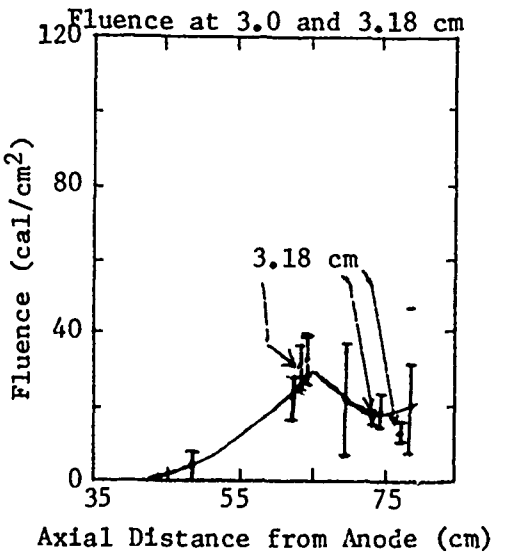

Figures 12 through 15. BJ3' axial fluence profiles.

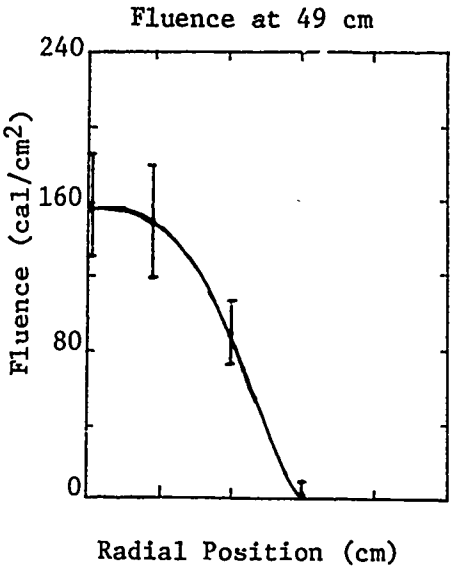

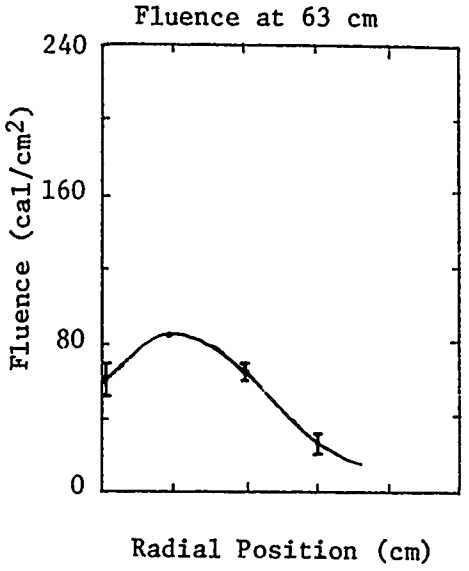

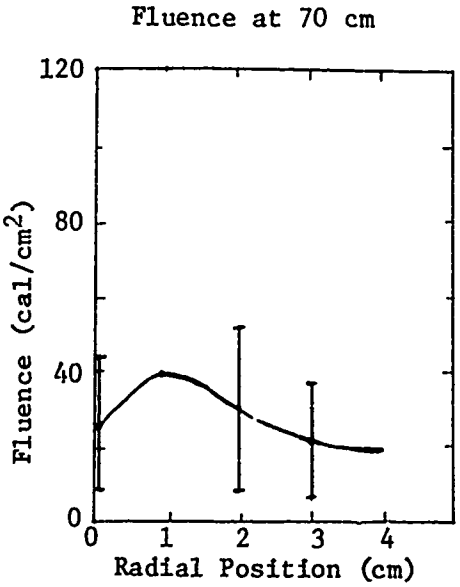

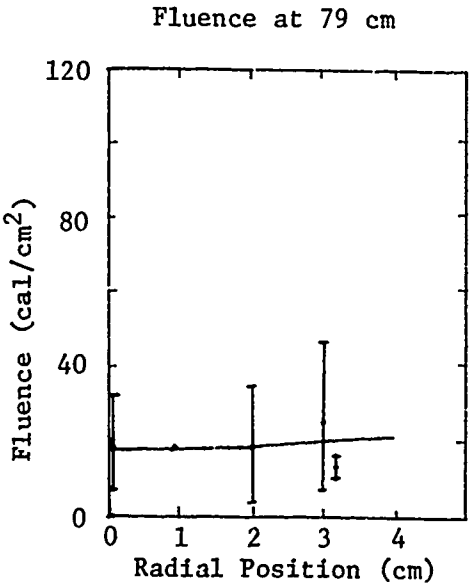

Figures 16 through 19. BJ3' radial fluence profiles.

tube down which the electrons had to flow to reach the sample. There were indications that this geometry induces beam perturbations, exagerating the hollowness of the beam and lowering still further the central sample fluence. This ring calorimeter also limited the possible one-dimensional read time of the experiments. For these reasons this ring calorimeter was replaced by a larger one of 1.9-cm mean radius. The latter was also used on BJ3.

Dose-depth measurements were done at the 64- and 79-cm stations. At high fluences the beam was less repeatable and was narrower. These facts, together with considerations of the deposition timings discussed below, prompted the decision to continue the high fluence stress measurements on BJ3. No dose-depth measurements were attempted at the high fluence stations for BJ3'.

It is seen from Figures 20 through 25 that a reasonable fit to the dose—depth data could be obtained using ELTRAN and a mean angle of the order of 20 to 30 degrees. In particular, where the thin carbon cloth was employed, on all but one shot, the better fits were obtained using the more complex ELTRAN II program, where the initial angle of incidence to the cloth was chosen to be 60 degrees.

The desired BJ3' beam was 800-keV mean energy, with 100 cal/cm^2 over 3 to 5 cm^2. The actual mean electron energy was 741 $\pm$ 128 keV. Figures 12 to 19 show that the fluence requirement could also be met, in particular at a position about 58 cm from the anode where 100 cal/cm^2 is maintained over an area of about 6 or 7 cm^2.

The requirement to achieve energy loadings of the order of 750 cal/g in Al or Ta implied fluences of the order of 150 cal/cm^2, assuming a mean coupling factor for these materials and these beams of about 5 (cal/g)/cal/cm^2). Figure 26 shows the general trend of coupling factors versus mean energy derived from ELTRAN computations. For BJ3' such a fluence exists over a radius of about 1.2 cm for $\leq$20 percent fluence drop. While this is adequate for one-dimensional irradiation

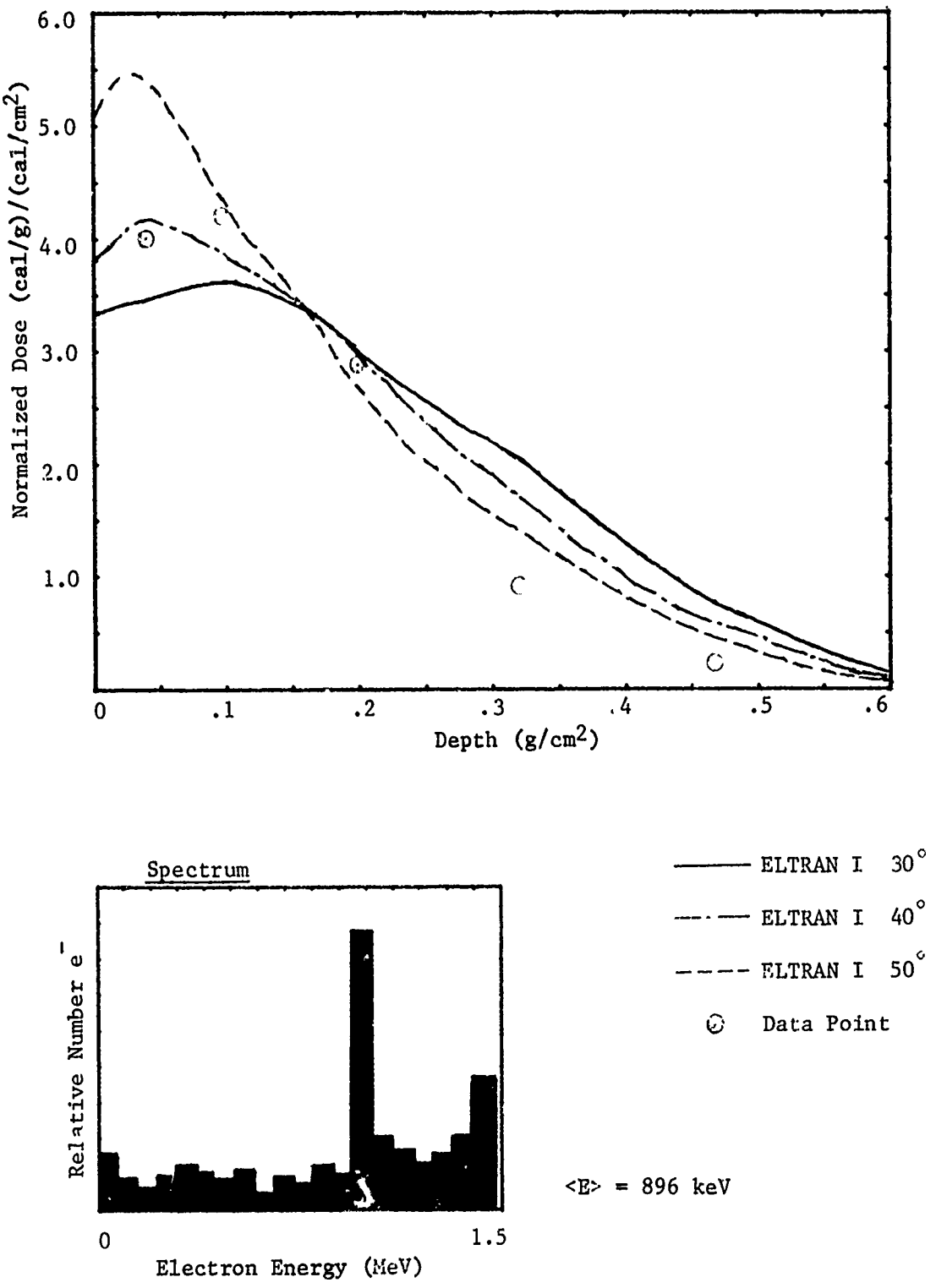

Figure 20. BJ3' dose-depth plot.

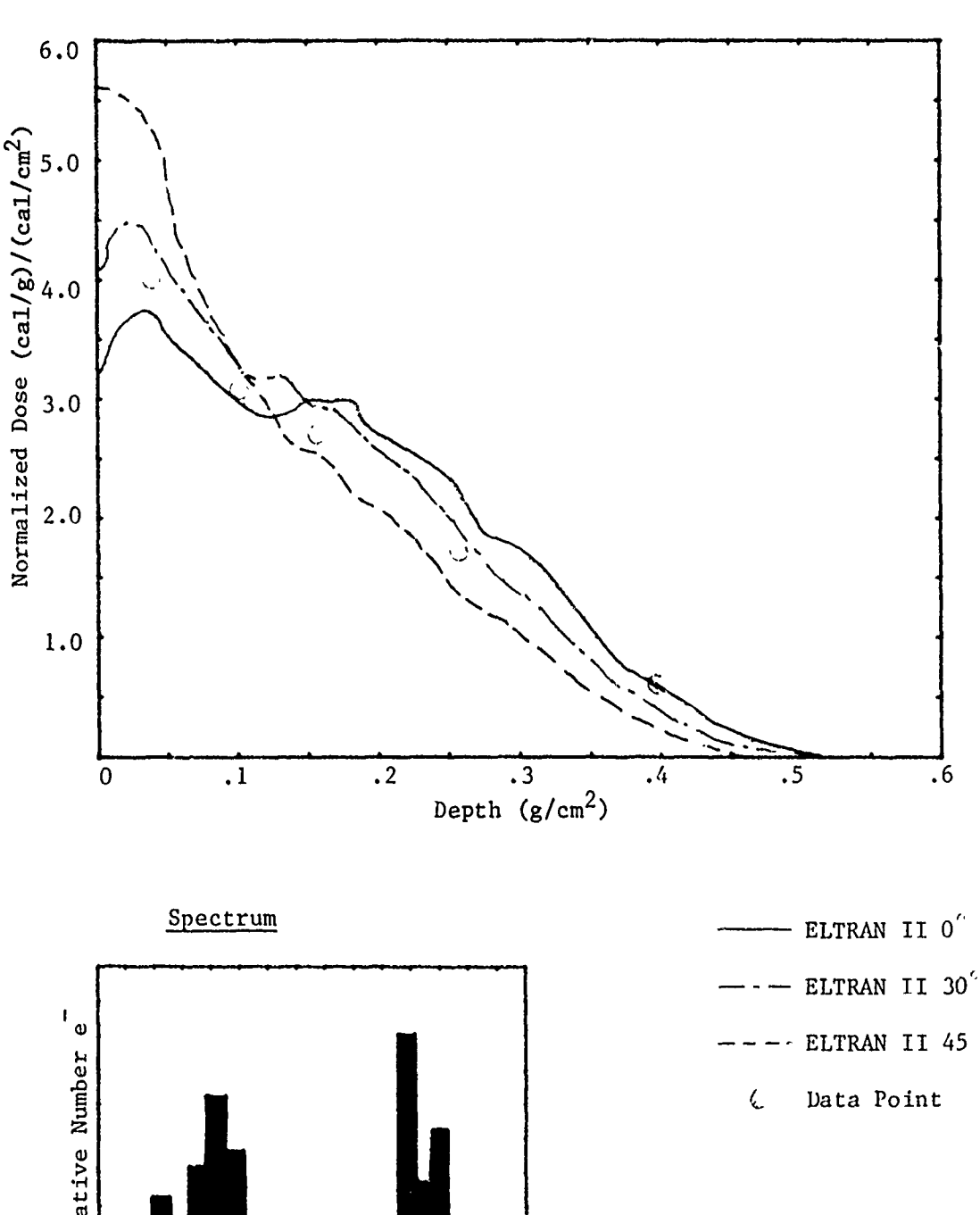

Figure 21. BJ3' dose-depth plot.

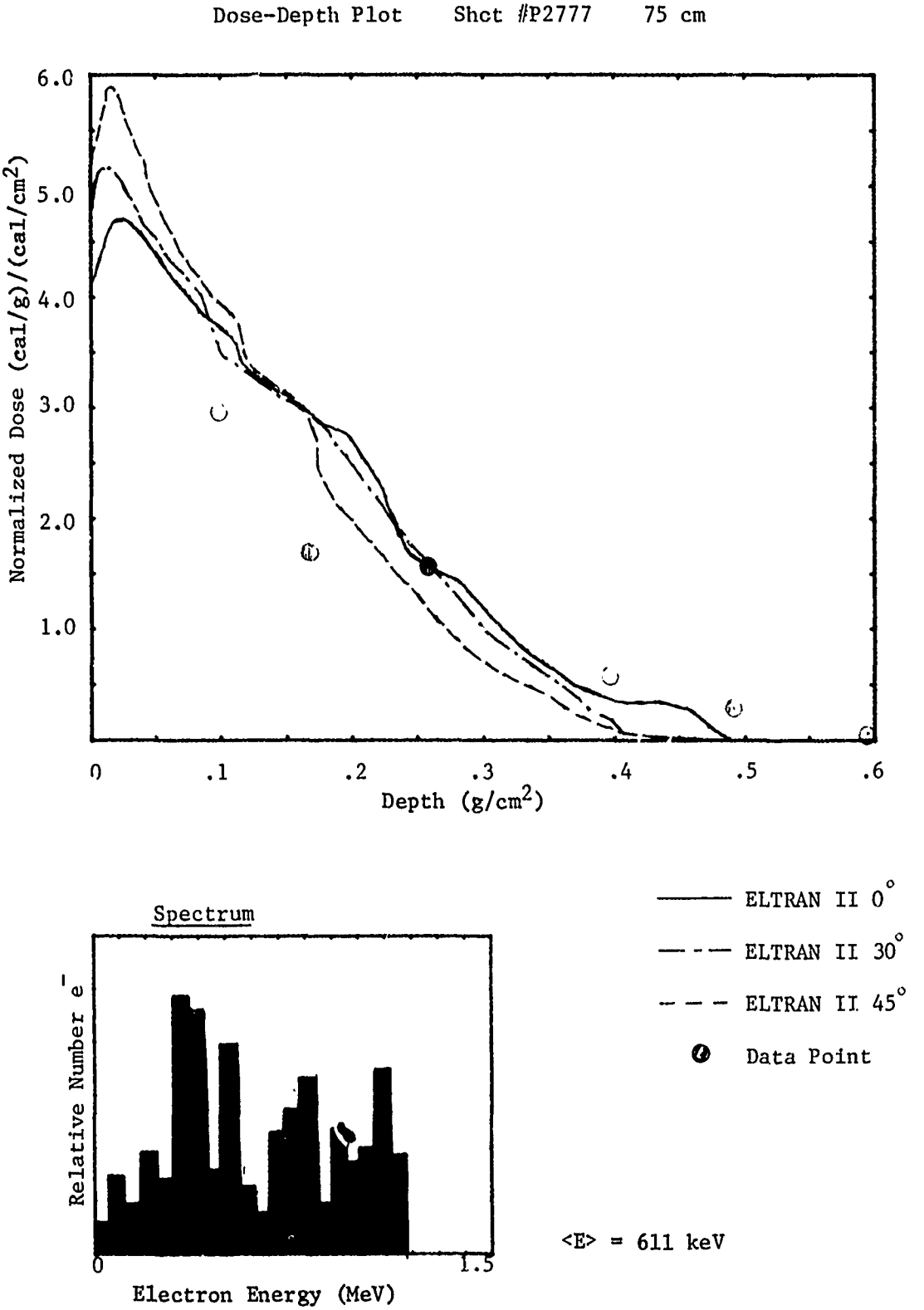

Figure 22. BJ3' dose-depth plot.

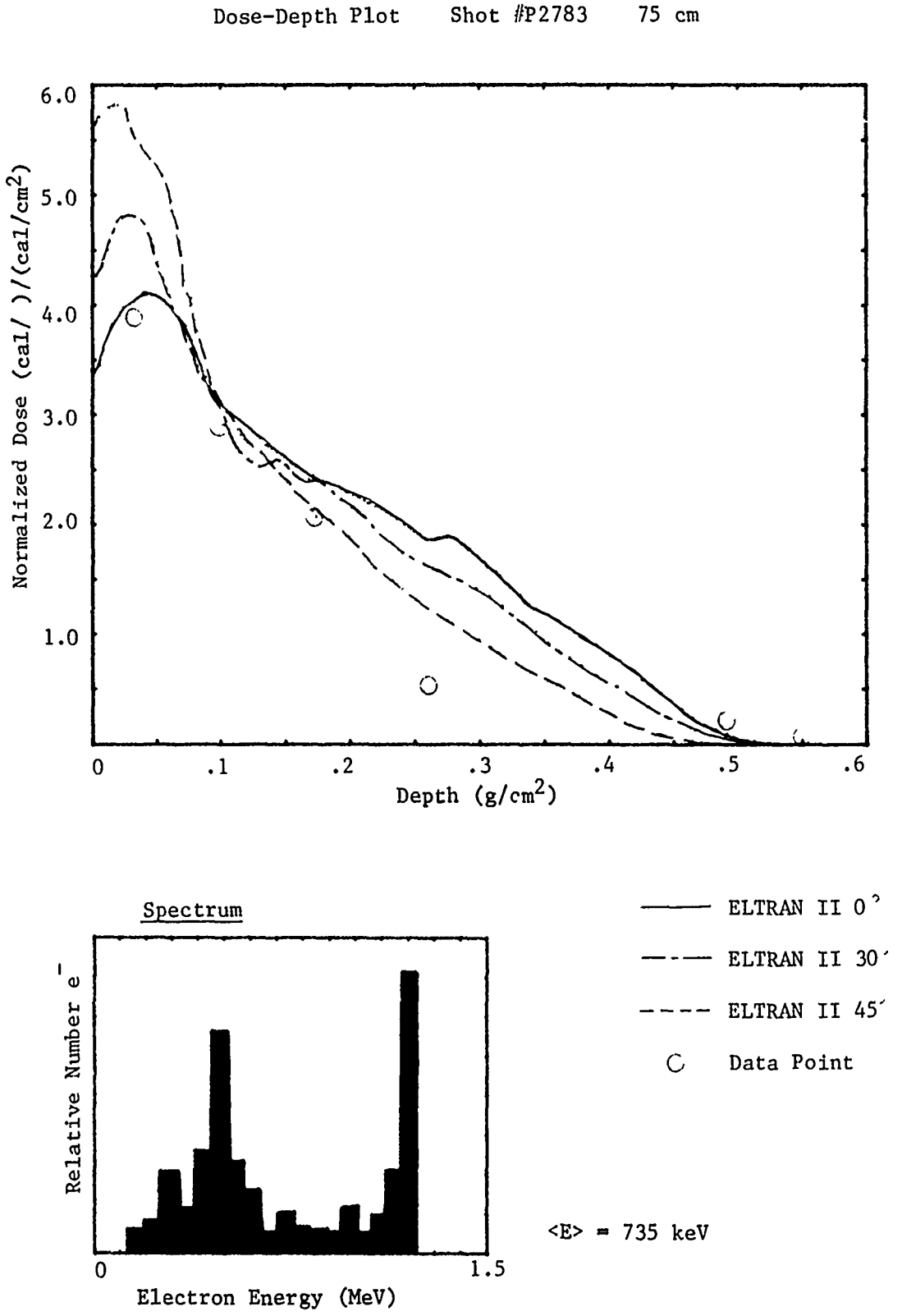

Figure 23. BJ3' dose-depth plot.

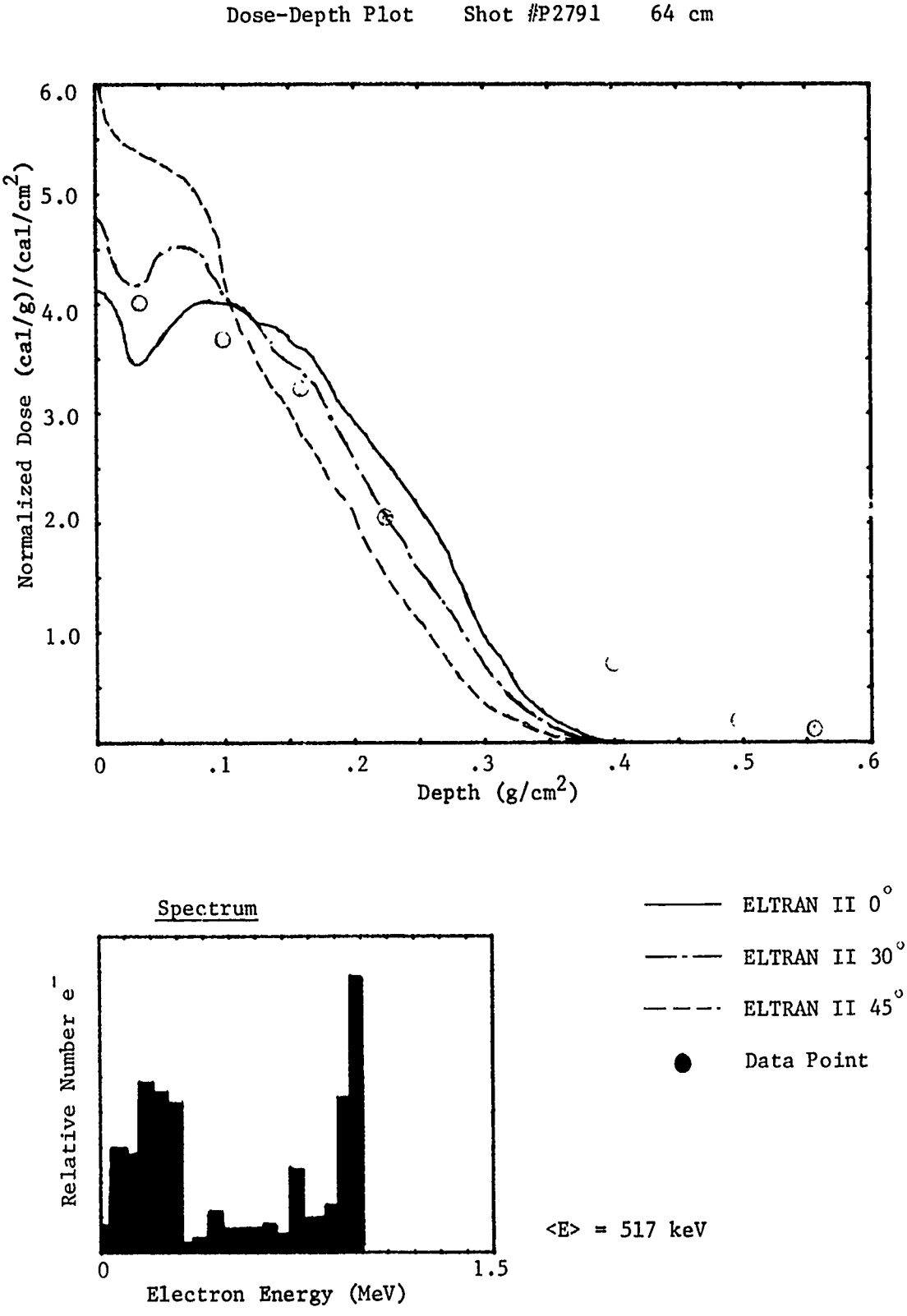

Figure 24. BJ3' dose-depth plot.

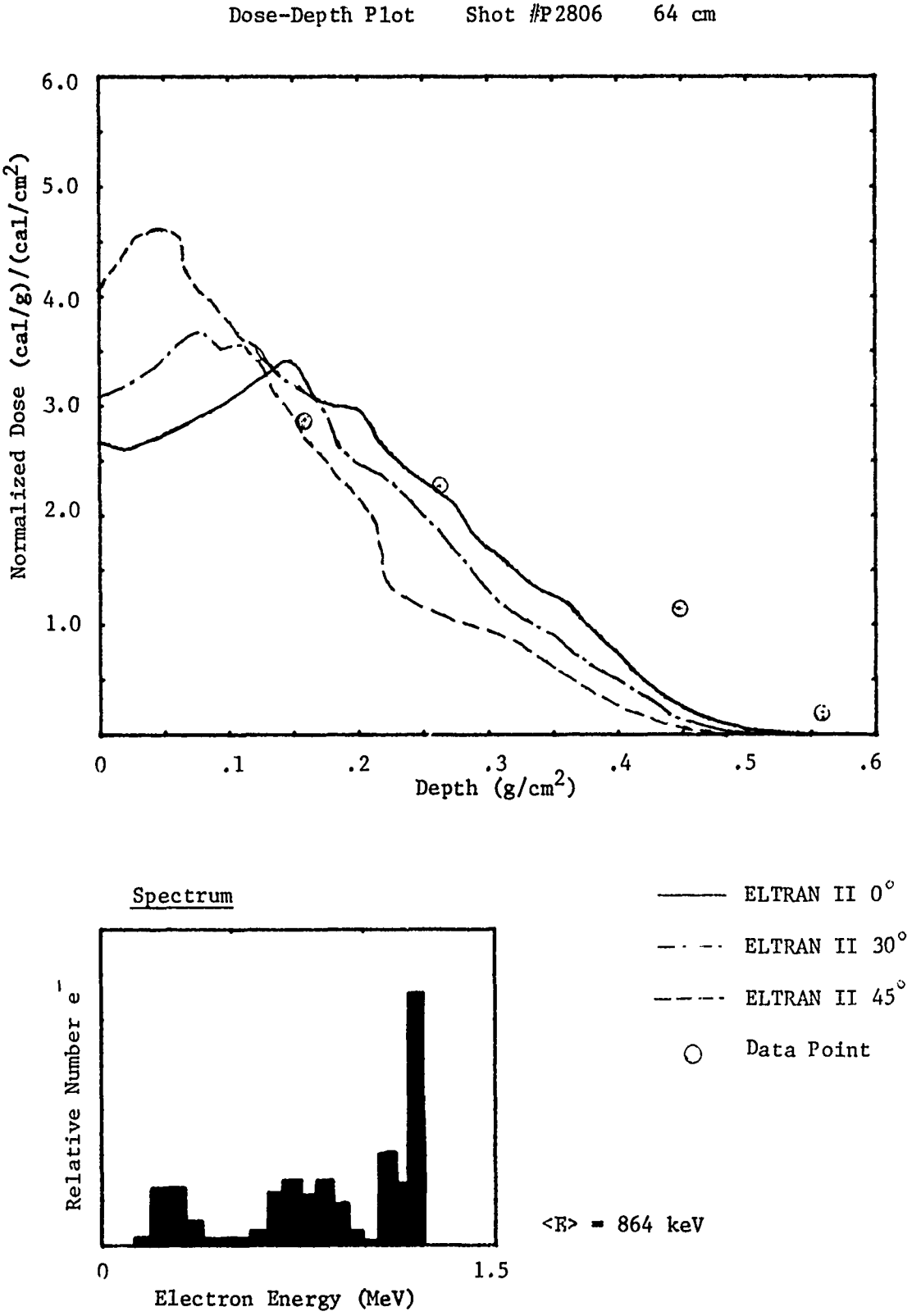

Figure 25. BJ3' dose-depth plot.

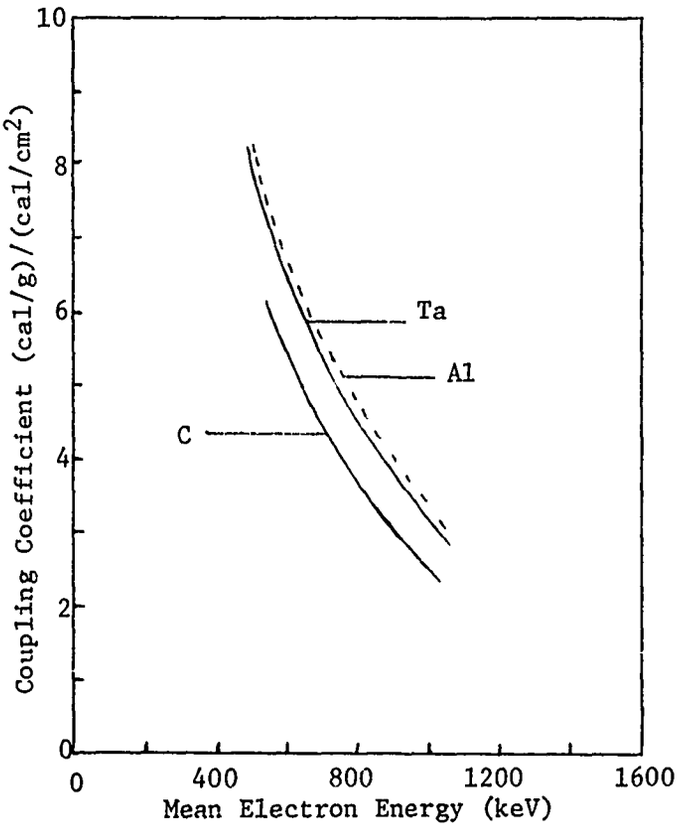

Trend of coupling coefficients derived from ELTRAN computations.

Note that exact value is dependent upon exact electron spectrum.

Figure 26. Coupling coefficient versus mean electron energy.

purposes, the BJ3' beam was less repeatable than that of BJ3. Inspection of Table 3 shows that BJ3 gave a similar mean electron energy, 747 $\pm$ 126 keV, and a higher total beam energy of 20.6 $\pm$ 4 kilojoules compared to 17.7 $\pm$ 3.3 kJ. The deposition time spanned the range of 26 to 56 ns for BJ3 alone, without the complications of a secondary power pulse tail seen on BJ3'. For these reasons, the majority of sample shots were performed on BJ3. (See also Section 4-4.)

4-2 CALORIMETRY: BLACKJACK 3

Use of BJ3 necessitated a similar beam characterization as for BJ3'. Figures 27 to 34 show the fluences as a function of axial position and radius. Again, all error bars are $\pm$1 standard deviation for fluence. A similar trend to that of BJ3' is observed; however, there are two major differences. Firstly, at no station does the beam become hollow*. The peak central fluence drops and the beam width increases in a monotonic, orderly fashion with axial distance from the anode. Secondly, the BJ3 beam width is greater than that of BJ3'. This accords with the greater overall total beam energy (see Table 3).

At 49 cm from the anode, peak fluences of about 170 cal/cm^2 are obtained, with the half-max fluence at a radius of about 2.0 cm. At 79 cm from the anode, the fluence is about 18 cal/cm^2 and essentially flat across the entire drift tube. This implies a total beam of about 13 kJ which is about 65 percent of the diode beam energy determined from the V and I records. This confirms that beam loss occurs during propagation down the drift tube.

At a radius of about 2 cm, two distinct sets of data were obtained. One was from the ring calorimeter system (4 thermocouples) with a mean radius of 1.9 cm. The other was from four independent calorimeters, 0.762-cm in diameter, with a mean radius of 2.0 cm. An apparent systematic difference was observed; however, closer inspection revealed that the limited number of shots using the 2.0-cm separate calorimeters were shots involving higher than average total beam energy.

* except slightly at the lowest fluences.

Table 3. Machine characteristics.

	Blackjack 3			Blackjack 3 Prime			
Session	FWHM (ns)	Total Beam (kJ)	Mean Energy (keV)	Session	FWHM (ns)	Total Beam (kJ)	Mean Energy (keV)
#1 18 Shots	43.9±7.8	21.58±5.39	708±165	24 Shots	33.6±5.0	15.8±4.0	862±143
#2 6 Shots	43.3±4.3	22.7±5.5	815±135	43 Shots	36.7±3.8	18.75±2.84	674±119
#3 70 Shots	43.5±7.0	20.18±3.41	752±111	---	---	---	---
Overall 94 Shots	43.57±7.02	20.64±4.06	747.3±125.6	67 Shots	35.59±4.3	17.69±3.30	741.3±128.1

Total number of shots = 161.

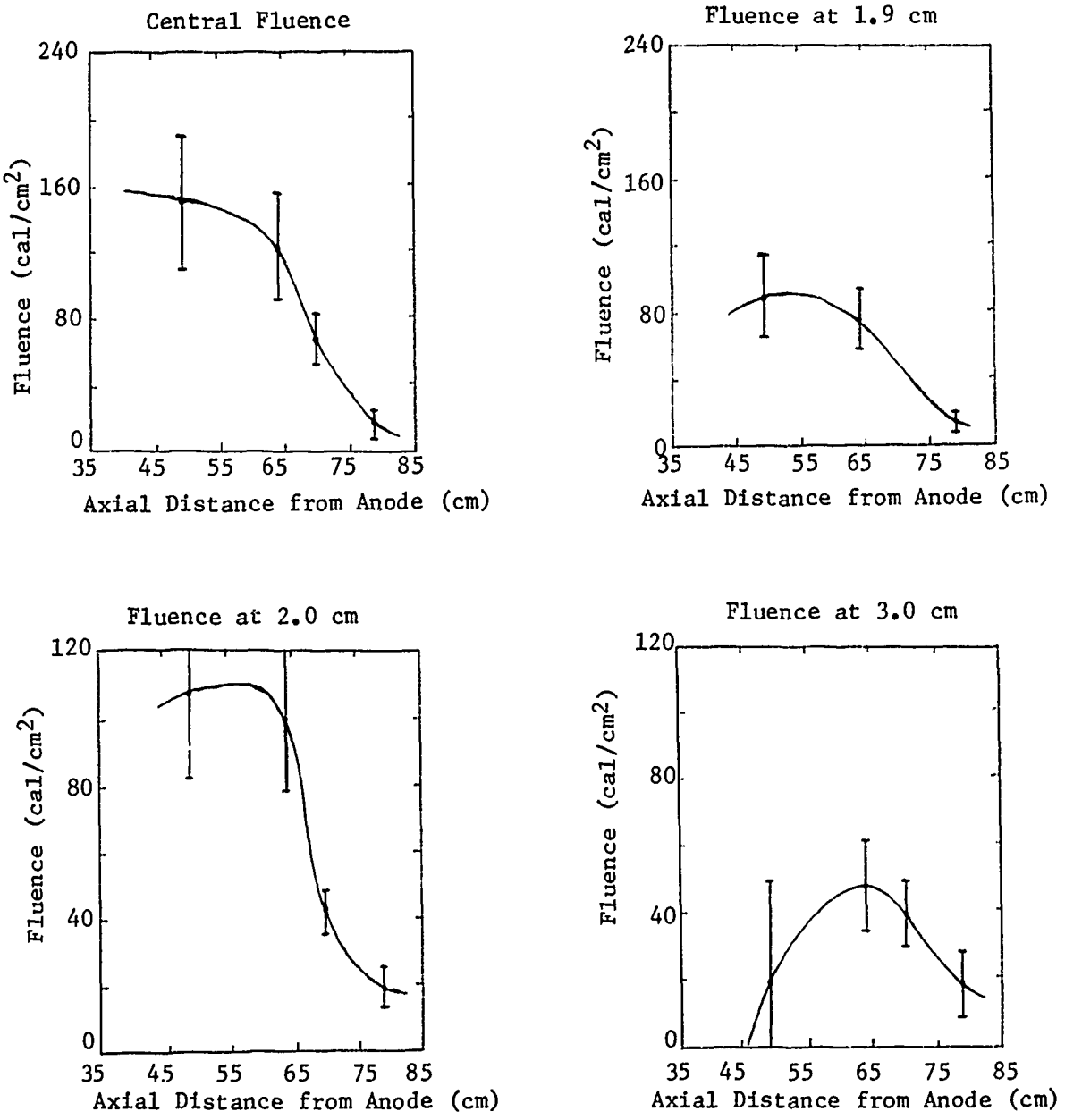

Figures 27 through 30. BJ3 axial fluence profiles.

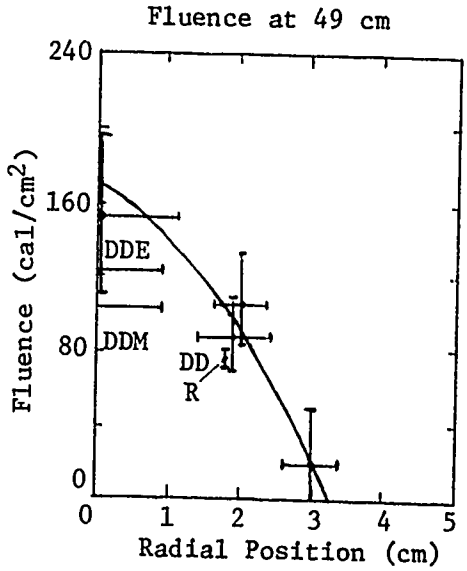

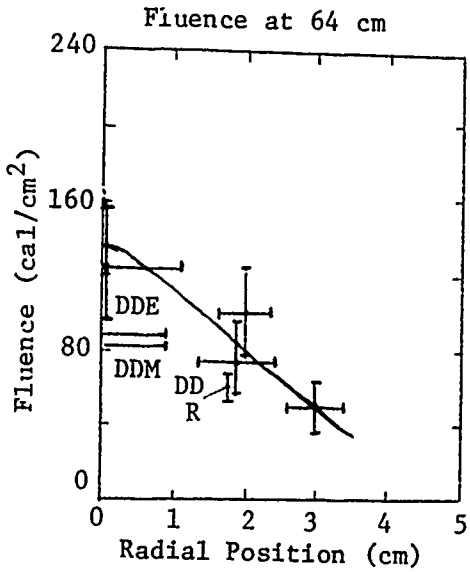

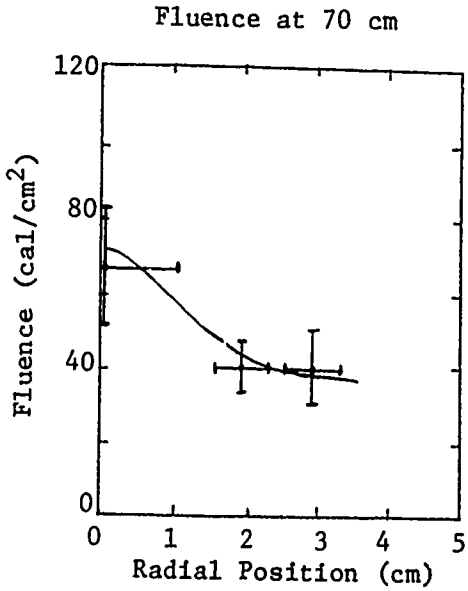

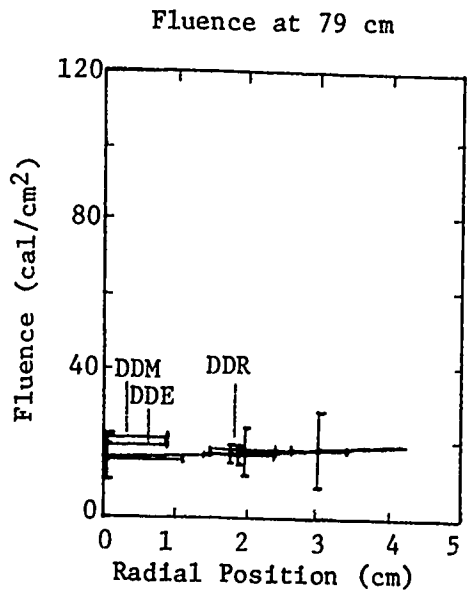

DDE: Dose-depth fitted to ELTRAN.
DDM: Dose-depth measured.
DDR: Ring calorimeter values for DD shots.

Figures 31 thr.ugh 34. BJ3 radial fluence profiles.

Inspection of all the shots revealed that there was an expected correlation between calorimetry values and the total beam energy. In addition to the normal shot-to-shot variations, there was also observed a slow variation in overall beam energy, with a corresponding variation in fluences. Indeed, a steady downward trend in behavior, culminating in bad voltage and current monitor performance, was the reason for a refurbishment of BJ3, accounting for some lost experimental time.

Figure 35 shows the sequential behavior of BJ3 at the 49-cm station. The importance of such behavior lies in the fact that a close packed group of shots, while having a small spread in results, can yield mean values different from other shots performed at significantly different times. This fact is demonstrated in Figures 31 to 34, where the fluence values for dose-depth measurements are seen to be offset from the mean values obtained by spatial calorimetry, especially at the 49- and 64-cm stations. Both the inferred fluences entering the foil stack and the corresponding ring calorimeter fluence values are offset downward for these two stations. Inspection of data reveals that these shots were done in groups and that the total beam energy was lower than average. At the 79-cm station the dose-depth values are offset slightly to the high fluence side of the mean values and, correspondingly, the total beam energies for these shots were higher than average.

Thus, it is concluded that Figures 27 to 34 show the overall average behavior of BJ3, while specific shot values maintain similar behavior but scale up or down in magnitude with the total beam energy of the shot. This factor, together with knowledge of the calorimetry values of a specific stress shot, allows more accurate assessment of fluences incident on the samples.

The dose-depth measurements and corresponding ELTRAN computations are shown in Figures 36 through 47. All but two of these shots utilized the 0.025 g/cm

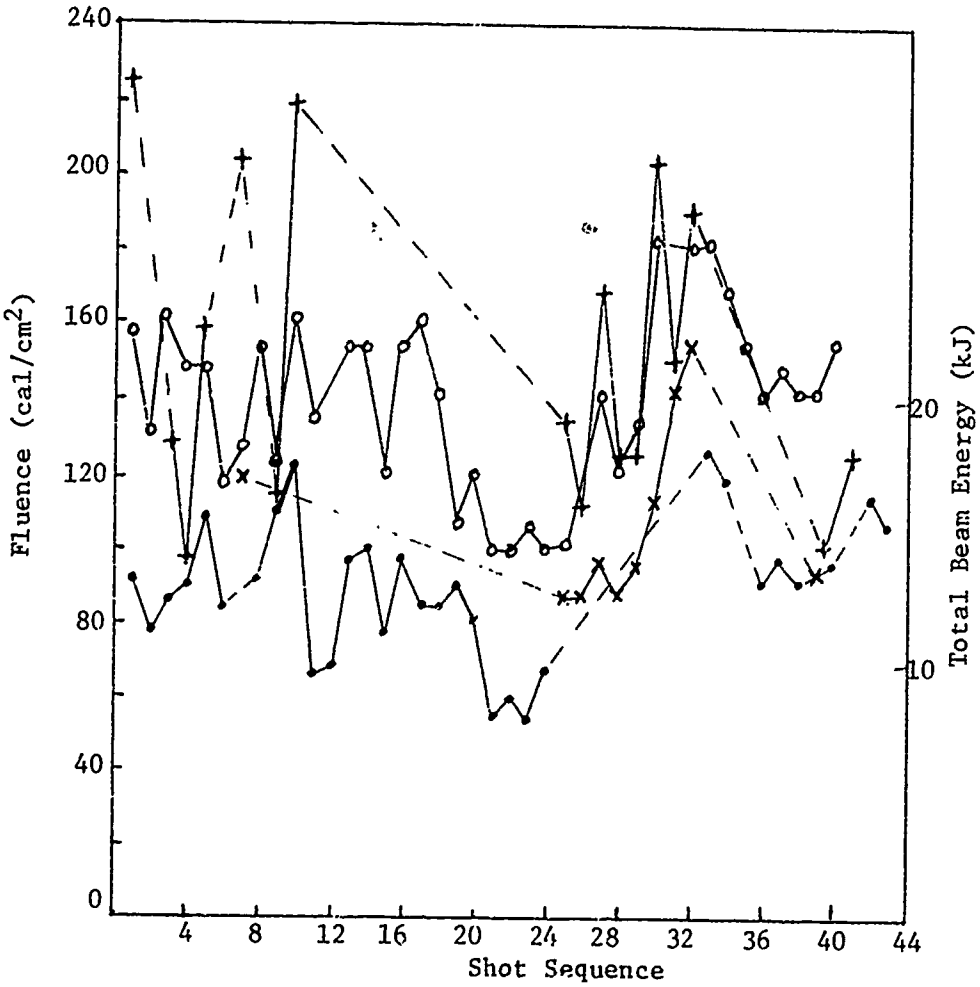

Illustration of sequential shot performance, indicating correlation of fluences with total beam energy.

+ Central Fluence

• Fluence at 1.9-cm radius

x Fluence at 2.0-cm radius

o Total Beam Energy

} All at 49-cm station

Figure 35. BJ3 sequential shot behavior.

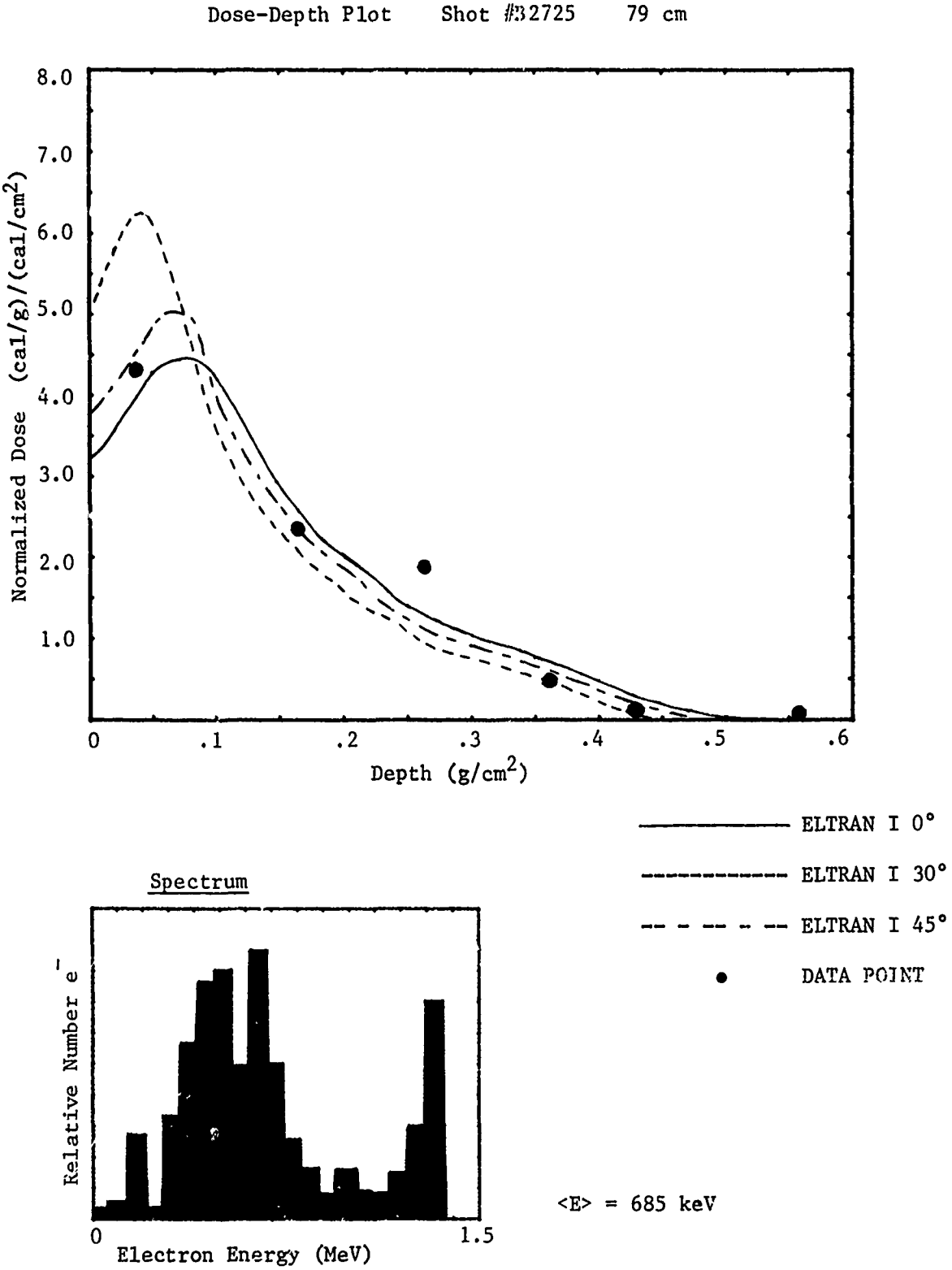

Figure 36. BJ3 dose-depth plot.

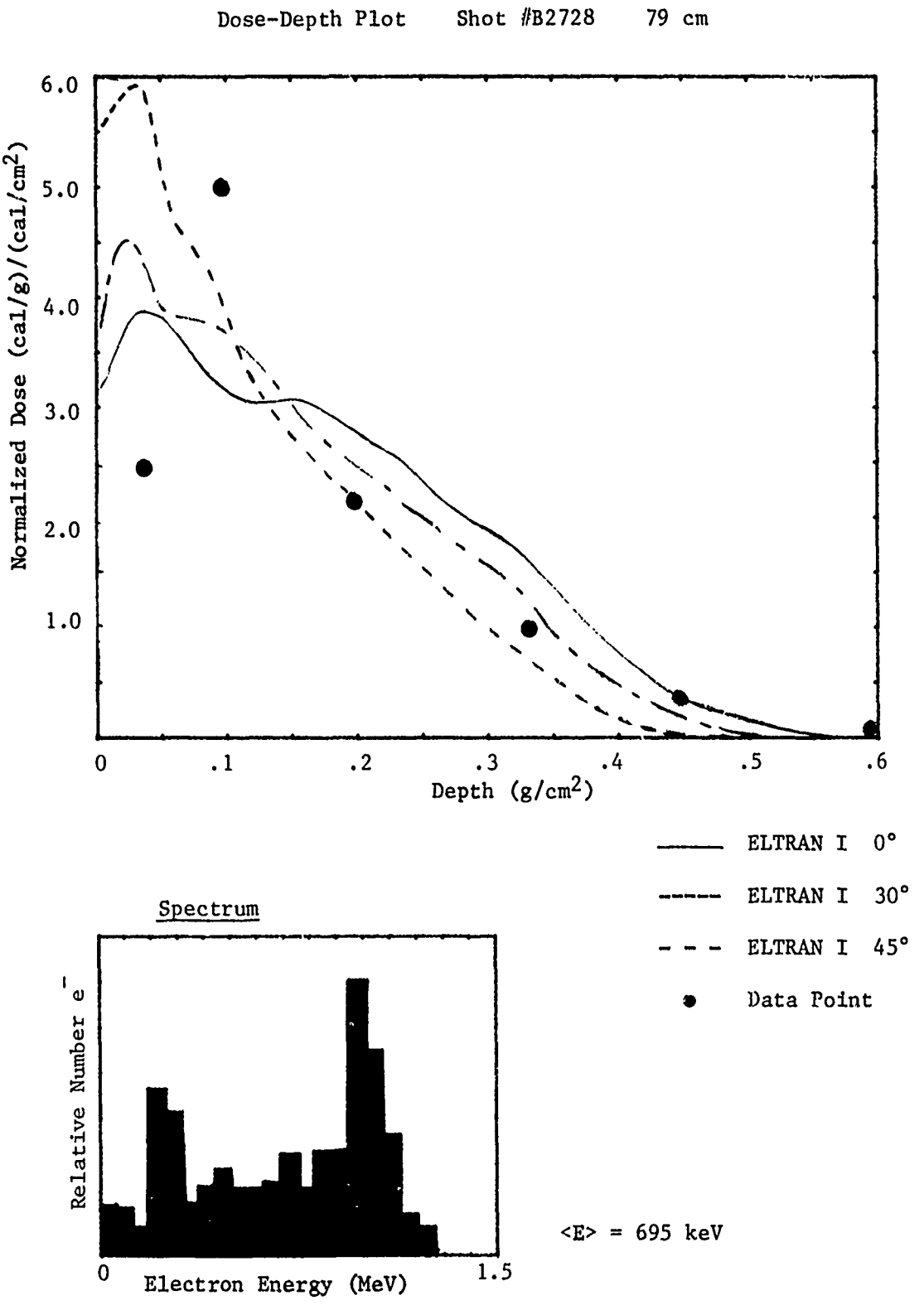

Figure 37. BJ3 dose-depth plot.

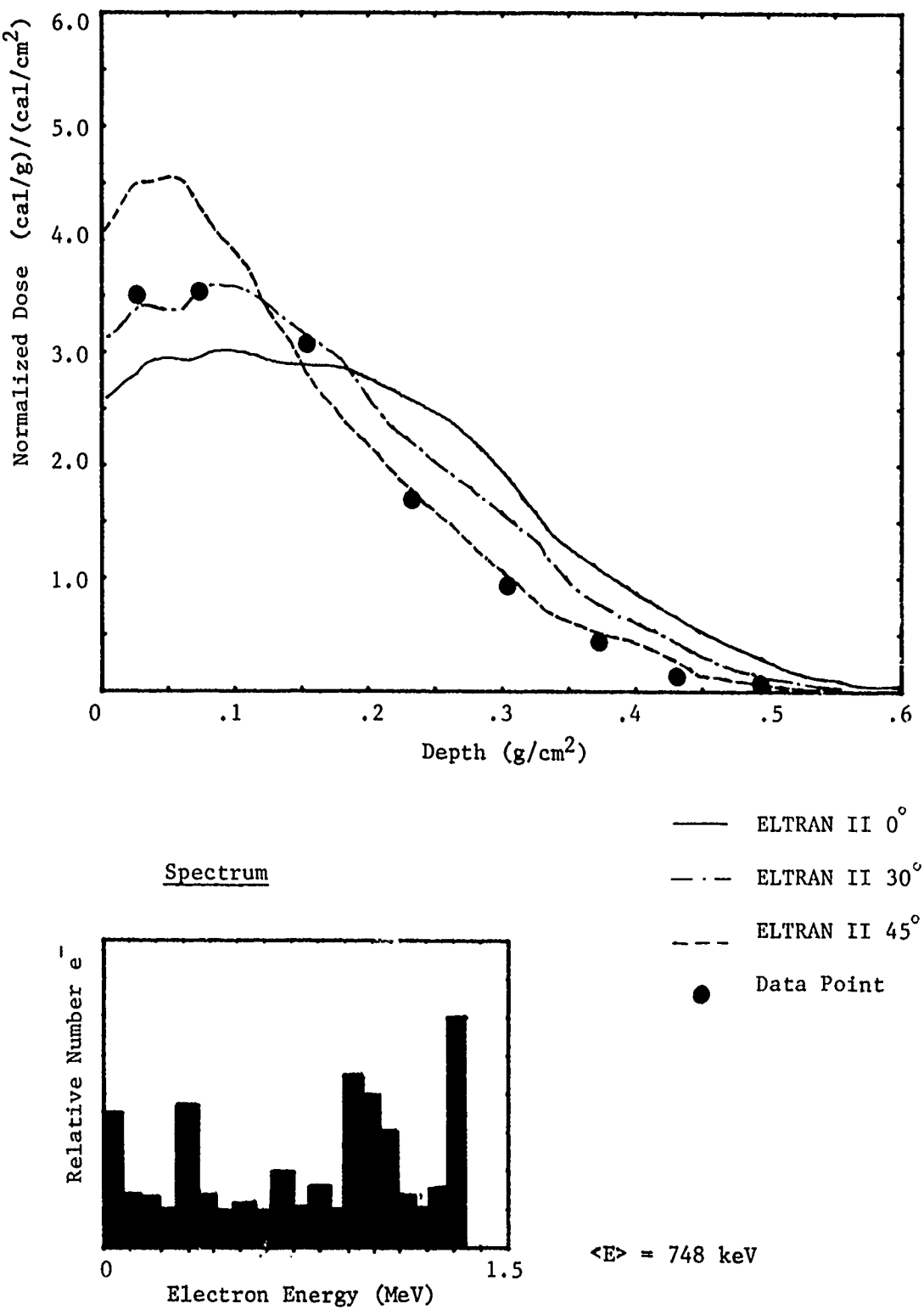

Figure 38. BJ3 dose-depth plot.

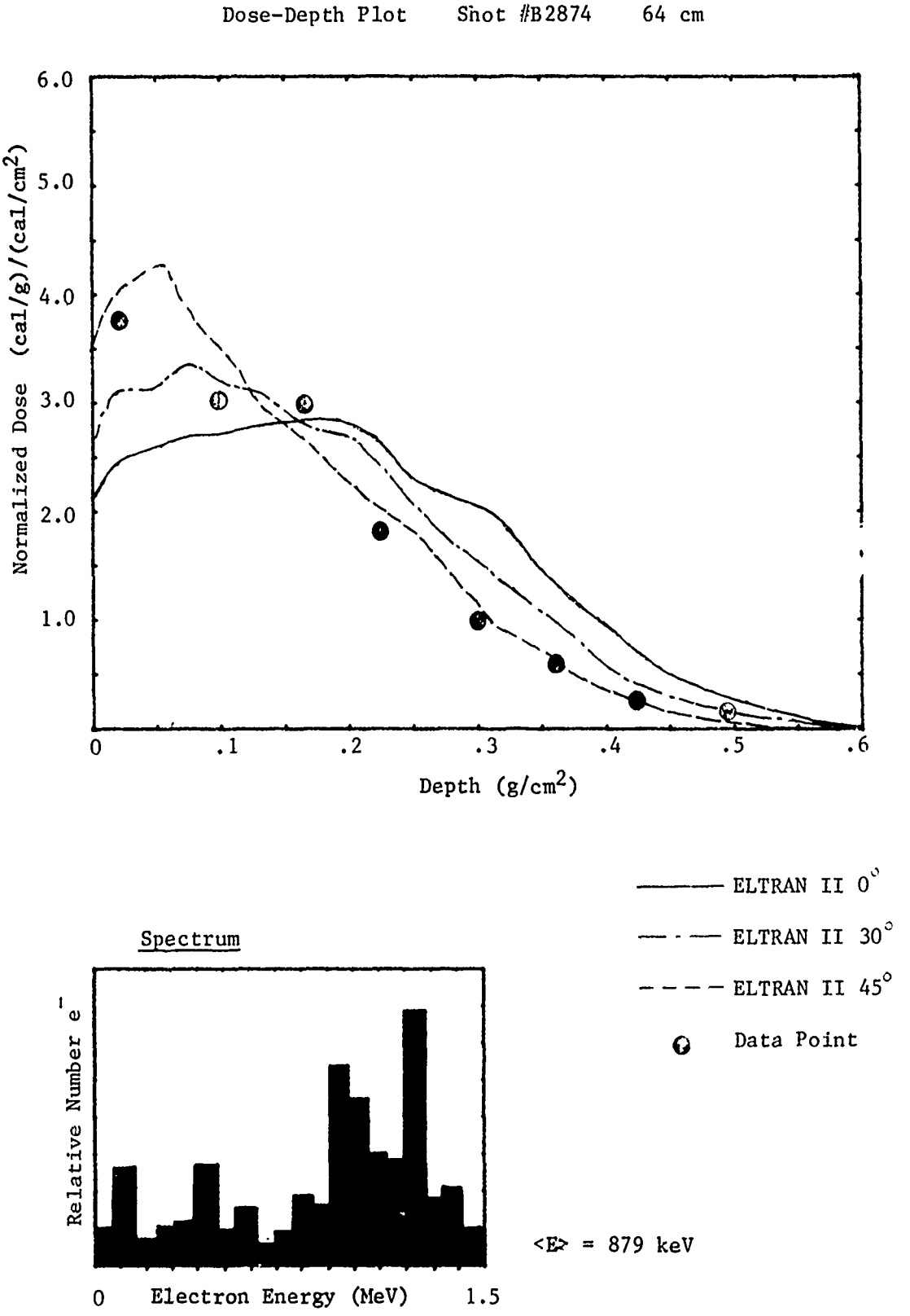

Figure 39. BJ3 dose-depth plot.

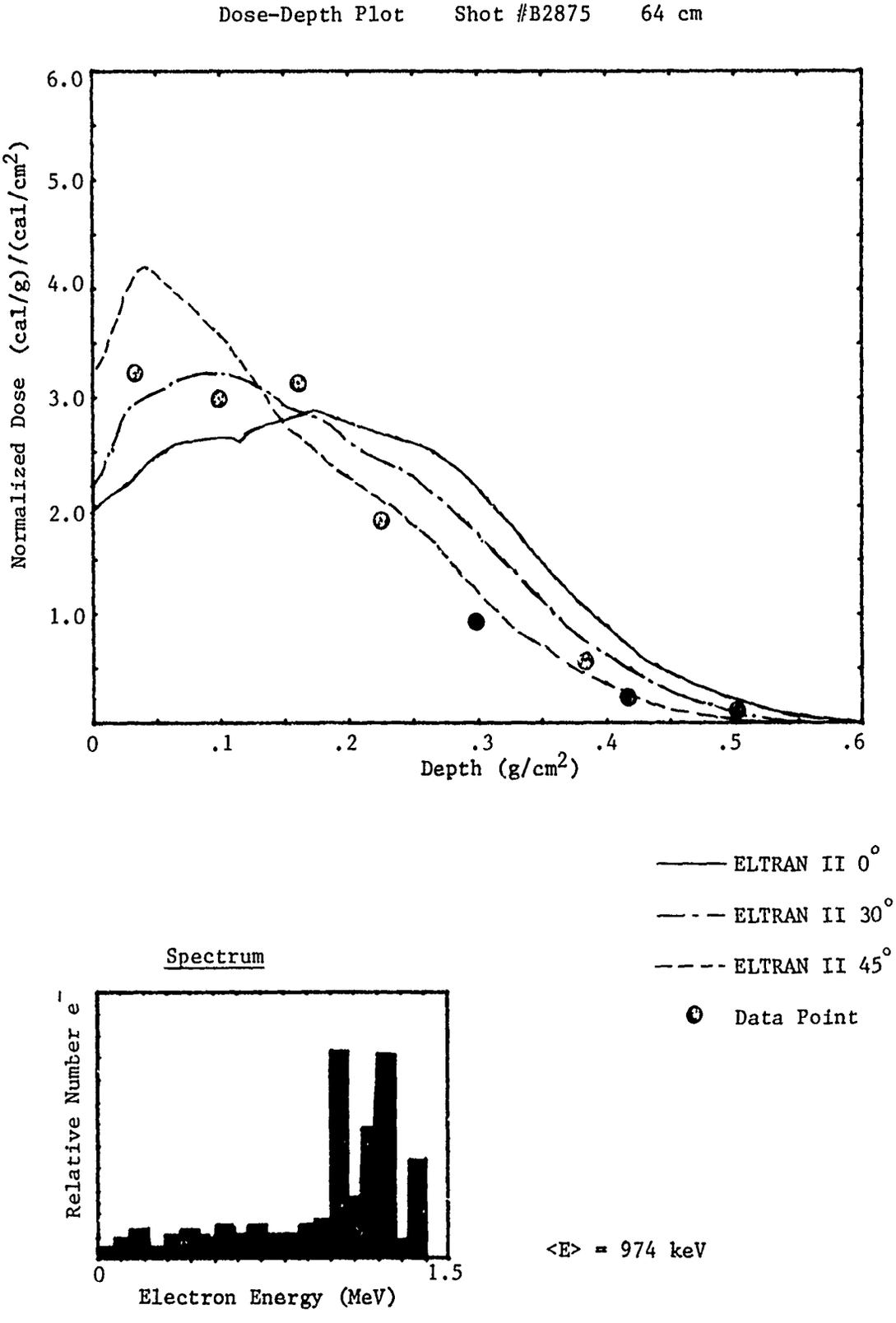

Figure 40. BJ3 dose-depth plot.

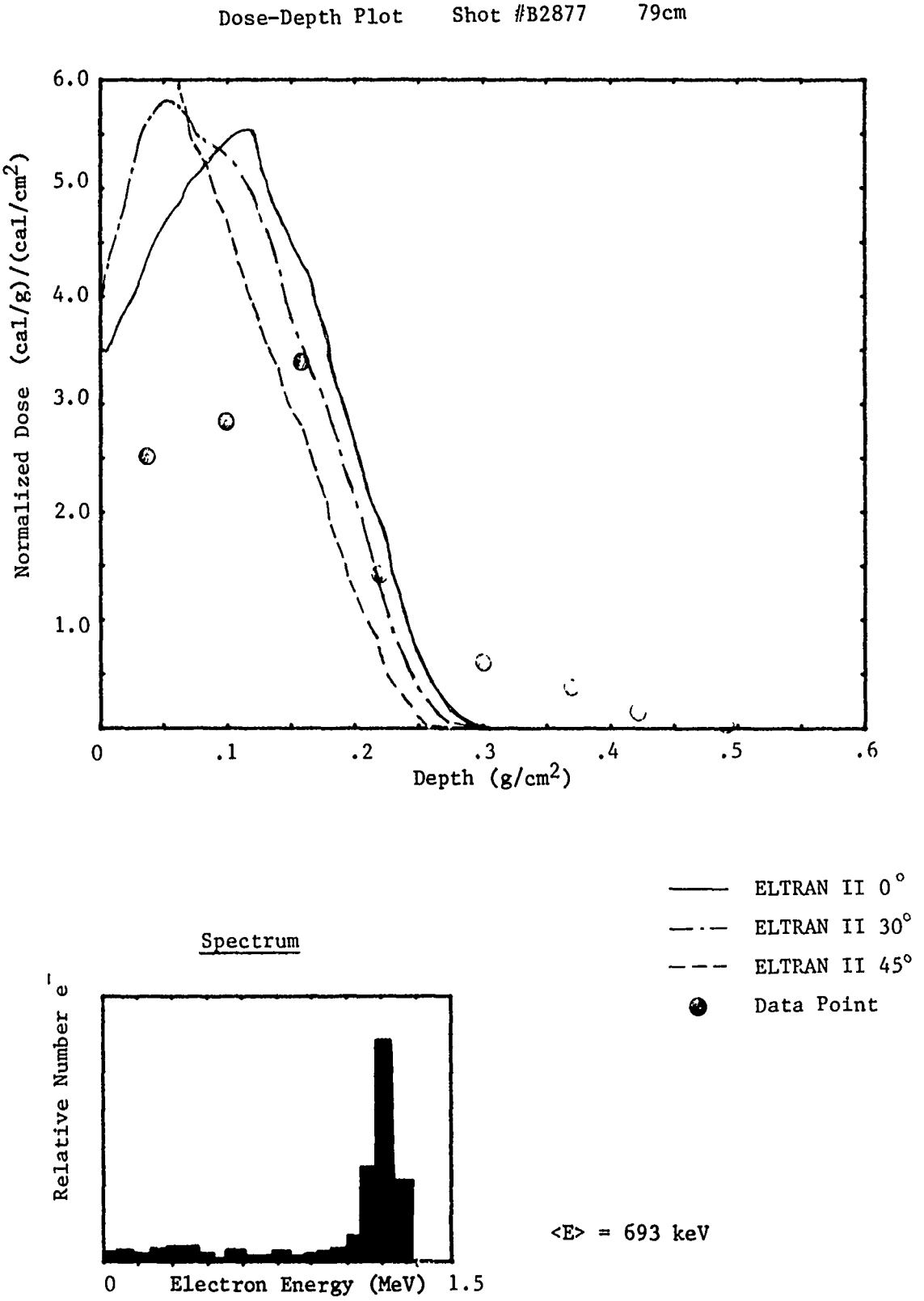

Figure 41. BJ3 dose-depth plot.

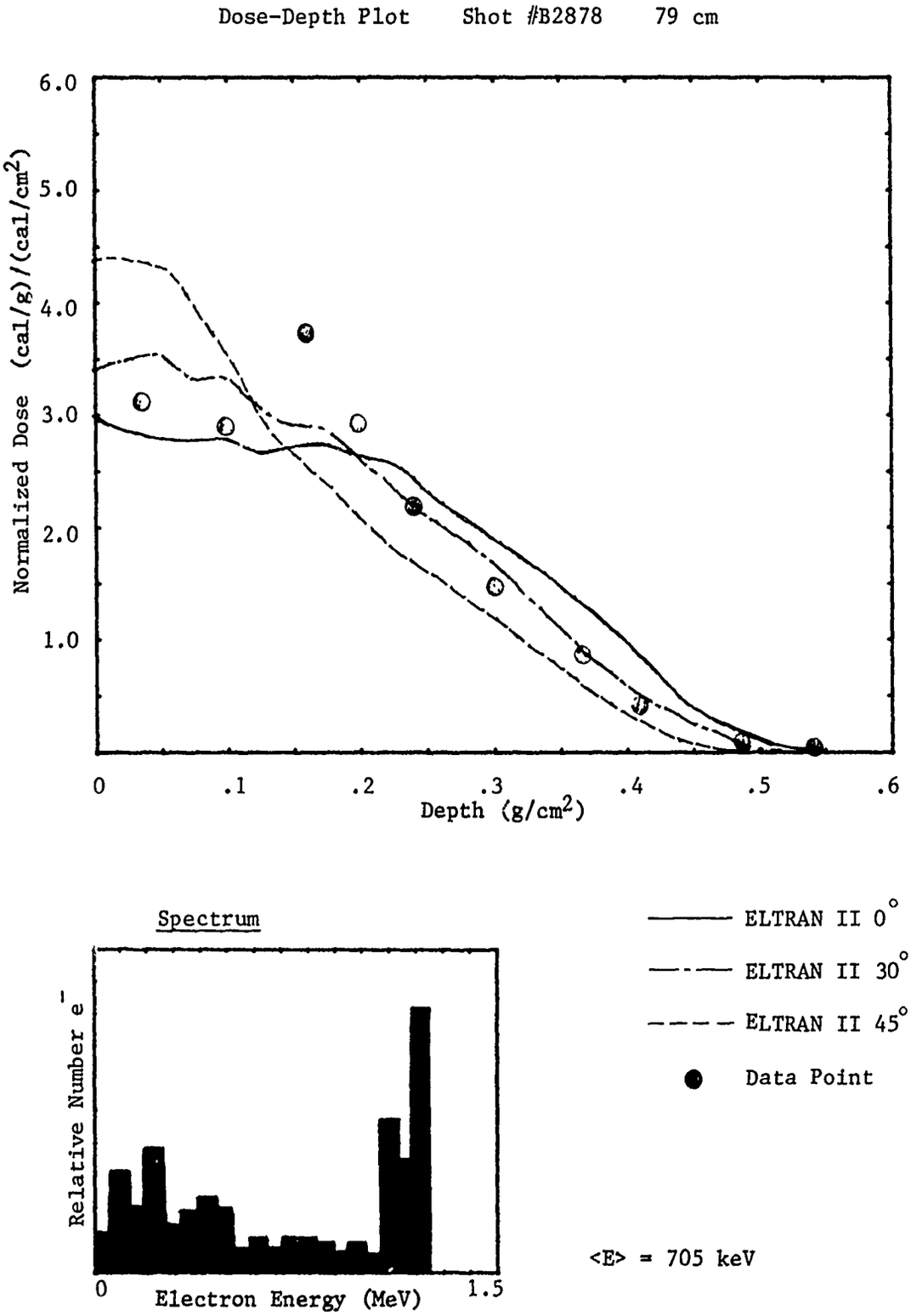

Figure 42. BJ3 dose-depth plot.

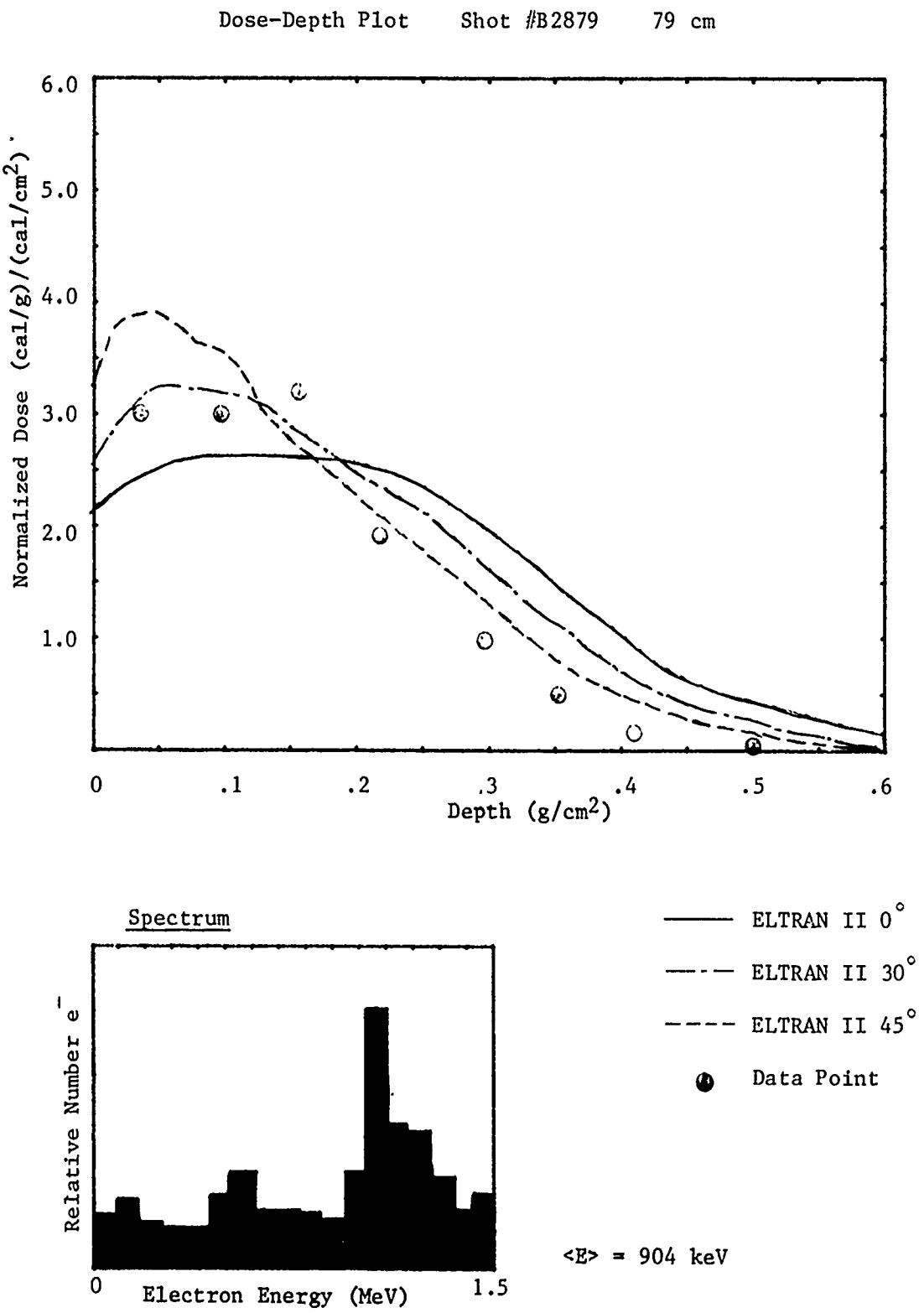

Figure 43. BJ3 dose-depth plot.

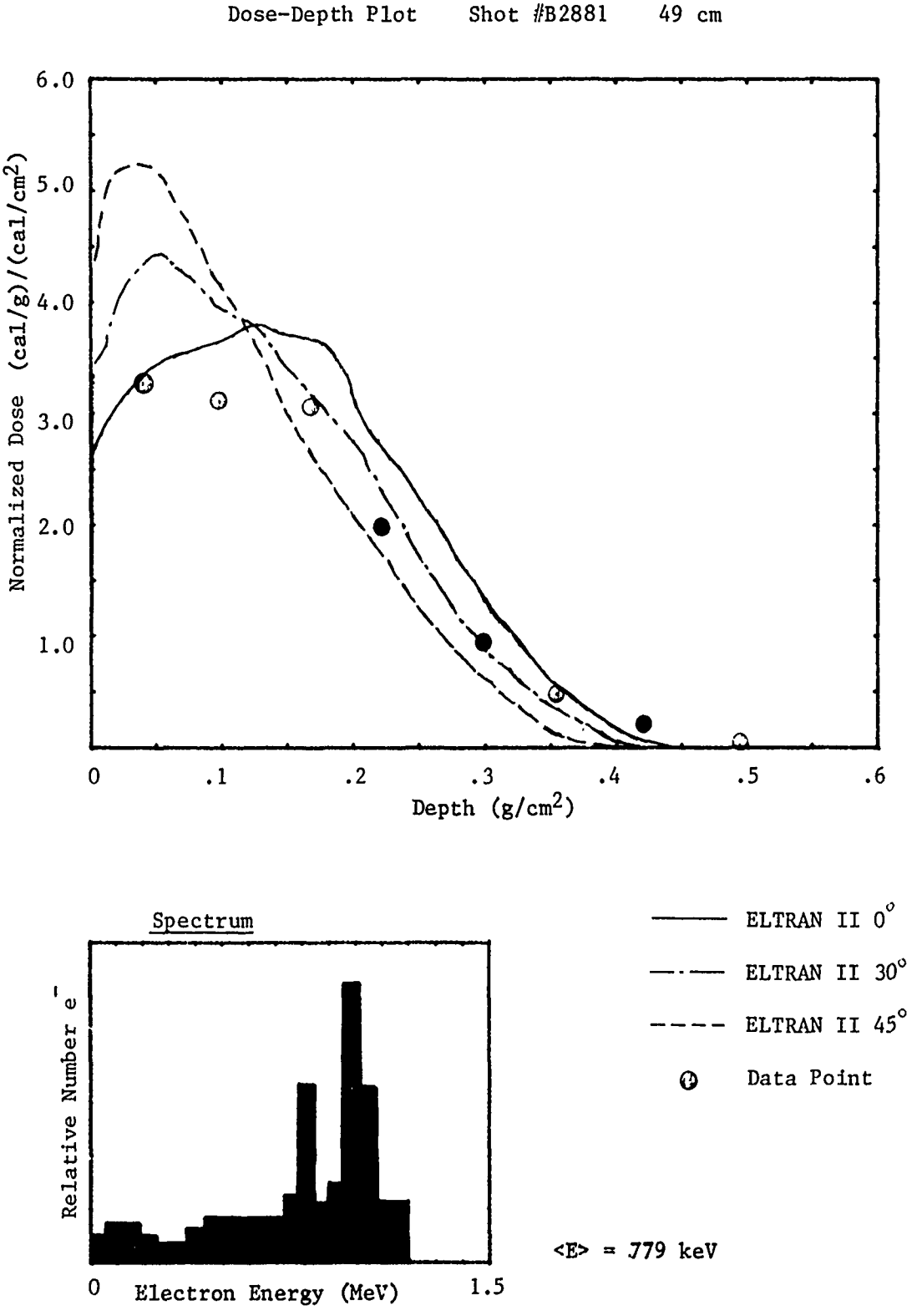

Figure 44. BJ3 dose-depth plot.

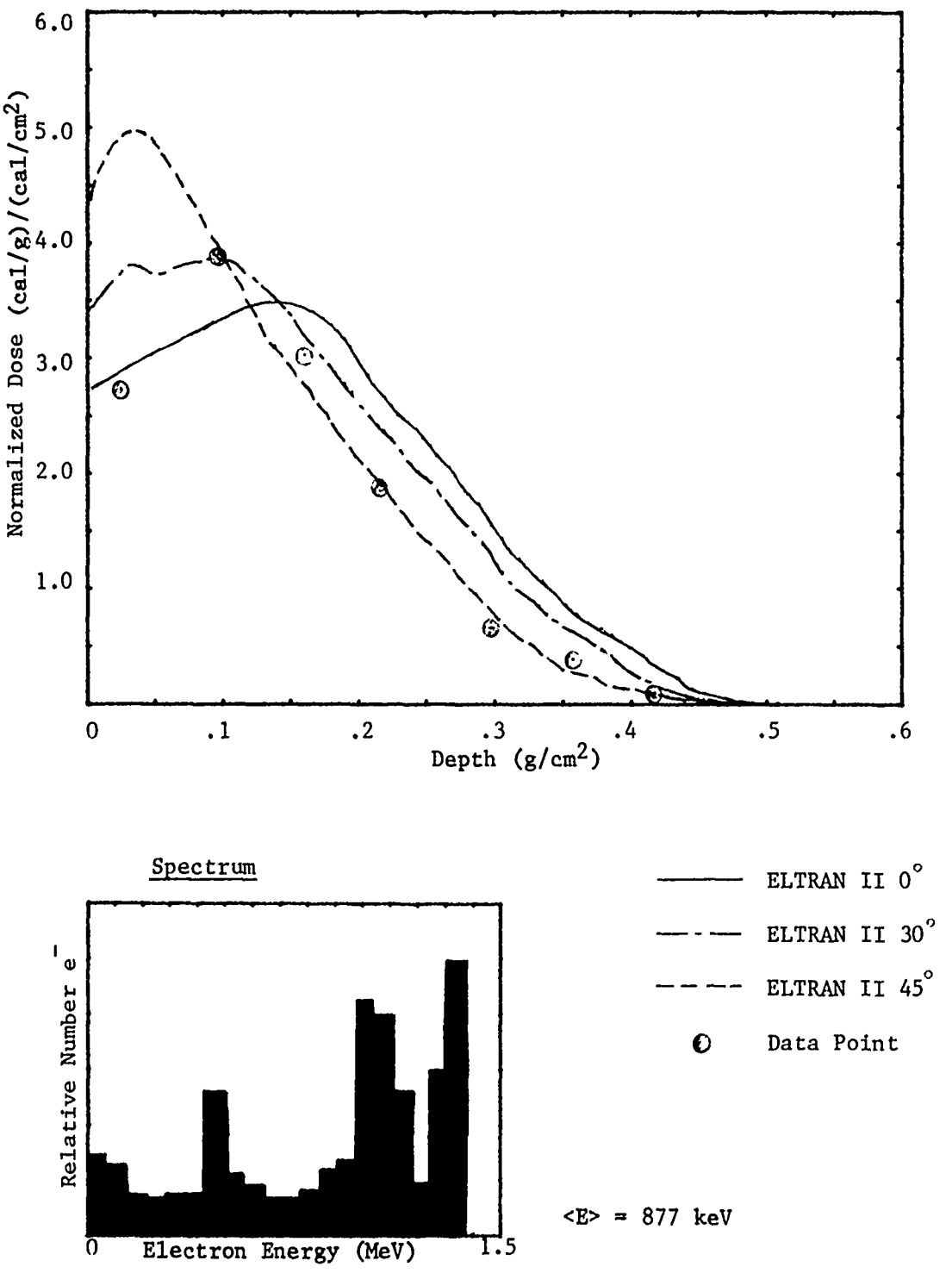

Figure 45. BJ3 dose-depth plot.

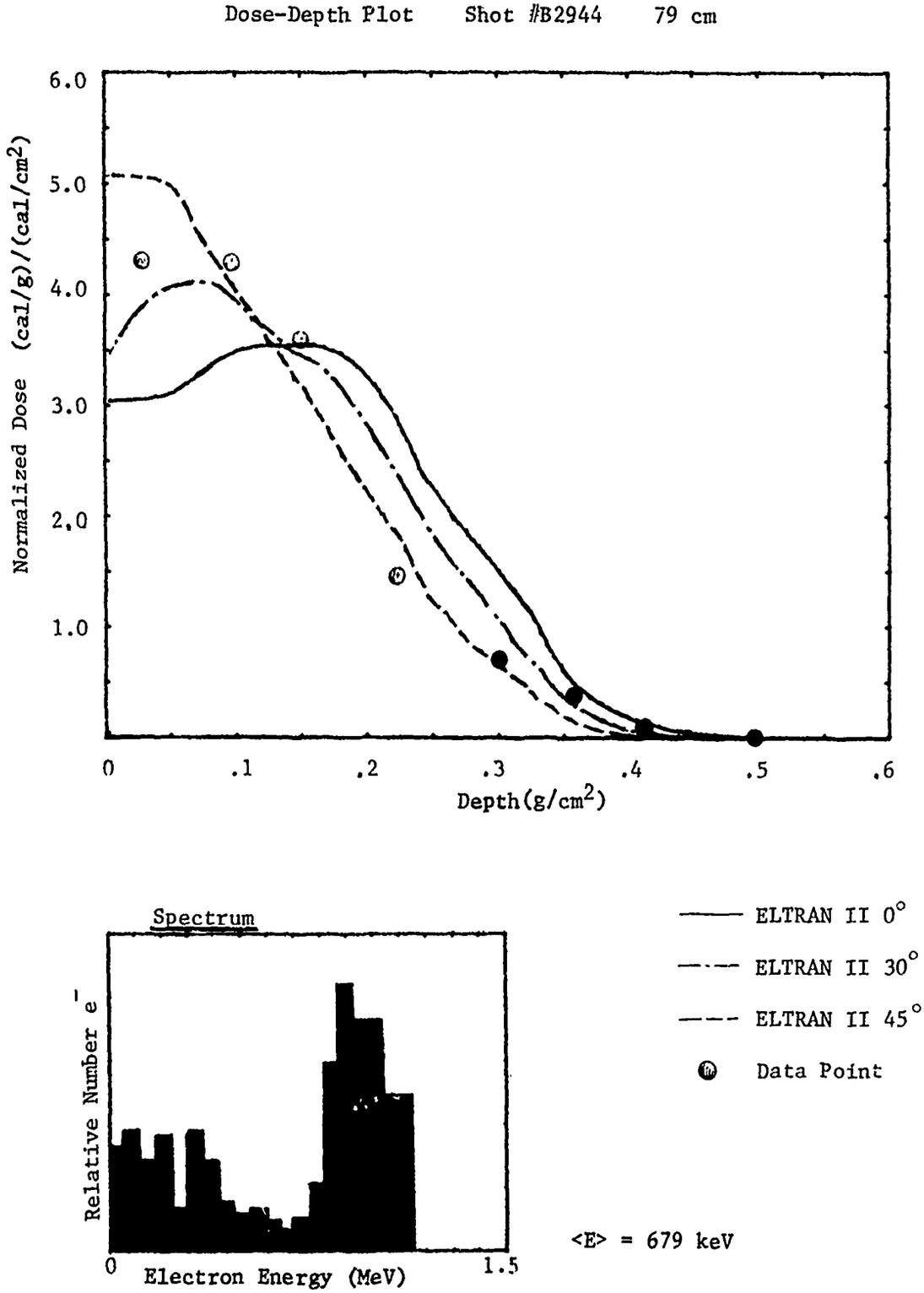

Figure 46. BJ3 dose-depth plot.

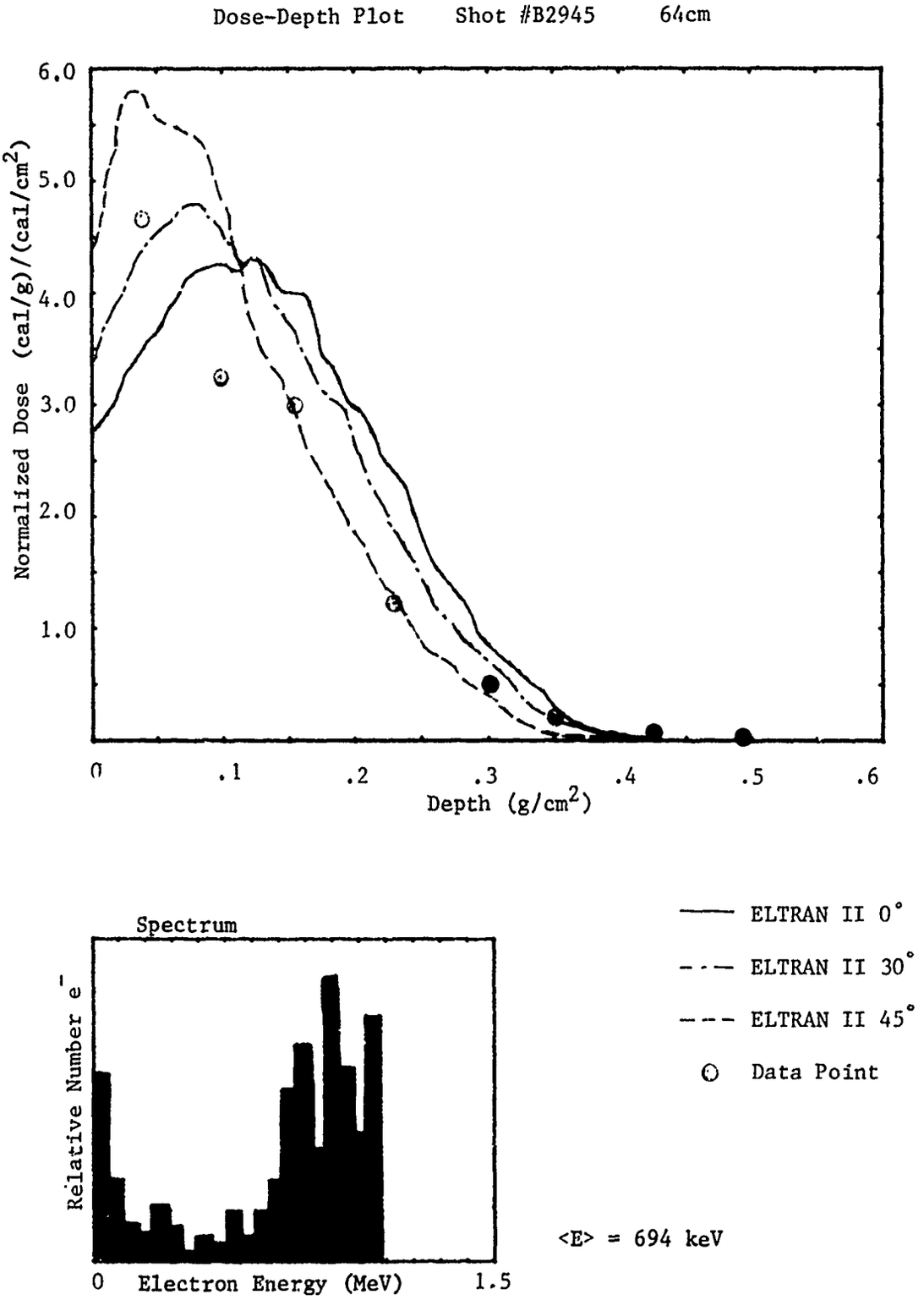

Figure 47. BJ3 dose-depth plot.

carbon cloth at maximum magnetic field position. Again, the more complex ELTRAN II computer program gives the better overall fit using a consistent angle of incidence into the dose-depth carbon cloth of 60 degrees. The best fit angle of incidence into the dose-depth stack is in the range of 30 to 45 degrees. There appears to be a cyclic trend in this best angle, going from 30 degrees at the highest (49-cm) and lowest (79-cm) to 45 degrees at the intermediate (64-cm) station.

The distinction between the "D-D ELTRAN" and "D-D measured" values in Figures 31 to 34 is that the latter represents the simple integrated fluence directly inferred from the foil stack, while the former represents the best fit of fluence to make ELTRAN match this experimental data. Scattered energy out of the carbon calorimeters is usually only a few percent.

The horizontal bars on the above figures indicate the histogram widths due to the finite sizes of the calorimeters.

The fluence quotes associated with each stress shot are based on the overall beam characteristics, but adjusted according to additional data such as calorimetry performed on the shot and the total beam energy of the shot. The error bars quoted are a reflection of the uncertainties in the radial profiles of any given shot. Thus, even though calorimetry data was obtained outboard of the sample, uncertainties in the radial profile reflect as uncertainties in the mean fluence existing across the sample.

4-3 MATERIAL STRESS MEASUREMENTS

Tables 4 and 5 summarize the overall material stress matrix, showing numbers of samples, sample type, instrumentation and rough fluence range. Tables 6 through 9 identify specific shots, giving instrumentation, geometry and inferred sample fluences.

Table 4. Experimental matrix.

Fluence Cals/cm^2	BJ3						BJ3 Prime					
	Al_k			Al_c			Al_k			Al_c		
	XQ	CG	LVI	XQ	CG	LVI	XQ	CG	LVI	XQ	CG	LVI
200		1	5		1	2						
115		1				1		1				
70			1			1						
25	1						1			2		
15	1			1	1		1			1		
0	1						1					
	Ta_k			Ta_c			Ta_k			Ta_c		
	XQ	CG	LVI	XQ	CG	LVI	XQ	CG	LVI	XQ	CG	LVI
200	3	1	1		1							
115			1		1							
70	1											
25	1						1			1		
15	1			1			1			1		
0												

Code: XQ = quartz, CG = carbon gauge,
LVI = laser velocity interferometer,
K = Ktech material,
C = Commonality material.

Table 5. Overall summary of experiments.

BJ3

Total dose-depth measurements = 12

Total spatial measurements = 52

Total sample measurements 11 Al_k, 7 Al_c, 9 Ta_k, 3 Ta_c

BJ3 Prime

Total dose-depth measurements = 6

Total spatial measurements = 50

Total sample measurements 4 Al_k, 3 Al_c, 2 Ta_k, 2 Ta_c

Combined

Total dose-depth measurements = 18

Total spatial measurements =102

Total sample measurements 14 Al_k, 10 Al_c, 11 Ta_k, 5 Ta_c

Code: Al_k = Ktech aluminum, etc.

Al_c = Commonality aluminum, etc.

GEOMETRICAL OPTIONS

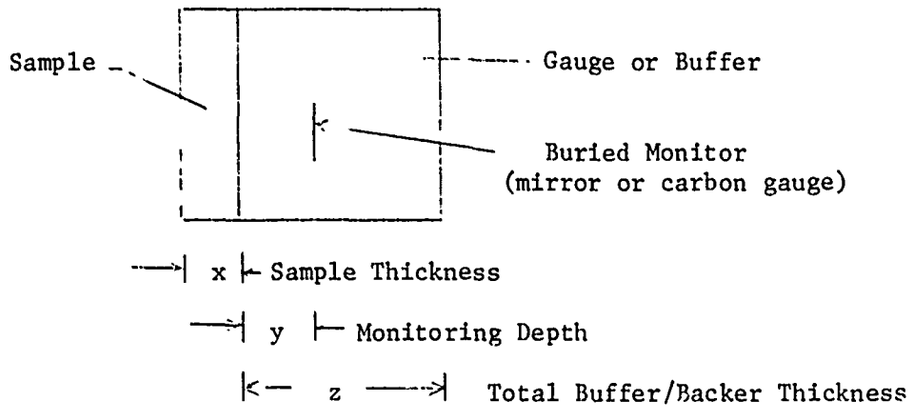

Table 6. Commonality aluminum: instrumentation, geometry, fluence.

Shot No.	Instrumentation	Material Dimensions x (cm)	y (cm)	z (cm)	Fluence (cal/cm^2)
P2785	X-cut Quartz	0.250	0.0	0.636	19 ± 3
P2801*	X-cut Quartz	0.257	0.0	0.636	55 ± 10
P2802	X-cut Quartz	0.255	0.0	0.637	55 ± 10
B2820*	X-cut Quartz	0.256	0.0	0.637	15 ± 10
B2937	Carbon Gauge in PMMA	0.249	0.3175	0.953	15 ± 10
B2940	Carbon Gauge in PMMA	0.250	0.3175	0.953	160 ± 25
B2894	LVI in SiO_2	0.256	0.635	1.902	120 ± 20
B2907	LVI in SiO_2	0.249	0.635	1.902	90 ± 30
B2919	LVI in SiO_2	0.253	0.635	1.902	150 ± 30
B2920	LVI in SiO_2	0.254	0.635	1.902	150 ± 20

* See Appendix B for stress record.

GEOMETRICAL OPTIONS

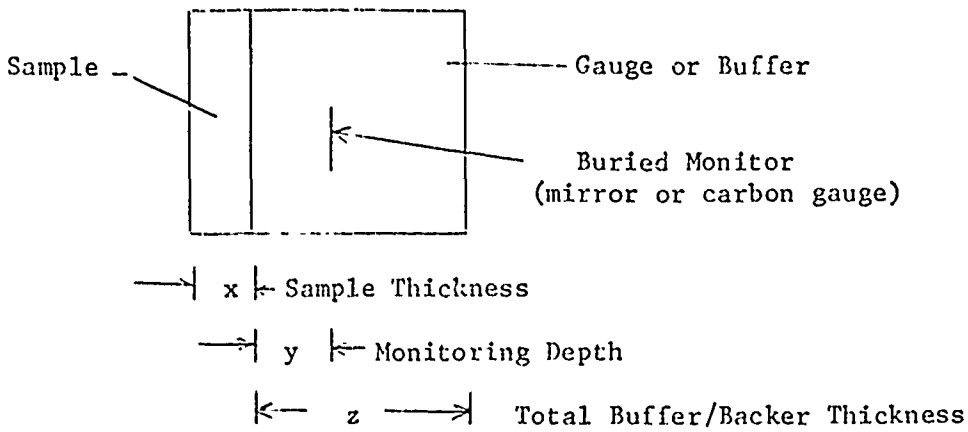

Table 7. Ktech aluminum: instrumentation, geometry, fluence.

Shot No.	Instrumentation	Material Dimensions x (cm)	y (cm)	z (cm)	Fluence (cal/cm^2)
P2715	X-cut Quartz	0.280	0.0	0.507	18 ± 4
B2729	X-cut Quartz	0.280	0.0	0.509	15 ± 3
B2738	X-cut Quartz	0.280	0.0	0.507	40 ± 5
P2779	X-cut Quartz	0.280	0.0	0.636	8 ± 3
P2782	X-cut Quartz	0.278	0.0	0.637	25 ± 5
B2922*	X-cut Quartz	0.281	0.0	0.509	13 ± 5
P2814	Carbon Gauge in PMMA	0.281	0.3175	0.953	120 ± 40
B2906	Carbon Gauge in PMMA	0.258	0.3175	0.953	112 ± 20
B2936	Carbon Gauge in PMMA	0.281	0.3175	0.953	155 ± 30
B2889	LVI in SiO_2	0.280	0.635	1.905	155 ± 30
B2890	LVI in SiO_2	0.280	0.635	1.905	170 ± 30
B2897	LVI free surface	0.280	0.0	0.0	150 ± 20
B2898	LVI free surface	0.280	0.0	0.0	170 ± 30
B2904	LVI free surface	0.279	0.0	0.0	145 ± 40
B2905	LVI in PMMA	0.274	0.0	1.27	100 ± 20

* See Appendix B for stress record.

71

GEOMETRICAL OPTIONS

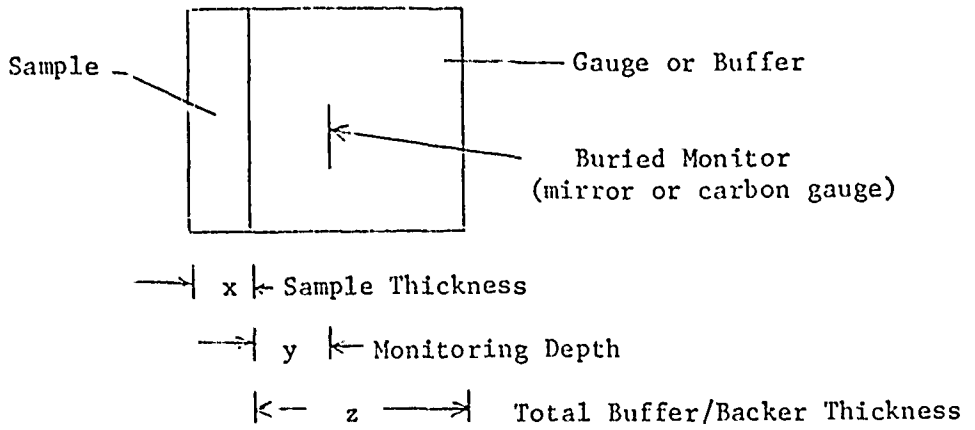

Table 8. Commonality tantalum: instrumentation, geometry, fluence.

Shot No.	Instrumentation	Material Dimensions x (cm)	y (cm)	z (cm)	Fluence (cal/cm^2)
P2788	X-cut Quartz	0.074	0.0	0.512	18 ± 5
P2809	X-cut Quartz	0.076	0.0	0.509	50 ± 15
P2896	X-cut Quartz	0.080	0.0	0.635	20 ± 10
B2908	Carbon Gauge in PMMA	0.080	0.3175	0.953	115 ± 25
B2943	Carbon Gauge in PMMA	0.079	0.3175	0.953	160 ± 30

GEOMETRICAL OPTIONS

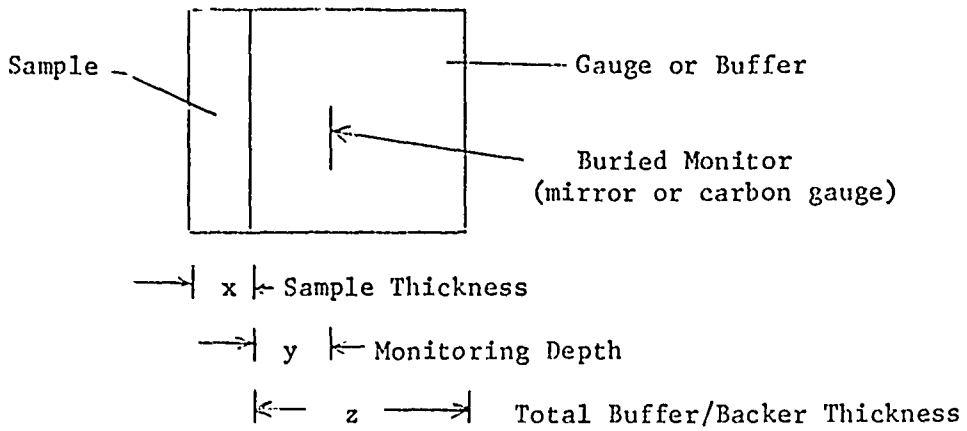

Table 9. Ktech tantalum: instrumentation, geometry, fluence.

Shot No.	Instrumentation	Material Dimensions x (cm)	y (cm)	z (cm)	Fluence (cal/cm^2)
P2716	X-cut Quartz	0.310	0.0	0.507	14 ± 10
B2732	X-cut Quartz	0.127	0.0	0.509	21 ± 4
P2803	X-cut Quartz	0.132	0.0	0.253	40 ± 15
B2824	X-cut Quartz	0.132	0.0	0.256	30 ± 10
B2885*	X-cut Quartz	0.130	0.0	0.256	130 ± 20
B2888	X-cut Quartz	0.130	0.0	0.256	150 ± 30
B2935	X-cut Quartz	0.131	0.0	0.256	60 ± 20
B2938	X-cut Quartz	0.130	0.0	0.256	135 ± 30
B2939	Carbon Gauge in PMMA	0.131	0.3175	0.952	170 ± 30
B2893	LVI in SiO_2	0.133	0.635	1.905	115 ± 30
B2895	LVI in SiO_2	0.130	0.635	1.905	170 ± 30

* See Appendix B for stress record.

The stress data are given in the form of quartz gauge stress, carbon gauge stress, or material velocity (for the LVI). Figures 48 through 55 show the Al_c* records, Figures 56 through 69 show the Al_k* records, while Figures 70 through 74 show the Ta_c* records and Figures 75 through 84 show the Ta_k* records. The X-cut quartz gauge records have been unfolded from voltage to stress using standard calibration data (ref. 7). The carbon gauge records have been unfolded from known calibration data for these gauges (ref. 8). The LVI records of velocity were unfolded using standard fringe counting techniques together with the knowledge of the delay leg length.

Tables 10 and 11 give the supporting machine parameters for these shots. Full details of the energy spectra (bin data) are given in Appendix A for all the sample stress shots.

Except for the LVI measurements of sample free rear surface velocity, none of the records directly measured conditions within the samples. Thus, the quartz gauge records need further unfolding to account for the hydrodynamic impedance mismatch between sample and gauge. Since the gauge monitors the interface stress, however, no attenuation need be accounted for, except that inherent within the sample itself.

For the carbon gauges the observed stress was that in the host matrix of PMMA. The small impedance mismatch between the very thin carbon gauge (and package of Kapton) and the PMMA allows the gauge to register the PMMA stress value within less than 20 ns. This is short compared with the observed stress rise times, allowing good resolution of the entire stress pulse shape. The PMMA has a low acoustic impedance and so gives a significant stress reduction at the sample/PMMA interface (see Appendix C), and results in multiple reverberations of the initial stress pulse within the sample. This can lead to additional tensile spalling within the sample on top of the vapor or melt loss that occurs

* C = Commonality material; K = Ktech-supplied material.

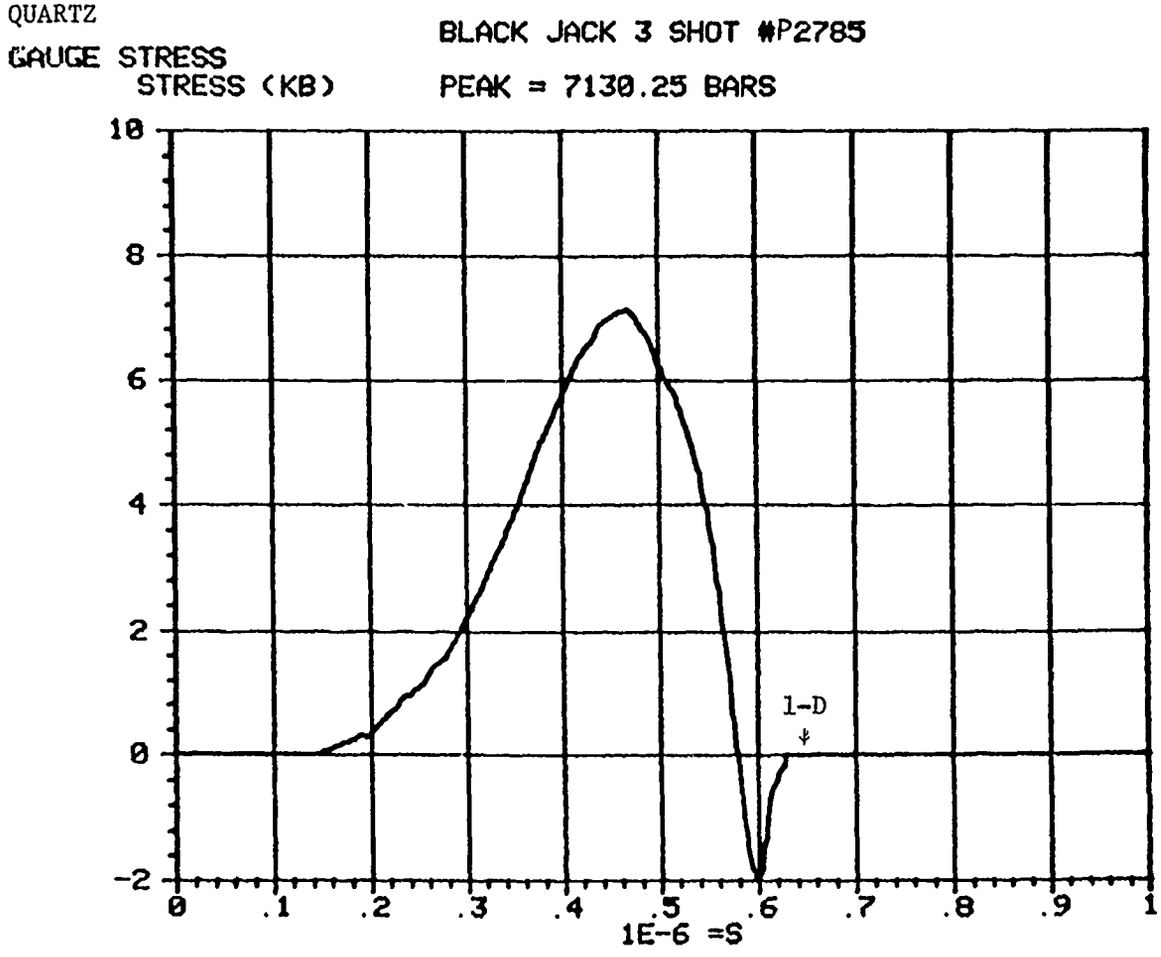

1-D ↓ Indicates limit of one-dimensionality (very conservative)

G ↓ Indicates limit of quartz gauge single-transit read time

Figure 48. Commonality aluminum quartz gauge record.

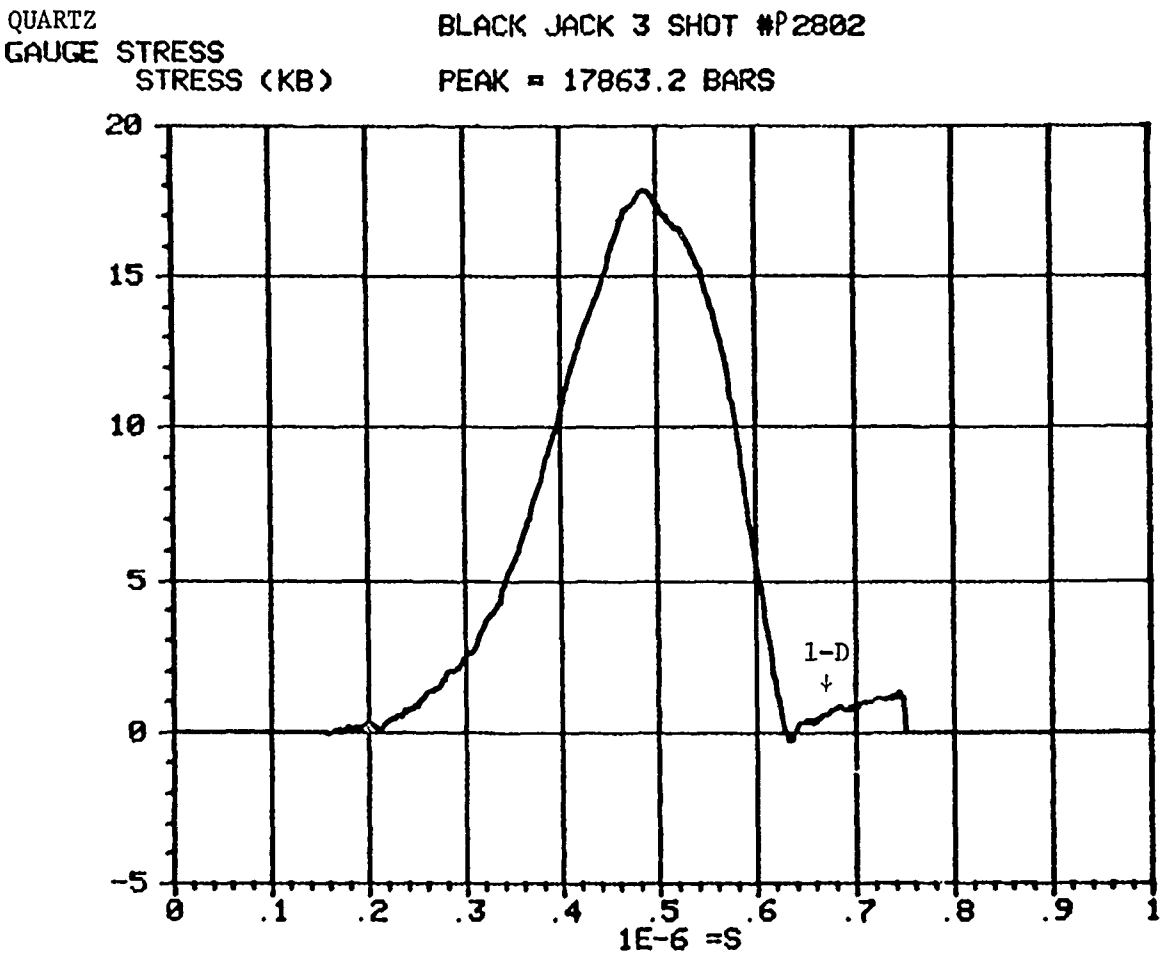

Figure 49. Commonality aluminum quartz gauge record.

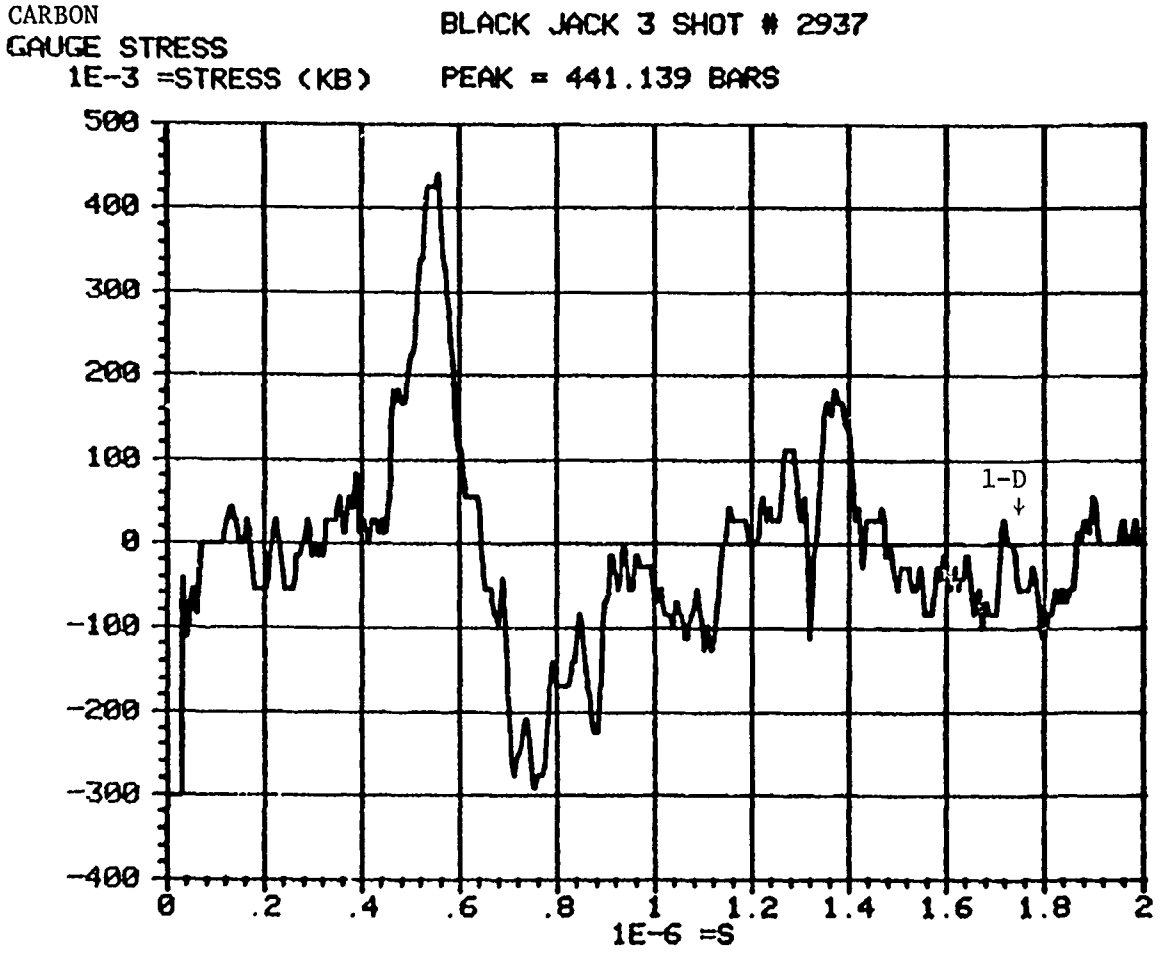

Figure 50. Commonality aluminum carbon gauge record.

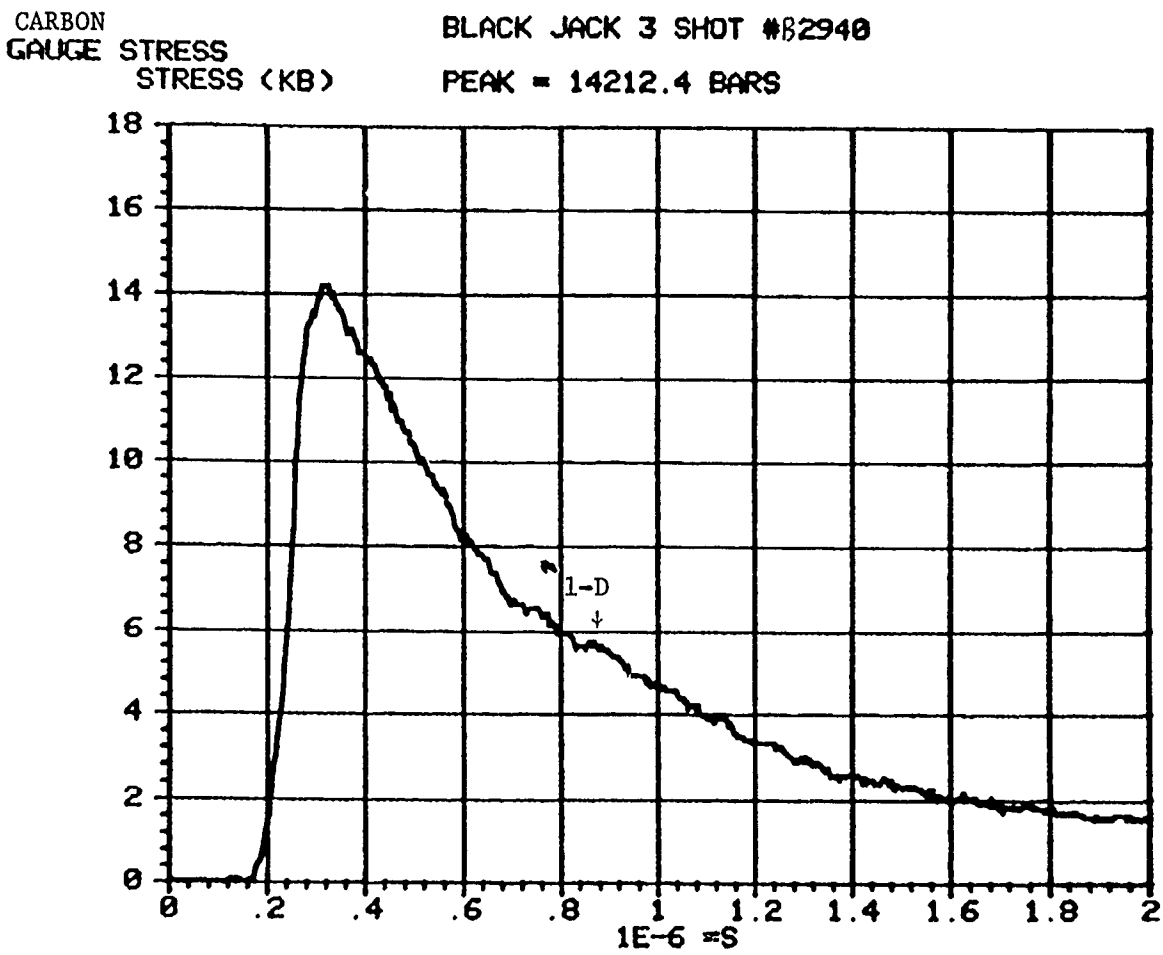

Figure 51. Commonality aluminum carbon gauge record.

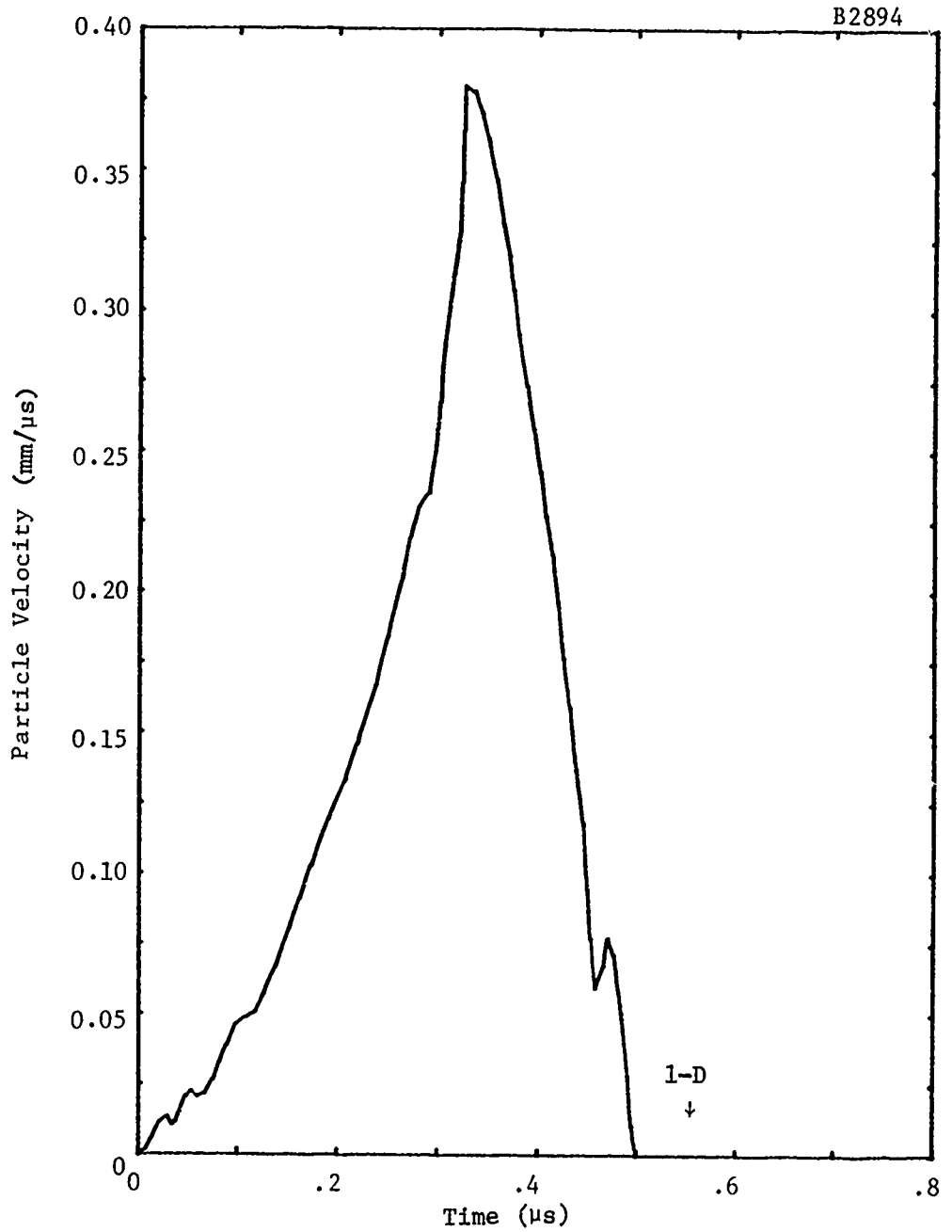

Figure 52. Commonality aluminum LVI record.

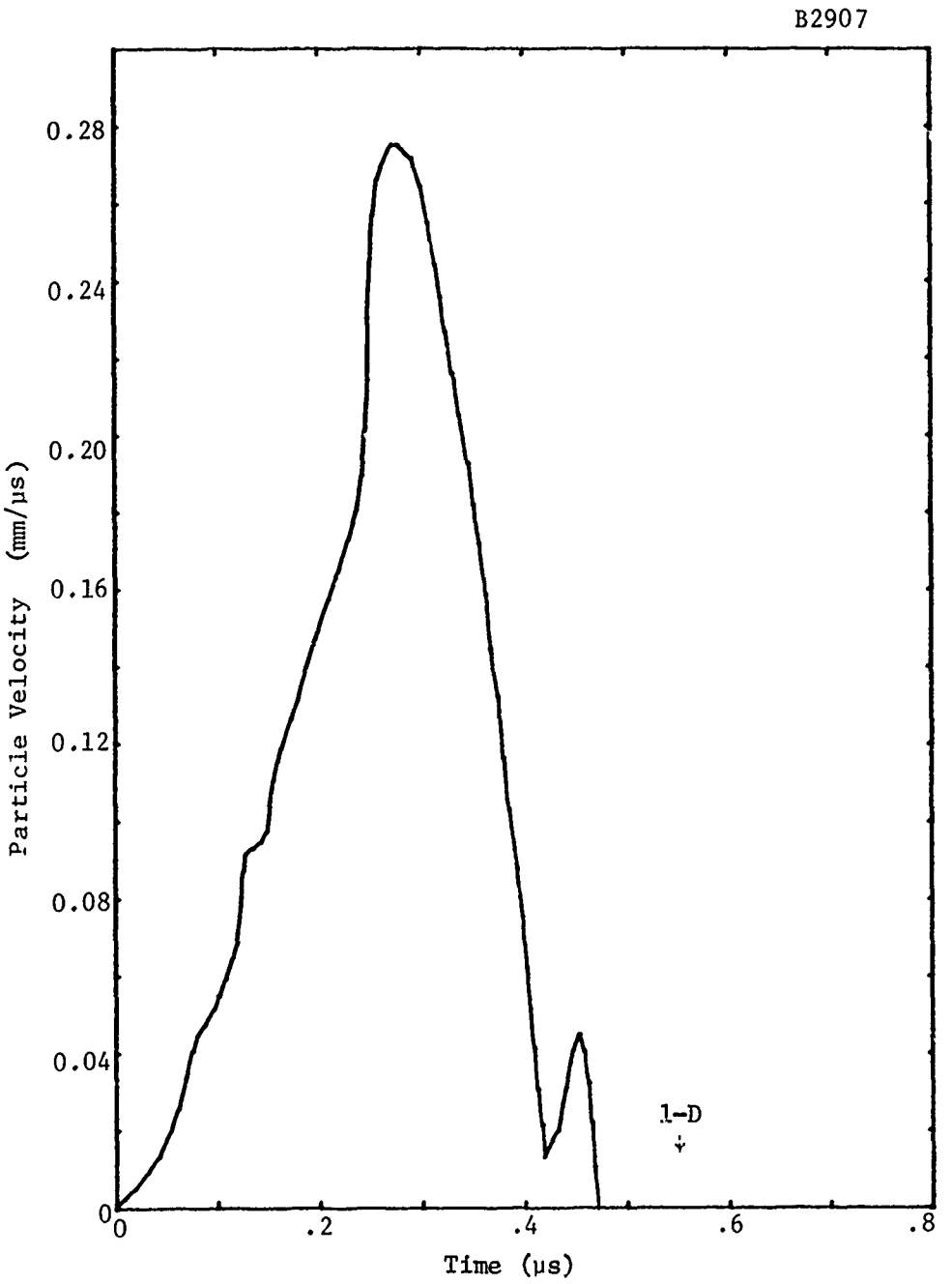

Figure 53. Commonality aluminum LVI record.

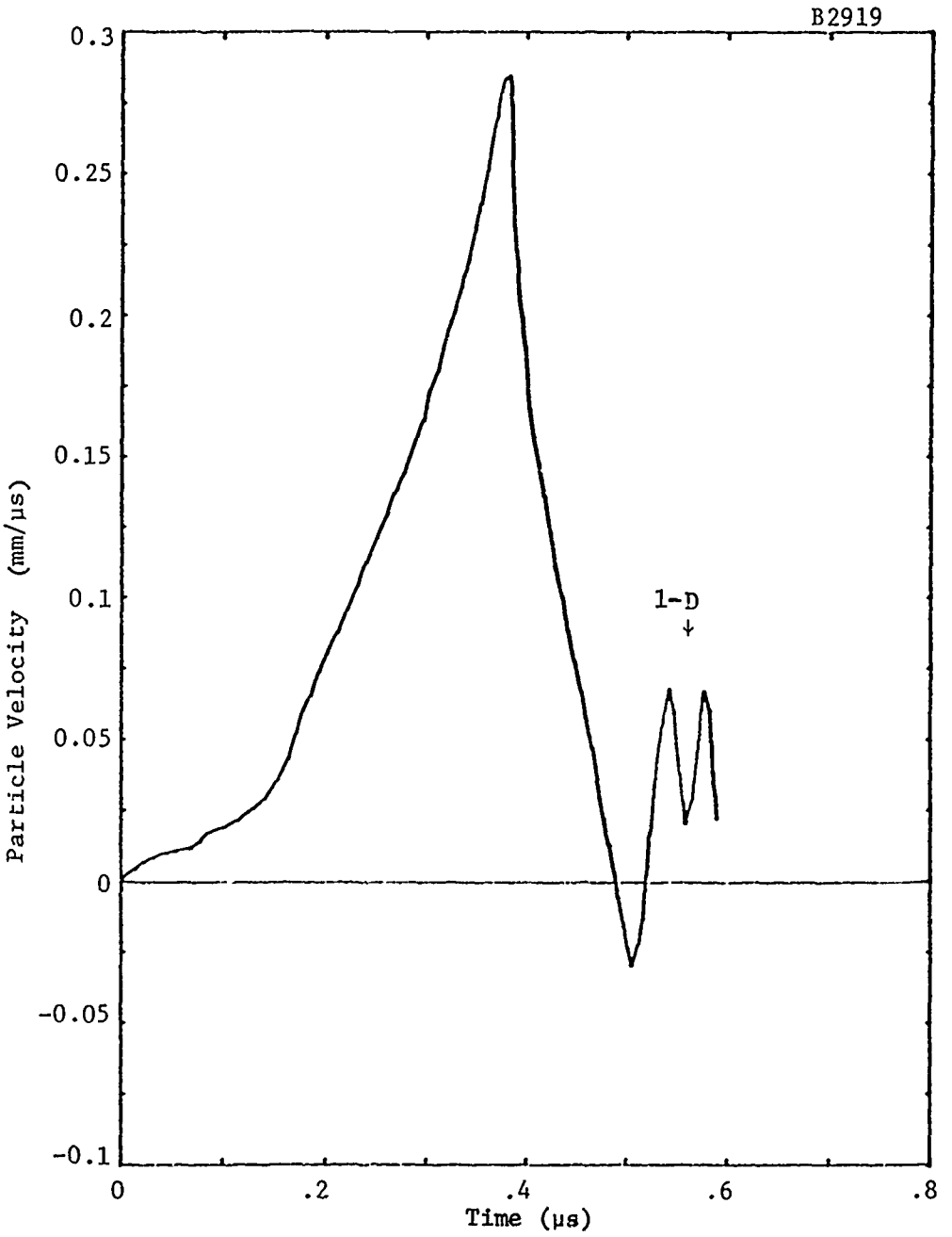

Figure 54. Commonality aluminum LVI record.

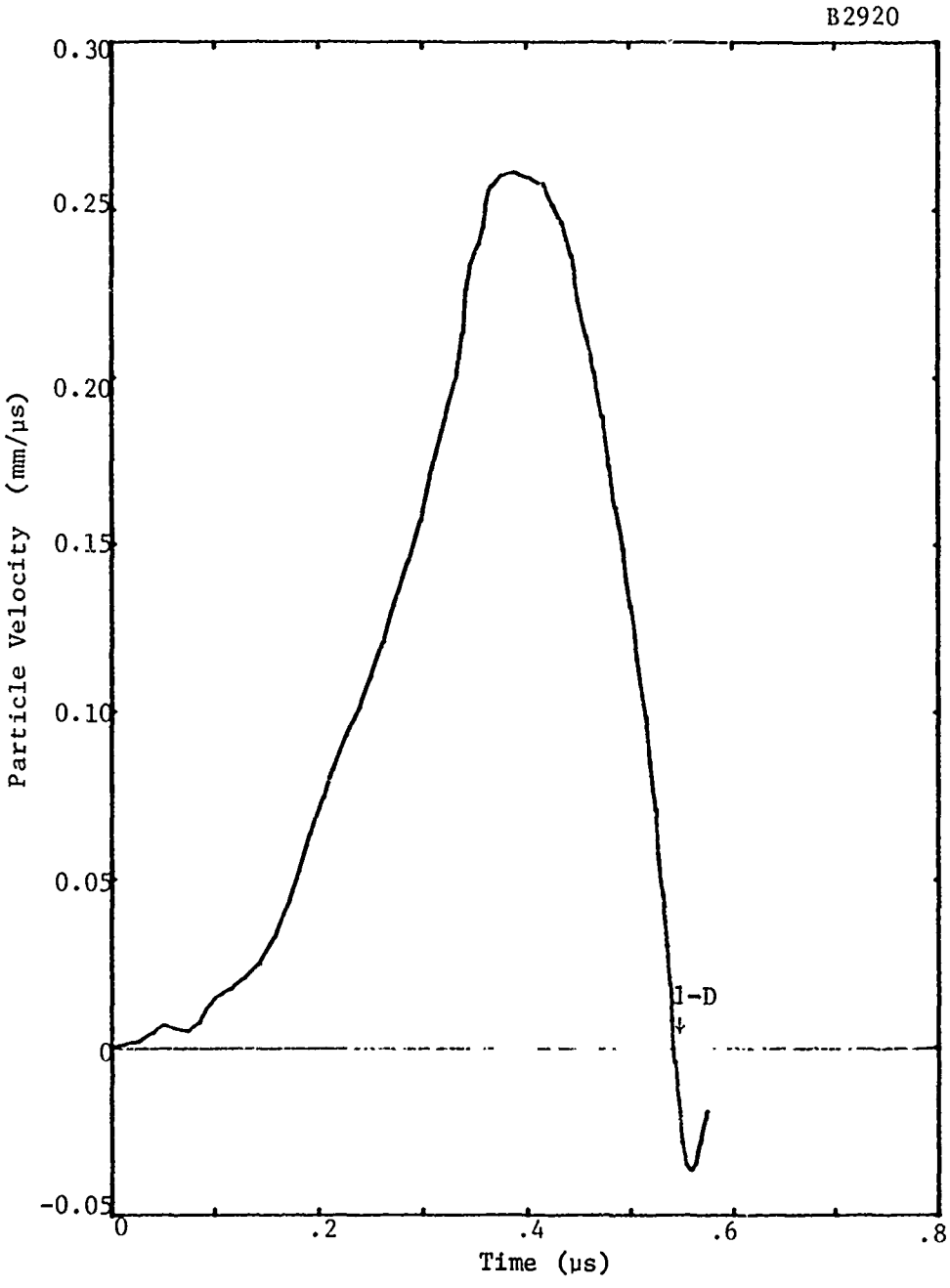

Figure 55. Commonality aluminum LVI record.

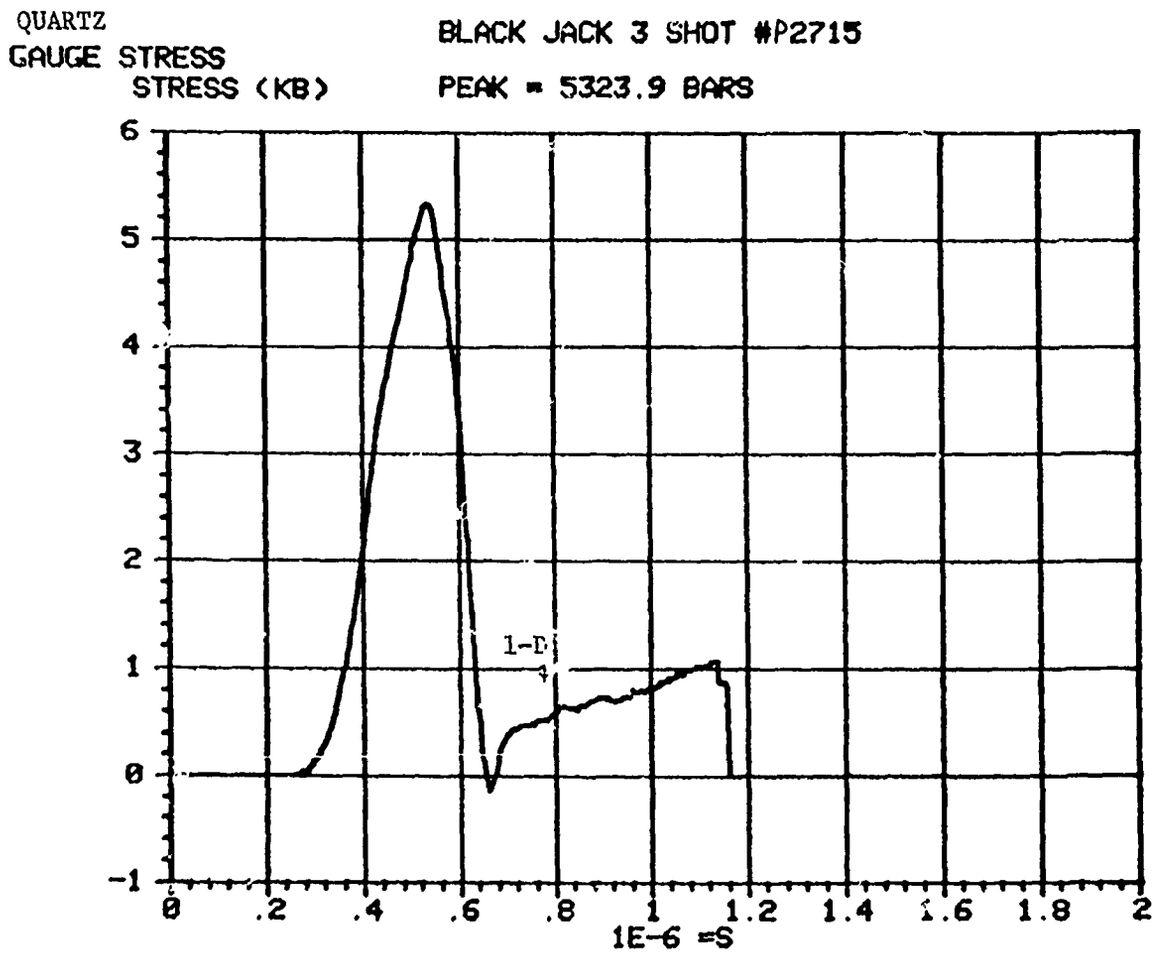

Figure 56. Ktech aluminum quartz gauge record.

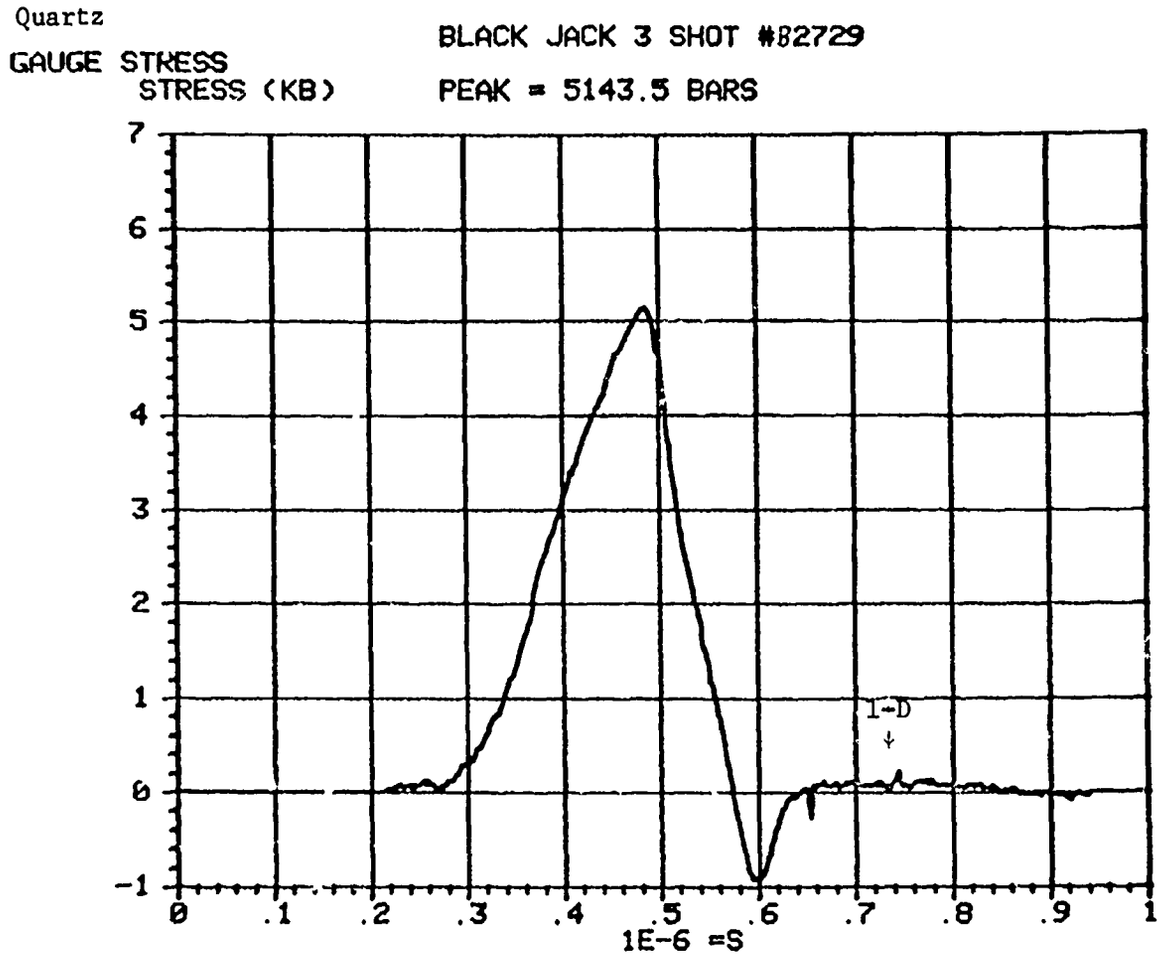

Figure 57. Ktech aluminum quartz gauge record.

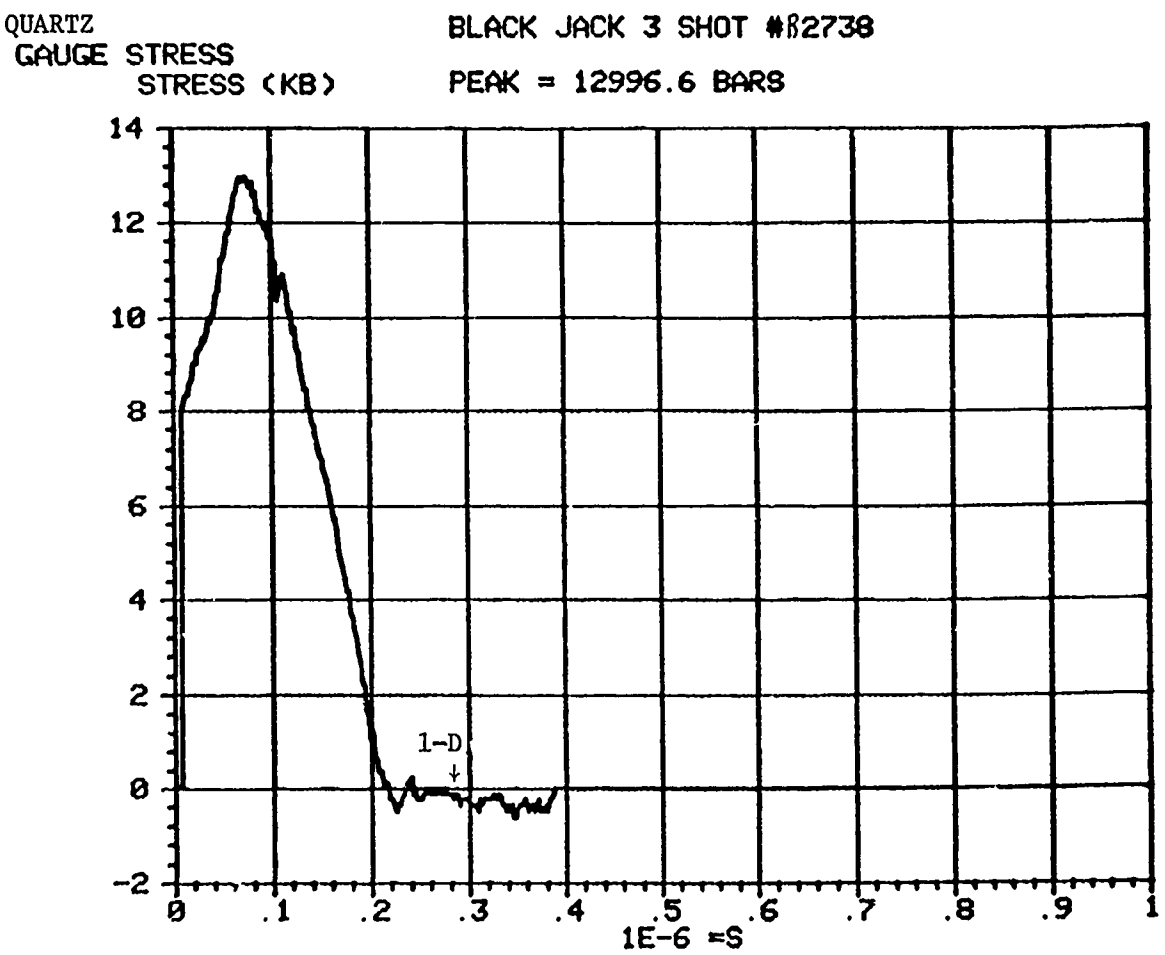

Figure 58. Ktech aluminum quartz gauge record.

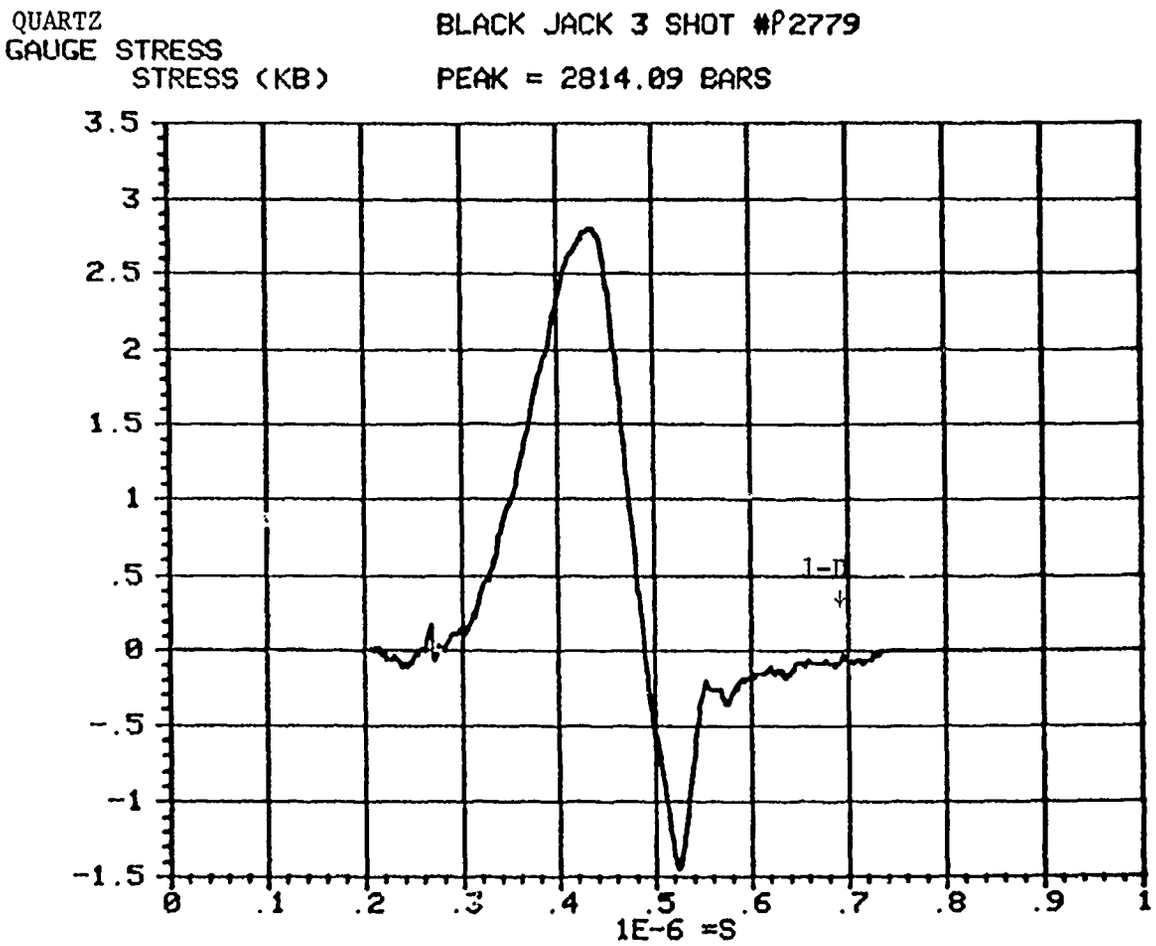

Figure 59. Ktech aluminum quartz gauge record.

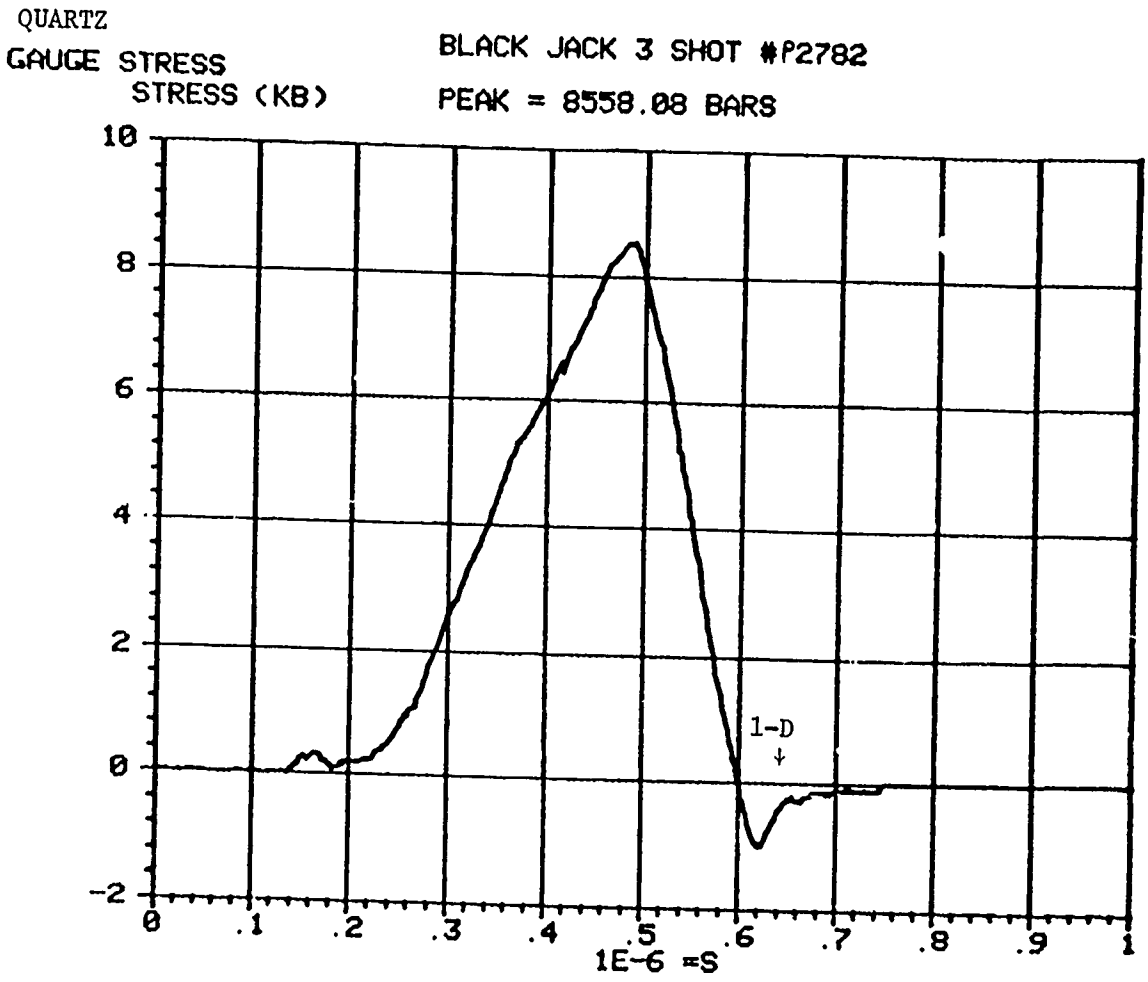

Figure 60. Ktech aluminum quartz gauge record.

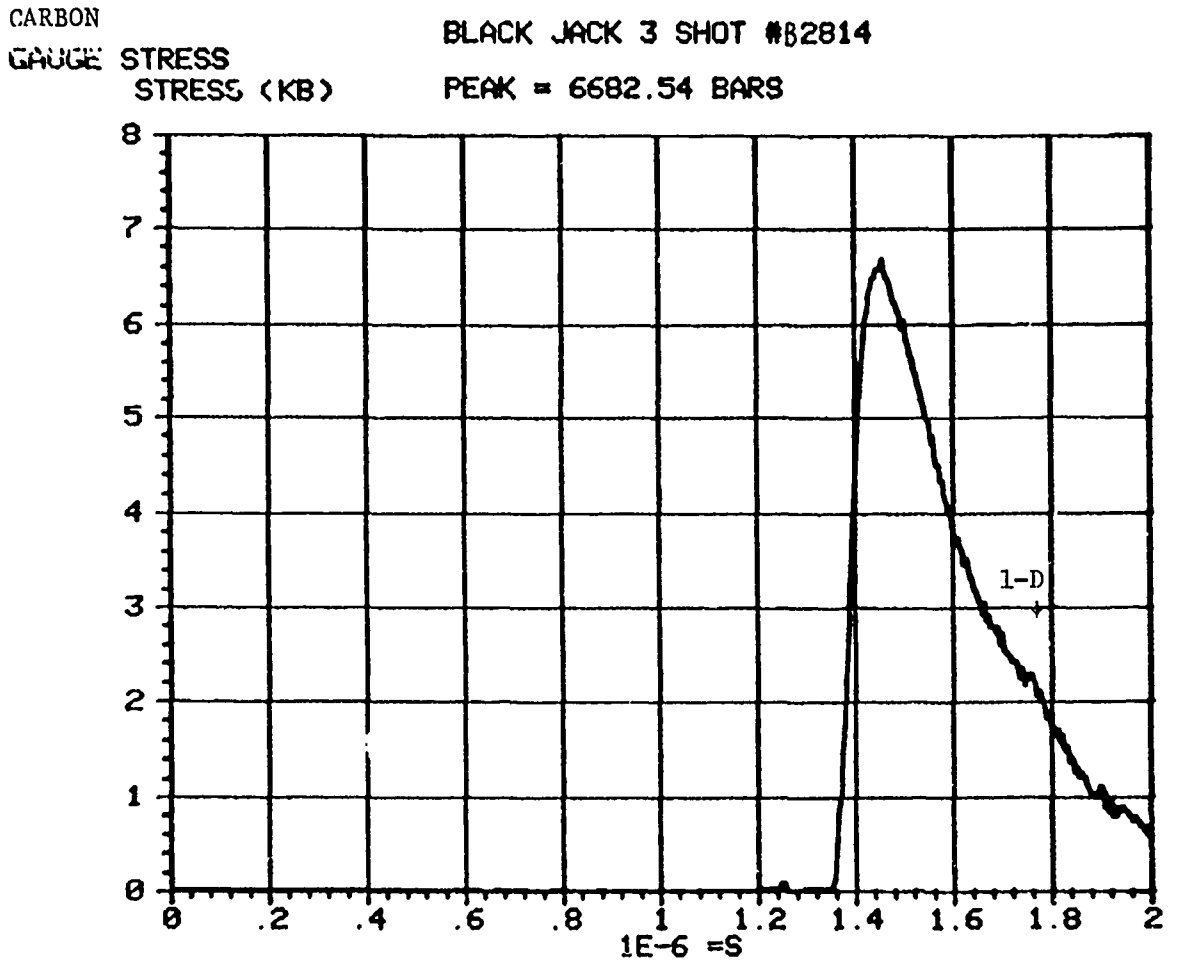

Figure 61. Ktech aluminum carbon gauge record.

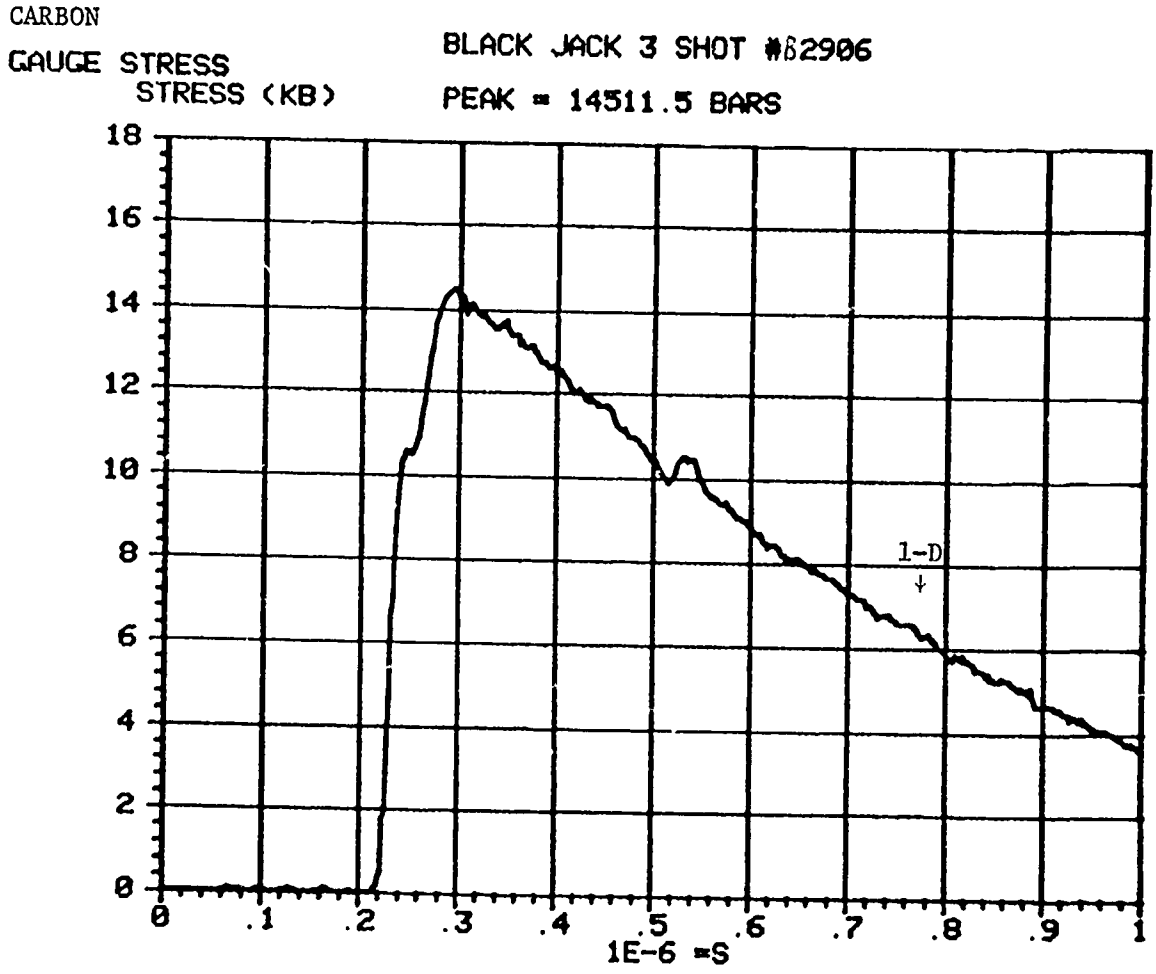

Figure 62. Ktech aluminum carbon gauge record.

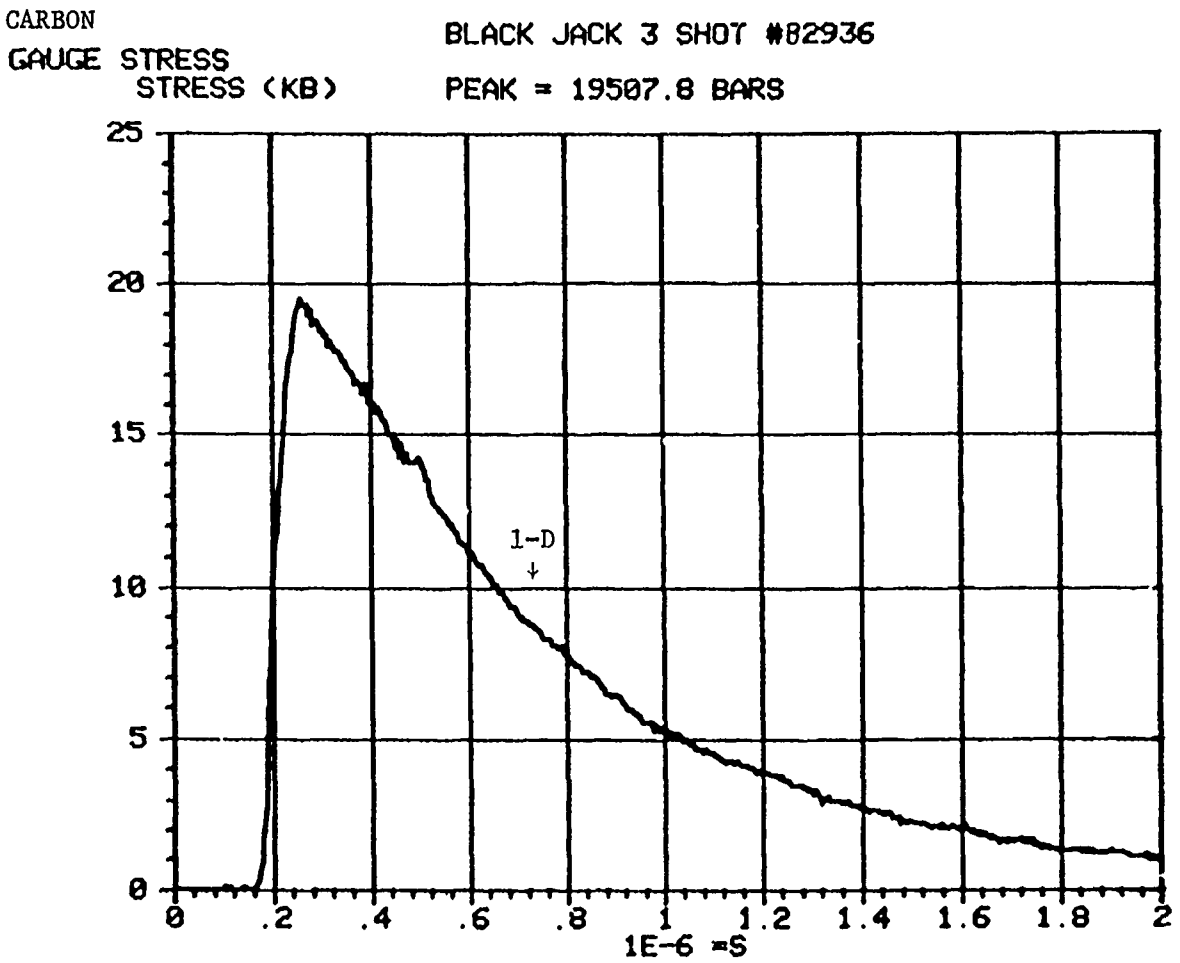

Figure 63. Ktech aluminum carbon gauge record.

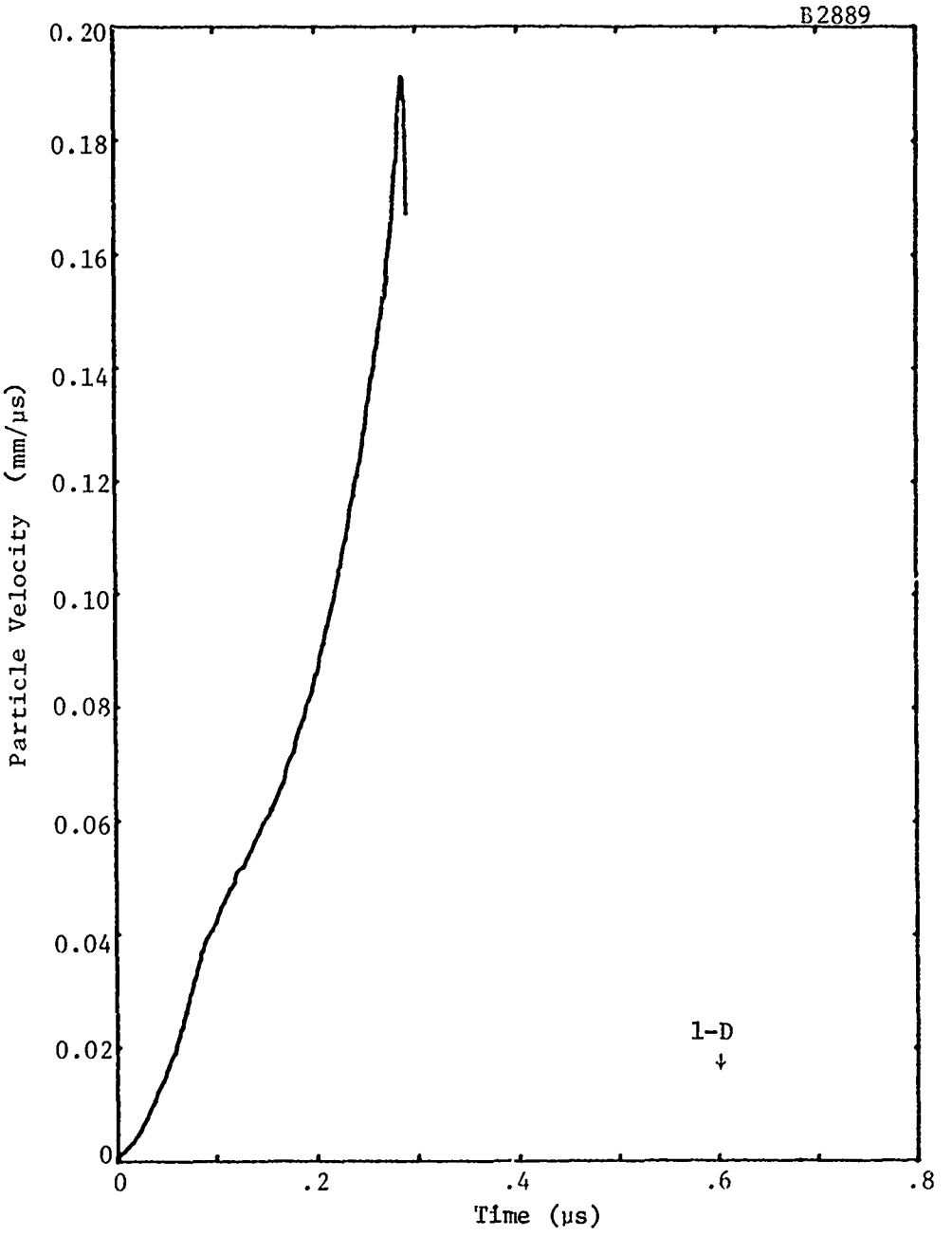

Figure 64. Ktech aluminum LVI record.

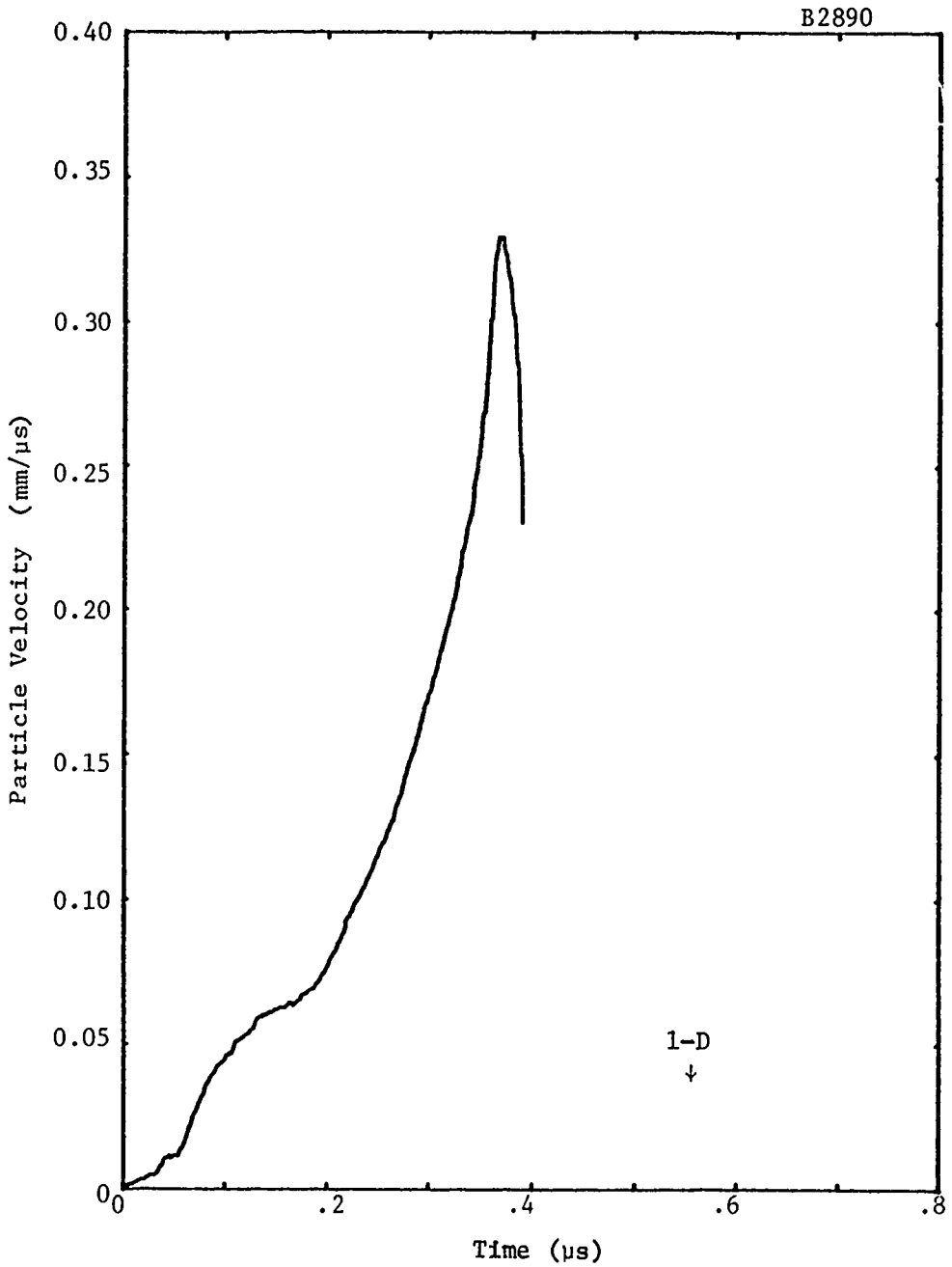

Figure 65. Ktech aluminum LVI record.

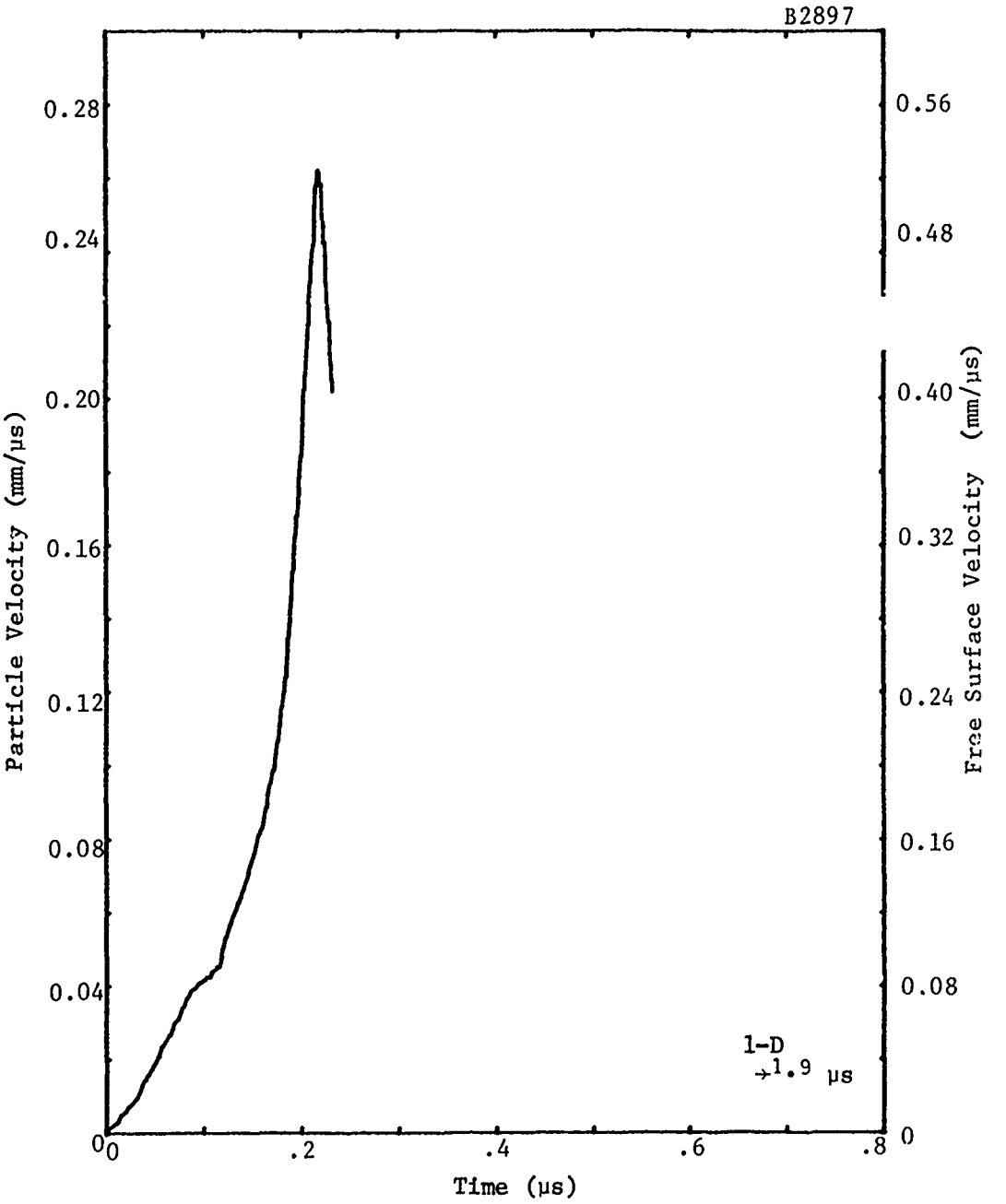

Figure 66. Ktech aluminum LVI record.

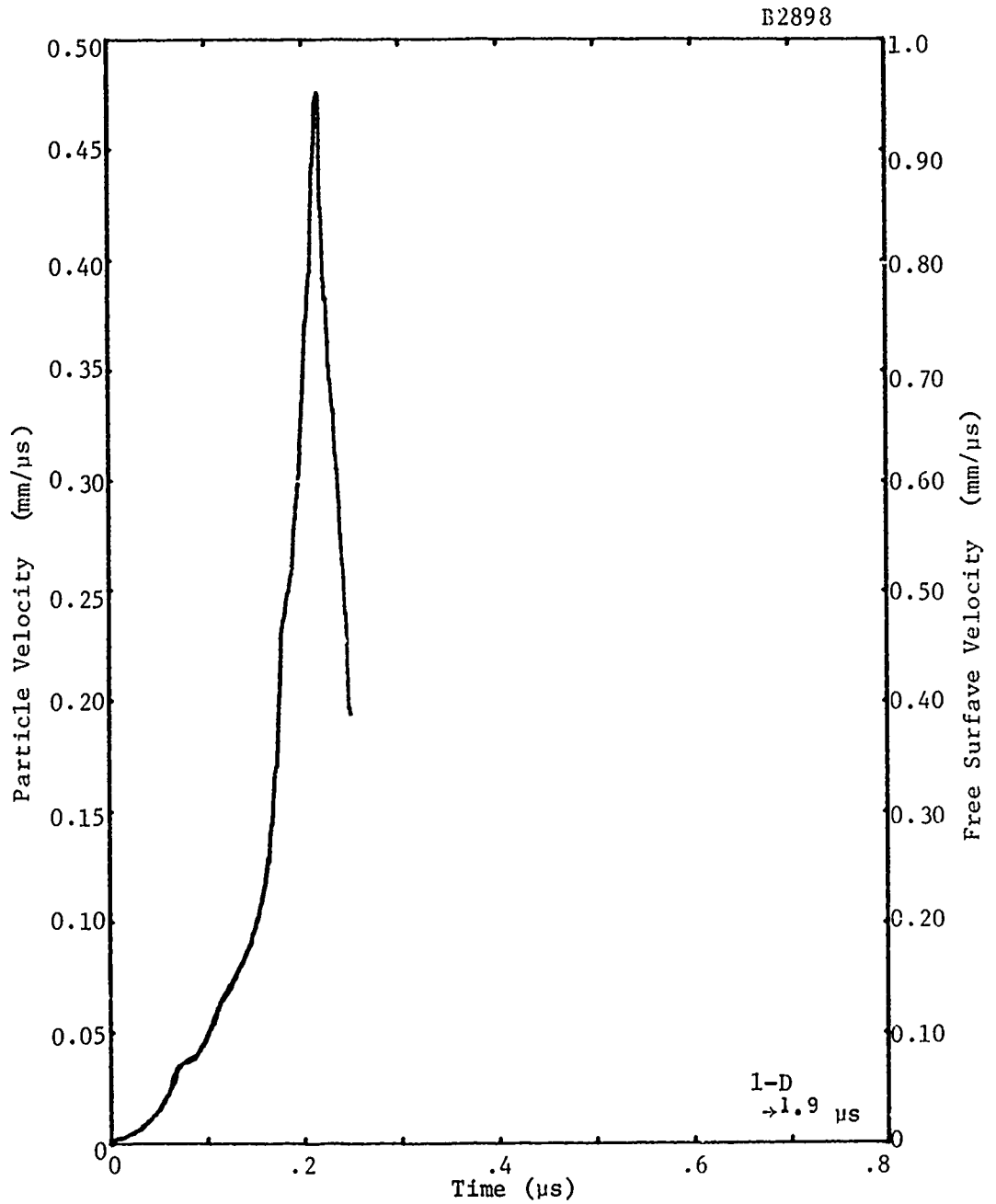

Figure 67. Ktech aluminum LVI record.

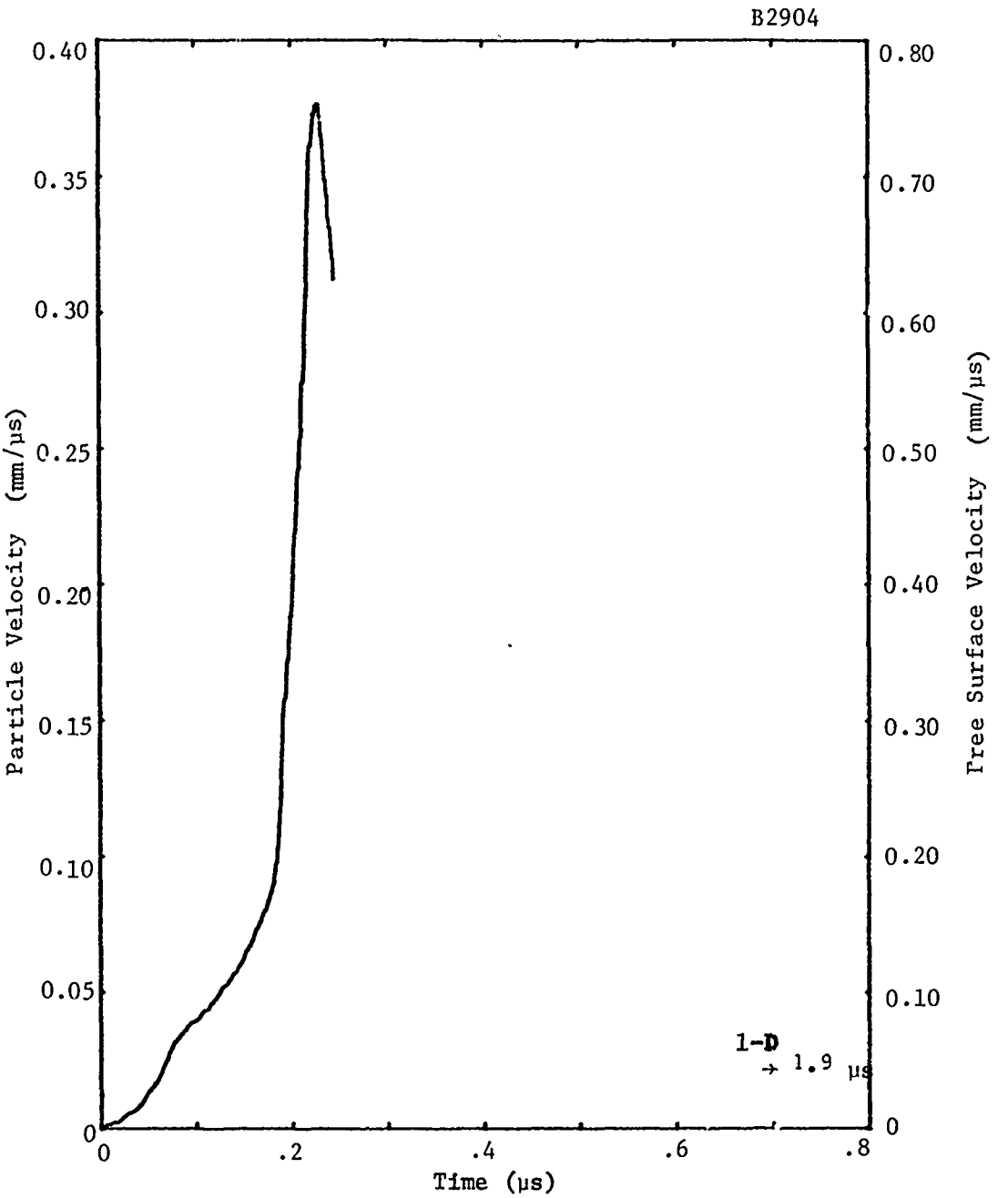

Figure 68. Ktech aluminum LVI record.

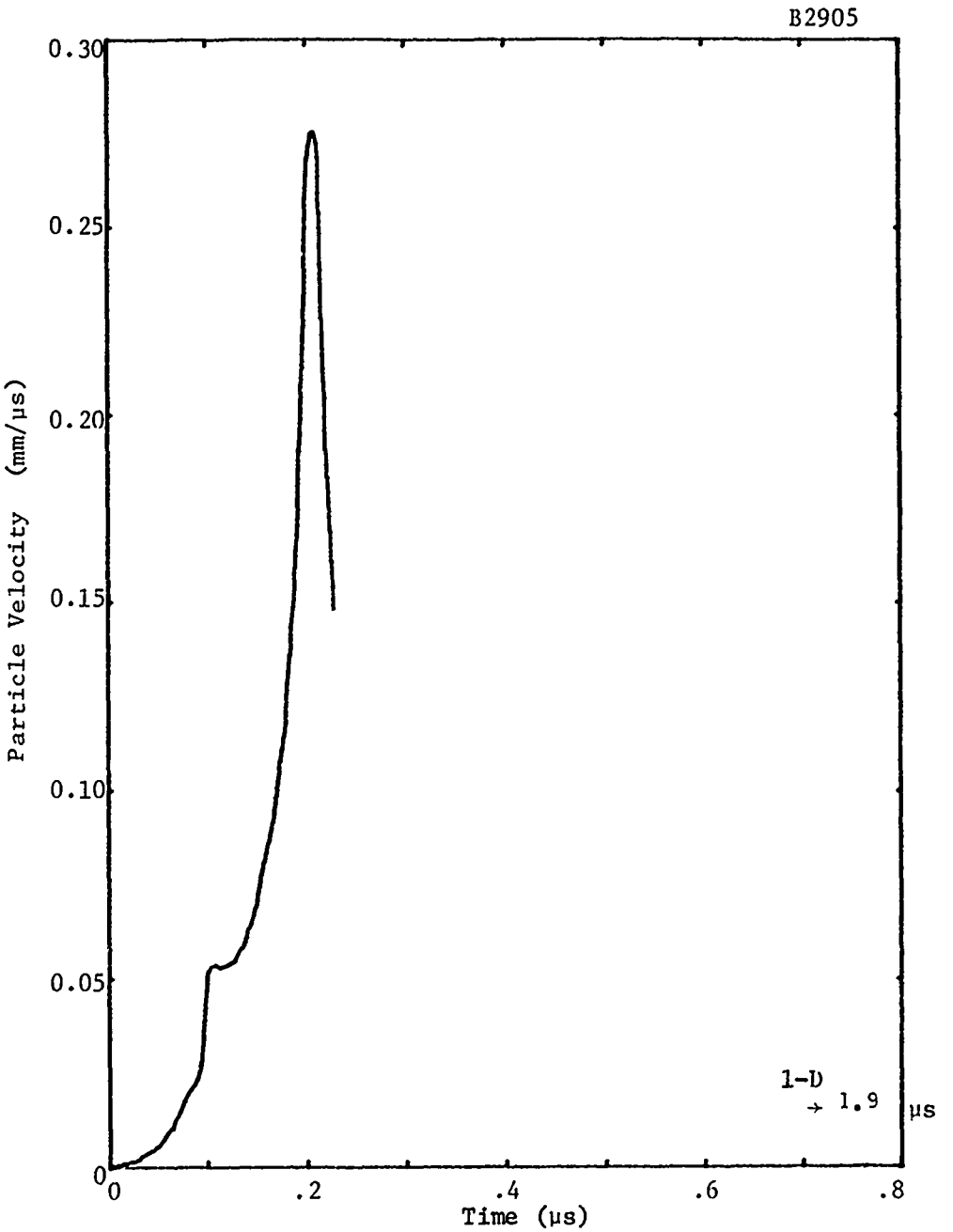

Figure 69. Ktech aluminum LVI record.

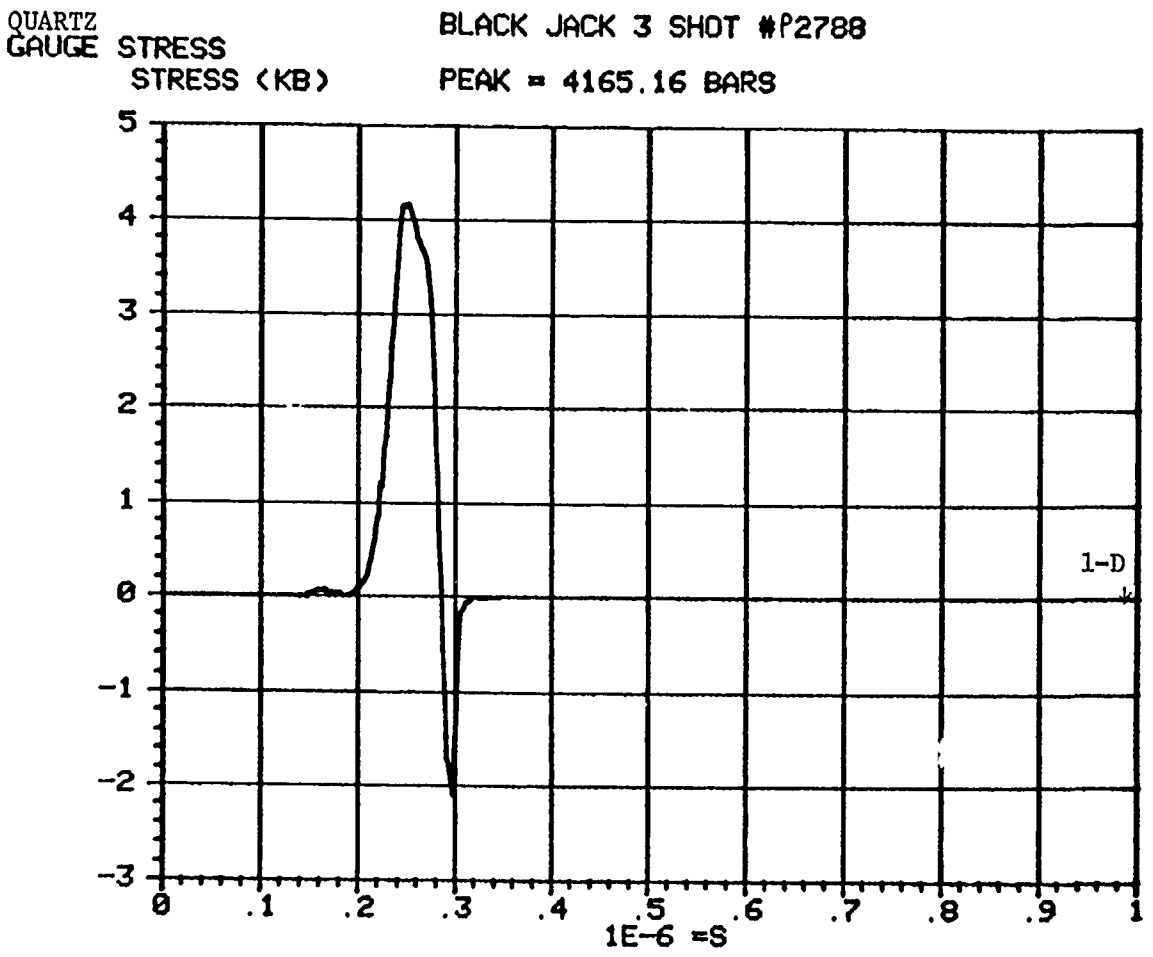

Figure 70. Commonality tantalum quartz gauge record.

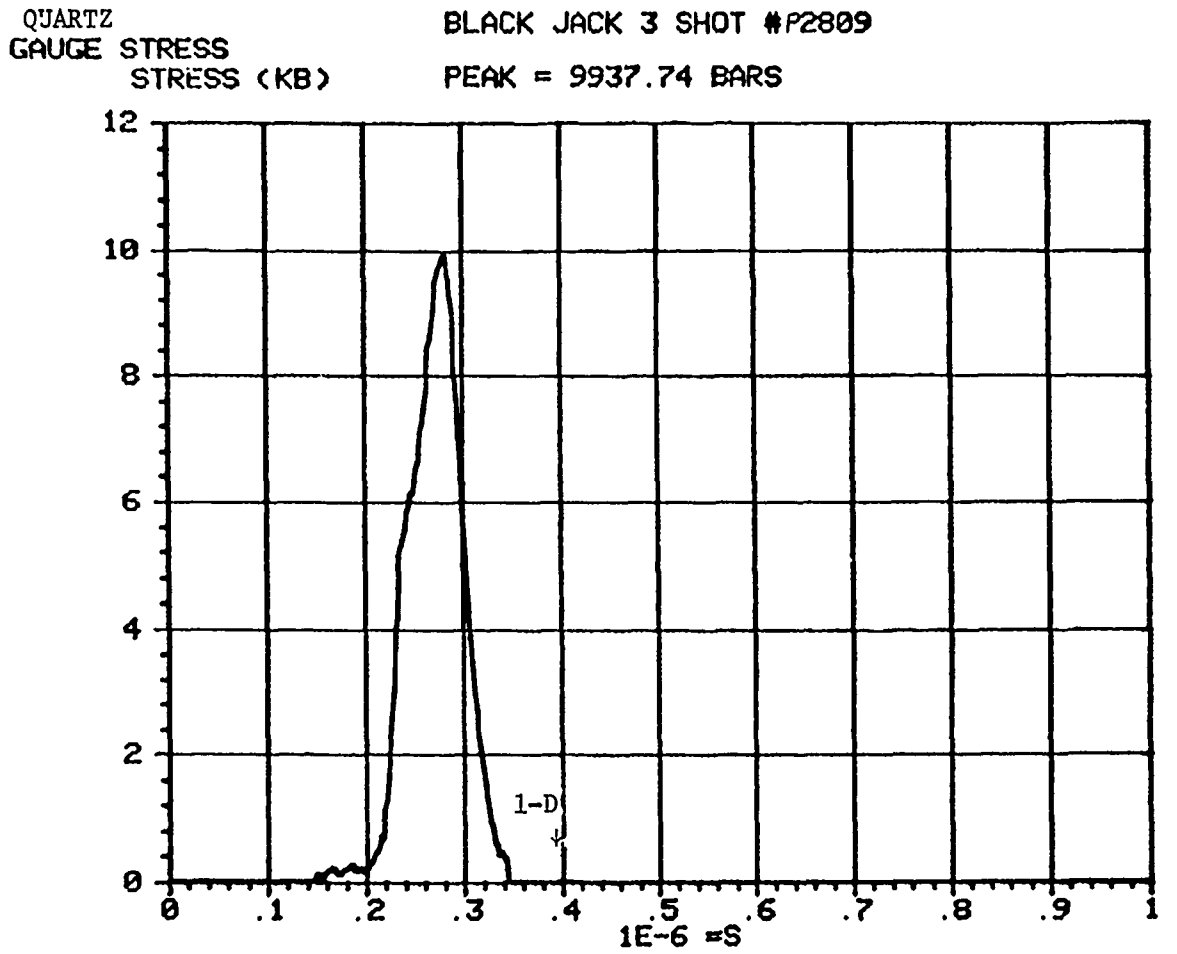

Figure 71. Commonality tantalum quartz gauge record.

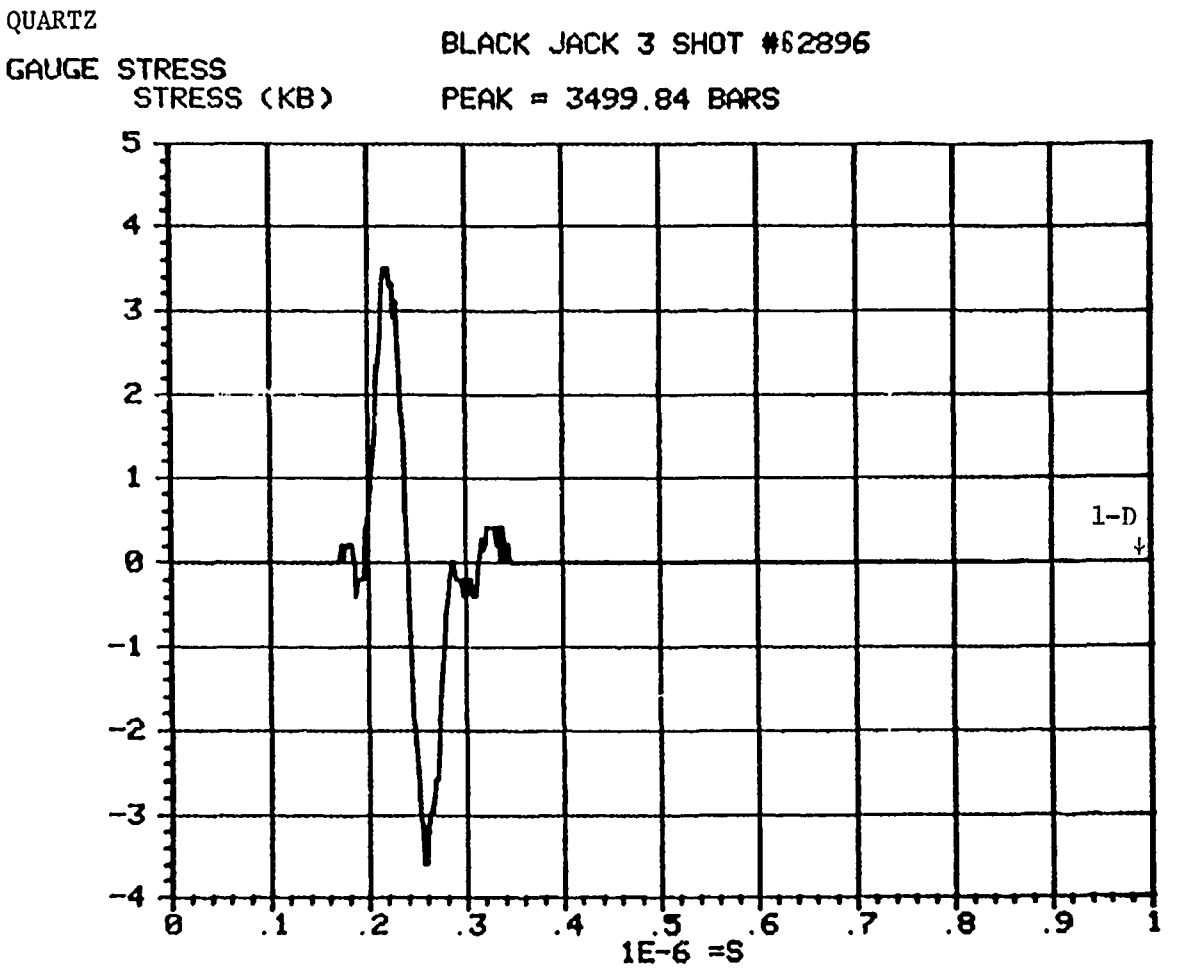

Figure 72. Commonality tantalum quartz gauge record.

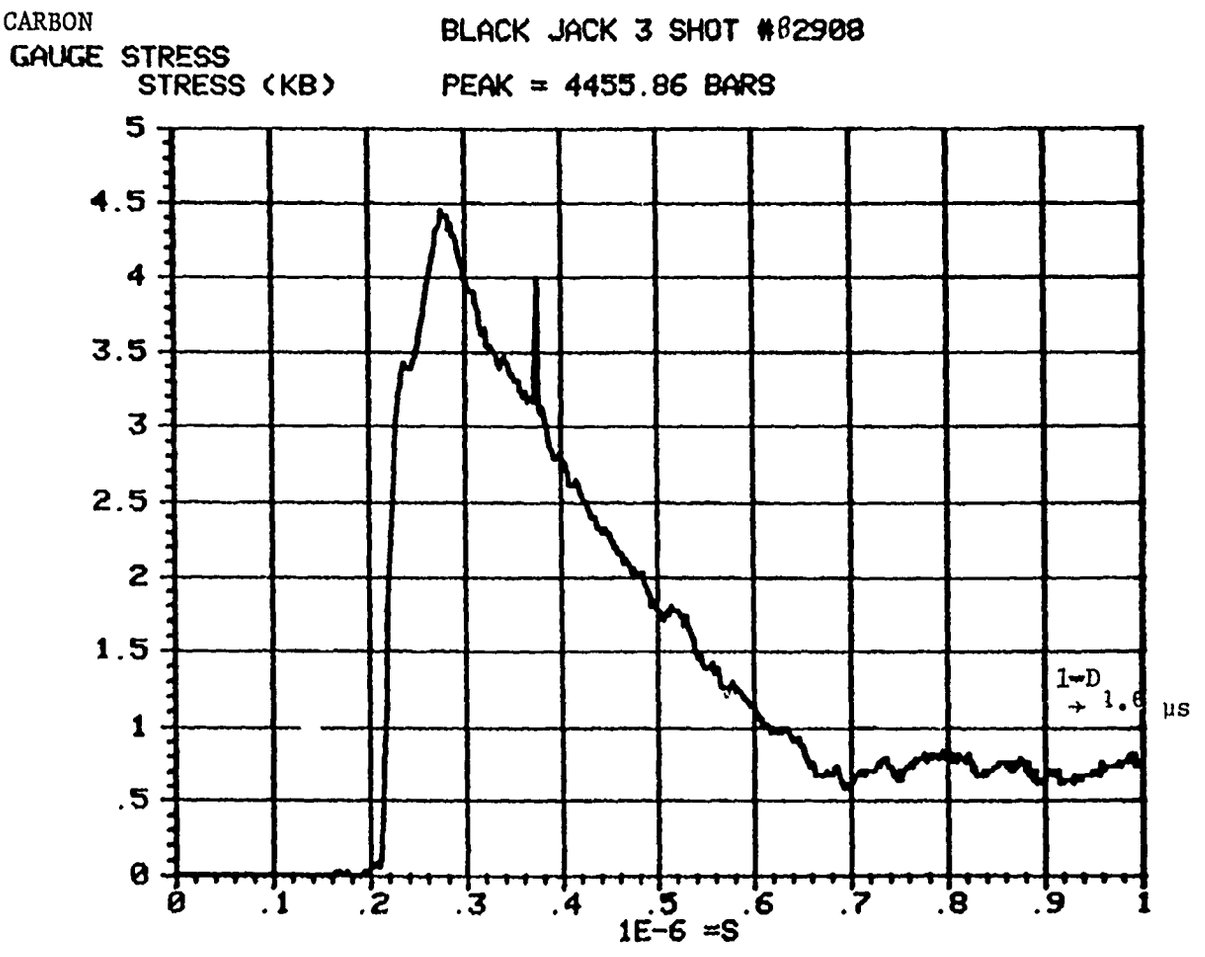

Figure 73. Commonality tantalum carbon gauge record.

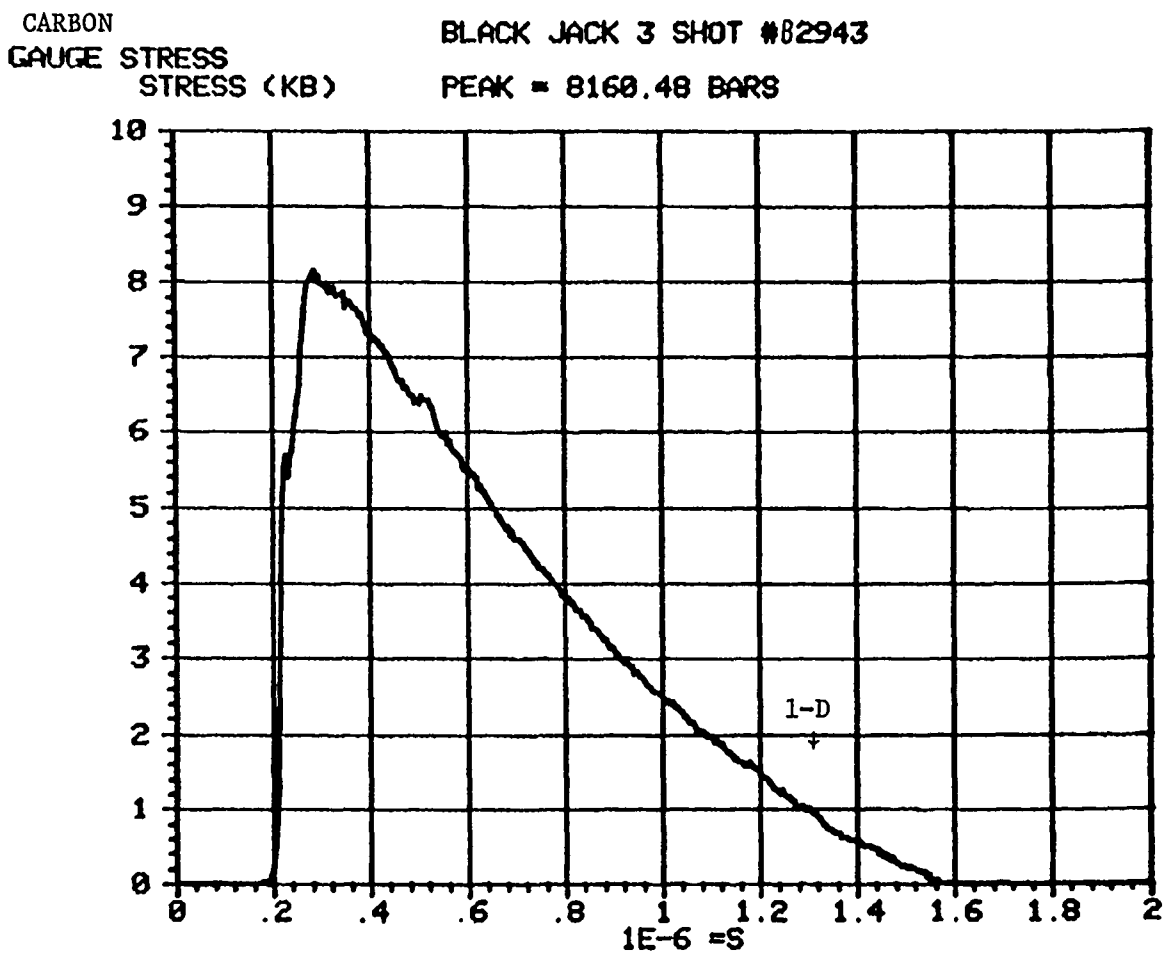

Figure 74. Commonality tantalum carbon gauge record.

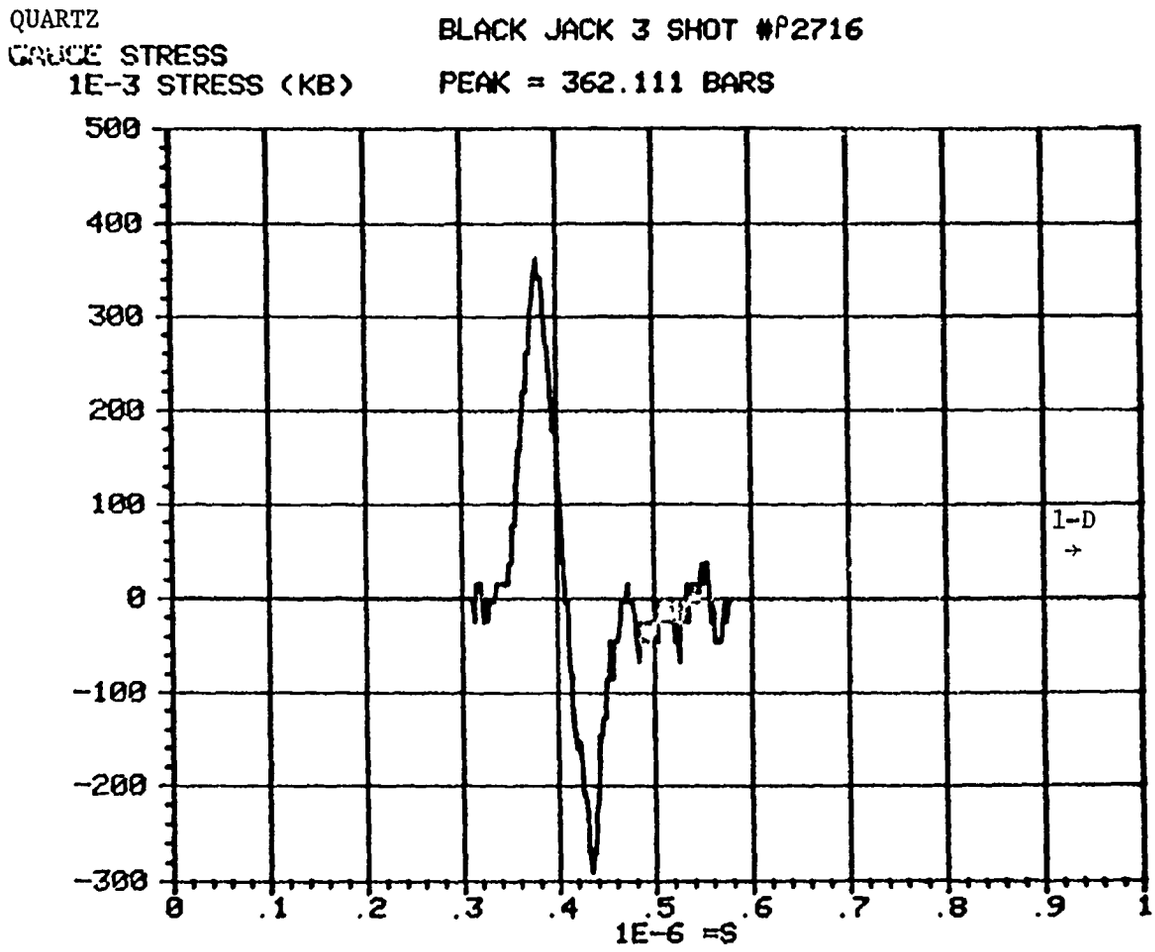

Figure 75. Ktech tantalum quartz gauge record.

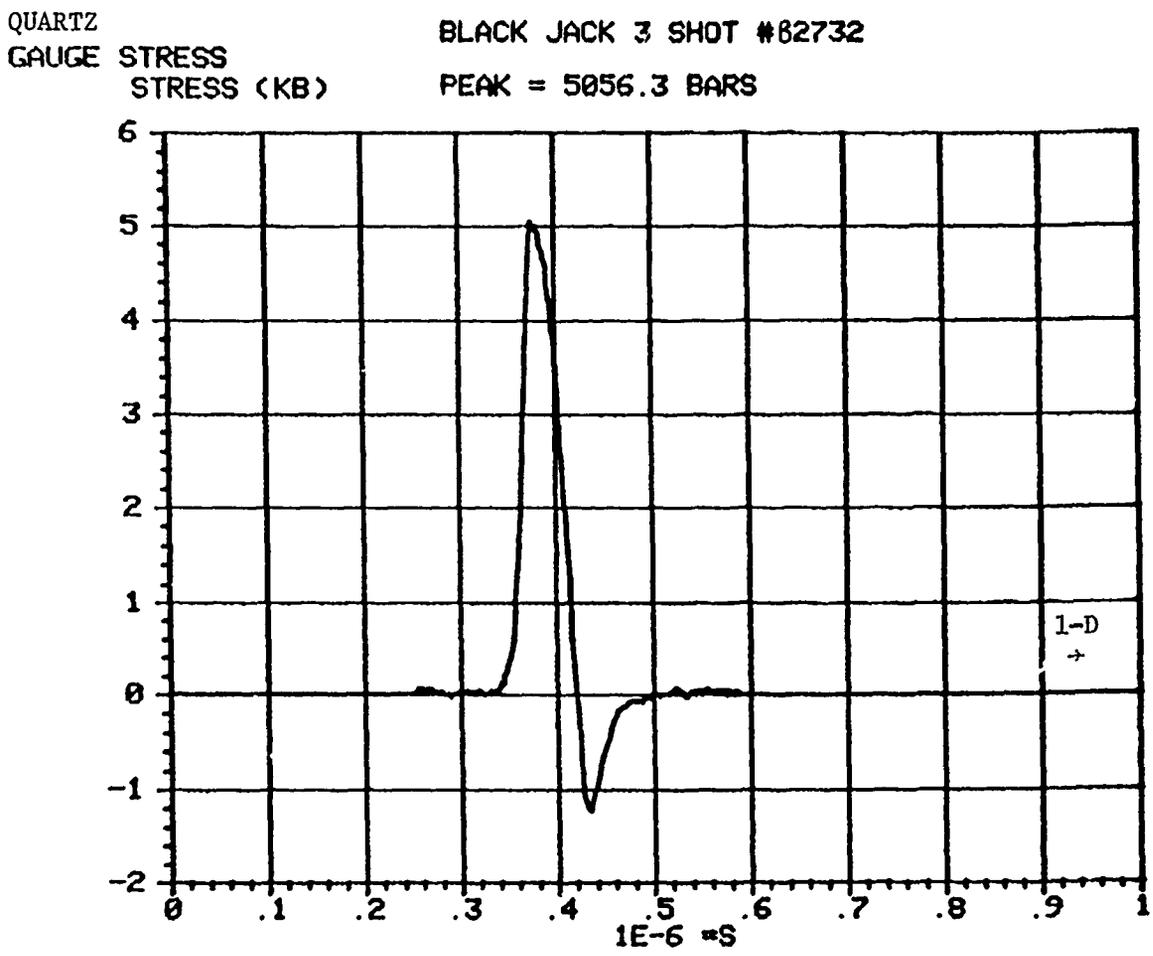

Figure 76. Ktech tantalum quartz gauge record.

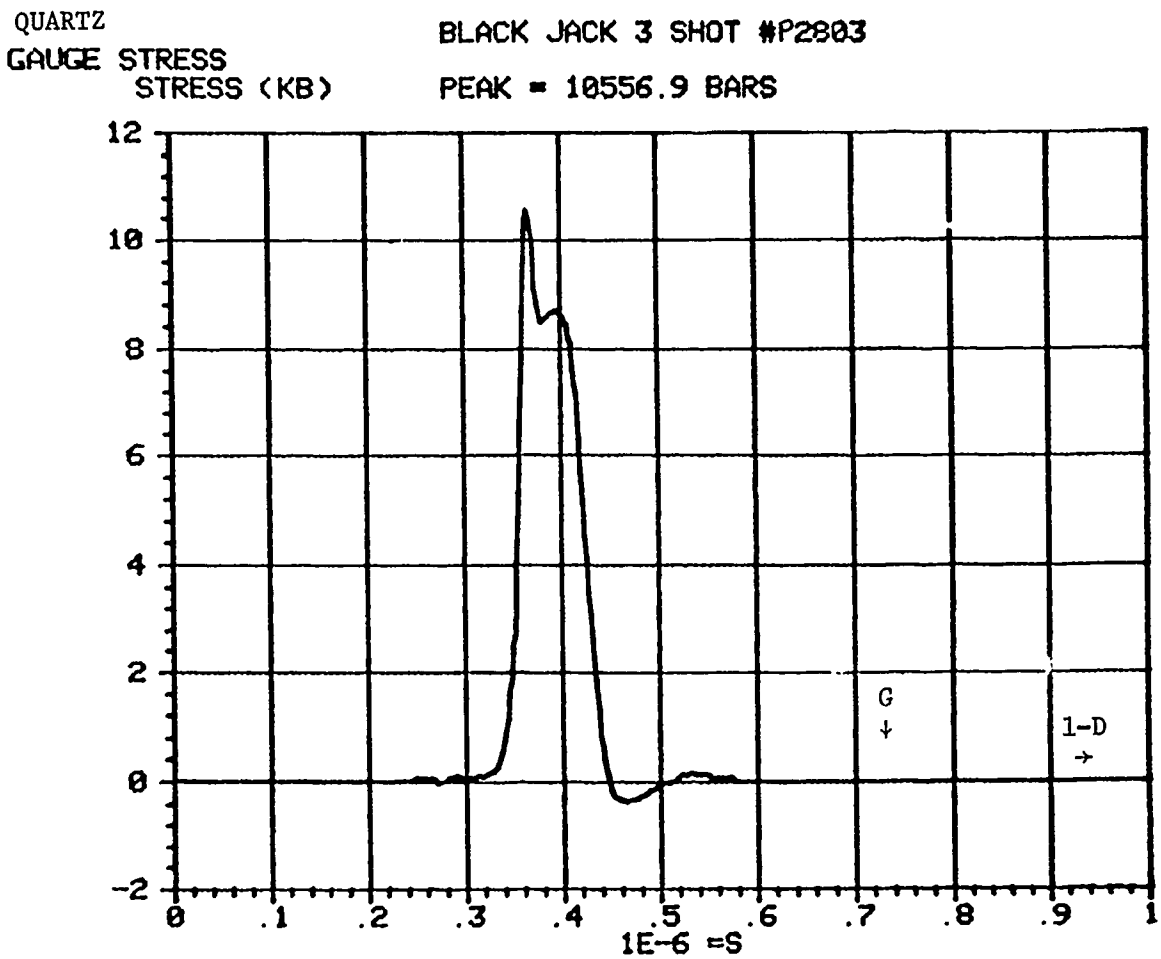

Figure 77. Ktech tantalum quartz gauge record.

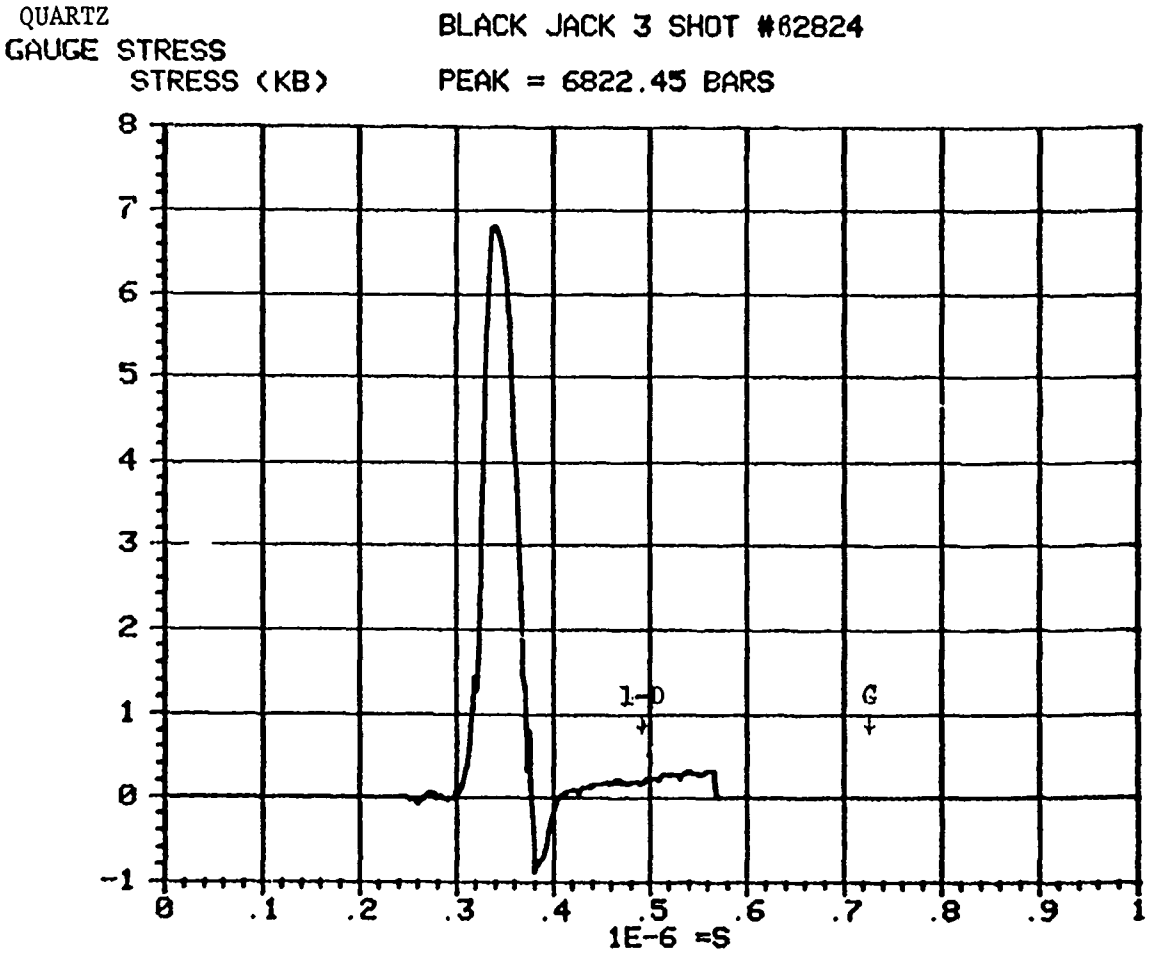

Figure 78. Ktech tantalum quartz gauge record.

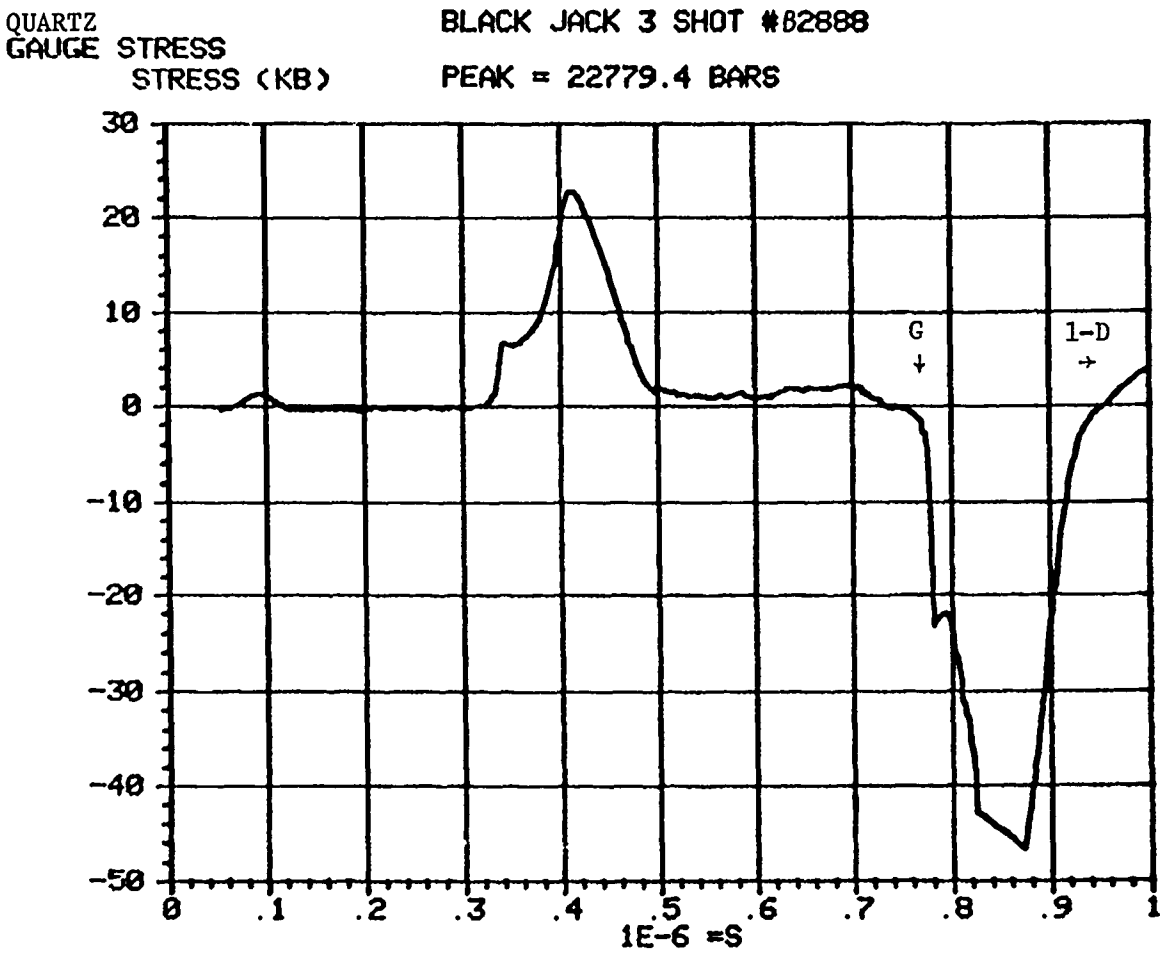

Figure 79. Ktech tantalum quartz gauge record.

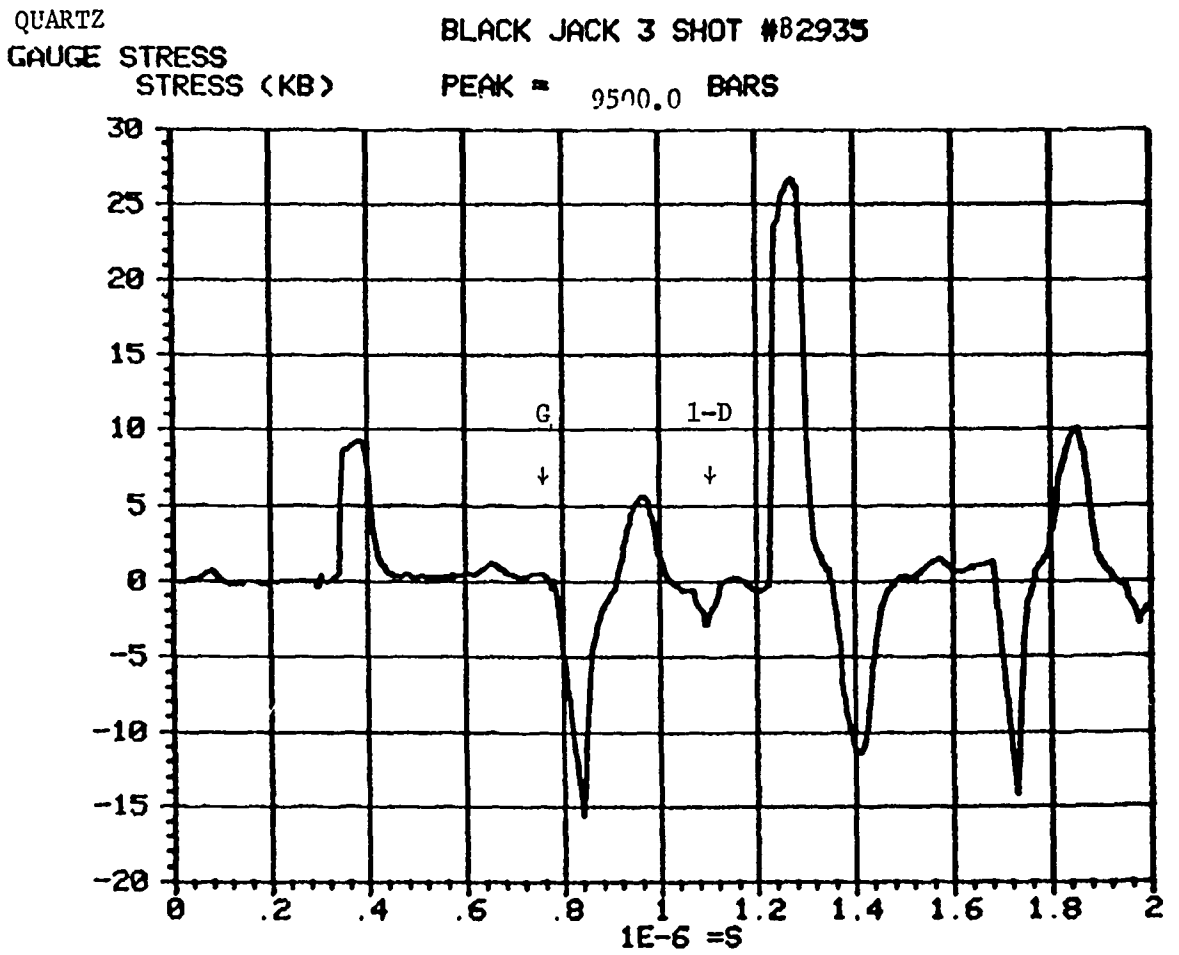

Figure 80. Ktech tantalum quartz gauge record.

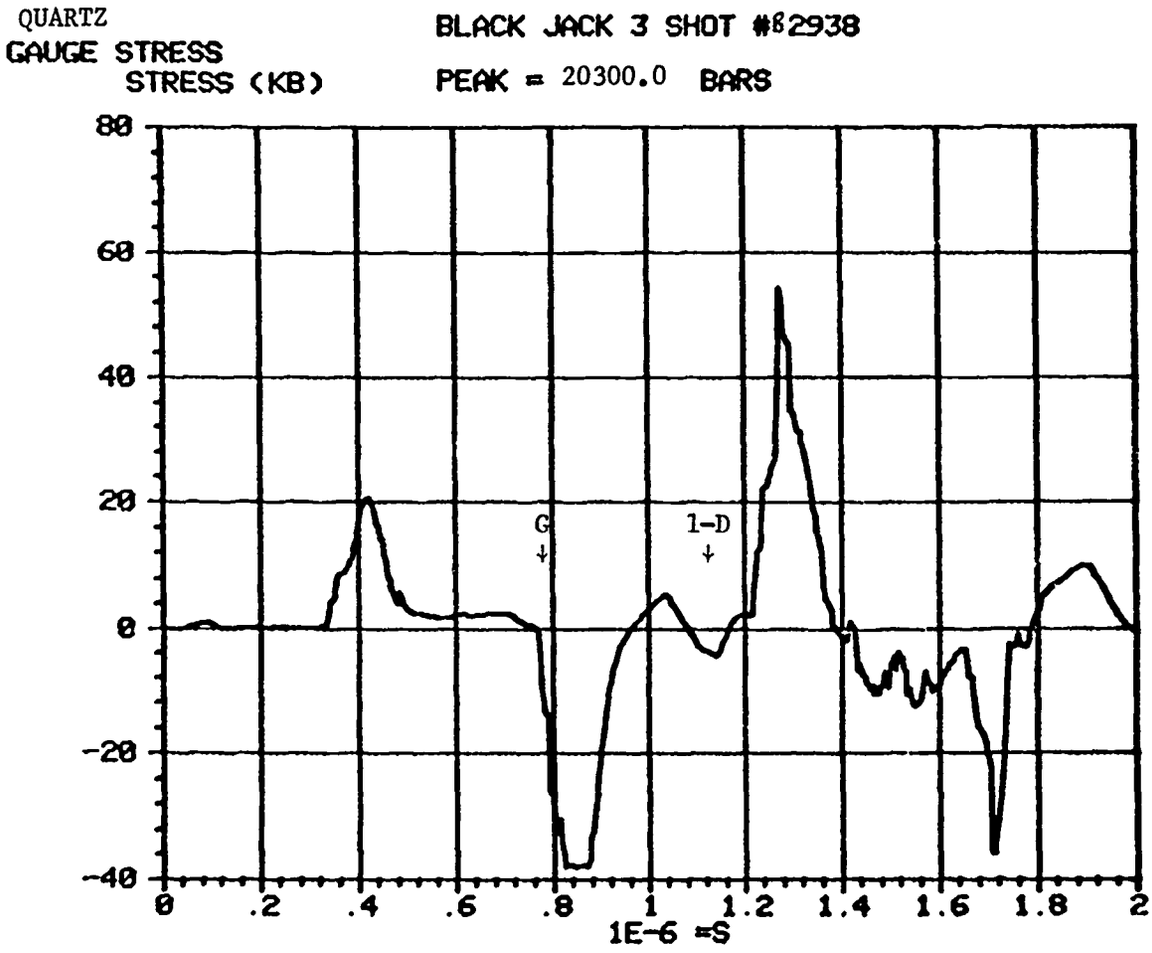

Figure 81. Ktech tantalum quartz gauge record.

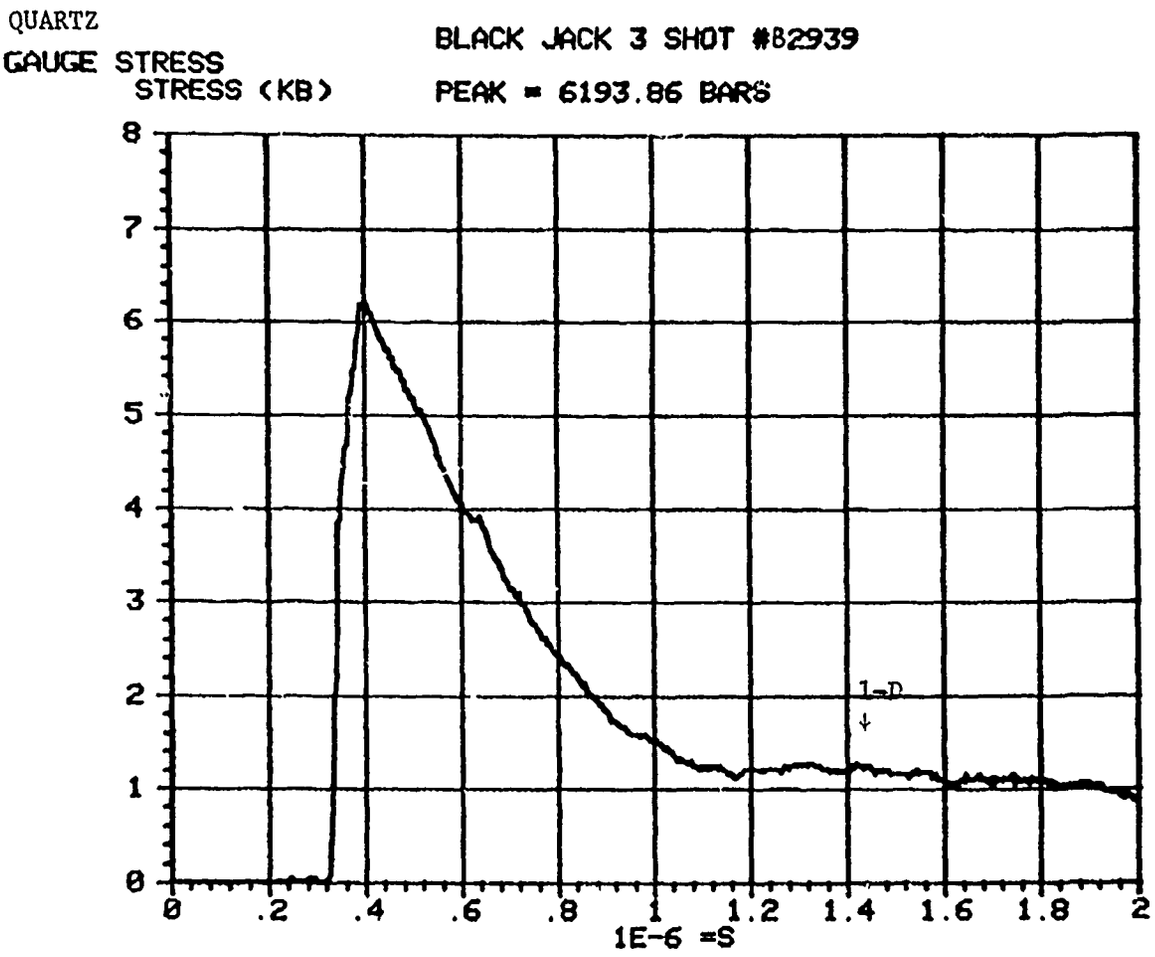

Figure 82. Ktech tantalum carbon gauge record.

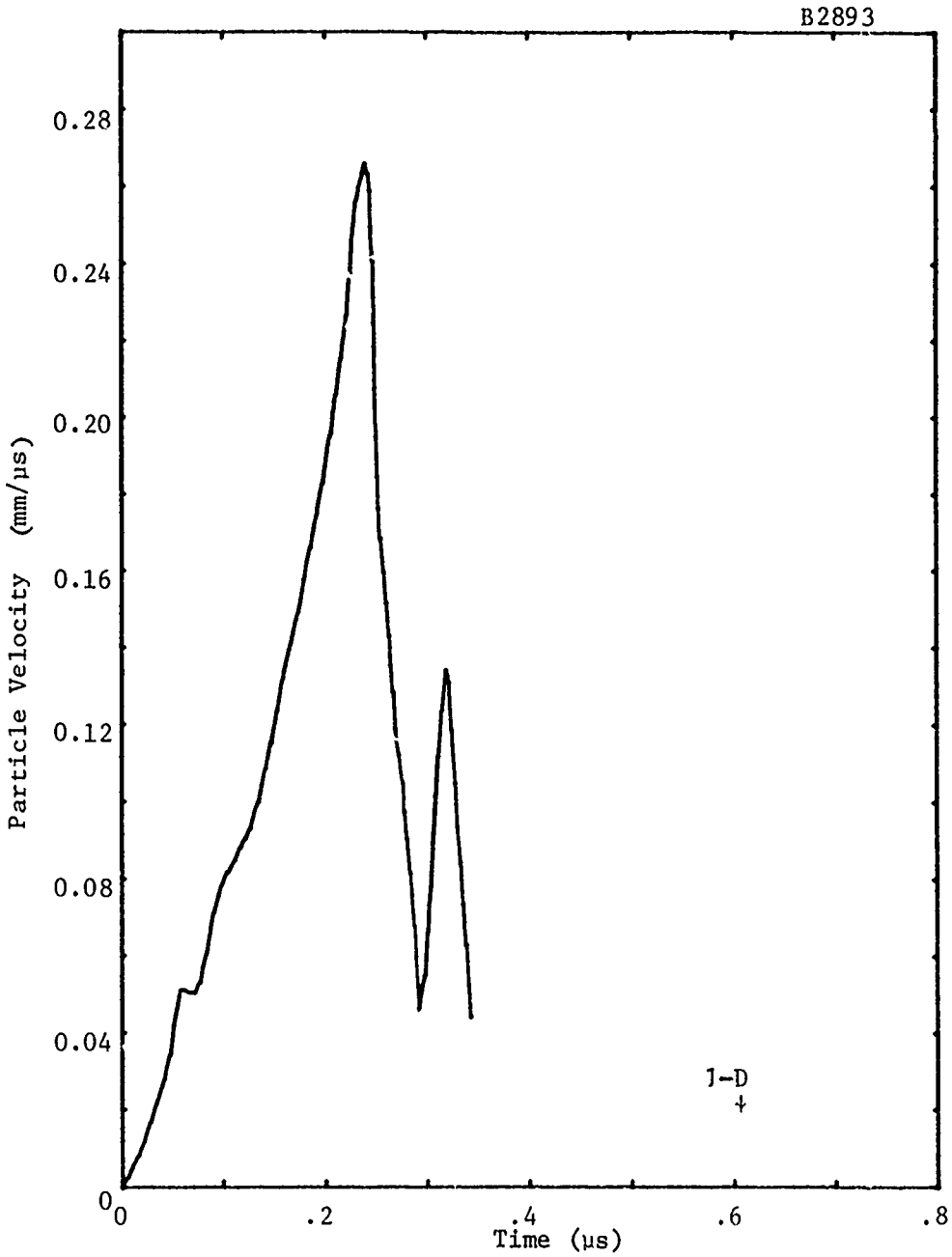

Figure 83. Ktech tantalum LVI record.

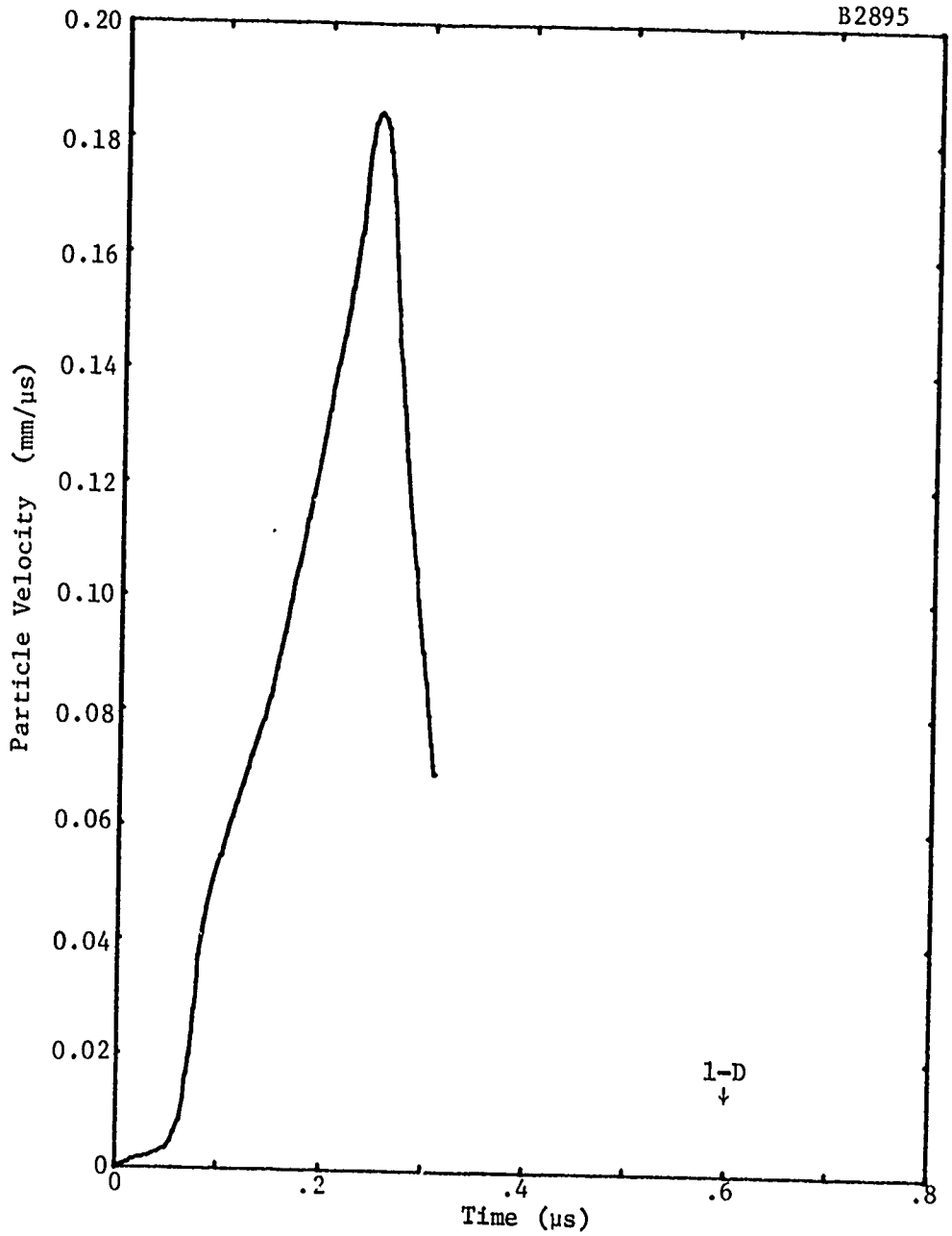

Figure 84. Ktech tantalum LVI record.

Table 10. Aluminum shots: machine characteristics summary.

Materials	Shot No.	Machine	Beam (kJ)	Mean Energy (keV)	FWHM (ns)	Peak Energy (MeV)
Al_c	P2785	BJ3P	20.7	800	41	1.35
	P2801	BJ3P	21.3	644	40	1.13
	P2802	BJ3P	17.2	622	34	1.16
Al_c	B2820	BJ3	25.7	724	44	1.28
Al_c	B2937	BJ3	10.9	337	40	0.97
	B2940	BJ3	21.9	744	53	1.19
	B2894	BJ3	12.34	706	33.5	1.20
	B2907	BJ3	15.0	818	32	1.36
	B2919	BJ3	23.1	800	47	1.31
Al_c	B2920	BJ3	21.1	797	40	1.44
Al_k	P2715	BJ3P	14.1	824	40	1.16
	B2729	BJ3	15.3	548	41	1.07
	B2738	BJ3	17.0	488	33	1.33
	P2779	BJ3P	4.6	466	38	0.83
	P2782	BJ3P	23.1	750	39	1.39
	B2922	BJ3	3.4	773	30	1.35
	P2814	BJ3P	17.0	510	38	0.98
	B2906	BJ3	14.0	825	29	1.39
	B2936	BJ3	20.9	618	53	0.94
	B2889	BJ3	22.6	537	39	1.08
	B2890	BJ3	18.1	952	36.5	1.72
	B2897	BJ3	25.0	978	46	1.52
	B2898	BJ3	23.0	900	47	1.50
	B2904	BJ3	17.3	849	39	1.47
Al_k	B2905	BJ3	14.0	892	30	1.51

Table 11. Tantalum shots: machine characteristics summary.

Materials	Shot No.	Machine	Beam (kJ)	Mean Energy (keV)	FWHM (ns)	Peak Energy (MeV)
Ta_c	P2788	BJ3P	19.5	663	32	1.27
	P2809	BJ3P	20.2	582	48	1.02
	B2896	BJ3	18.8	582	45	1.16
	B2908	BJ3	14.6	818	30	1.37
Ta_c	B2943	BJ3	22.1	756	47	1.37
Ta_k	P2716	BJ3P	14.0	846	29	1.33
	B2732	BJ3	16.5	483	36	1.33
	P2803	BJ3P	18.8	749	35	1.20
	B2824	BJ3	22.5	916	39	1.52
	B2885	BJ3	19.9	918	38	1.51
	B2888	BJ3	21.1	824	49	1.18
	B2935	BJ3	15.8	656	42	1.08
	B2938	BJ3	19.9	597	42	1.07
Ta_k	B2939	BJ3	19.8	623	53	0.99
Ta_k	B2893	BJ3	18.6	789	36.5	1.42
Ta_k	B2895	BJ3	22.9	900	49.6	1.56

at the front surface, and also accounts for the long pulse duration observed in the carbon gauge records.

Whereas the quartz gauge records give the overall appearance of a typical deposition-profile stress wave, the carbon gauge records do not except at low stresses. The PMMA shock speed is a rapidly increasing function of stress, and this causes rapid "shocking up" of the stress pulse as it propagates through the 0.3175-cm-thick PMMA in front of the gauge. Thus, the initial rise time of the records is shortened into a shock front. PMMA also has a rapid increasing release wave speed for increasing stress. This results in a long-lived Taylor expansion tail following the peak stress. These effects are readily predicted by PUFF (ref. 4) hydrocode computations. These wave profile distortions are accompanied by significant attenuation of the peak stresses. An illustration of such effects based on PUFF computations is given in Appendix D.

Typical narrow Ta stress waves of about 80-ns width at beam deposition time widen and distort to give stress pulse widths of the order of 1 μs after propagating through 0.3175 cm (1/8 inch) of PMMA. This long release tail is a mixture of the PMMA release behavior together with an overlay of reverberation behavior within the sample feeding successive pulses (of diminishing amplitude) into the PMMA. Unfolding of the carbon gauge data necessitates an accurate knowledge of the PMMA equation of state (EOS).

For the LVI records, three conditions applied. Some shots used the rear free surface of the samples as mirrors. For these measurements, only the inherent hydrodynamic behavior of the sample is involved, such as internal stress attenuation and the factor of 2 (approximately) jump in particle speed at the surface. One record used the sample rear surface as a mirror, but loaded the sample with PMMA. For this shot, the mismatch condition at the interface is involved, but the propagation through the PMMA is not relevant, except for the

small correction required due to changes in the refractive index (see ref. 2). The remaining LVI shots utilized samples loaded with fused silica containing a thin (1500 Å) buried mirror 0.635 cm (1/4 inch) from the sample/silica interface.

For these latter shots, both the interface impedance mismatch and the propagation through the silica must be accounted for. Unlike PMMA, silica exhibits a reducing stress wave speed with increasing stress over the range of 0 to 60 kbar, rising with stress only for higher stresses. This behavior results in a "ramping out" of the stress wave giving dispersion and an increasing rise time. Thus, again, narrow Ta pulses become widened, but the pulse profile more nearly resembles that of the initial deposition plot. Again, attenuation of the peak stress occurs, and unfolding of these buried mirror LVI records necessitates accurate knowledge of the fused silica EOS.

Differences in the behavior of the two aluminums are discerned. The Ktech supplied material is of 6061-T6 stock and displays an elasto-plastic knee in the neighborhood of 5 kbar. The commonality material is of 1100 type stock and displays a lower, less obvious elasto-plastic knee (1 to 3 kbar) as expected (refs. 10 and 11).

An important feature of the records is the existence of a sustained low stress at late times for high fluence shots on tantalum. This effect is not observed for the aluminum. Shots 2908 and 2939 most clearly show this. It is probable that this is caused by vapor production on the tantalum surface, and can be seen to occur before any significant limitations would be imposed on the records by one-dimensional read time considerations. The "vapor tail" is seen on all high dose records with carbon and LVI records, including some poor quality shots not itemized in this report.

4-4 MACHINE PERFORMANCE

During the experimental period, a total of 161 shots were performed. Of these, 41 were stress measurements, 18 were dose-depth calorimetry measurements and 102 were spatial fluence calorimetry measurements. Of the stress measurements, 15 were on material from the commonality stock (and of limited supply), while the remainder were of Ktech supply. These latter samples were used to (i) help verify the overall commonality results, and (ii) help determine the machine behavior and diagnostic setup to minimize accidental loss of commonality results due to inappropriate conditions.

Table 3 summarizes the two machine performances over all the experimental sessions, regardless of type of shot. The original anticipation had been for a deposition time (FWHM) of about 30 ns for BJ3' and 50 to 60 ns for BJ3. However, the data reveal that the differences were less than expected, and with variations sufficient to span the above range. Thus, BJ3' gave 35.6 ± 4.3 ns (standard deviation), and BJ3 gave 43.6 ± 7.0 ns. Individual shots ranged from 24 to 56 ns for both machines! An additional factor was that BJ3' frequently gave a second small power pulse following the main pulse which was low in mean energy. Low energy electrons are responsible for much of the peak sample energy loading near the front surface. Since these electrons were generated late in time, the effective overall deposition time for all low energy electrons was significantly longer than for the high energy electrons. This complicates the effects of "swiftness" and of hydrodynamic computations. Additionally, such low energy electrons are the most likely to be lost from the beam while propagating down the drift tube. Thus, the diode-drived energy spectrum may not be an accurate enough representation of the incident beam on the samples. Figure 85 illustrates this late tail behavior of BJ3' and contrasts it with the single pulse behavior of BJ3.

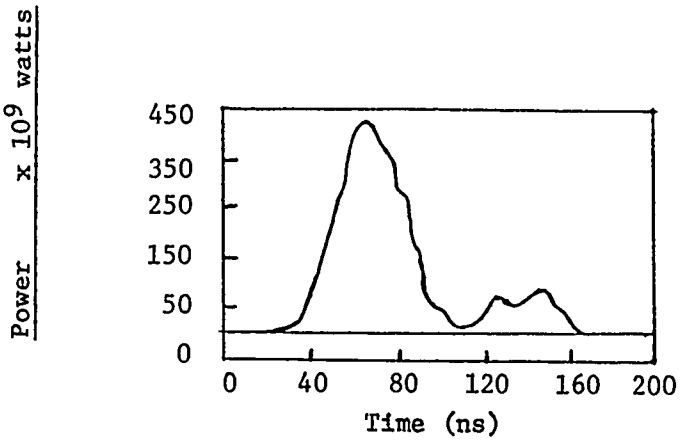

Top: Typical BJ3' power curve showing late secondary pulse

Bottom: Typical BJ3 power curve

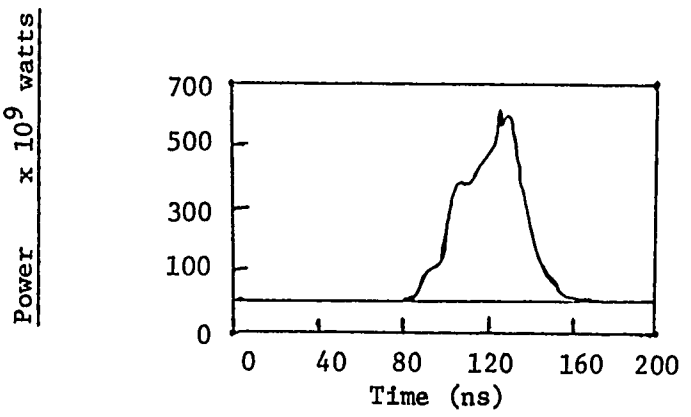

Figure 85. Typical power curves.

4-5 ACCURACY

The accuracy of fluence measurements on individual calorimeters is about ±10 percent. This is essentially determined by the extrapolation of temperature back to time zero (shot time) to allow for heat leakage from the calorimeters, and is greater than the uncertainties in either the thermocouple calibration (known to ±1 percent [ref. 9]), or the enthalpy data (known to ±5 percent [ref. 1]).

Stress and velocity measurements are better than ±5 percent, with the quartz and carbon calibration data being good to ±1 percent (ref. 7) and ±5 percent (ref. 8), and fringe measurements being good to ±1 percent for low velocities and ±5 percent for peak velocities.*

The 7912 digital analysis of machine behavior gives precise values. However, the system output is known to be quite sensitive to adjustment in various parameters. For example, during short-circuit shots the time stagger between the voltage and current recordings is established. This parameter (of a few ns) is important for establishing the true power curve, the electron energy spectrum and the inductively corrected voltages. Depending on the electron pulse (overall time width, etc.), these various properties can be sensitive in value to the time stagger. Likewise, an adjustment to the "zero" of voltage can significantly influence the analysis of the pulse. This is especially true of the BJ3' pulse in which the significance of the secondary power pulse varies according to the choice of zero voltage. Thus, while the system has precision, it is not necessarily accurate in assessing the true electron spectrum. The fits of the ELTRAN computations to the measured dose-depth data give the relevance of the assessed diode data. It is seen that while some fits are very good, others are less so, and the fitted angle of incidence can vary by up to ±30 percent.

* To unfold the quartz and carbon gauge records also involves use of the EOS of quartz and PMMA. These Hugoniot data are quoted in Appendix C.

SECTION 5

CONCLUSIONS AND RECOMMENDATIONS

5-1 CONCLUSIONS

The objectives of this contract have been well met. Both Blackjack 3 Prime and Blackjack 3 have been well characterized. Energy density loadings of up to about 1000 cal/g are possible in Al and Ta over irradiation areas large enough to give reliable stress measurements which are one-dimensional for long times, between 500 ns and 2 μs, depending on exact geometry of recording system. These are also very conservative one-dimensional read times; the useful one-dimensional read times are longer. In addition, dose-depth measurements were accomplished at energy loadings in carbon of up to 750 cal/g, which to our knowledge is a level not previously achieved by other experimenters.

In particular, BJ3 gives a wide, high fluence beam (e.g., ≈100 cal/cm^2 over 10 cm^2) and by suitable adjustment of the diode impedance match to the Blumlein can be made to give pulses of time duration (FWHM) of between 30 and 60 ns. This time range coupled with the deposition profile characteristics of BJ3 provides a very useful combination of beam properties for investigating many aspects of sample response. For example, vaporization can be induced in Ta in such a way as to still allow easy measurement of stress owing to the ability to irradiate a large area. BJ3' is not presently very useful owing to the late secondary power pulse of low energy, giving long ambiguous deposition times.

A great deal of information has been obtained on both Al and Ta and over energy loadings of between about 10 and 1000 cal/g. Thus the complete range of material responses, of small stress solid behavior through to copious vaporization (for Ta), have been investigated. The results agree well with initial predictions, taking into account the induced energies, stress relief during deposition, and

wave attenuation during propagation. The few anomalous records are understood (e.g., gauge saturation or break down) and such records have been included, for completeness, in Appendix B.

Of great significance is the observation of a residual late time low stress in those samples of Ta irradiated sufficiently intensely to induce surface vaporization. This effect was not seen for Al samples, and was quite repeatable for the Ta at the highest dose. It is thus a function of vaporization. This vapor tail is much higher in amplitude than predicted with the PUFF equation-of-state model.

5-2 RECOMMENDATIONS

In view of the above mentioned "vapor stress tail," it is recommended that detailed analysis of the three-phase (solid, liquid, vapor) behavior of Ta be done. The PUFF hydrocode does not compute the liquid/vapor transition adequately as it does not have a liquid phase. The CHART-D code is more realistic in this regard, and is particularly relevant for situations such as those of the high fluence Ta shots. In these, vaporization was initiated but the energy loadings were not intense enough to take the material above total vaporization (i.e., including latent heat of vaporization at a total enthalpy of 1290 cal/g). The deposition profile also induced loadings giving states between vapor and cool solid, and the observed stress records integrate these effects. A complete equation of state such as that in the CHART-D hydrocode is needed to adequately describe these effects.

It is recommended that future studies be made on Ta, at several values of specific energy in the vapor region, to generate an understanding of the vapor pressure tail and to increase the data base for this material. Such studies should also be made of other materials which can be vaporized (e.g., Au, Pb, Cu) to correlate their behavior with that of Ta.

Future work should include the study of porous metals, especially porous high Z ones such as Ta (85 percent dense). Porous material response is strongly coupled to deposition time, and is a function of pore size and vapor behavior. Many shielding materials contain high Z constituents and are frequently porous. In addition to Ta, the solid and porous versions of vanadium at levels up to and including vaporization should be studied. Vanadium is an important cermet constituent.

Design of experiments with porous Ta (and V) should fully anticipate the elasto-plastic properties of porous materials such as the fast elastic wave, slow plastic (core collapse) wave and the rapid release waves. This necessitates care on sample thickness and one-dimensionality considerations. Situations similar to those used for the Al and Ta on BJ3 should yield good data. Owing to toxicity problems of various cermet constituents, such work needs to be done on a machine such as REHYD. This machine has similar behavior to BJ3 and can handle toxic materials.

The wave propagation studies mentioned above need to be fully supported by studies of the effective Gruneisen parameter for porous materials. To do this a high energy beam, such as that of HERMES, is needed to induce a uniform energy loading within a sample (rather than a profiled deposition dropping to zero loading). Particle motions can be monitored (by LVI) to ascertain the induced stresses. The Gruneisen constant is an essential parameter for prediction and correlation of stress generation and measurement.

In view of the known sensitivity of the electron spectrum to current and voltage time correlation and the inductive voltage correction, and the consequences on predicted deposition profiles and stress profiles, it is recommended that a detailed study be made to assess this sensitivity. Ktech Corporation is in an

ideal position to do this study. Such a study would complement the analysis done by SRI, providing them a matrix of calculated deposition profiles against which their own hydrodynamic predictions of observed stress could be compared; the study would also generate the electron spectrum and (ELTRAN) deposition profiles as functions of time during the deposition. This information is needed as input to the hydrocodes for accurate stress generation calculation, especially for cases such as Ta where considerable stress relief occurs during energy deposition.

It is recommended that further work be done by MLI on the BJ3' to eliminate the second pulse. For example, the pulse can be crowbarred immediately after the first main pulse. Although this would reduce the total beam energy a little, it would result in a well controlled beam with a short deposition time of about 30 ns. This would make it a very useful machine for studying narrow stress profiles (such as solid Ta) where little "swiftness" stress relief has occurred. A better, more costly, solution would be to better match the BJ3' machine components to reduce reflections and eliminate the second pulse without sacrificing total beam energy.

REFERENCES

1. Phelps, D. A. and Rauch, J. E., "Description of Blackjack 3 and Blackjack 3 Prime," MLR-748, Maxwell Laboratories, Inc., 1978.

2. Barker, L. M. and Hollenbach, R. E., "Shock-Wave Studies of PMMA, Fused Silica, and Sapphire," J. Appl. Phys., 41, pp 4208-4226, Sept. 1970.

3. Barker, L. M. and Hollenbach, R. E., "Laser Interferometer for Measuring High Velocities on Any Reflecting Surface," J. Appl. Phys., 43, p 4669, 1972.

4. Cecil, R., Newlander, C. D. and Scammon, R. J., PUFF 74 - A Material Response Computer Code, AFWL-TR-76-43, Vols. 1 and 2, Air Force Weapons Laboratory, Kirtland AFB, NM, 1976.

5. Brittain, F. H., "ELTRAN: An Electron Deposition Code," SC-TM-68-713, Sandia Laboratories, Albuquerque, NM, 1973.

6. Beezhold, W., Keller, D. V. and Rice, D. A., "Characterization of the Blackjack 3 Prime Electron Beam," Ktech TR-79-9, Ktech Corporation, Albuquerque, NM, 1979.

7. Graham, R. A. and Reed, R. P., "Selected Papers on Piezoelectricity and Impulsive 'Pressure' Measurements," SAND-78-1911, Sandia Laboratories, Albuquerque, NM, 1978.

8. "Carbon Shot Pressure Gauges," Technical Information Data Sheet No. 2, Dynasen, Inc., Goleta, CA, Sept. 1972.

9. "Chromel/Alumel Type K Calibration," Omega Engineering Inc. Data Book, 1978 (superseding N.B.S. Circular #561).

10. Munson, D. E. and Barker, L. M., "Dynamically Determined Pressure-Volume Relationships for Aluminum, Copper, and Lead," J. Appl. Phys., 37, pp 1652-1660, 15 Mar. 1966.

11. Karnes, C. H. and Ripperger, E. A., "Strain Rate Effects in Cold Worked High-Purity Aluminum," J. Mech. Phys. Solids, 14, pp 75-88, 1966.

APPENDIX A

SPECTRAL INFORMATION ON STRESS SHOTS

Histograms of stress-shot data are presented first, followed by tabulations of stress and dose-depth data. The shot numbers are listed according to material type.

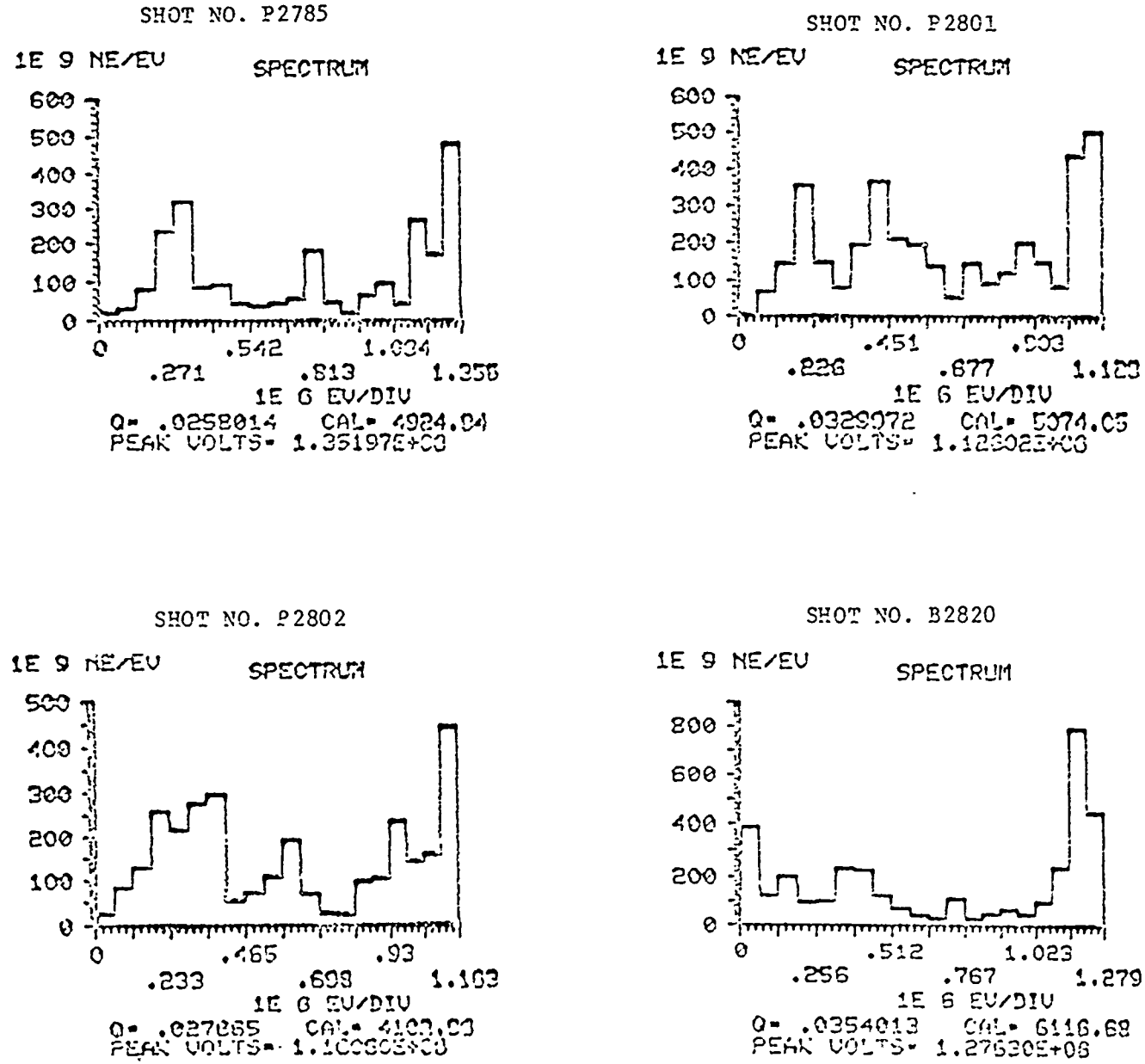

Figurea A1-A4. Commonality aluminum spectral graphs: quartz gauge.

Al - Commonality

SHOT NO. B2937

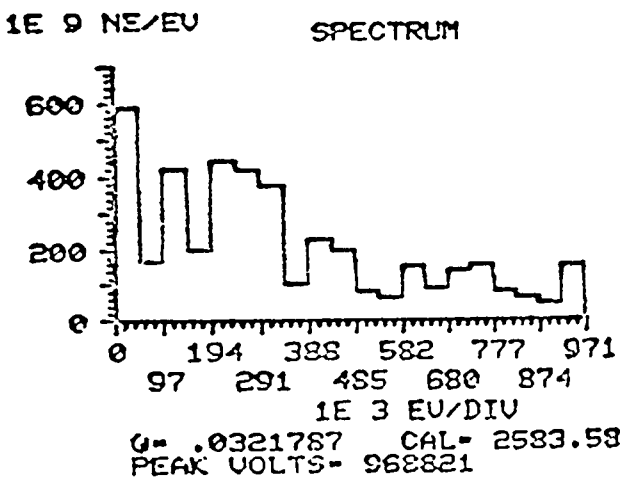

SHOT NO. B2940

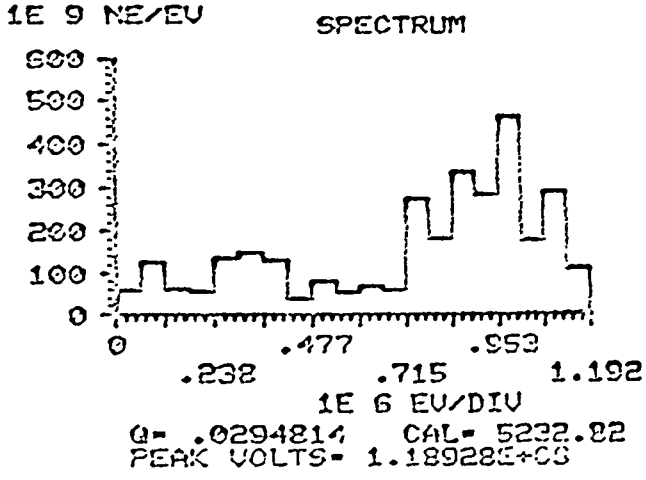

Figures A5-A6. Commonality aluminum spectral graphs: carbon gauge.

SHOT NO. B2894

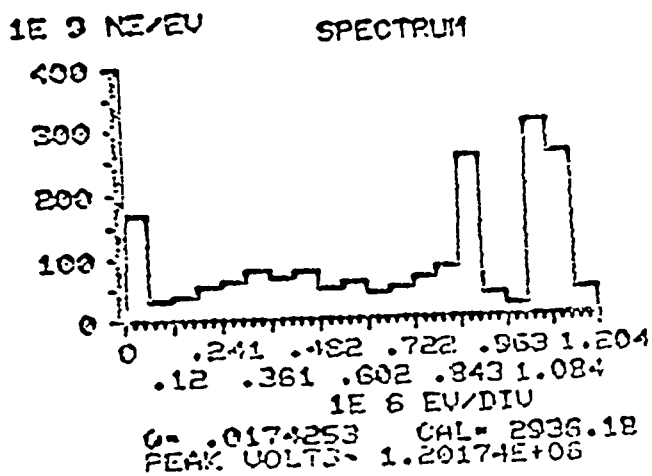

SHOT NO. B2907

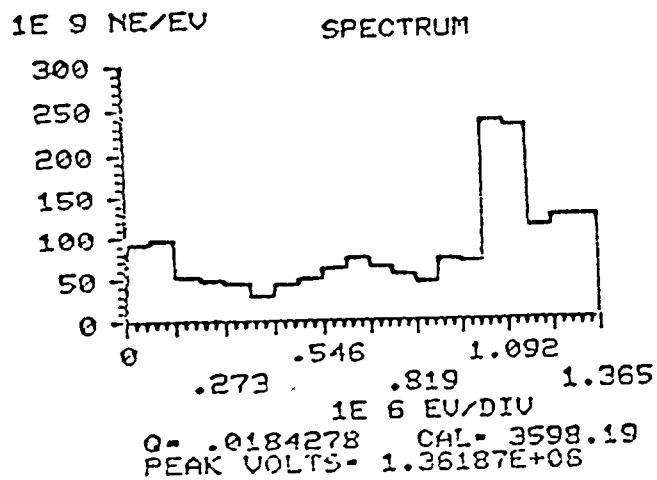

SHOT NO. B2919

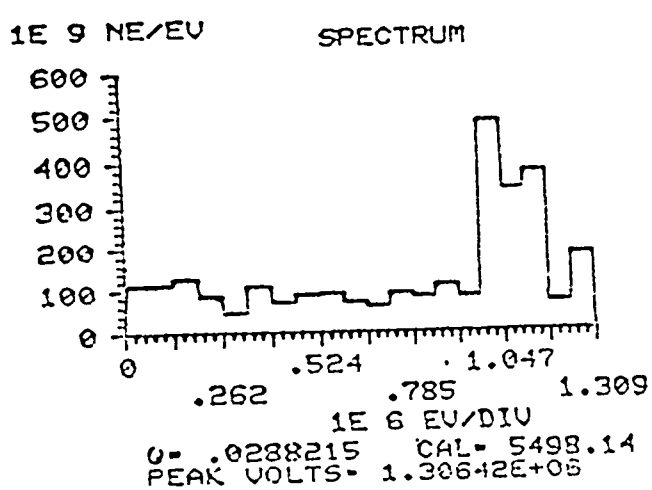

SHOT NO. B2920

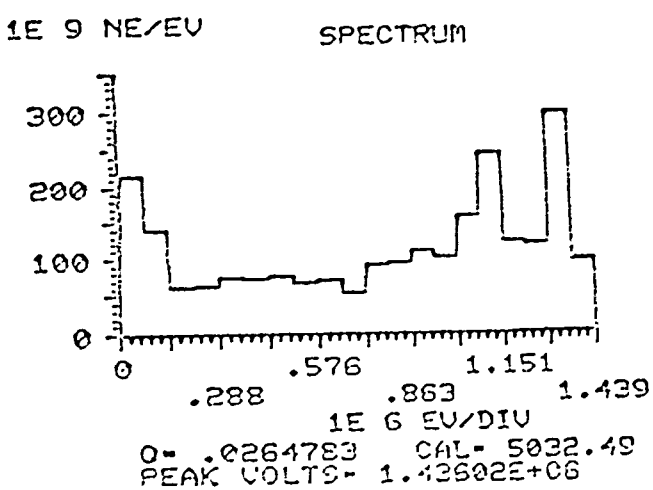

Figures A7-A10. Commonality aluminum spectral graphs: LVI.

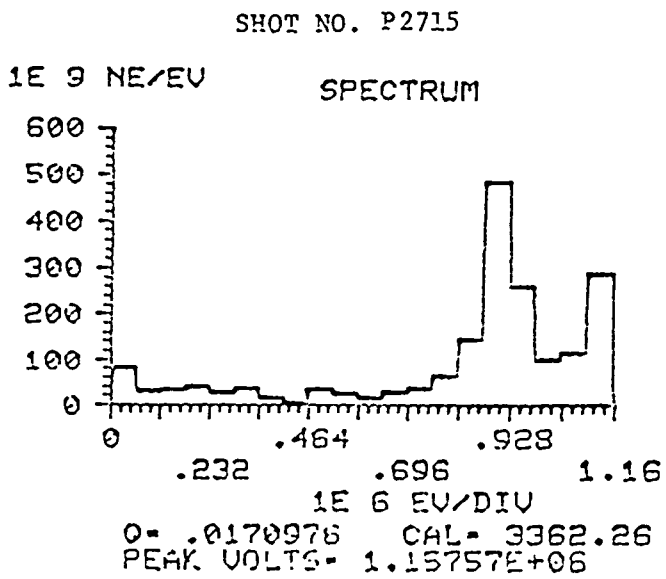

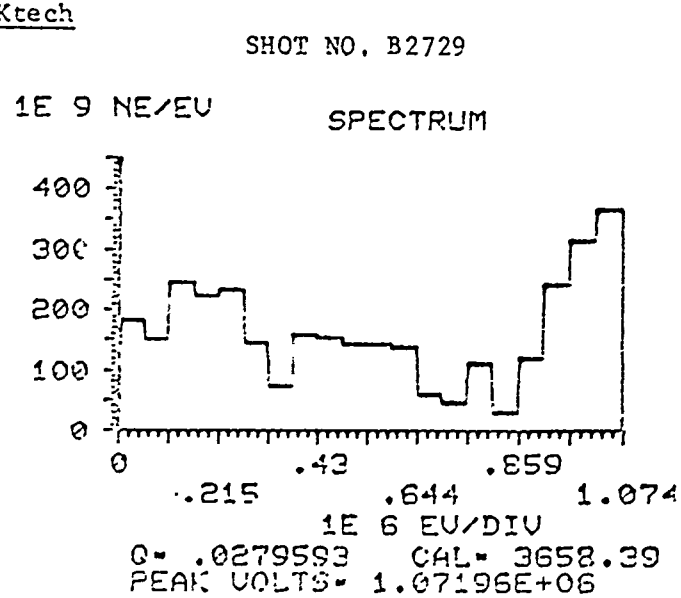

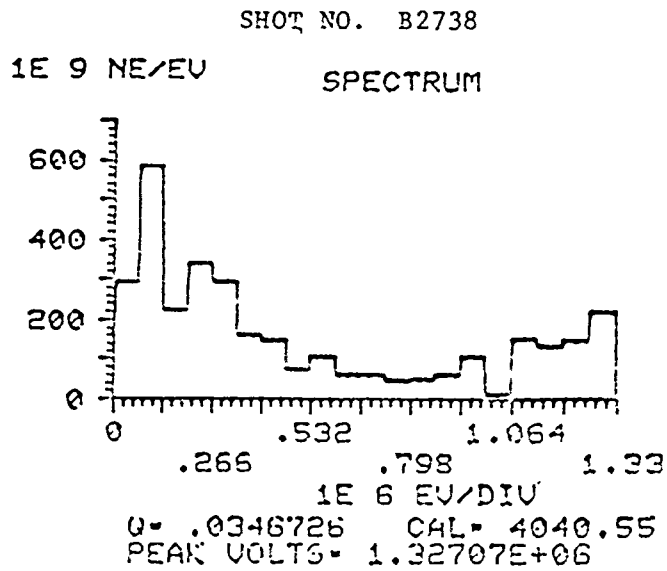

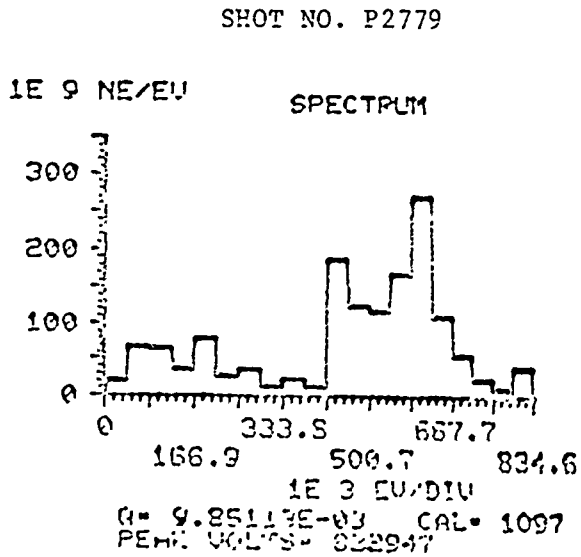

Figures A11-A14. Ktech aluminum spectral graphs: quartz gauge.

SHOT NO. P2782

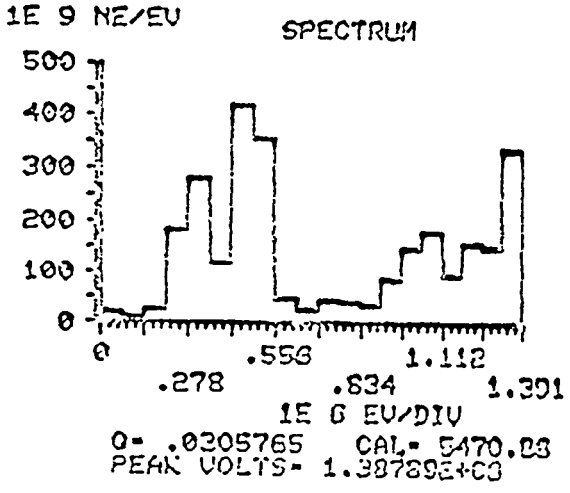

SHOT NO. B2922

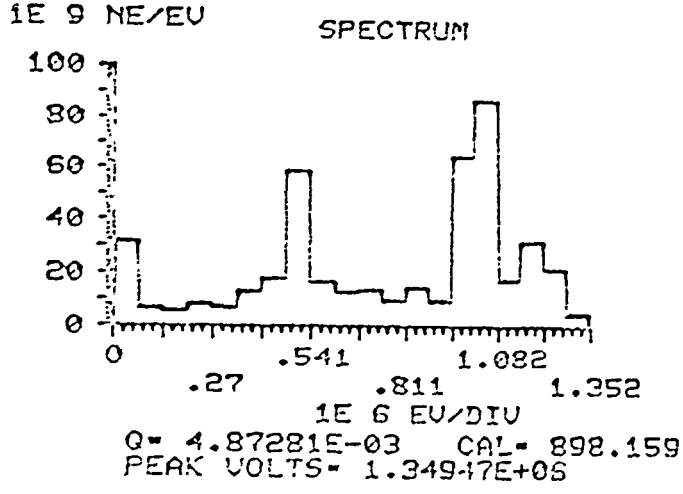

Figures A15-A16. Ktech aluminum spectral graphs: quartz gauge.

Al-Ktech

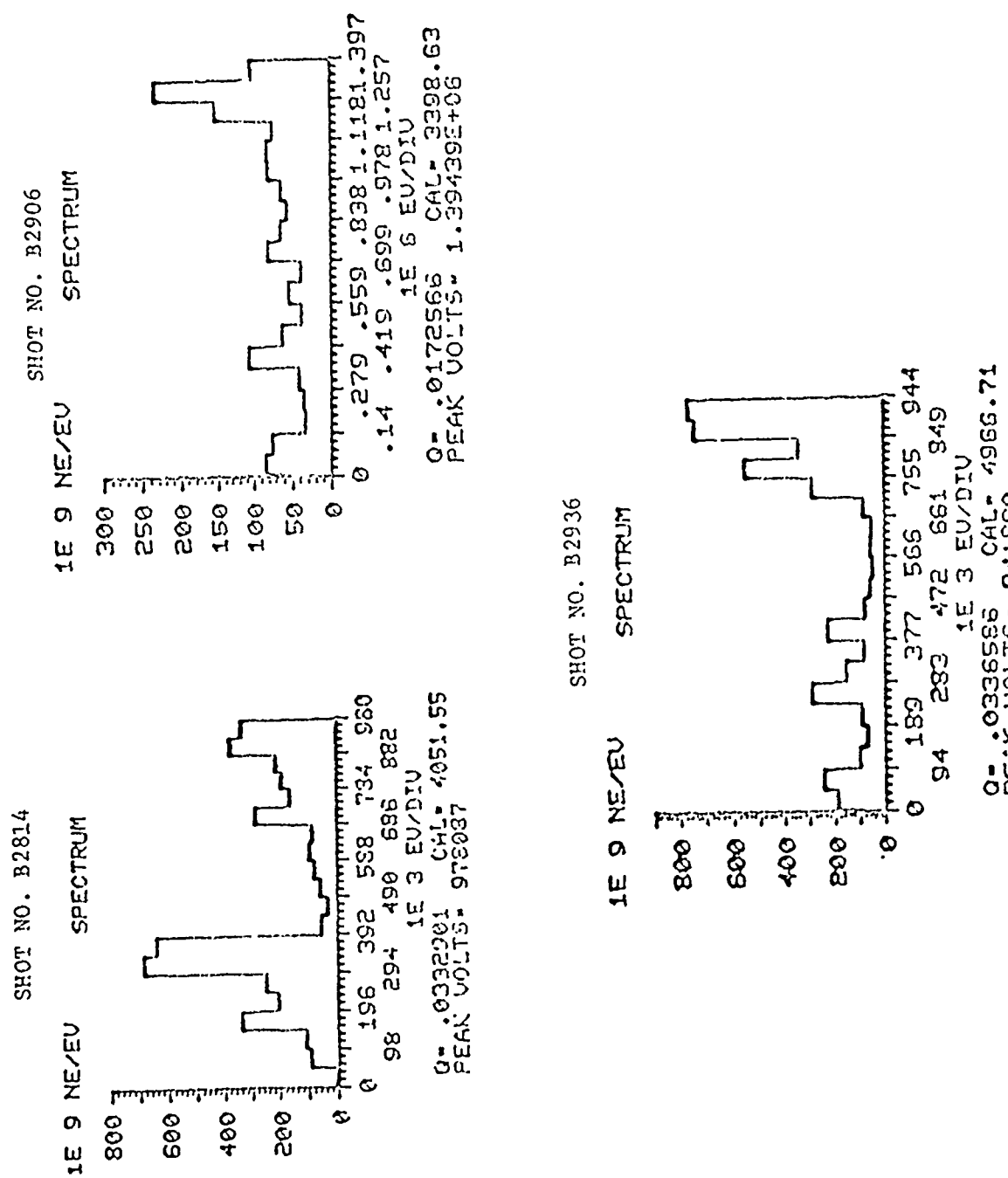

Figures A17-A19. Ktech aluminum spectral graphs: carbon gauge.

SHOT NO. B2889

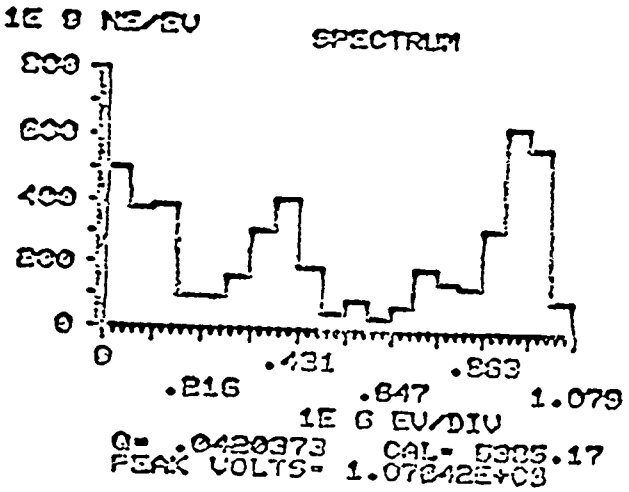

SHOT NO. B2890

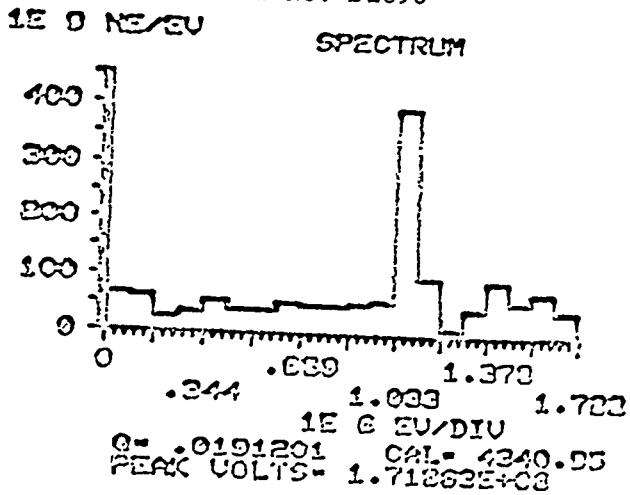

SHOT NO. B2897

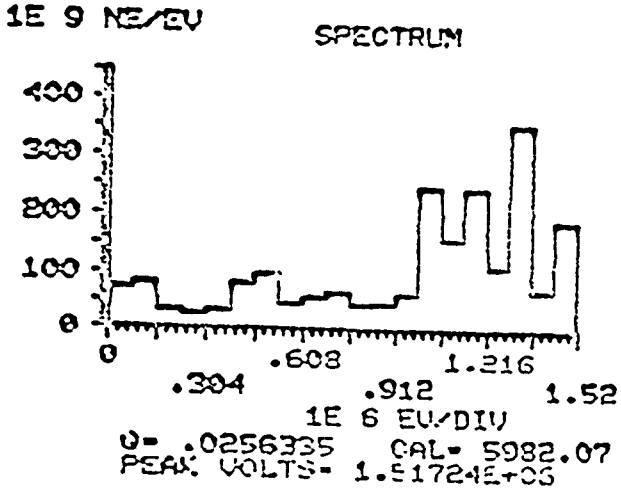

SHOT NO. B2898

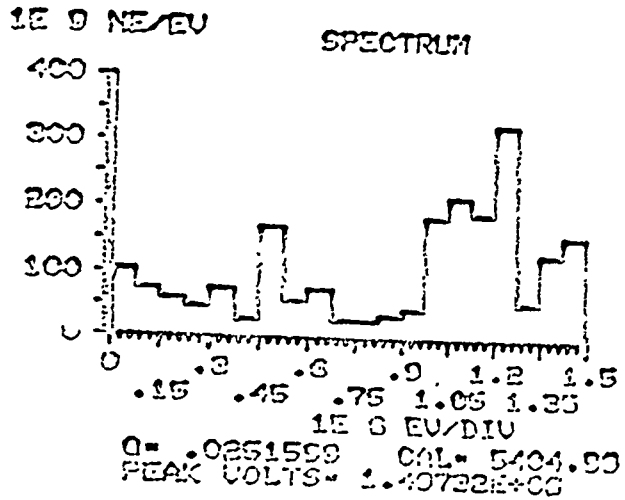

Figures A20-A23. Ktech aluminum spectral graphs: LVI.

Al-Ktech

Figures A24-A25. Ktech aluminum spectral graphs: LVI.

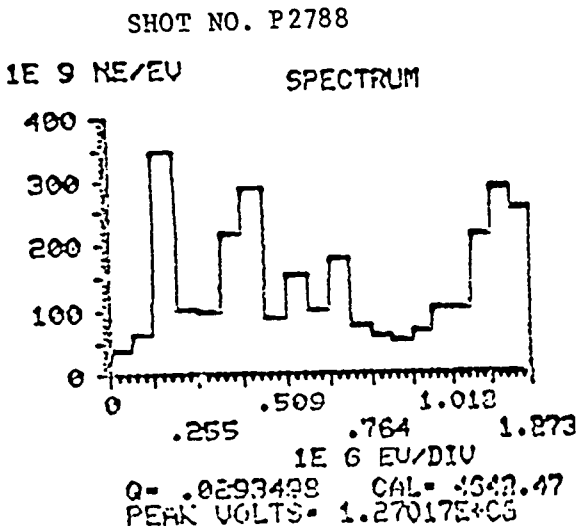

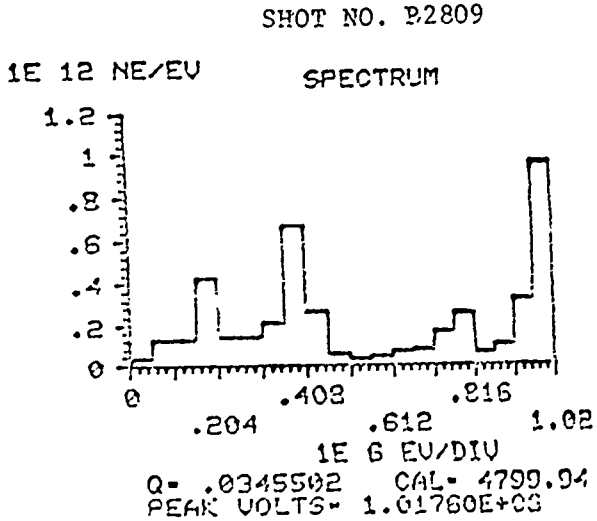

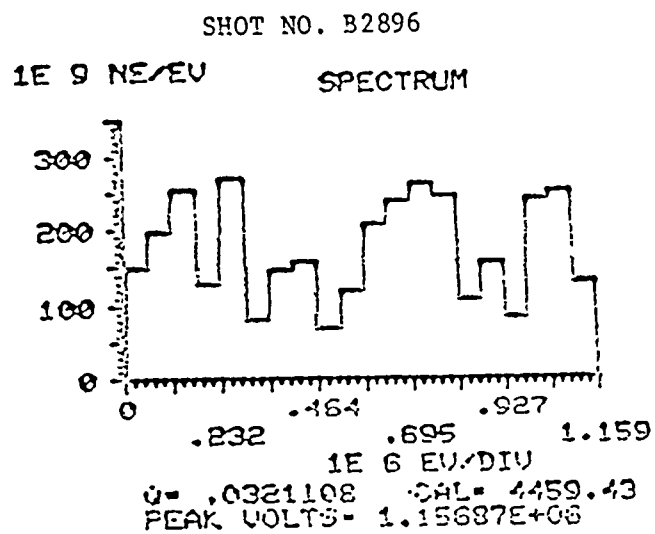

Figures A30-A32. Commonality tantalum spectral graphs: quartz gauge.

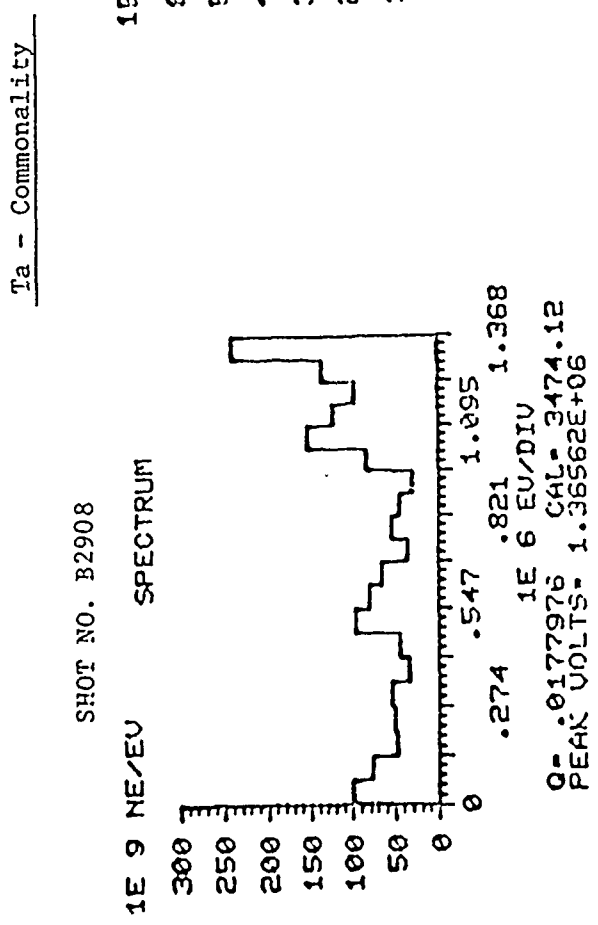

Figures A33-A34. Commonality tantalum spectral graphs: carbon gauge.

SHOT NO. P2716

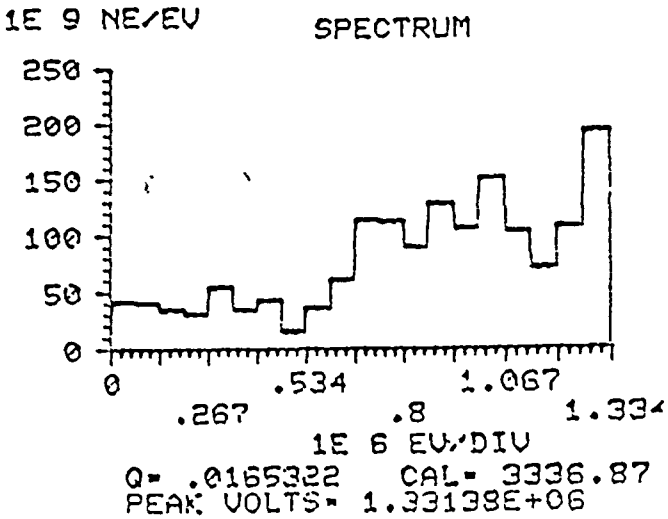

SHOT NO. B2732

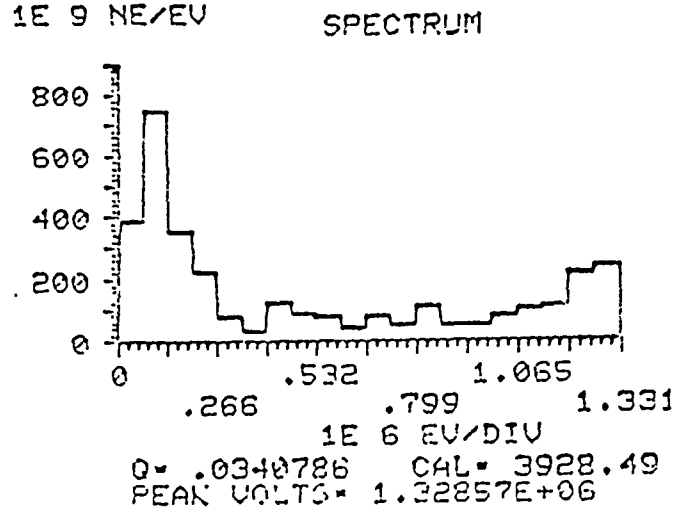

SHOT NO. P2803

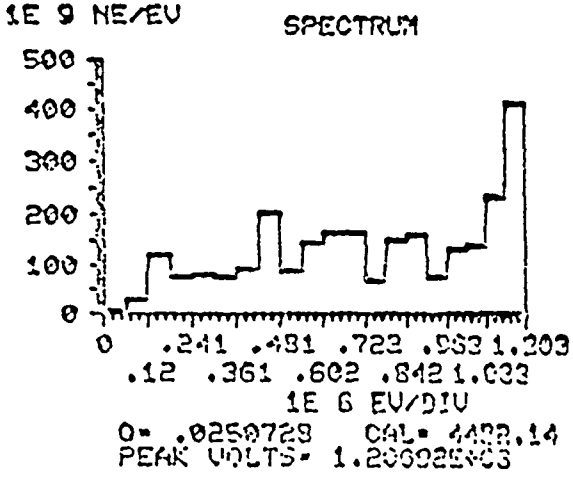

SHOT NO. B2824

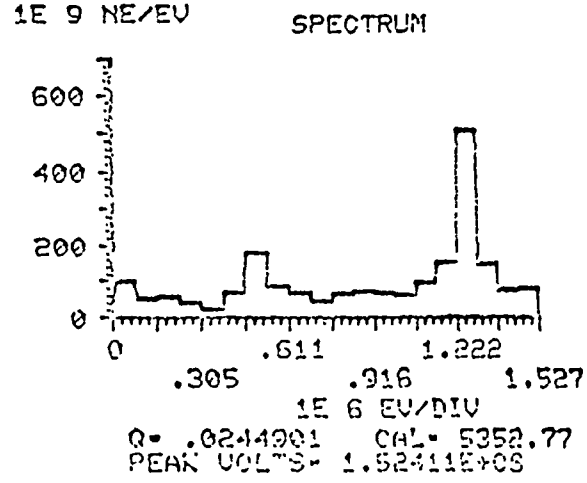

Figures A35-A38. Ktech tantalum spectral graphs: quartz gauge.

Ta - Ktech

SHOT NO. B2885

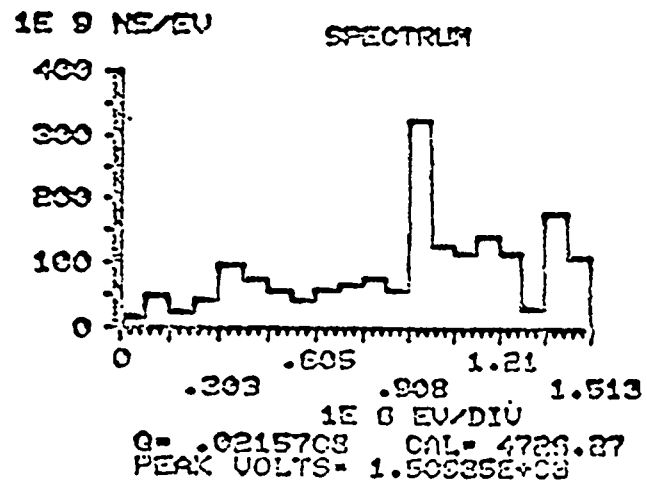

SHOT NO. B2888

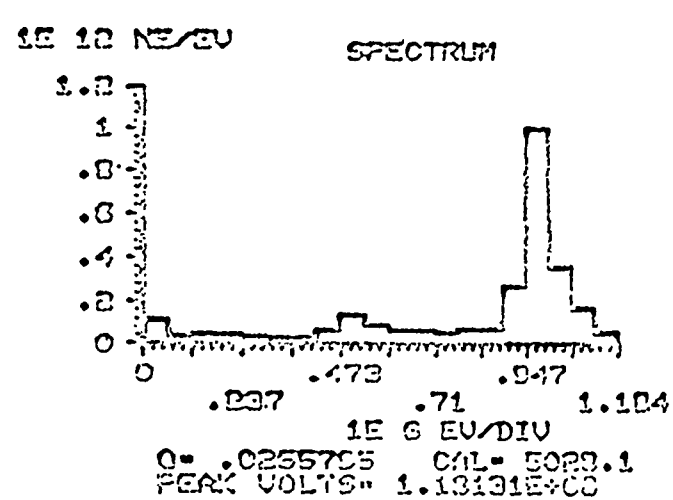

SHOT NO. B2935

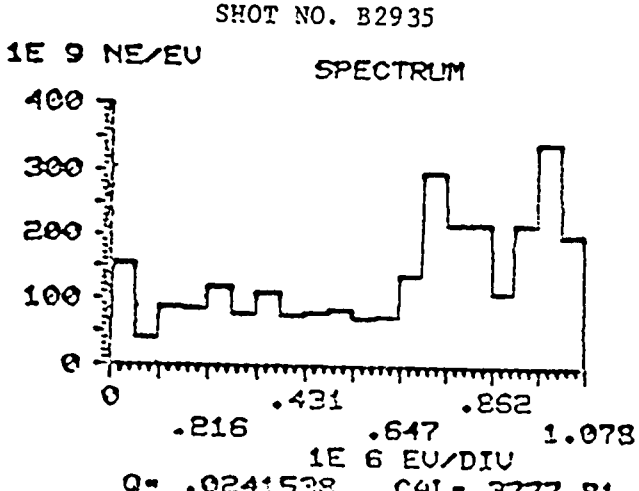

SHOT NO. B2938

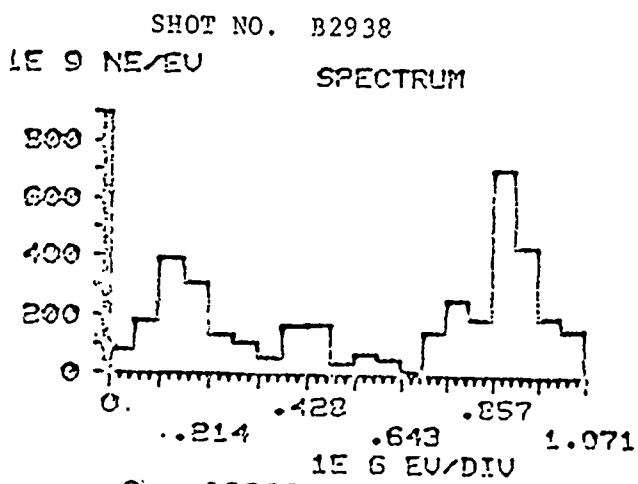

Figures A39-A42. Ktech tantalum spectral graphs: quartz gauge.

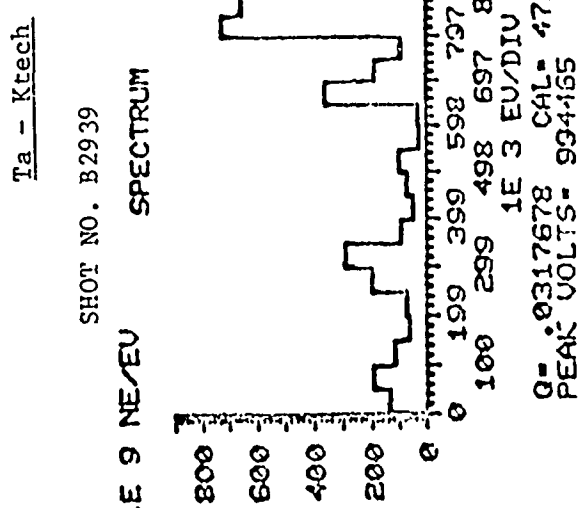

Figure 113. Ktech tantalum spectral graph: carbon gauge.

Ta - Ktech

SHOT NO. B2893

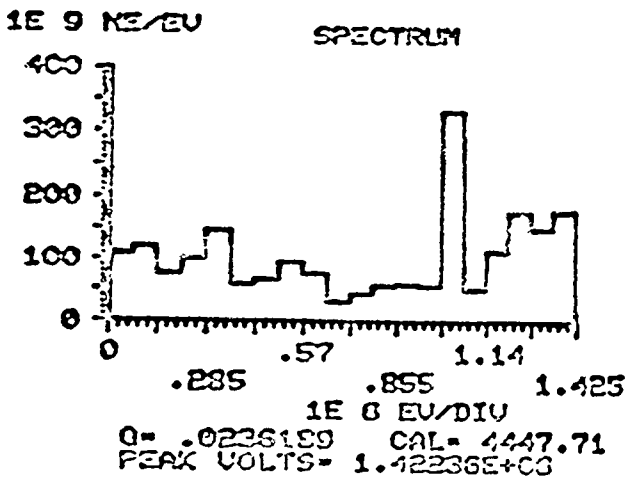

SHOT NO. B2895

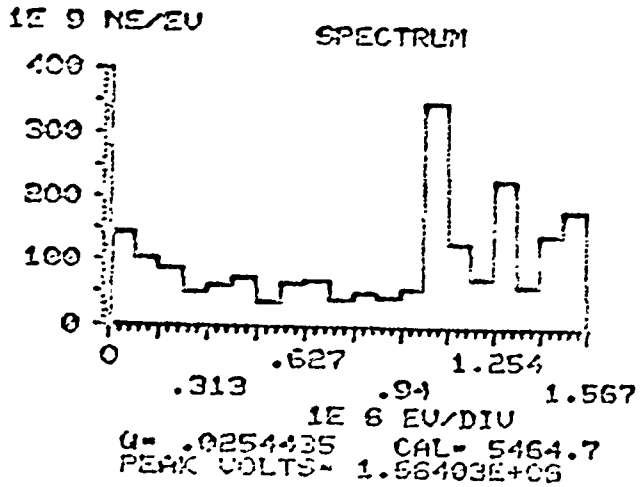

Figures A44-A45. Ktech tantalum spectral graphs: LVI.

BLKJACK-3' SHOT # P2710 27-APR-79 8:45

BINS	VALUES	VOLTS	VALUES/MAX
1	5.47431E+15	36691.7	.193018
2	2.98080E+15	110075	.1051
3	2.41023E+15	183458	.0849821
4	3.16339E+15	256842	.111538
5	4.25721E+15	330225	.150105
6	3.81975E+15	403609	.13468
7	2.90993E+15	476992	.102601
8	3.73128E+15	550375	.131561
9	1.33462E+15	623759	.0470571
10	3.13514E+15	697142	.110542
11	2.48668E+15	770526	.0876778
12	3.88193E+15	843909	.136873
13	3.09906E+15	917292	.109269
14	2.83616E+16	990676	1
15	7.15064E+15	1.06406E+06	.252124
16	5.91376E+15	1.13744E+06	.208513
17	4.52965E+15	1.21083E+06	.159711
18	5.23395E+15	1.28421E+06	.184543
19	6.88927E+15	1.35759E+06	.242908
20	1.32640E+16	1.43098E+06	.467673

AVE. ENERGY= 896255

RMS DEVIATION= 410573

DEVIATION= 45.8099%

BLKJACK-3' SHOT # P2715 30-APR-79 10:45

BINS	VALUES	VOLTS	VALUES/MAX
1	4.71888E+15	28939.3	.168752
2	1.65702E+15	86818	.0592568
3	1.97425E+15	144697	.0706012
4	2.22165E+15	202575	.0794424
5	1.47745E+15	260454	.052835
6	2.09039E+15	318333	.0747545
7	8.05619E+14	376211	.0288097
8	1.68678E+14	434090	6.03210E-03
9	1.87039E+15	491969	.0668333
10	1.42624E+15	549847	.050988
11	9.50556E+14	607726	.0339928
12	1.52519E+15	665605	.0545424
13	2.11516E+15	723483	.0756401
14	3.66149E+15	781362	.130938
15	8.35716E+15	839241	.29886
16	2.79634E+16	897120	1
17	1.48300E+16	954998	.530122
18	5.80918E+15	1.01288E+06	.207742
19	6.57247E+15	1.07076E+06	.235038
20	1.64822E+16	1.12863E+06	.589421

AVE. ENERGY= 824211

RMS DEVIATION= 303196

DEVIATION= 36.7862%

BLKJACK-3' SHOT # P2716 30-APR-79 11:30

BINS	VALUES	VOLTS	VALUES/MAX
1	2.70928E+15	33284.6	.213115
2	2.69605E+15	99853.7	.212074
3	2.28596E+15	166423	.179816
4	1.97119E+15	232992	.155056
5	3.61490E+15	299561	.284352
6	2.24576E+15	366130	.176654
7	2.81162E+15	432699	.221165
8	1.00191E+15	499268	.0788115
9	2.32882E+15	565838	.183188
10	4.02137E+15	632407	.316325
11	7.47394E+15	698976	.587908
12	7.40674E+15	765545	.582623
13	5.90069E+15	832114	.464154
14	8.48348E+15	898683	.66732
15	6.98333E+15	965252	.549316
16	9.97125E+15	1.03182E+06	.78435
17	6.84307E+15	1.09839E+06	.538283
18	4.64659E+15	1.16496E+06	.365506
19	7.08847E+15	1.23153E+06	.557587
20	1.27128E+16	1.29810E+06	1

AVE. ENERGY= 845962

RMS DEVIATION= 353405

DEVIATION= 41.7755%

BLKJACK-3 SHOT # B2725 2-MAY-79 16:45

BINS	VALUES	VOLTS	VALUES/MAX
1	9.27047E+14	34069.8	.0314197
2	1.28207E+15	102209	.0434522
3	8.98778E+15	170349	.304616
4	6.82571E+14	238489	.0231339
5	1.10647E+16	306628	.375007
6	1.88496E+16	374768	.638857
7	2.59214E+16	442907	.878535
8	2.72876E+16	511047	.924837
9	1.64361E+16	579186	.557058
10	2.95053E+16	647326	1
11	1.70214E+16	715465	.576895
12	8.58847E+15	783605	.291082
13	5.37744E+15	851745	.182254
14	2.65097E+15	919884	.0898473
15	5.12161E+15	988024	.173583
16	2.92034E+15	1.05616E+06	.0989768
17	2.80178E+15	1.12430E+06	.0949535
18	4.88472E+15	1.19244E+06	.165554
19	9.83628E+15	1.26058E+06	.333374
20	2.38629E+16	1.32372E+06	.808768

AVE. ENERGY= 685288

RMS DEVIATION= 337573

DEVIATION= 49.2599%

BLKJACK-3 SHOT # B2728 3-MAY-79 10:20

BINS	VALUES	VOLTS	VALUES/MAX
1	3.38203E+15	31689	.17859
2	3.09073E+15	95067.1	.163207
3	1.91834E+15	158445	.101299
4	1.15839E+16	221823	.611695
5	9.91343E+15	285201	.523484
6	3.38938E+15	348579	.178978
7	4.71681E+15	411957	.249074
8	6.02583E+15	475335	.318197
9	4.62077E+15	538713	.244002
10	4.67971E+15	602092	.247114
11	4.90810E+15	665470	.259175
12	6.84789E+15	728848	.361609
13	4.30674E+15	792226	.22742
14	7.21487E+15	855604	.380985
15	7.09037E+15	918982	.374411
16	1.89374E+16	982360	1
17	1.42900E+16	1.04574E+06	.75459
18	8.40766E+15	1.10912E+06	.443971
19	2.85760E+15	1.17249E+06	.150897
20	1.92458E+15	1.23587E+06	.101628

AVE. ENERGY= 694485

RMS DEVIATION= 341941

DEVIATION= 49.2366%

BLKJACK-3 SHOT # B2729 3-MAY-79 11:20

BINS	VALUES	VOLTS	VALUES/MAX
1	9.71232E+15	26799.1	.497824
2	8.07451E+15	80397.3	.413875
3	1.31436E+16	133996	.673701
4	1.19624E+16	187594	.613154
5	1.25459E+16	241192	.643064
6	7.73012E+15	294790	.396222
7	3.81654E+15	348388	.195624
8	8.38630E+15	401987	.429856
9	8.19675E+15	455585	.42014
10	7.57938E+15	509183	.388496
11	7.54466E+15	562781	.386716
12	7.34117E+15	616379	.376286
13	3.07914E+15	669977	.157827
14	2.40360E+15	723576	.123201
15	5.96541E+15	777174	.305769
16	1.53253E+15	830772	.0785527
17	6.34507E+15	884370	.325229
18	1.29510E+16	937968	.663829
19	1.67075E+16	991567	.856376
20	1.95096E+16	1.04516E+06	1

AVE. ENERGY= 548410

RMS DEVIATION= 352515

DEVIATION= 64.2795%

BLKJACK-3 SHOT # B2732 3-MAY-79 15:00

BINS	VALUES	VOLTS	VALUES/MAX
1	2.55914E+16	33214.1	.515398
2	4.96537E+16	99642.4	1
3	2.33245E+16	166071	.469743
4	1.47886E+16	232499	.297834
5	5.08137E+15	298927	.102336
6	2.01892E+15	365356	.04066
7	8.11588E+15	431784	.16345
8	5.61540E+15	498212	.113091
9	5.12392E+15	564640	.103193
10	2.65759E+15	631069	.0535226
11	4.99649E+15	697497	.100627
12	3.32153E+15	763925	.0668939
13	7.21922E+15	830353	.145391
14	3.34581E+15	896782	.0673829
15	3.40467E+15	963210	.0685683
16	4.94155E+15	1.02964E+06	.0995203
17	6.63711E+15	1.09607E+06	.133668
18	7.25128E+15	1.16249E+06	.146037
19	1.41143E+16	1.22892E+06	.284255
20	1.55220E+16	1.29535E+06	.312605

AVE. ENERGY= 483155

RMS DEVIATION= 455814

DEVIATION= 94.3411%

BLKJACK-3 SHOT # B2730 4-MAY-79 15:40

BINS	VALUES	VOLTS	VALUES/MAX
1	1.95282E+16	33176.7	.504708
2	3.86921E+16	99530.2	1
3	1.49259E+16	165884	.385761
4	2.25323E+16	232237	.582348
5	1.95084E+16	298591	.504197
6	1.06271E+16	364944	.274659
7	9.73945E+15	431298	.251717
8	4.86419E+15	497651	.125715
9	6.98036E+15	564004	.180408
10	4.06346E+15	630358	.105021
11	3.84138E+15	696711	.0992803
12	2.98574E+15	763065	.0771666
13	3.36652E+15	829418	.087003
14	4.02109E+15	895772	.103925
15	7.00183E+15	962125	.180963
16	7.96855E+14	1.02848E+06	.0205948
17	1.00377E+16	1.09483E+06	.259426
18	8.71306E+15	1.16119E+06	.22519
19	9.85256E+15	1.22754E+06	.25464
20	1.43549E+16	1.29389E+06	.371004

AVE. ENERGY= 483423

RMS DEVIATION= 427389

DEVIATION= 87.5038%

BLKJACK-3' SHOT # P2776 22-MAY-79 1655

#INS	VALUES	VOLTS	VALUES/MAX
1	1.21782E+15	30813.5	.0450184
2	6.90002E+15	92440.6	.277053
3	3.71670E+15	154058	.148502
4	9.94747E+15	215695	.409347
5	3.21424E+15	277322	.12933
6	1.27001E+16	338949	.511189
7	1.91524E+16	400576	.770897
8	1.37588E+16	462203	.553737
9	6.44894E+15	523830	.259544
10	5.36405E+15	585457	.215882
11	3.77362E+15	647084	.151873
12	3.82362E+15	708711	.153885
13	2.15676E+15	770338	.086801
14	7.73832E+15	831965	.311437
15	3.67401E+15	893593	.147884
16	1.76117E+15	955220	.0708802
17	5.07771E+15	1.01685E+06	.204358
18	2.48472E+16	1.07847E+06	1
19	1.09935E+16	1.14010E+06	.442443
20	1.59982E+16	1.20173E+06	.643884

AVE. ENERGY= .684533

RMS DEVIATION= 369250

DEVIATION= 53.9419%

BLKJACK-3' SHOT # P2777 23-MAY-79 0950

BINS	VALUES	VOLTS	VALUES/MAX
1	1.67770E+15	29284.6	.11963
2	4.36120E+15	87853.9	.310979
3	2.73400E+15	146423	.194951
4	5.73044E+15	204993	.408615
5	4.00937E+15	263562	.285892
6	1.40241E+16	322131	1
7	1.33724E+16	380700	.953528
8	4.58070E+15	439270	.326631
9	1.14913E+16	497839	.819397
10	3.58150E+15	556408	.255382
11	2.35938E+15	614977	.168238
12	6.72238E+15	673547	.479345
13	7.89395E+15	732116	.562886
14	9.57475E+15	790685	.682738
15	2.75186E+15	849255	.196224
16	6.97103E+15	907824	.497075
17	5.03672E+15	966393	.359148
18	5.86448E+15	1.02496E+06	.418172
19	1.02217E+16	1.08353E+06	.728565
20	5.23517E+15	1.14210E+06	.373299

AVE. ENERGY= 610991

RMS DEVIATION= 313189

DEVIATION= 51.2592%

BLKJACK-3' SHOT # P2779 14-MAY-79 1130

BINS	VALUES	VOLTS	VALUES/MAX
1	8.22889E+14	20823.7	.0733754
2	2.75140E+15	62471	.245337
3	2.68404E+15	104118	.239331
4	1.44289E+15	145766	.12866
5	3.26726E+15	187413	.291335
6	1.05750E+15	229060	.094295
7	1.45433E+15	270708	.129684
8	5.28822E+14	312355	.0471605
9	9.26853E+14	354002	.0826453
10	5.25478E+14	395650	.0468553
11	7.80320E+15	437297	.695705
12	5.16936E+15	478944	.460941
13	4.89715E+15	520592	.436669
14	6.93194E+15	562239	.618065
15	1.12148E+16	603886	1
16	4.58575E+15	645534	.408902
17	2.36824E+15	687181	.211171
18	9.28542E+14	728828	.0827962
19	4.63366E+14	770476	.0413174
20	1.61943E+15	812123	.144401

AVE. ENERGY= 466726

RMS DEVIATION= 196327

DEVIATION= 42.0649%

BLKJACK-3' SHOT # P2782 29-MAY-79 1315

BINS	VALUES	VOLTS	VALUES/MAX
1	1.33546E+15	34697.2	.041041
2	7.53805E+14	104091	.0231071
3	1.78956E+15	173486	.055004
4	1.27915E+16	242880	.437015
5	1.94487E+16	312274	.660009
6	8.10712E+15	381669	.279305
7	2.90229E+16	451063	1
8	2.46164E+16	520457	.843171
9	3.37042E+15	589852	.116133
10	1.73005E+15	659246	.0590316
11	2.99034E+15	728640	.10302
12	2.73068E+15	798035	.0930977
13	2.49353E+15	867429	.0859154
14	5.86410E+15	936823	.202051
15	1.03192E+16	1.00682E+06	.355394
16	1.25638E+16	1.07581E+06	.432901
17	6.52152E+15	1.14501E+06	.224703
18	1.08463E+16	1.21440E+06	.373714
19	1.04226E+16	1.28320E+06	.359117
20	2.32347E+16	1.35315E+06	.800564

AVE. ENERGY= 749911

RMS DEVIATION= 401007

DEVIATION= 53.4739%

IV

BLKJACK-3' SHOT # P2783 29-MAY-79 1410

BINS	VALUES	VOLTS	VALUES/MAX
1	8.22417E+13	30942.1	1.85667E-03
2	4.66283E+13	92826.2	1.05267E-03
3	3.24274E+15	154710	.0732074
4	3.88290E+15	216594	.0876595
5	1.18706E+16	278479	.267958
6	6.20274E+15	340363	.140032
7	1.53919E+16	402247	.347485
8	3.51912E+16	464131	.79447
9	1.40493E+16	526015	.317174
10	9.19010E+15	587899	.207474
11	2.81662E+15	649783	.0635674
12	5.67394E+15	711667	.128094
13	3.87581E+15	773552	.0874994
14	3.48866E+15	835436	.0787592
15	2.75091E+15	897320	.062104
16	6.73517E+15	959204	.152052
17	3.13907E+15	1.02109E+06	.0708571
18	5.23562E+15	1.08297E+06	.118188
19	1.26416E+16	1.14486E+06	.285393
20	4.42952E+16	1.20674E+06	1

AVE. ENERGY= 735472

RMS DEVIATION= 356137

DEVIATION= 48.4311%

BLKJACK-3' SHOT # P2765 29-MAY-79 1635

BINS	VALUES	VOLTS	VALUES/MAX
1	1.30024E+15	33799.1	.0401837
2	2.02041E+15	101397	.0624172
3	5.33623E+15	168996	.164894
4	1.57629E+16	236594	.486939
5	2.14558E+16	304192	.662839
6	5.70431E+15	371791	.176225
7	6.05800E+15	439389	.187152
8	2.74936E+15	506987	.0849035
9	2.42972E+15	574586	.075032
10	2.81589E+15	642184	.0869921
11	3.75058E+15	709782	.115863
12	1.21653E+16	777380	.375935
13	3.03259E+15	844979	.0936868
14	1.19139E+15	912577	.0368069
15	4.35318E+15	980175	.134484
16	6.33247E+15	1.04777E+06	.195631
17	2.81331E+15	1.11537E+06	.0869123
18	1.77710E+16	1.18297E+06	.549005
19	1.16413E+16	1.25057E+06	.359633
20	3.23695E+16	1.31817E+06	1

AVE. ENERGY= 800016

RMS DEVIATION= 438327

DEVIATION= 54.7898%

BLKJACK-3' SHOT # P2788 30-MAY-79 1125

BINS	VALUES	VOLTS	VALUES/MAX
1	2.42226E+15	31754.3	.109453
2	4.10339E+15	95262.8	.18544
3	2.21306E+16	158771	1
4	6.43764E+15	222280	.290893
5	6.28707E+15	285788	.28409
6	1.37602E+16	349297	.621771
7	1.83490E+16	412806	.829185
8	5.62164E+15	476314	.254021
9	9.67000E+15	539823	.436958
10	6.36714E+15	603331	.287707
11	1.12058E+16	666840	.506348
12	4.80044E+15	730348	.216914
13	3.77863E+15	793857	.170745
14	3.34599E+15	857365	.151193
15	4.35822E+15	920874	.196902
16	6.45451E+15	984382	.291656
17	6.53717E+15	1.04789E+06	.295391
18	1.34247E+16	1.11140E+06	.606615
19	1.81087E+16	1.17491E+06	.818284
20	1.60437E+16	1.23842E+06	.724953

AVE. ENERGY= 662958

RMS DEVIATION= 389695

DEVIATION= 58.7813%

BLKJACK-3' SHOT # P2791 30-MAY-79 1545

BINS	VALUES	VOLTS	VALUES/MAX
1	3.46933E+15	25133.6	.0916093
2	1.45975E+16	75400.7	.382929
3	1.42166E+16	125668	.372937
4	2.41404E+16	175935	.633263
5	2.25973E+16	226202	.592784
6	2.10939E+16	276469	.553347
7	7.42145E+14	326736	.0194683
8	1.09287E+15	377003	.0286686
9	5.54025E+15	427270	.145335
10	2.70687E+15	477538	.0710079
11	2.47594E+15	527805	.0649501
12	2.18796E+15	578072	.0573958
13	2.94371E+15	628339	.0772208
14	1.53501E+15	678606	.0402667
15	1.16091E+16	728873	.304536
16	3.99123E+15	779140	.1047
17	4.35769E+15	829407	.114313
18	5.93159E+15	879674	.156124
19	2.17821E+16	929942	.571398
20	3.81206E+16	980209	1

AVE. ENERGY= 516619

RMS DEVIATION= 355189

DEVIATION= 68.7525%

BLKJACK-3' SHOT # P2801 1-JUN-79 1500

BINS	VALUES	VOLTS	VALUES/MAX
1	1.47272E+14	28150.5	5.24307E-03
2	3.66258E+15	84451.4	.130393
3	8.15893E+15	140752	.290469
4	1.99542E+16	197053	.710306
5	8.26616E+15	253354	.294287
6	4.34859E+15	309655	.154816
7	1.09939E+16	365956	.391309
8	2.06500E+16	422257	.735167
9	1.17847E+16	478558	.419549
10	1.08991E+16	534859	.388023
11	7.81115E+15	591160	.278083
12	2.93176E+15	647461	.104375
13	8.13431E+15	703762	.289592
14	5.01064E+15	760063	.178376
15	6.79679E+15	816363	.241975
16	1.11560E+16	872664	.39717
17	8.28069E+15	928965	.294804
18	4.63757E+15	985266	.165104
19	2.42621E+16	1.04157E+06	.863762
20	2.80888E+16	1.09787E+06	1

AVE. ENERGY= 644494

RMS DEVIATION= 334578

DEVIATION= 51.9133%

BLKJACK-3' SHOT # P2802 1-JUN-79 1555

BINS	VALUES	VOLTS	VALUES/MAX
1	1.39763E+15	29014.9	.0547618
2	4.79232E+15	87044.8	.187708
3	7.44197E+15	145075	.29153
4	1.49797E+16	203105	.586911
5	1.24363E+16	261134	.487231
6	1.59844E+16	319164	.626278
7	1.70865E+16	377194	.669458
8	2.97865E+15	435224	.116705
9	4.01070E+15	493254	.157141
10	6.03763E+15	551284	.236568
11	1.10508E+16	609313	.432975
12	3.89835E+15	667343	.152712
13	1.40531E+15	725373	.0550553
14	1.30300E+15	783403	.0510459
15	5.45723E+15	841433	.213819
16	5.92465E+15	899463	.232131
17	1.3551CE+16	957493	.530936
18	8.24235E+15	1.01552E+06	.322939
19	9.12391E+15	1.07355E+06	.35748
20	2.56229E+16	1.13159E+06	1

AVE. ENERGY= 621597

RMS DEVIATION= 361458

DEVIATION= 58.1499%

BLKJACK-3 SHOT # P2803 1-JUN-79 1655

BINS	VALUES	VOLTS	VALUES/MAX
1	3.52340E+14	30022.9	.0142994
2	1.58445E+15	90088.7	.064211
3	7.16237E+15	150115	.29025
4	4.57432E+15	210160	.185373
5	4.73667E+15	270206	.191957
6	4.56040E+15	330252	.184813
7	5.53308E+15	390298	.224232
8	1.21560E+16	450344	.49253
9	5.30499E+15	510389	.214938
10	8.73637E+15	570435	.354047
11	9.83620E+15	630481	.400645
12	9.88785E+15	690527	.400712
13	4.00860E+15	750573	.162451
14	8.94099E+15	810618	.36234
15	9.57653E+15	870664	.388095
16	4.55092E+15	930710	.184429
17	7.97528E+15	990756	.323204
18	8.33395E+15	1.05080E+06	.337739
19	1.39719E+16	1.11085E+06	.56622
20	2.46757E+16	1.17089E+06	1

AVE. ENERGY= 749245

RMS DEVIATION= 329333

DEVIATION= 43.9554%

BLKJACK-3' SHOT # P2806 4-JUNE-79 10:45

BINS	VALUES	VOLTS	VALUES/MAX
1	2.41514E+13	30859.7	7.03822E-04
2	6.13880E+13	92579.2	1.78897E-03
3	4.14792E+14	154299	.0120879
4	7.84429E+15	216018	.228599
5	7.91422E+15	277738	.230637
6	3.19149E+15	339457	.0930066
7	8.23675E+14	401177	.0240036
8	6.71803E+14	462896	.0195777
9	1.09190E+15	524615	.0318203
10	1.46542E+15	586335	.0427053
11	7.32615E+15	648054	.213499
12	9.10197E+15	709774	.26525
13	7.37650E+15	771493	.214966
14	9.19727E+15	833213	.268027
15	5.79934E+15	894932	.169005
16	2.18570E+15	956652	.0636959
17	5.01870E+14	1.01837E+06	.0146255
18	1.27309E+16	1.08009E+06	.371004
19	8.35871E+15	1.14181E+06	.24359
20	3.43147E+16	1.20353E+06	1

AVE. ENERGY= 864375

RMS DEVIATION= 335342

DEVIATION= 38.7958%

BLKJACK-3' SHOT # P2809 4-JUNE-79 15:20

BINS	VALUES	VOLTS	VALUES/MAX
1	1.81592E+15	25440.1	.0377512
2	6.36765E+15	76320.2	.132377
3	6.36323E+15	127200	.132285
4	2.16466E+16	178020	.450013
5	6.96130E+15	228961	.144719
6	7.08413E+15	279841	.147272
7	1.07087E+16	330721	.222624
8	3.42078E+16	381601	.711143
9	1.34241E+16	432481	.279074
10	2.63130E+15	483361	.0547021
11	1.67471E+15	534241	.0348156
12	2.20486E+15	585121	.0458369
13	3.44228E+15	636001	.0715617
14	3.52673E+15	686882	.0733174
15	8.32250E+15	737762	.173017
16	1.27718E+16	788642	.265512
17	3.19844E+15	839522	.0664924
18	5.02712E+15	890402	.104509
19	1.61880E+16	941282	.336532
20	4.81023E+16	992162	1

AVE. ENERGY= 582273

RMS DEVIATION= 323719

DEVIATION= 55.5957%

BLKJACK-3' SHOT # P2814 5-JUNE-79 14:04

BINS	VALUES	VOLTS	VALUES/MAX
1	1.65440E+14	24452.2	4.95901E-03
2	4.43919E+15	73356.5	.133063
3	5.30688E+15	122261	.159132
4	1.63355E+16	171165	.489651
5	9.99081E+15	220070	.299471
6	1.21822E+16	268974	.365157
7	3.33615E+16	317878	1
8	3.13299E+16	366783	.939102
9	2.46858E+15	415687	.0739949
10	1.47516E+15	464591	.0442173
11	2.65040E+15	513496	.0794446
12	3.77761E+15	562400	.113232
13	4.58488E+15	611304	.13743
14	4.13936E+15	660209	.124076
15	1.38681E+16	709113	.415692
16	7.91768E+15	758017	.237329
17	9.15528E+15	806922	.274426
18	1.02300E+16	855826	.30664
19	1.81098E+16	904730	.542836
20	1.63132E+16	953635	.488982

AVE. ENERGY- 510091

RMS DEVIATION- 279694

DEVIATION- 54.8321%

BLKJACK-3 SHOT # B2820 7-JUNE-79 13:30

BINS	VALUES	VOLTS	VALUES/MAX
1	2.47299E+16	31907.4	.483831
2	7.73177E+15	95722.2	.152833
3	1.26510E+16	159537	.25007
4	5.89809E+15	223352	.116587
5	6.24489E+15	287167	.123442
6	1.47728E+16	350982	.292011
7	1.42315E+16	414796	.281311
8	7.80405E+15	478611	.154261
9	4.37511E+15	542426	.0864821
10	2.59384E+15	606241	.051272
11	1.77951E+15	670056	.0351753
12	6.77327E+15	733870	.133886
13	1.86111E+15	797685	.0367882
14	2.84183E+15	861500	.056174
15	3.89406E+15	925315	.0769732
16	2.94115E+15	989130	.0581372
17	6.00311E+15	1.05294E+06	.118663
18	1.48285E+16	1.11676E+06	.293113
19	5.05898E+16	1.18057E+06	1
20	2.84369E+16	1.24439E+06	.562108

AVE. ENERGY= 724166

RMS DEVIATION= 462564

DEVIATION= 63.8754%

BLKJACK-3 SHOT # B2824 8-JUNE-79 1445

BINS	VALUES	VOLTS	VALUES/MAX
1	7.50302E+15	38102.9	.195855
2	3.82993E+15	114309	.0999748
3	4.25471E+15	190514	.111063
4	3.02422E+15	266720	.078943
5	1.71007E+15	342926	.044639
6	5.08671E+15	419131	.132781
7	1.36243E+16	495337	.355644
8	6.49959E+15	571543	.169662
9	5.01453E+15	647749	.130897
10	3.20410E+15	723954	.0836335
11	4.87592E+15	800160	.127279
12	5.26404E+15	876366	.13741
13	5.00818E+15	952571	.130731
14	4.41915E+15	1.02878E+06	.115355
15	7.08522E+15	1.10498E+06	.184949
16	1.14435E+16	1.18119E+06	.298716
17	3.83090E+16	1.25739E+06	1
18	1.12962E+16	1.33360E+06	.29487
19	5.64837E+15	1.40981E+06	.147442
20	5.77146E+15	1.48601E+06	.150655

AVE. ENERGY= 916071

RMS DEVIATION= 428878

DEVIATION= 46.8171%

BLKJACK-3 SHOT # B2271 24-JULY-79 13:04

BINS	VALUES	VOLTS	VALUES/MAX
1	1.18906E+16	33654.5	.582549
2	4.61513E+15	100964	.226106
3	4.40973E+15	168273	.216043
4	3.23488E+15	235582	.158484
5	1.26064E+16	302891	.617616
6	4.31988E+15	370200	.211641
7	3.33044E+15	437509	.163166
8	3.62652E+15	504818	.177672
9	3.02754E+15	572127	.148326
10	6.51218E+15	639436	.319047
11	3.29989E+15	706745	.161669
12	5.27203E+15	774054	.258288
13	3.06445E+15	841363	.150134
14	1.55194E+16	908672	.760329
15	1.35371E+16	975981	.663213
16	1.03639E+16	1.04329E+06	.507753
17	4.40865E+15	1.11060E+06	.21599
18	3.45416E+15	1.17791E+06	.169227
19	5.16843E+15	1.24522E+06	.253213
20	2.04114E+16	1.31253E+06	1

AVE. ENERGY= 748075

RMS DEVIATION= 421124

DEVIATION= 56.2943%

BLKJACK-3 SHOT # B2874 25-JUL.-79 1338

BINS	VALUES	VOLTS	VALUES/MAX
1	4.20067E+15	36751.9	.162751
2	8.64853E+15	110256	.335079
3	2.54507E+15	183759	.0986064
4	2.97293E+15	257263	.115183
5	6.63127E+15	330767	.256922
6	7.69791E+15	404271	.298249
7	3.38110E+15	477775	.130998
8	4.76180E+15	551278	.184491
9	1.87478E+15	624782	.0726366
10	5.17500E+15	698286	.2005
11	6.18231E+15	771790	.239528
12	5.79373E+15	845294	.224473
13	1.96888E+16	918797	.762794
14	1.66322E+16	992301	.644398
15	1.02306E+16	1.06581E+06	.396374
16	1.03161E+16	1.13931E+06	.399689
17	2.58104E+16	1.21281E+06	1
18	6.60075E+15	1.28632E+06	.25574
19	7.80848E+15	1.35982E+06	.302532
20	3.85629E+15	1.43332E+06	.149409

AVE. ENERGY= 867681

RMS DEVIATION= 385222

DEVIATION= 44.3967%

BLKJACK-3 SHOT # B2875 25-JUL-79 1550

BINS	VALUES	VOLTS	VALUES/MAX
1	1.22466E+15	34843.7	.0388306
2	3.58480E+15	104531	.113664
3	3.01122E+15	174219	.0954773
4	2.19501E+15	243906	.0695977
5	2.38928E+15	313593	.0757575
6	4.03979E+15	383281	.12809
7	3.97631E+15	452968	.126078
8	4.51555E+15	522656	.143176
9	3.29435E+15	592343	.104455
10	4.68219E+15	662030	.148459
11	3.77779E+15	731718	.119783
12	4.41010E+15	801405	.139832
13	4.18512E+15	871093	.132699
14	5.83454E+15	940780	.184997
15	3.15386E+16	1.01047E+06	1
16	8.80717E+15	1.08015E+06	.279251
17	2.04224E+16	1.14984E+06	.647537
18	3.05554E+16	1.21953E+06	.968825
19	1.92095E+15	1.28922E+06	.060908
20	1.54317E+16	1.35890E+06	.489295

AVE. ENERGY= 963691

RMS DEVIATION= 333300

DEVIATION= 34.5858%

BLKJACK-3 SHOT # B2877 26-JUL-79 1030

BINS	VALUES	VOLTS	VALUES/MAX
1	1.59420E+15	21360.3	.0306239
2	1.88759E+15	64081	.0362599
3	9.66457E+14	106802	.0185652
4	2.71940E+15	149522	.0522306
5	3.64417E+15	192243	.0700031
6	2.91069E+15	234964	.0559132
7	9.25254E+14	277684	.0177737
8	1.39199E+15	320405	.0267395
9	1.44598E+15	363126	.0277767
10	1.49867E+15	405846	.0287889
11	2.08732E+15	448567	.0400965
12	1.61261E+15	491288	.0309776
13	1.10442E+15	534008	.0212155
14	2.26843E+15	576729	.0435756
15	2.35959E+15	619449	.0453267
16	3.03498E+15	662170	.0583008
17	6.56739E+15	704891	.126157
18	2.10928E+16	747611	.405183
19	5.20573E+16	790332	1
20	1.95476E+16	833053	.375502

AVE. ENERGY= 679398

RMS DEVIATION= 213172

DEVIATION= 31.3767%

BLKJACK-3 SHOT # B2878 26-JUL-79 1125

BINS	VALUES	VOLTS	VALUES/MAX
1	8.45197E+15	30747	.165377
2	2.12217E+16	92241.1	.415239
3	1.11322E+16	153735	.21782
4	1.77675E+16	215229	.347651
5	1.05651E+16	276723	.206723
6	1.30173E+16	338217	.254705
7	9.78173E+15	399711	.191396
8	1.19296E+16	461205	.233423
9	5.69799E+15	522699	.111491
10	4.79671E+15	584193	.0938557
11	5.32718E+15	645688	.104235
12	8.79513E+15	707182	.172091
13	2.77181E+15	768676	.054235
14	5.27214E+15	830170	.103158
15	3.22471E+15	891664	.0630969
16	5.45745E+15	953158	.106784
17	2.64378E+15	1.01465E+06	.0517283
18	2.97199E+16	1.07615E+06	.58152
19	1.90124E+16	1.13764E+06	.37201
20	5.11073E+16	1.19913E+06	1

AVE. ENERGY= 694789

RMS DEVIATION= 430686

DEVIATION= 61.9881%

BLKJACK-3 SHOT # B2879 27-JUL-79 1316

BINS	VALUES	VOLTS	VALUES/MAX
1	7.00037E+15	41210.4	.2375
2	7.23149E+15	123631	.245341
3	4.19109E+15	206052	.14219
4	4.61709E+15	288473	.156643
5	4.51736E+15	370893	.15326
6	9.52841E+15	453314	.323268
7	8.22944E+15	535735	.279199
8	7.85765E+15	618156	.266585
9	5.91608E+15	700577	.200714
10	5.36751E+15	782997	.182102
11	6.27365E+15	865418	.212845
12	1.13374E+16	947839	.384641
13	2.94752E+16	1.03026E+06	1
14	1.62994E+16	1.11268E+06	.552988
15	1.66545E+16	1.19510E+06	.565032
16	7.92850E+15	1.27752E+06	.268989
17	6.70824E+15	1.35994E+06	.227589
18	6.92318E+15	1.44236E+06	.234881
19	6.00013E+15	1.52478E+06	.203565
20	4.00723E+15	1.60721E+06	.135953

AVE. ENERGY= 808287

RMS DEVIATION= 413380

DEVIATION= 46.5368%

BLKJACK-3 SHOT # B2881 26-JUL-79 1558

BINS	VALUES	VOLTS	VALUES/MAX
1	2.72717E+15	29308.1	.0875826
2	4.54482E+15	87924.4	.145956
3	3.32314E+15	146541	.106722
4	2.81928E+15	205157	.0905405
5	1.25098E+15	263773	.0401749
6	2.16198E+15	322389	.0694315
7	4.33058E+15	381006	.139076
8	4.74824E+15	439622	.152489
9	4.73656E+15	498238	.152114
10	4.59838E+15	556855	.147676
11	3.63463E+15	615471	.116726
12	5.74854E+15	674087	.184613
13	9.93331E+15	732703	.319006
14	1.68342E+16	791320	.540626
15	6.38776E+15	849936	.205142
16	9.14763E+15	908552	.293774
17	3.11383E+16	967168	1
18	1.81004E+16	1.02578E+06	.581549
19	6.33791E+15	1.08440E+06	.203541
20	6.15198E+15	1.14302E+06	.19757

AVE. ENERGY= 768698

RMS DEVIATION= 290466

DEVIATION= 37.7868%

BLKJACK-3 SHOT # B2885 27-JUL-79 1452

BINS	VALUES	VOLTS	VALUES/MAX
1	1.09093E+15	37484.9	.0431349
2	3.99293E+15	112455	.157879
3	1.46357E+15	187424	.0578688
4	3.71991E+15	262394	.147083
5	6.92658E+15	337364	.273874
6	5.60104E+15	412334	.221462
7	3.74759E+15	487304	.148178
8	3.78977E+15	562273	.149846
9	4.46358E+15	637243	.176488
10	4.96988E+15	712213	.196507
11	4.99995E+15	787183	.197696
12	4.39451E+15	862153	.173757
13	2.52911E+16	937122	1
14	9.52450E+15	1.01209E+06	.376594
15	7.67551E+15	1.08706E+06	.303486
16	1.12785E+16	1.16203E+06	.445947
17	7.89156E+15	1.23700E+06	.312029
18	2.28710E+15	1.31197E+06	.090431
19	1.32869E+16	1.38694E+06	.525357
20	8.11197E+15	1.46191E+06	.320744

AVE. ENERGY= 909185

RMS DEVIATION= 374597

DEVIATION= 41.2014%

BLKJACK-3 SHOT # B2886 27-JUL-79 1558

BINS	VALUES	VOLTS	VALUES/MAX
1	6.00942E+15	33568.3	.394899
2	3.42623E+15	100705	.225149
3	2.42145E+15	167841	.159121
4	1.73609E+15	234978	.114084
5	2.58282E+15	302114	.169726
6	4.22126E+15	369251	.277393
7	8.23227E+15	436387	.54097
8	3.08693E+15	503524	.202852
9	2.33578E+15	570660	.153492
10	1.38211E+15	637797	.0908227
11	2.51075E+15	704933	.16499
12	1.88265E+15	772070	.123715
13	4.02841E+15	839206	.26472
14	4.90729E+15	906343	.322474
15	1.41544E+16	973479	.930132
16	1.36589E+16	1.04062E+06	.897574
17	9.62648E+15	1.10775E+06	.632582
18	3.47273E+15	1.17489E+06	.228205
19	1.10061E+16	1.24203E+06	.723246
20	1.52176E+16	1.30916E+06	1

AVE. ENERGY= 849371

RMS DEVIATION= 396114

DEVIATION= 46.6361%

BLKJACK-3 SHOT # B2888 30-JUL-79 1040

BINS	VALUES	VOLTS	VALUES/MAX
1	6.34566E+15	29459.7	.106128
2	1.92456E+15	88379	.0321873
3	2.07511E+15	147298	.0347051
4	2.43868E+15	206218	.0407956
5	1.89777E+15	265137	.0317392
6	1.32198E+15	324056	.0221094
7	1.37717E+15	382976	.0230324
8	4.02284E+15	441895	.06728
9	7.38318E+15	500815	.12348
10	4.90999E+15	559734	.0821172
11	3.39403E+15	618653	.0567635
12	3.53156E+15	677573	.0590636
13	2.93661E+15	736492	.0491134
14	3.77202E+15	795411	.0630852
15	4.69457E+15	854331	.0785143
16	1.61133E+16	913250	.269487
17	5.97925E+16	972169	1
18	1.93731E+16	1.03109E+06	.324006
19	9.55500E+15	1.09001E+06	.159803
20	2.81232E+15	1.14893E+06	.0470347

AVE. ENERGY= 820307

RMS DEVIATION= 288743

DEVIATION= 35.1994%

BLKJACK-3 SHOT # B2889 31-JUL-79 0930

BINS	VALUES	VOLTS	VALUES/MAX
1	2.94202E+16	26746.2	.858582
2	2.21134E+16	80238.5	.645345
3	1.64315E+16	133731	.479527
4	5.06562E+15	187223	.147832
5	5.61121E+15	240716	.163754
6	9.84924E+15	294208	.287435
7	1.57087E+16	347700	.4582
8	2.30542E+16	401193	.672801
9	8.81200E+15	454685	.257167
10	2.62514E+15	508177	.0766107
11	4.72582E+15	561670	.137915
12	1.86783E+15	615162	.0545098
13	3.95650E+15	668654	.115464
14	1.12227E+16	722147	.327516
15	6.93648E+15	775639	.20243
16	7.29256E+15	829131	.212822
17	1.74543E+16	882624	.509375
18	3.42660E+16	936116	1
19	3.09217E+16	989609	.9024
20	5.07815E+15	1.04310E+06	.148198

AVE. ENERGY= 531104

RMS DEVIATION= 361768

DEVIATION= 68.1162%

BLKJACK-3 SHOT # B2890 31-JUL-79 1350

BINS	VALUES	VOLTS	VALUES/MAX
1	7.20135E+15	42557.6	.220981
2	3.60377E+15	127673	.110586
3	2.42291E+15	212788	.0743496
4	3.11911E+15	297903	.0957132
5	4.15857E+15	383019	.12761
6	3.51852E+15	468134	.10797
7	3.30006E+15	553249	.101267
8	3.82150E+15	638364	.117267
9	4.42549E+15	723479	.135801
10	4.29711E+15	808595	.131861
11	3.81818E+15	893710	.117165
12	6.03721E+15	978825	.185258
13	3.25881E+16	1.06394E+06	1
14	8.52353E+15	1.14906E+06	.261554
15	1.86590E+15	1.23417E+06	.0572571
16	3.02172E+15	1.31929E+06	.0927246
17	8.14165E+15	1.40440E+06	.249835
18	5.08189E+15	1.48952E+06	.155943
19	6.29530E+15	1.57463E+06	.193178
20	3.84655E+15	1.65975E+06	.118035

AVE. ENERGY= 938551

RMS DEVIATION= 441821

DEVIATION= 47.0748%

BLKJACK-3 SHOT # B2893 1-AUG-79 0945

BINS	VALUES	VOLTS	VALUES/MAX
1	6.98697E+15	35332.6	.297635
2	8.17871E+15	105998	.348401
3	6.58403E+15	176663	.28047
4	7.05739E+15	247328	.300635
5	9.16684E+15	317993	.390494
6	4.10280E+15	388659	.174773
7	5.38916E+15	459324	.229571
8	6.72723E+15	529989	.28657
9	4.70341E+15	600654	.200359
10	2.09569E+15	671319	.0892736
11	2.95278E+15	741984	.125784
12	3.92554E+15	812650	.167222
13	4.14962E+15	883315	.176768
14	3.97308E+15	953980	.169248
15	2.34750E+16	1.02465E+06	1
16	3.57572E+15	1.09531E+06	.152321
17	8.83881E+15	1.16598E+06	.376521
18	1.22383E+16	1.23664E+06	.521333
19	9.83402E+15	1.30731E+06	.418915
20	1.25306E+16	1.37797E+06	.533785

AVE. ENERGY= 786251

RMS DEVIATION= 442912

DEVIATION= 56.3321%

BLKJACK-3 SHOT # B2894 1-AUG-79 1125

BINS	VALUES	VOLTS	VALUES/MAX
1	1.03448E+16	29636.9	.58589
2	1.82999E+15	88910.8	.103644
3	1.94505E+15	148185	.11016
4	2.72016E+15	207458	.154059
5	4.13536E+15	266732	.234211
6	4.74648E+15	326006	.268823
7	3.85277E+15	385280	.218206
8	4.14073E+15	444554	.234515
9	4.00174E+15	503828	.226643
10	2.31593E+15	563102	.131165
11	2.39045E+15	622375	.135386
12	4.20375E+15	681649	.238085
13	2.58231E+15	740923	.146252
14	5.70269E+15	800197	.322979
15	1.42070E+16	859471	.804632
16	2.15738E+15	918745	.122181
17	1.70764E+15	978018	.0967146
18	1.76565E+16	1.03729E+06	1
19	1.53123E+16	1.09657E+06	.86723
20	2.54975E+15	1.15584E+06	.144408

AVE. ENERGY= 694574

RMS DEVIATION= 365452

DEVIATION= 52.6152%

BLKJACK-3 SHOT # B2895 1-AUG-79 1505

BINS	VALUES	VOLTS	VALUES/MAX
1	1.28405E+16	38448.4	.456043
2	8.08821E+15	115345	.287262
3	5.76848E+15	192242	.204874
4	3.31068E+15	269139	.117582
5	5.55962E+15	346036	.197456
6	4.20008E+15	422933	.14917
7	3.36264E+15	499830	.119428
8	5.74681E+15	576727	.204104
9	4.18951E+15	653623	.148795
10	3.73452E+15	730520	.132636
11	3.30941E+15	807417	.117537
12	3.46872E+15	884314	.123195
13	3.61488E+15	961211	.128387
14	2.81562E+16	1.03811E+06	1
15	1.06218E+16	1.11500E+06	.377244
16	4.15956E+15	1.19190E+06	.147731
17	1.80019E+16	1.26880E+06	.639358
18	4.89501E+15	1.34570E+06	.173852
19	1.10655E+16	1.42259E+06	.393004
20	1.40997E+16	1.49949E+06	.500766

AVE. ENERGY= 879506

RMS DEVIATION= 475384

DEVIATION= 54.0463%

BLKJACK-3 SHOT # B2390 1-JUL-79 0855

BINS	VALUES	VOLTS	VALUES/MAX
1	8.64472E+15	28921.2	.55625
2	1.12997E+16	86765.4	.727083
3	1.46455E+16	144609	.942396
4	7.41454E+15	202453	.477093
5	1.55411E+16	260296	1
6	4.68073E+15	318140	.301184
7	8.37583E+15	375983	.538951
8	9.00201E+15	433827	.57924
9	3.96510E+15	491671	.255142
10	6.91322E+15	549514	.444835
11	1.18104E+16	607358	.759946
12	1.36593E+16	665202	.878913
13	1.50353E+16	723045	.967458
14	1.40866E+16	780889	.905105
15	6.20175E+15	838732	.399055
16	8.92281E+15	896576	.574143
17	4.78001E+15	954420	.307573
18	1.37433E+16	1.01228E+06	.884342
19	1.43323E+16	1.07071E+06	.922218
20	7.40756E+15	1.12795E+06	.476644

AVE. ENERGY= 582062

RMS DEVIATION= 337946

DEVIATION= 53.0602%

BLKJACK-3 SHOT # B2897 2-AUG-79 1115

BINS	VALUES	VOLTS	VALUES/MAX
1	4.38505E+15	37923.5	.165837
2	5.47485E+15	113770	.207052
3	2.30093E+15	189617	.0870183
4	1.86296E+15	265464	.0704546
5	2.24794E+15	341311	.0850143
6	5.90441E+15	417158	.223297
7	7.06206E+15	493005	.267078
8	3.36872E+15	568852	.128157
9	4.12453E+15	644699	.155985
10	4.91039E+15	720546	.185705
11	3.19132E+15	796393	.120692
12	3.28013E+15	872240	.12405
13	4.76701E+15	948087	.180282
14	1.82664E+16	1.02393E+06	.690812
15	1.19367E+16	1.09978E+06	.451433
16	1.80759E+16	1.17563E+06	.683609
17	8.44843E+15	1.25147E+06	.319509
18	2.64419E+16	1.32732E+06	1
19	5.46402E+15	1.40317E+06	.206642
20	1.41233E+16	1.47902E+06	.534127

AVE. ENERGY= 987983

RMS DEVIATION= 405260

DEVIATION= 41.019%

BLKJACK-3 SHOT # B2898 2-AUG-79 1420

BINS	VALUES	VOLTS	VALUES/MAX
1	7.57005E+15	37473.4	.313516
2	5.40647E+15	112420	.223911
3	4.37787E+15	187367	.181311
4	3.50957E+15	262314	.14535
5	5.54558E+15	337261	.229672
6	2.03970E+15	412208	.0844749
7	1.25312E+16	487155	.518982
8	4.23460E+15	562102	.175377
9	5.63225E+15	637048	.233262
10	2.00068E+15	711995	.0828569
11	2.04310E+15	786942	.0846156
12	2.71451E+15	861889	.112422
13	3.42402E+15	936836	.141807
14	1.28300E+16	1.01178E+06	.531359
15	1.70001E+16	1.08673E+06	.704055
16	1.42996E+16	1.16168E+06	.592222
17	2.41457E+16	1.23662E+06	1
18	4.29857E+15	1.31157E+06	.178027
19	9.73169E+15	1.38652E+06	.403041
20	1.17399E+16	1.46146E+06	.486213

AVE. ENERGY= 904148

RMS DEVIATION= 433853

DEVIATION= 47.9848%

BLKJACK-3 SHOT # B2904 6-AUG-79 14:23

BINS	VALUES	VOLTS	VALUES/MAX
1	6.55295E+15	36659.2	.252927
2	6.14[illegible]E+15	109977	.237335
3	2.72877E+15	183296	.105224
4	3.29694E+15	256614	.127253
5	5.79[illegible]E+15	329932	.223311
6	6.80375E+15	403251	.2628
7	2.70737E+15	476569	.104517
8	4.717[illegible]E+15	549887	.182075
9	5.2354[illegible]E+15	623206	.202074
10	3.9372[illegible]E+15	696524	.151987
11	2.41478E+15	769842	.0932047
12	4.75207E+15	843161	.183418
13	3.40204E+15	916479	.13131
14	4.33562E+15	989797	.167344
15	2.59085E+16	1.06312E+06	1
16	3.60731E+15	1.13642E+06	.139233
17	5.57392E+15	1.20975E+06	.215139
18	6.80208E+15	1.28307E+06	.262543
19	1.69801E+16	1.35635E+06	.655389
20	5.24479E+15	1.42971E+06	.202435

AVE. ENERGY= 848575

RMS DEVIATION= 433611

DEVIATION= 51.0987%

BLKJACK-3 SHOT # B2905 6-AUG-79 15:50

BINS	VALUES	VOLTS	VALUES/MAX
1	5.14965E+15	37664.2	.343688
2	4.18454E+15	112993	.279277
3	2.04754E+15	188321	.136653
4	2.37592E+15	263649	.158569
5	1.84506E+15	338978	.12314
6	2.65301E+15	414306	.177062
7	2.80259E+15	489634	.187045
8	1.30460E+16	564963	.870691
9	3.64288E+15	640291	.243126
10	2.11550E+15	715619	.141189
11	3.18556E+15	790948	.212605
12	2.57330E+15	866276	.171742
13	3.12278E+15	941604	.208414
14	4.06975E+15	1.01693E+06	.271615
15	5.37827E+15	1.09226E+06	.358946
16	3.90550E+15	1.16759E+06	.260654
17	4.52924E+15	1.24292E+06	.302282
18	1.49835E+16	1.31825E+06	1
19	5.32990E+15	1.39357E+06	.355718
20	1.12484E+16	1.46890E+06	.750717

AVE. ENERGY= 892023

RMS DEVIATION= 457457

DEVIATION= 51.2831%

BLKJACK-3 SHOT # B2906 7-AUG-79 9:05

BINS	VALUES	VOLTS	VALUES/MAX
1	5.88862E+15	34859.8	.363378
2	5.19147E+15	104579	.320358
3	2.33719E+15	174299	.144224
4	2.43411E+15	244019	.150205
5	2.80454E+15	313738	.173064
6	7.47589E+15	383458	.461387
7	4.24296E+15	453178	.262197
8	2.59330E+15	522897	.160028
9	3.66483E+15	592617	.226154
10	2.58454E+15	662337	.159488
11	5.52235E+15	732056	.340776
12	4.42972E+15	801776	.273351
13	3.90384E+15	871496	.2409
14	4.42602E+15	941215	.273123
15	5.53590E+15	1.01093E+06	.341612
16	5.59574E+15	1.08065E+06	.345304
17	5.11874E+15	1.15037E+06	.31587
18	1.06334E+16	1.22009E+06	.656168
19	1.62052E+16	1.28981E+06	1
20	7.12397E+15	1.35953E+06	.439609

AVE. ENERGY- 825448

RMS DEVIATION- 429565

DEVIATION- 52.0402%

BLKJACK-3 SHOT # B2907 7-AUG-79 11:10

BINS	VALUES	VOLTS	VALUES/MAX
1	6.24219E+15	34046.9	.391385
2	6.57015E+15	102141	.411948
3	3.52314E+15	170234	.220901
4	3.13270E+15	238328	.19642
5	2.97743E+15	306422	.186685
6	1.90856E+15	374515	.119667
7	2.86293E+15	442609	.179505
8	3.26028E+15	510703	.204419
9	4.12734E+15	578796	.258784
10	4.86916E+15	646890	.305296
11	4.19884E+15	714984	.263267
12	3.55356E+15	783078	.222808
13	2.92210E+15	851171	.183216
14	4.83808E+15	919265	.303347
15	4.55548E+15	987359	.285628
16	1.59490E+16	1.05545E+06	1
17	1.55040E+16	1.12355E+06	.972101
18	7.40609E+15	1.19164E+06	.464362
19	8.32246E+15	1.25973E+06	.521818
20	8.30670E+15	1.32783E+06	.520833

AVE. ENERGY= 818373

RMS DEVIATION= 410406

DEVIATION= 50.1491%

BLKJACK-3 SHOT # B2908 7-AUG-79 13:40

BINS	VALUES	VOLTS	VALUES/MAX
1	6.73479E+15	34140.5	.411877
2	5.17347E+15	102421	.316392
3	3.21645E+15	170702	.196708
4	3.34625E+15	238983	.204645
5	3.57545E+15	307264	.218663
6	2.23597E+15	375545	.136745
7	2.94021E+15	443826	.179813
8	6.57778E+15	512107	.402275
9	5.40478E+15	580388	.330538
10	4.44777E+15	648669	.272011
11	2.31001E+15	716950	.141272
12	3.59960E+15	785231	.220139
13	2.95187E+15	853512	.180526
14	2.08211E+15	921793	.127335
15	5.64391E+15	990074	.345162
16	1.04339E+16	1.05835E+06	.638101
17	8.31814E+15	1.12664E+06	.508709
18	6.50485E+15	1.19492E+06	.397815
19	9.24745E+15	1.26320E+06	.565543
20	1.63514E+16	1.33148E+06	1

AVE. ENERGY= 818134

RMS DEVIATION= 432393

DEVIATION= 52.8511%

BLKJACK-3 SHOT # B2919 10-AUG-79 10:30

BINS	VALUES	VOLTS	VALUES/MAX
1	7.21379E+15	32660.6	.228113
2	7.26383E+15	97981.7	.229695
3	8.21241E+15	163303	.259691
4	5.46835E+15	228624	.172919
5	2.85515E+15	293945	.0902849
6	7.14638E+15	359266	.225982
7	4.42548E+15	424587	.139942
8	5.59969E+15	489908	.177072
9	5.89049E+15	555229	.186268
10	4.56325E+15	620551	.144292
11	3.99599E+15	685872	.12636
12	5.89007E+15	751193	.186255
13	5.22033E+15	816514	.165076
14	7.01919E+15	881835	.221959
15	5.34427E+15	947156	.168995
16	3.16237E+16	1.01248E+06	1
17	2.17444E+16	1.07780E+06	.687593
18	2.43534E+16	1.14312E+06	.770098
19	4.27090E+15	1.20844E+06	.135054
20	1.18085E+16	1.27376E+06	.373407

AVE. ENERGY- 799541

RMS DEVIATION- 382262

DEVIATION- 47.8102%

BLKJACK-3 SHOT # B2920 10-AUG-79 11:55

BINS	VALUES	VOLTS	VALUES/MAX
1	1.54265E+16	35900.6	.731591
2	1.00414E+16	107702	.476207
3	4.38295E+15	179503	.207859
4	4.46070E+15	251304	.211546
5	5.30804E+15	323105	.25173
6	5.17278E+15	394907	.245316
7	5.36417E+15	466708	.254392
8	4.81344E+15	538509	.228274
9	4.99718E+15	610310	.236988
10	3.79010E+15	682111	.179743
11	6.35822E+15	753913	.301535
12	6.64719E+15	825714	.315239
13	7.82730E+15	897515	.371205
14	7.13527E+15	969316	.338386
15	1.11362E+16	1.04112E+06	.528127
16	1.73655E+16	1.11292E+06	.823546
17	8.68557E+15	1.18472E+06	.411908
18	8.43920E+15	1.25652E+06	.400224
19	2.10862E+16	1.32832E+06	1
20	6.84472E+15	1.40012E+06	.324607

AVE. ENERGY= 796590

RMS DEVIATION= 454226

DEVIATION= 57.0213%

BLKJACK-3 SHOT # B2922 13-AUG-79 1038

BINS	VALUES	VOLTS	VALUES/MAX
1	2.13906E+15	33736.7	.363823
2	4.29931E+14	101210	.0731248
3	3.66190E+14	168683	.0622835
4	5.49204E+14	236157	.0934115
5	4.59760E+14	303630	.0781983
6	8.61509E+14	371103	.14653
7	1.19890E+15	438577	.203916
8	3.93447E+15	506050	.669195
9	1.13002E+15	573523	.1922
10	8.84518E+14	640997	.150443
11	9.15576E+14	708470	.155726
12	6.27276E+14	775943	.10669
13	9.64968E+14	843417	.164127
14	6.56596E+14	910890	.111677
15	4.34197E+15	978363	.738505
16	5.87941E+15	1.04584E+06	1
17	1.18736E+15	1.11331E+06	.201952
18	2.13121E+15	1.18078E+06	.362486
19	1.44432E+15	1.24826E+06	.245658
20	3.14773E+14	1.31573E+06	.0535382

AVE. ENERGY= 772530

RMS DEVIATION= 359132

DEVIATION= 46.4877%

BLKJACK-3 SHOT # B2935 16-AUG-79 1105

BINS	VALUES	VOLTS	VALUES/MAX
1	8.29408E+15	26894.4	.450524
2	2.16020E+15	80633.4	.117339
3	4.70322E+15	134472	.255473
4	4.61541E+15	188261	.250703
5	6.35009E+15	242050	.344929
6	4.14198E+15	295839	.224986
7	5.94456E+15	349628	.322923
8	4.09383E+15	403417	.222154
9	4.35363E+15	457206	.236487
10	4.53918E+15	510995	.246563
11	3.84943E+15	564783	.209056
12	3.93142E+15	618572	.21355
13	7.41536E+15	672361	.402793
14	1.59893E+16	726150	.868518
15	1.17365E+16	779939	.63751
16	1.17411E+16	833728	.63776
17	5.97683E+15	887517	.324654
18	1.17462E+16	941306	.638041
19	1.84099E+16	995095	1
20	1.07843E+16	1.04888E+06	.585789

AVE. ENERGY= 655535

RMS DEVIATION= 312519

DEVIATION= 47.674%

BLKJACK-3 SHOT # B2936 16-AUG-79 1318

BINS	VALUES	VOLTS	VALUES/MAX
1	8.79748E+15	23547.2	.246
2	1.13934E+16	70641.7	.318726
3	4.70727E+15	117736	.131627
4	3.28239E+15	164831	.0912246
5	4.15438E+15	211925	.116167
6	1.36121E+16	259020	.380628
7	7.21000E+15	306114	.20161
8	3.80743E+15	353209	.106467
9	1.05515E+16	400303	.295058
10	3.61039E+15	447398	.100956
11	2.62375E+15	494492	.0733666
12	2.07730E+15	541587	.0580864
13	2.58785E+15	588681	.0723627
14	2.22794E+15	635776	.0622989
15	3.90924E+15	682870	.109312
16	1.33935E+16	729965	.374516
17	2.58731E+16	777059	.723476
18	1.58378E+16	824154	.442865
19	3.46991E+16	871248	.970275
20	3.57622E+16	918343	1

AVE. ENERGY- 618464

RMS DEVIATION- 303890

DEVIATION- 49.1362%

BLKJACK-3 SHOT # B2937 16-AUG-79 1440

BINS	VALUES	VOLTS	VALUES/MAX
1	2.85540E+16	24220.5	1
2	8.06933E+15	72661.6	.282606
3	2.03532E+16	121103	.712272
4	9.66795E+15	169544	.338525
5	2.13119E+16	217985	.746366
6	2.01672E+16	266426	.706303
7	1.80870E+16	314867	.63343
8	4.92334E+15	363308	.172422
9	1.10564E+16	411749	.38721
10	9.54662E+15	460190	.334336
11	3.96915E+15	508631	.139005
12	3.04853E+15	557072	.106764
13	7.29517E+15	605513	.255487
14	4.15534E+15	653954	.145526
15	6.81702E+15	702395	.238741
16	7.49079E+15	750836	.262338
17	3.85215E+15	799277	.134907
18	3.06349E+15	847718	.107288
19	2.14206E+15	896159	.0750179
20	7.30947E+15	944601	.255988

AVE. ENERGY= 336507

RMS DEVIATION= 260102

DEVIATION= 77.2945%

BLKJACK-3 SHOT # B2933 16-AUG-79 1600

BINS	VALUES	VOLTS	VALUES/MAX
1	4.33480E+15	26719.6	.115036
2	9.56308E+15	80158.8	.253782
3	2.09824E+16	133598	.556825
4	1.66705E+16	187037	.442407
5	7.32041E+15	240476	.194532
6	5.86595E+15	293915	.155669
7	3.07101E+15	347355	.0814975
8	8.89645E+15	400794	.236091
9	9.13684E+15	454233	.242545
10	2.21475E+15	507672	.0587742
11	3.94411E+15	561111	.104668
12	2.80101E+15	614551	.0743323
13	8.06911E+14	667990	.0214136
14	8.05391E+15	721429	.213732
15	1.36065E+16	774868	.361084
16	1.03679E+16	828307	.275141
17	3.76822E+16	881746	1
18	2.34355E+16	935186	.621925
19	1.06982E+16	988625	.283906
20	8.32216E+15	1.04206E+06	.220851

AVE. ENERGY- 596787

RMS DEVIATION- 337192

DEVIATION- 58.5012%

BLKJACK-3 SHOT # B2939 16-AUG-79 1735

BINS	VALUES	VOLTS	VALUES/MAX
1	6.68870E+15	24861.6	.184072
2	9.72824E+15	74584.9	.26772
3	5.91463E+15	124308	.16277
4	3.19971E+15	174031	.0880556
5	3.62004E+15	223755	.0996231
6	9.78421E+15	273478	.26926
7	1.45256E+16	323201	.399744
8	4.75231E+15	372924	.130783
9	2.39127E+15	422648	.0658076
10	3.48964E+15	472371	.0960344
11	4.89570E+15	522094	.134729
12	1.44201E+15	571817	.0396838
13	1.48261E+15	621541	.0408012
14	1.78172E+16	671264	.490327
15	9.37711E+15	720987	.258057
16	4.78781E+15	770710	.13176
17	3.63374E+16	820434	1
18	3.24705E+16	870157	.893585
19	1.89163E+16	919880	.520574
20	6.67970E+15	969603	.183824

AVE. ENERGY= 622554

RMS DEVIATION= 294034

DEVIATION= 47.2302%

BLKJACK-3 SHOT # B2940 16-AUG-79 1840

BINS	VALUES	VOLTS	VALUES/MAX
1	3.45985E+15	29732.1	.127087
2	7.47975E+15	89196.3	.274414
3	3.50107E+15	148661	.128601
4	3.17751E+15	208125	.116716
5	8.03804E+15	267589	.295252
6	8.65968E+15	327053	.318086
7	7.67670E+15	386517	.281979
8	2.10267E+15	445982	.0771614
9	4.66491E+15	505446	.171351
10	3.05247E+15	564910	.112123
11	3.97255E+15	624374	.145919
12	3.32399E+15	683838	.122096
13	1.62433E+16	743303	.596648
14	1.07600E+16	802767	.395236
15	1.98689E+16	862231	.72982
16	1.68234E+16	921695	.617953
17	2.72243E+16	981160	1
18	1.05102E+16	1.04062E+06	.38606
19	1.71153E+16	1.10009E+06	.628677
20	6.38497E+15	1.15955E+06	.234531

AVE. ENERGY- 743925

RMS DEVIATION- 318141

DEVIATION- 42.7652%

BLKJACK--3 SHOT # B2943 17-AUG-79 1350

BINS	VALUES	VOLTS	VALUES/MAX
1	1.30480E+16	34171.3	.386244
2	4.53142E+15	102514	.134138
3	3.59055E+15	170856	.10629
4	6.41226E+15	239199	.189814
5	1.63387E+16	307541	.483655
6	9.20707E+15	375884	.272546
7	4.67309E+15	444226	.138332
8	4.06027E+15	512569	.120191
9	2.41702E+15	580911	.0715481
10	2.49065E+15	649254	.0737278
11	4.18508E+15	717596	.123885
12	3.39400E+15	785939	.100468
13	9.36381E+15	854281	.277186
14	3.37817E+16	922624	1
15	1.03840E+16	990966	.307386
16	1.07448E+16	1.05931E+06	.318066
17	1.44133E+16	1.12765E+06	.426659
18	1.46487E+16	1.19599E+06	.433629
19	1.04464E+16	1.26434E+06	.309234
20	4.30028E+15	1.33268E+06	.127296

AVE. ENERGY= 756138

RMS DEVIATION= 396254

DEVIATION= 52.4049%

BLKJACK-3 SHOT # B2944 17-AUG-79 1554

BINS	VALUES	VOLTS	VALUES/MAX
1	9.39434E+15	28634.3	.38931
2	1.10115E+16	85903	.456325
3	7.82207E+15	143172	.324154
4	1.03493E+16	200440	.428886
5	3.48322E+15	257709	.144555
6	1.09918E+16	314978	.455509
7	8.06260E+15	372246	.334122
8	4.09130E+15	429515	.169547
9	3.29875E+15	486784	.136703
10	3.38698E+15	544052	.140774
11	2.61538E+15	601321	.108384
12	1.77079E+15	658589	.0733834
13	2.68125E+15	715858	.111114
14	5.50881E+15	773127	.22829
15	1.70359E+16	830395	.705984
16	2.41307E+16	887664	1
17	2.10705E+16	944933	.873182
18	2.09703E+16	1.00220E+06	.869028
19	1.40697E+16	1.05947E+06	.583064
20	1.40532E+16	1.11674E+06	.582379

AVE. ENERGY= 679185

RMS DEVIATION= 361971

DEVIATION= 53.2949%

BLKJACK-3 SHOT # 52945B 18 AUG 79 0918

BINS	VALUES	VOLTS	VALUES/MAX
1	1.81113E+16	26862.8	.64639
2	7.45275E+15	80588.5	.265937
3	3.23534E+15	134314	.115469
4	2.29293E+15	188040	.0818342
5	5.48650E+15	241766	.195812
6	2.87062E+15	295491	.102738
7	5.87655E+14	349217	.0209726
8	2.09231E+15	402943	.0746743
9	1.27805E+15	456668	.0456132
10	4.84799E+15	510394	.173024
11	2.27495E+15	564120	.0811925
12	4.72289E+15	617845	.168559
13	7.44418E+15	671571	.265682
14	1.60779E+16	725297	.573816
15	2.12671E+16	779022	.75902
16	1.06465E+16	832748	.37997
17	2.80192E+16	886474	1
18	1.89945E+16	940199	.677912
19	1.24936E+16	993925	.445893
20	2.38448E+16	1.04765E+06	.851017

AVE. ENERGY= 693779

RMS DEVIATION= 331051

DEVIATION= 47.717%

APPENDIX B

ANOMALOUS STRESS RECORDS

Figures B1 and B2 show peak stress clipped on Shots P2801 and B2820. Figure B3 shows odd peak stress, with an unusual pulse shape on Shot B2885. Figure B4 had poor electron beam current monitoring, hence suspect 7912 data for Shot B2922.

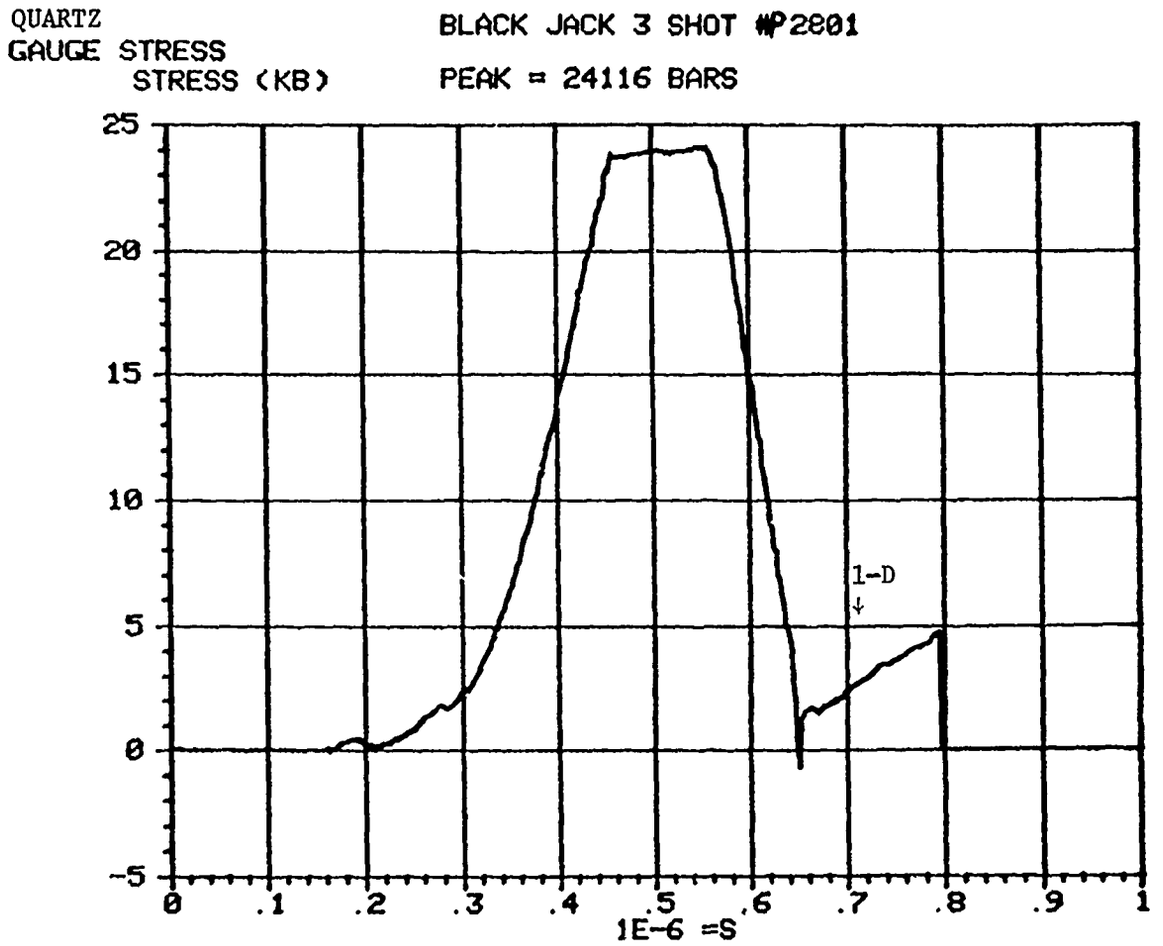

Figure B1. Commonality aluminum quartz gauge record.

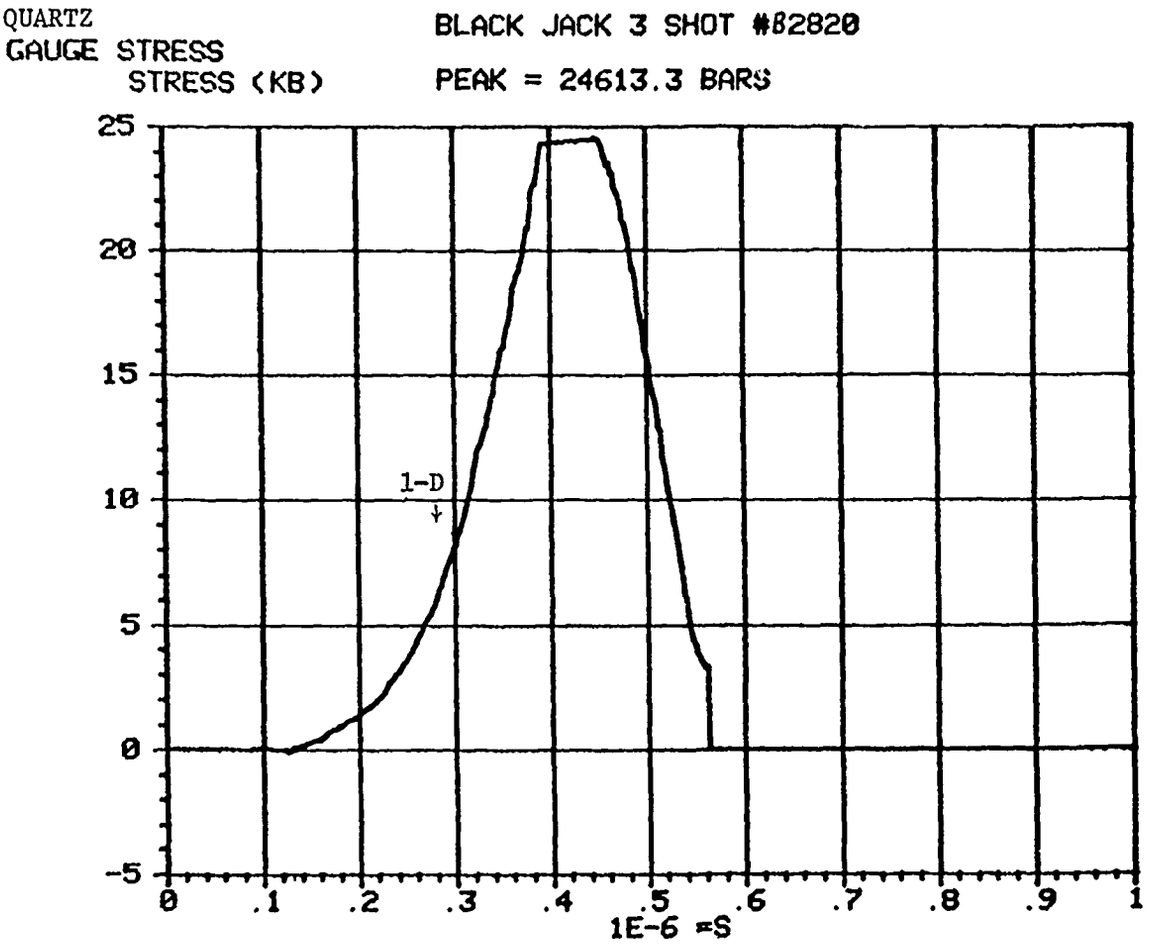

Figure B2. Ktech aluminum quartz gauge record.

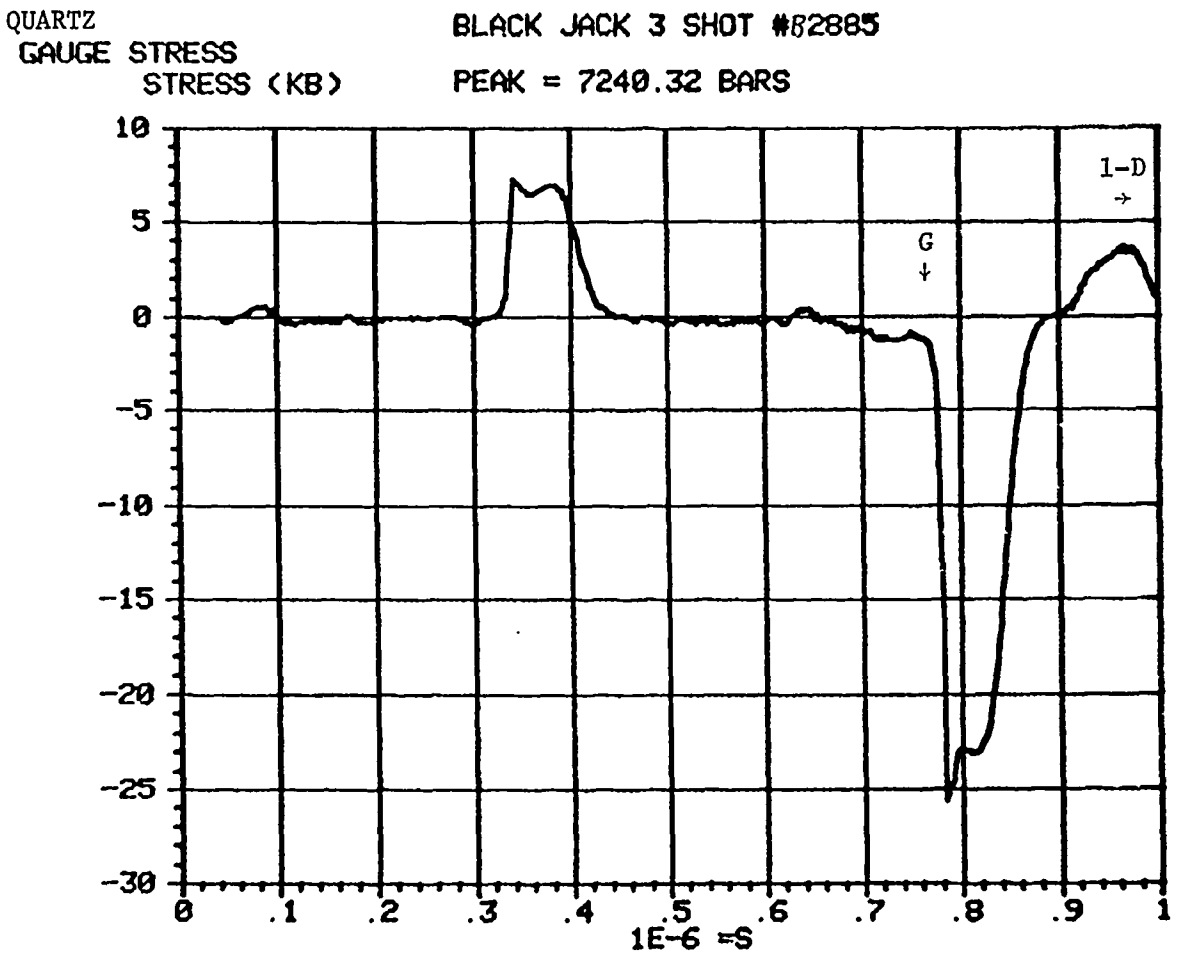

Figure B3. Ktech tantalum quartz gauge record.

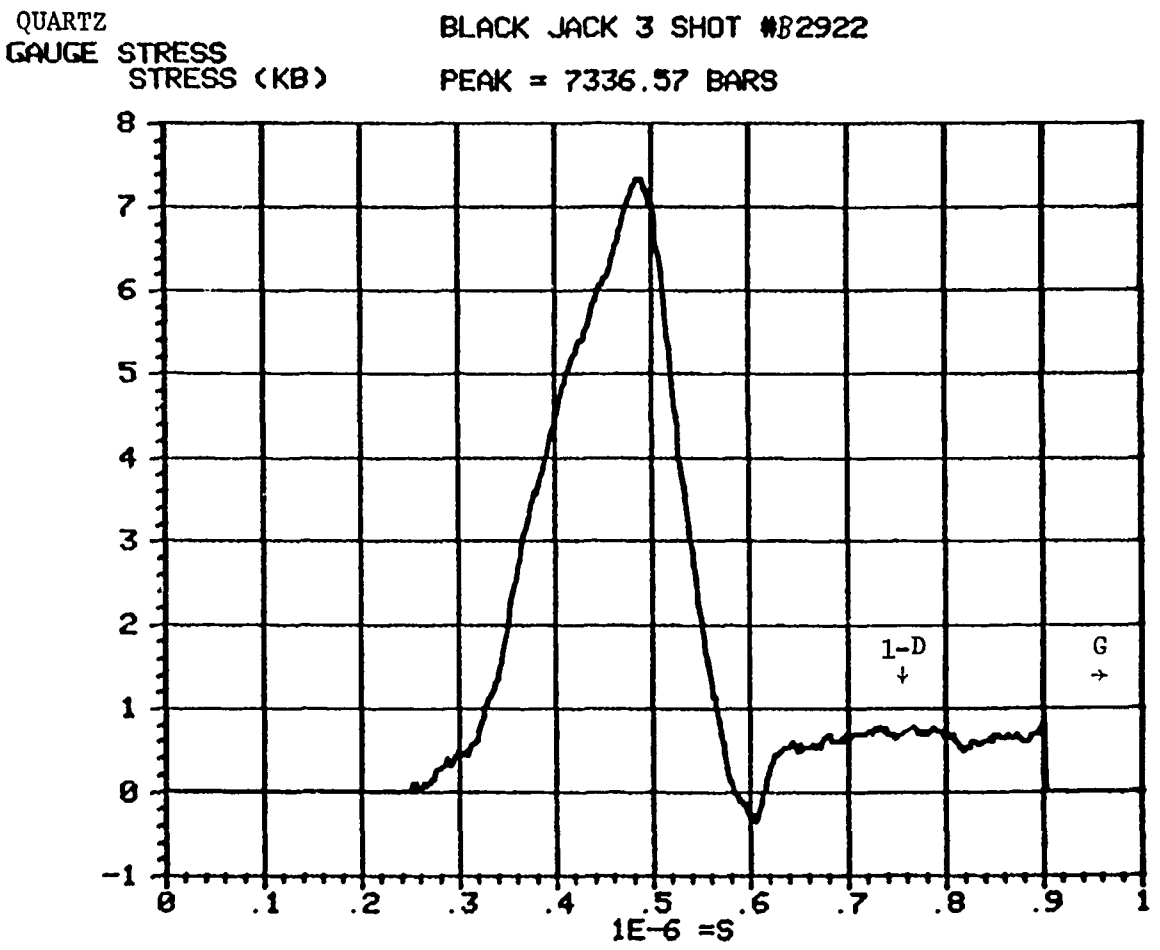

Figure B4. Commonality aluminum quartz gauge record.

APPENDIX C

HUGONIOT DATA, MATERIAL PROPERTIES AND IMPEDANCES

C-1 HUGONIOT EQUATIONS OF STATE

The Hugoniot equations of state for the materials of interest are listed below.

Aluminum	$P = 143.86u + 36.13u^2$	
Tantalum	$P = 566.72u + 199.37u^2$	
X-cut Quartz	$P = 151.22u + 8.24u^2$	
Fused Silica	$P = 131.7u - 73.61u^2 + 99.47u^3 - 41.63u^4$	
PMMA	$P = 32.971u + 24.219u^2$	$P \leq 6$ kbar
	$0.679 + 31.815u + 8.718u^2 + 6.924u^2$	$P > 6$ kbar

P = material stress in kbar.

u = material velocity in mm/μs.

C-2 MATERIAL PROPERTIES

Material properties data for aluminum, tantalum, X-cut quartz, fused silica and PMMA are shown in the following table.

Material	Density (g/cm^3)	Longitudinal Wave Velocity (cm/μs)	Gruneisen Constant	Z Number
Aluminum	2.7	0.64	2.14	13
Tantalum	16.6	0.415	1.7	73
X-cut Quartz	2.65	0.57	0.6	--
Fused Silica	2.2	0.59	0.05	--
PMMA	1.184	0.27	0.3	--

C-3 MECHANICAL IMPEDANCES

Typical mechanical impedance values are shown below for the materials of interest.

Material	Impedance Z[a]	Mismatch Condition[b]	Mismatch Value[c]
Aluminum	173	Al/Quartz	0.93
		Al/Fused Silica	0.86
		Al/PMMA	0.31
Tantalum	689	Ta/Quartz	0.36
		Ta/Fused Silica	0.32
		Ta/PMMA	0.09
X-cut Quartz	151	----------	----
Fused Silica	130	----------	----
PMMA	32	----------	----

[a]Units of kbar/(mm/μs).

[b]Interface, stress passing from metal to backer.

[c]Transmitted stress/incident stress = $2Z_2/(Z_1+Z_2)$

where Z_1 = impedance of sample,

Z_2 = impedance of backer.

Note: Exact values of (a) and (c) are stress dependent according to the Hugoniot data for each material.

APPENDIX D

TYPICAL PUFF COMPUTATIONS

The following three plots are examples of the waveforms to be anticipated for measurements of stress from a given deposition profile in tantalum, when monitored either using (1) a quartz gauge, (2) a carbon gauge within PMMA, or (3) a buried mirror within fused silica (for LVI).

All three cases used a sample of tantalum, 0.127-cm-thick, and assumed the deposition profile appropriate to Shot B2732 with a beam incident angle of 30 degrees. The deposition time was set at 36 ns, and all were given an input fluence of 300 cal/cm^2 (to exaggerate high fluence behavior including stress attenuation). The initial stress profile generated within the tantalum was thus common for all three computations.

The three plots indicate both the profile shape anticipated and the stress level at the monitoring position.

The EOS data used for these computations are the "standard" ones called by the PUFF 74 code (ref. 4). It is seen that the quartz record yields the narrowest pulse width and maintains the initial deposition-profile induced in the sample. For the fused silica record (LVI), the dispersion involved has widened the pulse width and dropped the peak stress, while maintaining the overall pulse shape. For the PMMA record, however, severe pulse shape distortion has occurred. A shock has developed and a dispersive increase in pulse width has occurred.

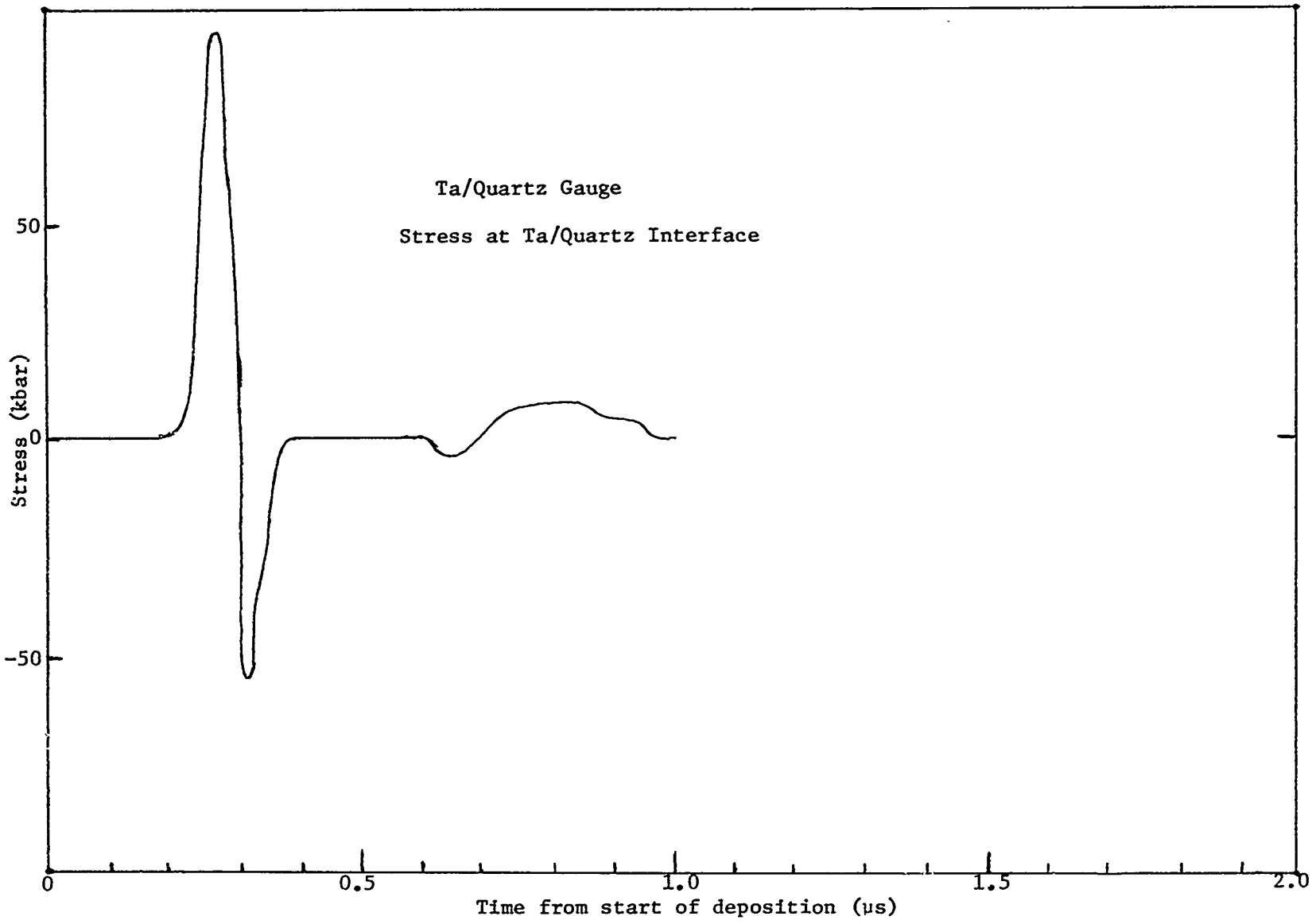
Ta/Quartz Gauge
Stress at Ta/Quartz Interface
50
0
-50
Stress (kbar)
0
0.5
1.0
1.5
2.0
Time from start of deposition (μs)

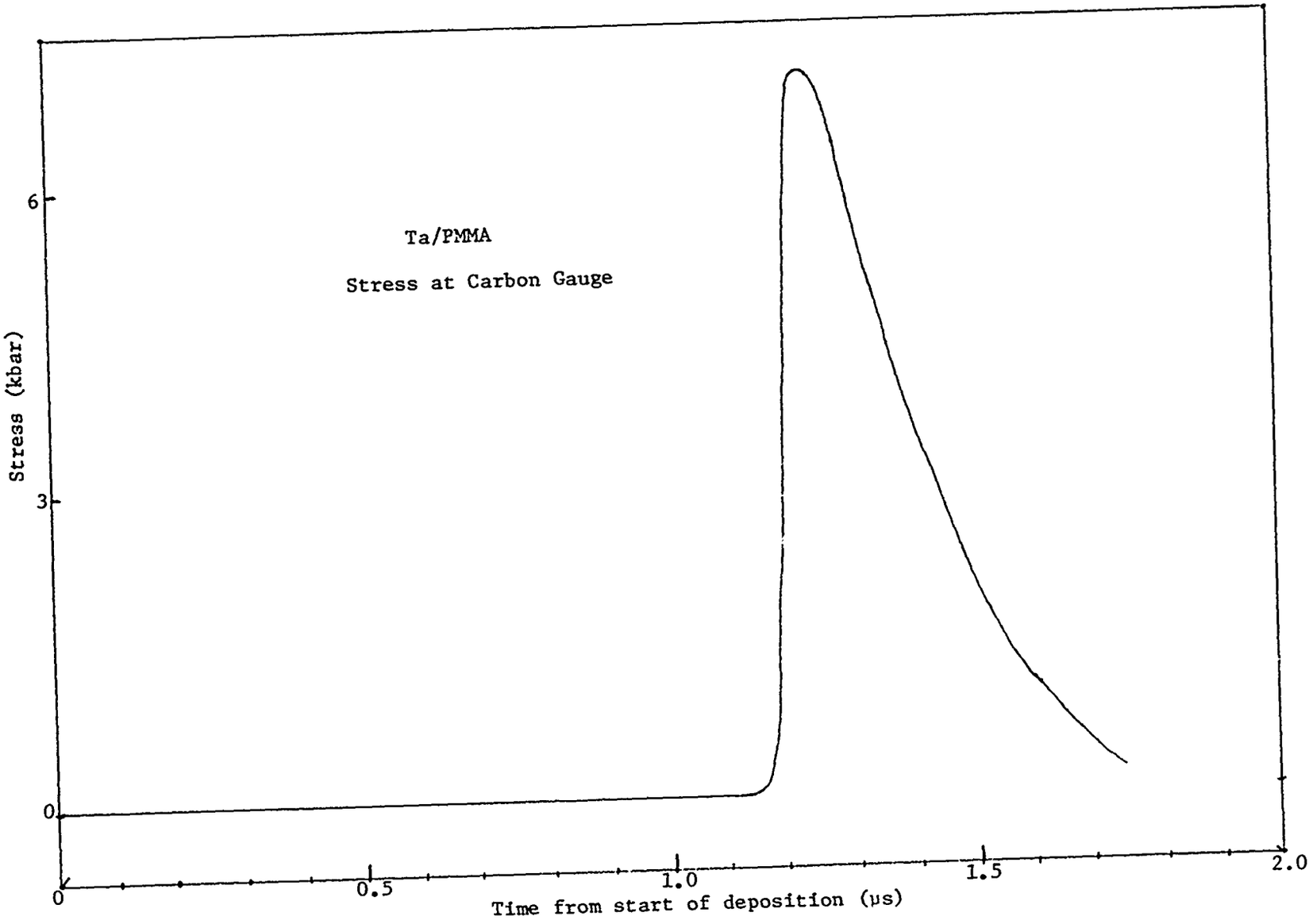
Ta/PMMA
Stress at Carbon Gauge
Stress (kbar)
6
3
0
0
0.5
1.0
1.5
2.0
Time from start of deposition (μs)

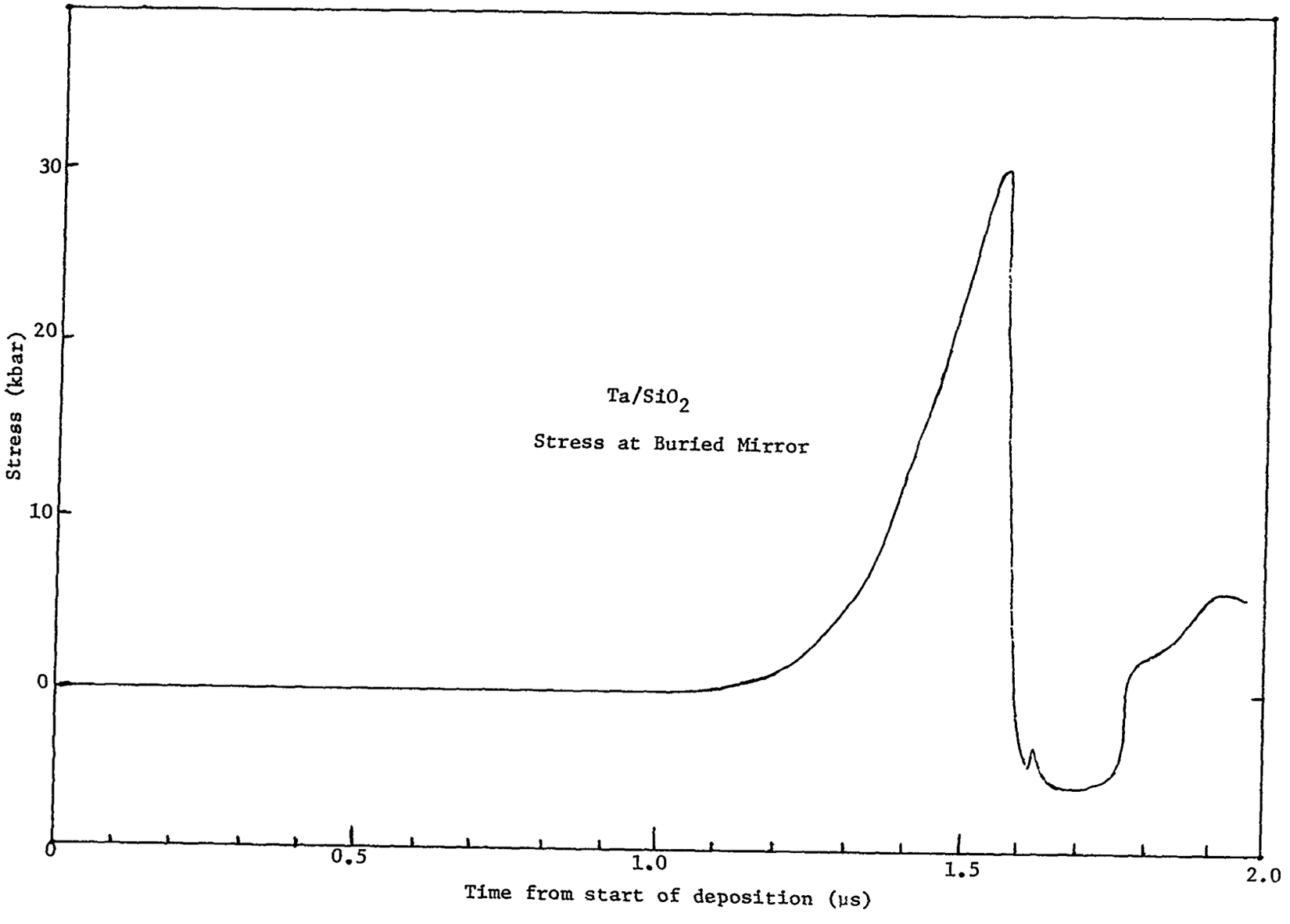
Ta/SiO2
Stress at Buried Mirror
Stress (kbar)
30
20
10
0
0
0.5
1.0
1.5
2.0
Time from start of deposition (μs)

APPENDIX E

TYPICAL PHOTOGRAPHS OF IRRADIATED SAMPLES

The following are views of a small selection of samples illustrating irradiation surfaces.

Al_c, Shot No. B2894

Al_c, Shot No. B2907

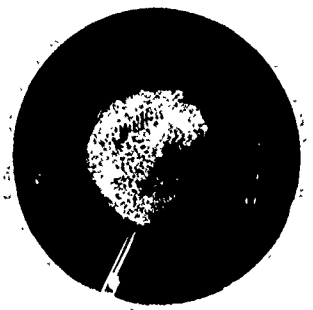

Al_c, Shot No. B2940

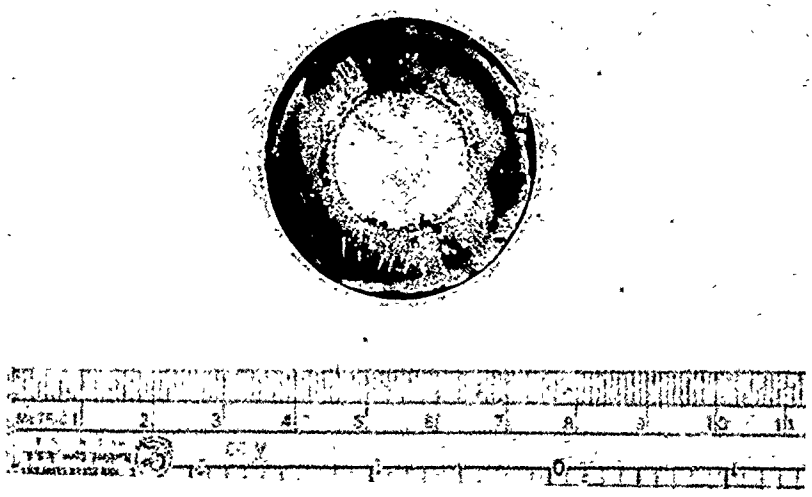

Al_k, Shot No. P2814

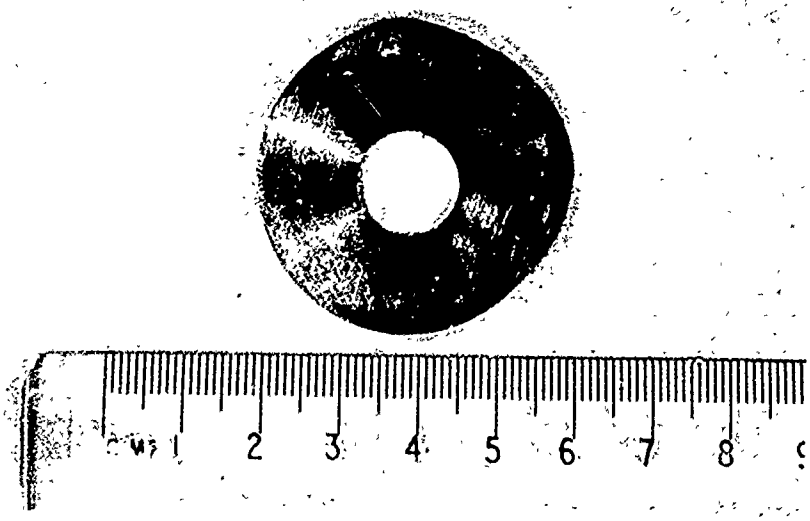

Al_k, Shot No. B2889

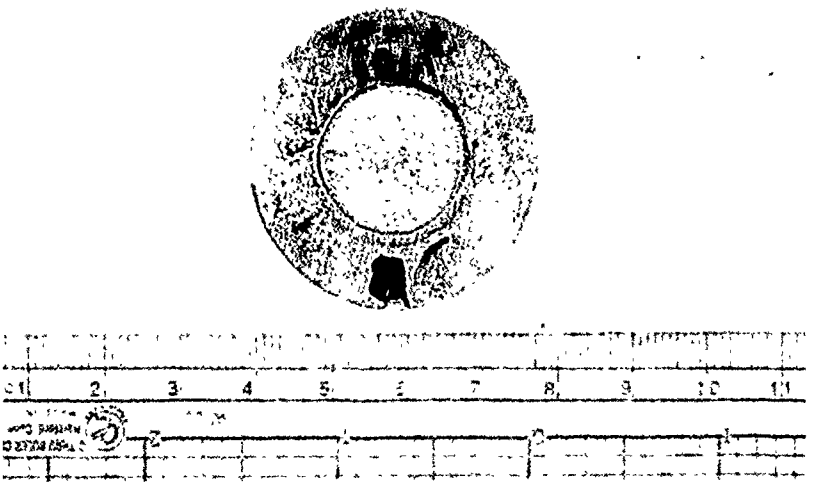

Al_k, Shot No. B2890

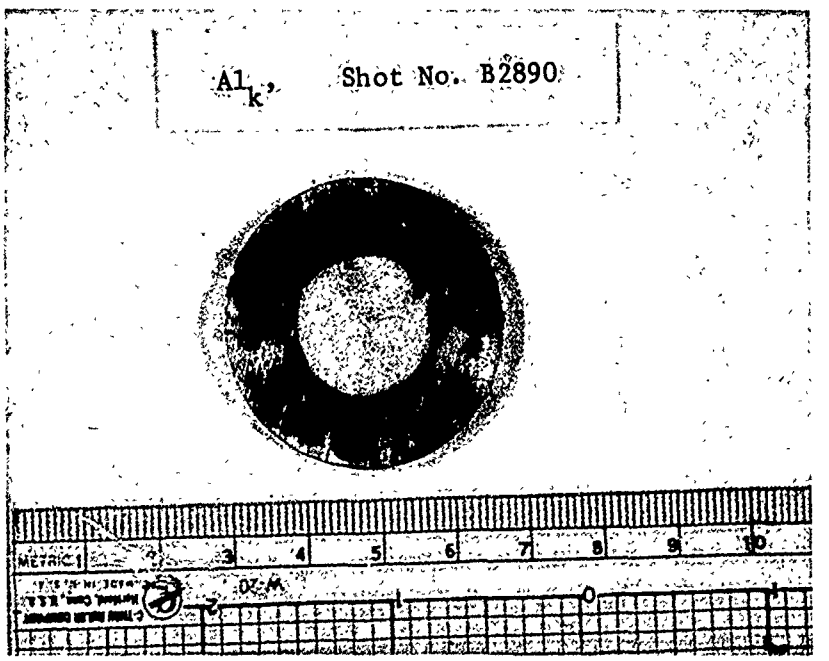

Ta_c, Shot No. P2809

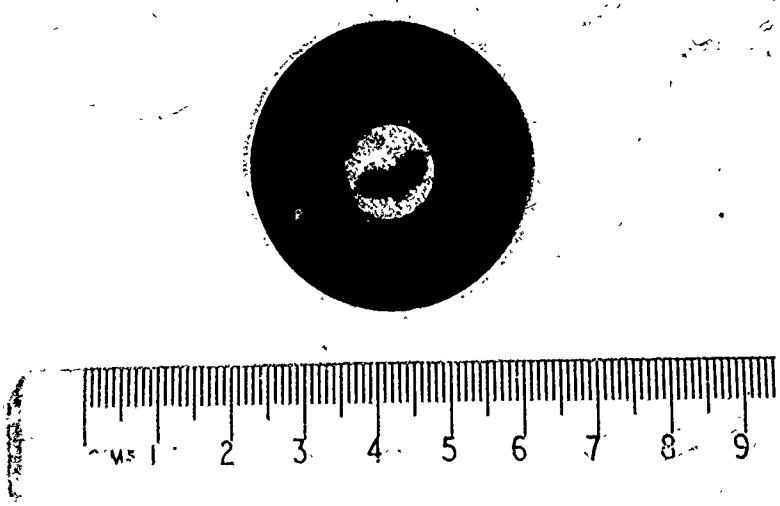

Ta_c, Shot No. B2908

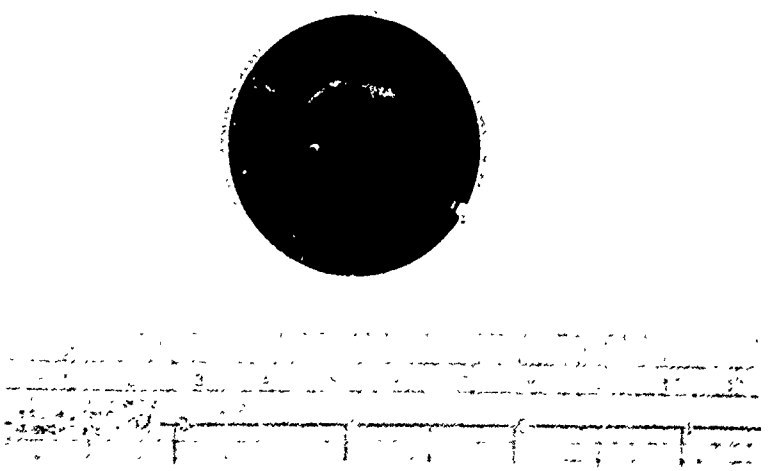

Ta_c, Shot No. B2943

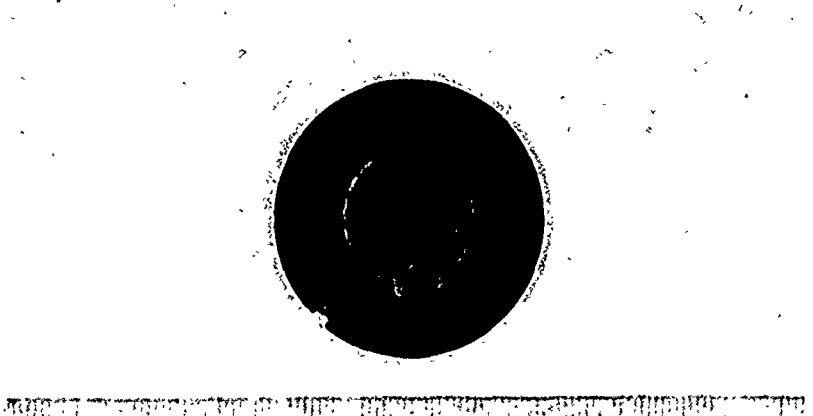

Ta_k, Shot No. B2885

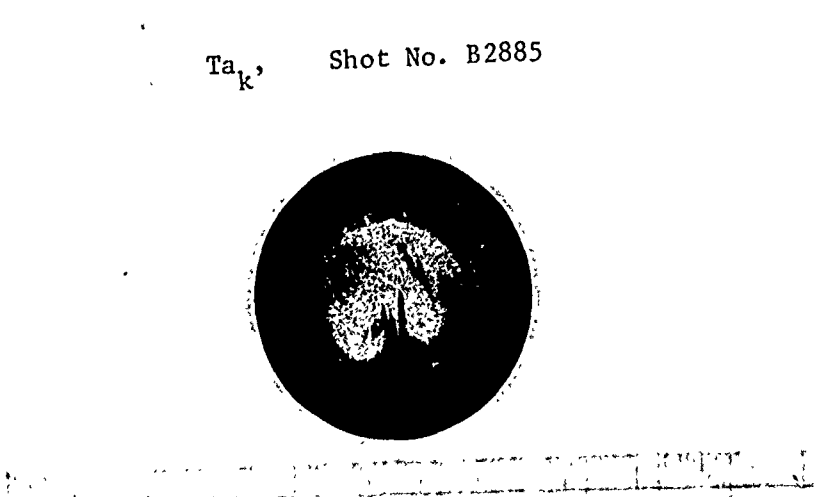

Ta_k, Shot No. B2893

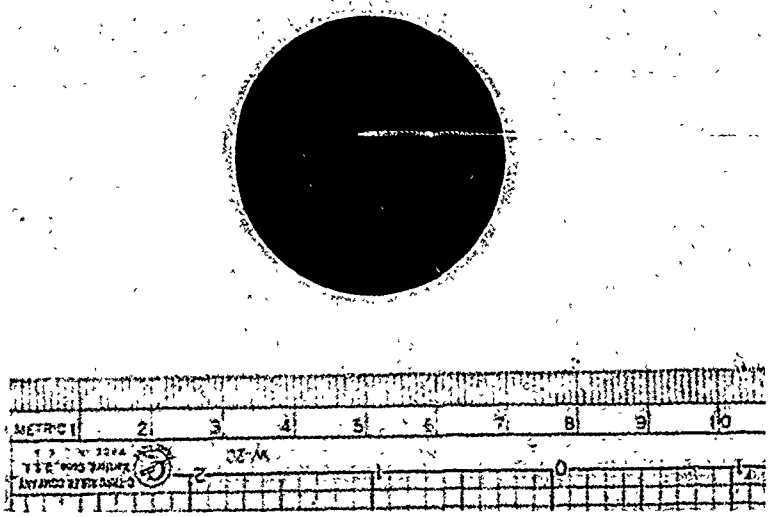

Ta_k, Shot No. B2895

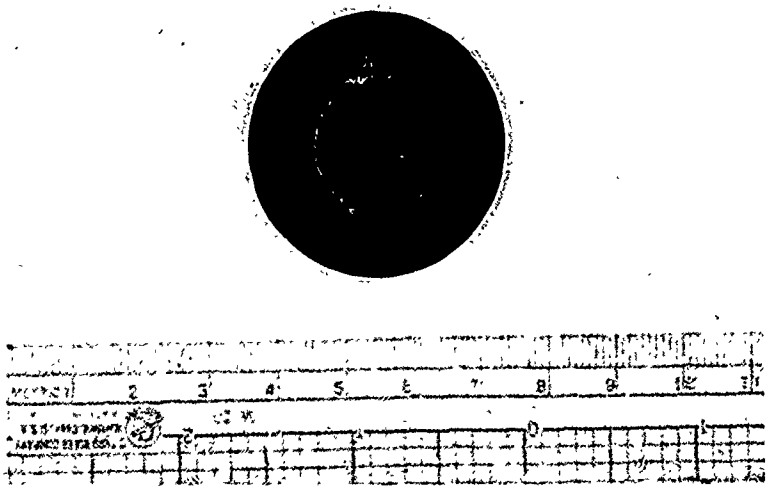

APPENDIX F

ELTRAN Dose-Depth Computations

Ktech Electron Beam Commonality Experiments on Blackjack 3 and 3 Prime

Ktech 79-11

DNA Contract 001-79-C-0127

The following tables should be used in conjunction with the main report listed above.

These tables list the appropriate ELTRAN deposition code computations for all the itemized stress experiments in the main report organized by shot number. The data are given in the form of normalized deposition (cals/gm per incident cal/cm^2) versus mass depth (gm/cm^2) from the irradiated surfaces. In all cases the inclusion of the carbon filter and choice of beam angles of incidence have been incorporated as appropriate for each experiment.

To obtain true dose-depth values these normalized doses should be scaled up directly according to the quoted fluences in the main report, and the material densities (ρ=2.7 gm/cm^3 for Al, and ρ=16.6 gm/cm^3 for Ta) should be used to convert mass depths to linear cm scale.

P2715

MASS DEPTH (GM/CM$$2)	NORM DOSE INT=1.0
.0069	3.2832
.0206	3.6389
.0343	3.9665
.0480	3.9479
.0617	4.1726
.0754	3.9740
.0891	3.9727
.1028	3.7857
.1165	3.7349
.1302	3.5315
.1439	3.3735
.1576	3.2238
.1713	2.8795
.1850	2.7138
.1987	2.4097
.2124	2.1364
.2261	1.9871
.2398	1.7088
.2535	1.5628
.2672	1.3520
.2809	1.1835
.2946	.9333
.3083	.7809
.3220	.6221
.3357	.5345
.3494	.4175
.3631	.2991
.3768	.2871
.3905	.1911
.4042	.1435
.4179	.0904
.4316	.0436
.4453	.0450
.4590	.0240
.4727	.0148
.4864	.0126
.5001	.0015
.5138	.0036
.5275	0.0000
.5412	0.0000
.5549	0.0000
.5686	0.0000
.5823	0.0000
.5960	0.0000
.6097	0.0000
.6234	0.0000

P2716

MASS DEPTH (GM/CM$$2)	NORM DOSE INT=1.0
.0065	3.6772
.0195	4.0564
.0325	4.3519
.0455	4.2303
.0585	3.8820
.0715	3.5678
.0845	3.0587
.0975	2.8687
.1105	2.6451
.1235	2.3634
.1365	2.2490
.1495	2.0324
.1625	1.8141
.1755	1.5094
.1885	1.3264
.2015	1.2803
.2145	1.0725
.2275	.8754
.2405	.7906
.2535	.6689
.2665	.5288
.2795	.4808
.2925	.4541
.3055	.3288
.3185	.2821
.3315	.2886
.3445	.2452
.3575	.1533
.3705	.1305
.3835	.1085
.3965	.0767
.4095	.0729
.4225	.0544
.4355	.0563
.4485	.0369
.4615	.0216
.4745	.0112
.4875	.0114
.5005	.0145
.5135	.0111
.5265	.0016

B2729

MASS DEPTH (GM/CM**2)	NORM DOSE INT=1.0
.0069	5.4845
.0206	6.2023
.0343	5.5379
.0480	5.2297
.0617	4.9114
.0754	4.5520
.0891	3.8307
.1028	3.5609
.1165	3.2052
.1302	2.7228
.1439	2.6771
.1576	2.3659
.1713	2.1333
.1850	2.0045
.1987	1.8556
.2124	1.4943
.2261	1.3879
.2398	1.1958
.2535	1.1453
.2672	.9333
.2809	.7575
.2946	.6626
.3083	.5757
.3220	.4723
.3357	.3617
.3494	.2758
.3631	.2112
.3768	.1286
.3905	.0736
.4042	.0419
.4179	.0247
.4316	.0104
.4453	.0025
.4590	.0045
.4727	0.0000
.4864	0.0000
.5001	0.0000
.5138	0.0000
.5275	0.0000
.5412	0.0000
.5549	0.0000
.5686	0.0000
.5823	0.0000
.5960	0.0000

B2732

MASS DEPTH (GM/CM**2)	NORM DOSE INT=1.0
.0065	8.5304
.0195	4.8014
.0325	4.2319
.0455	3.6545
.0585	3.1823
.0715	2.9720
.0945	2.7005
.0975	2.6554
.1105	2.4144
.1235	2.2119
.1365	1.9859
.1495	1.6768
.1625	1.4708
.1755	1.3955
.1885	1.2517
.2015	.8831
.2145	.8197
.2275	.8117
.2405	.7840
.2535	.7303
.2665	.6056
.2795	.4353
.2925	.3995
.3055	.3386
.3185	.2627
.3315	.2771
.3445	.2602
.3575	.2140
.3705	.1584
.3835	.0933
.3965	.0773
.4095	.0597
.4225	.0908
.4355	.0883
.4485	.0520
.4615	.0349
.4745	.0448
.4875	.0174
.5005	.0229
.5135	.0205
.5265	.0162
.5395	0.0000
.5525	0.0000

B2738

MASS DEPTH (GM/CM**2)	NORM DOSE INT=1.0
.0069	8.2709
.0206	5.8687
.0343	5.3012
.0480	4.4649
.0617	3.7427
.0754	3.2815
.0891	3.0563
.1028	2.7933
.1165	2.5975
.1302	2.4743
.1439	2.2810
.1576	2.1187
.1713	1.7560
.1850	1.7271
.1987	1.6066
.2124	1.6491
.2261	1.6029
.2398	1.3591
.2535	1.3529
.2672	1.2464
.2809	1.1122
.2946	1.0711
.3083	.9762
.3220	.9446
.3357	.7354
.3494	.6645
.3631	.5303
.3768	.5302
.3905	.4016
.4042	.2872
.4179	.2794
.4316	.3136
.4453	.2662
.4590	.2021
.4727	.1564
.4864	.0826
.5001	.0747
.5138	.0380
.5275	.0306
.5412	.0215
.5549	.0067
.5686	.0066
.5823	0.0000
.5960	0.0000
.6097	0.0000
.6234	0.0000

B2779

MASS DEPTH (GM/CM**2)	NORM DOSE INT=1.0
.0069	8.3920
.0206	10.0582
.0343	6.9999
.0480	8.7326
.0617	7.6252
.0754	6.0056
.0891	4.6195
.1028	3.8832
.1165	2.8912
.1302	1.7741
.1439	1.1311
.1576	.6796
.1713	.3948
.1850	.2650
.1987	.1677
.2124	.1075
.2261	.0625
.2398	.0208
.2535	.0111
.2672	.0002
.2809	0.0000
.2946	0.0000
.3083	0.0000
.3220	0.0000
.3357	0.0000
.3494	0.0000
.3631	0.0000
.3768	0.0000
.3905	0.0000
.4042	0.0000
.4179	0.0000
.4316	0.0000
.4453	0.0000
.4590	0.0000
.4727	0.0000
.4864	0.0000
.5001	0.0000
.5138	0.0000
.5275	0.0000
.5412	0.0000
.5549	0.0000
.5686	0.0000
.5823	0.0000
.5960	0.0000
.6097	0.0000
.6234	0.0000
.6371	0.0000

P2782

MASS DEPTH (GM/CM**2)	NORM COSE INT=1.0
.0069	4.5752
.0206	4.2508
.0343	4.6495
.0480	4.4067
.0617	4.0200
.0754	3.6317
.0891	3.3097
.1028	2.9579
.1165	2.8449
.1302	2.8164
.1439	2.7309
.1576	2.5559
.1713	2.4313
.1850	2.3262
.1987	2.3001
.2124	2.0757
.2261	1.9415
.2398	1.7254
.2535	1.5191
.2672	1.4073
.2809	1.1752
.2946	1.1069
.3083	1.0161
.3220	.8742
.3357	.7282
.3494	.6024
.3631	.4784
.3768	.4666
.3905	.3830
.4042	.3262
.4179	.2611
.4316	.2308
.4453	.1975
.4590	.1392
.4727	.1055
.4864	.0934
.5001	.0444
.5138	.0428
.5275	.0119
.5412	.0081
.5549	.0039
.5686	.0030

P2785

MASS DEPTH (GM/CM**2)	NORM COSE INT=1.0
.0069	3.9621
.0206	3.8729
.0343	3.7755
.0480	3.7157
.0617	3.5753
.0754	3.4138
.0891	3.3997
.1028	3.2374
.1165	3.0952
.1302	3.0953
.1439	2.9404
.1576	2.7102
.1713	2.5707
.1850	2.4071
.1987	2.2633
.2124	2.1176
.2261	1.9446
.2398	1.8212
.2535	1.6054
.2672	1.4974
.2809	1.3556
.2946	1.3057
.3083	1.1691
.3220	1.0305
.3357	.9056
.3494	.8044
.3631	.7021
.3768	.6260
.3905	.4919
.4042	.3785
.4179	.3694
.4316	.3229
.4453	.2570
.4590	.1566
.4727	.1112
.4864	.0694
.5001	.0583
.5138	.0306
.5275	.0215
.5412	.0265
.5549	.0186
.5686	.0039
.5823	.0019

P2488

MASS DEPTH (GM/CM**2)	NORM DOSE INT=1.0
.0055	4.9976
.0165	5.3398
.0275	5.2439
.0385	4.8576
.0495	4.2150
.0605	3.8966
.0715	3.5119
.0825	3.2706
.0935	3.0466
.1045	2.8555
.1155	2.3621
.1265	2.2424
.1375	2.0687
.1485	1.8591
.1595	1.5646
.1705	1.4335
.1815	1.1972
.1925	1.0128
.2035	.8243
.2145	.7889
.2255	.8048
.2365	.7577
.2475	.7075
.2585	.6105
.2695	.5201
.2805	.5060
.2915	.3732
.3025	.3293
.3135	.2283
.3245	.1795
.3355	.2078
.3465	.1562
.3575	.1288
.3685	.0989
.3795	.0798
.3905	.0409
.4015	.0175
.4125	.0135
.4235	.0222
.4345	.0121
.4455	.0040
.4565	.0070
.4675	.0077
.4785	.0113
.4895	.0113
.5005	.0032
.5115	.0000

P2801

MASS DEPTH (GM/CM**2)	NORM DOSE INT=1.0
.0069	5.0057
.0206	5.2828
.0343	5.2446
.0480	5.1114
.0617	4.6178
.0754	4.4159
.0891	3.9415
.1028	3.4788
.1165	3.3222
.1302	3.2190
.1439	2.8503
.1576	2.6785
.1713	2.4396
.1850	2.3473
.1987	2.1694
.2124	1.8977
.2261	1.5877
.2398	1.3624
.2535	1.1625
.2672	1.0173
.2809	.8859
.2946	.7658
.3083	.6169
.3220	.5230
.3357	.3809
.3494	.2741
.3631	.1770
.3768	.1145
.3905	.0666
.4042	.0300
.4179	.0156
.4316	.0066
.4453	.0046
.4590	.0046
.4727	.0021
.4864	0.0000
.5001	0.0000
.5138	0.0000
.5275	0.0000
.5412	0.0000
.5549	0.0000
.5686	0.0000
.5823	0.0000
.5960	0.0000
.6097	0.0000
.6234	0.0000
.6371	0.0000
.6508	0.0000

P2802

MASS DEPTH (GM/CM**2)	NORM DOSE INT=1.0
.0069	5.5258
.0206	5.5295
.0343	4.8865
.0480	4.6489
.0617	4.5715
.0754	4.2559
.0891	3.8871
.1028	3.5562
.1165	3.4417
.1302	3.1347
.1439	2.8998
.1576	2.6906
.1713	2.2904
.1850	2.1825
.1987	2.0722
.2124	1.8067
.2261	1.6394
.2398	1.4326
.2535	1.2614
.2672	1.2243
.2809	.9064
.2946	.7440
.3083	.6185
.3220	.5276
.3357	.4381
.3494	.2613
.3631	.2216
.3768	.1974
.3905	.1559
.4042	.1165
.4179	.0561
.4316	.0342
.4453	.0269
.4590	.0016
.4727	0.0000
.4864	0.0000
.5001	0.0000
.5138	0.0000
.5275	0.0000
.5412	0.0000
.5549	0.0000
.5686	0.0000
.5823	0.0000
.5960	0.0000
.6097	0.0000
.6234	0.0000

P2803

MASS DEPTH (GM/CM**2)	NORM DOSE INT=1.0
.0055	4.3228
.0165	4.9487
.0275	5.1003
.0385	4.6710
.0495	4.4127
.0605	4.0559
.0715	3.8018
.0825	3.2903
.0935	3.0623
.1045	2.8620
.1155	2.6942
.1265	2.3276
.1375	1.9894
.1485	1.7767
.1595	1.6260
.1705	1.4273
.1815	1.2097
.1925	1.0285
.2035	.8286
.2145	.7434
.2255	.6297
.2365	.6062
.2475	.5365
.2585	.4307
.2695	.3797
.2805	.3301
.2915	.2661
.3025	.1970
.3135	.1856
.3245	.1490
.3355	.1192
.3465	.1266
.3575	.1111
.3685	.0576
.3795	.0621
.3905	.0454
.4015	.0247
.4125	.0148
.4235	.0101
.4345	.0024
.4455	.0024
.4565	0.0000
.4675	0.0000
.4785	0.0000
.4895	0.0000

P2809

MASS DEPTH (GM/CM$$2)	NORM DOSE INT=1.0
.0065	6.1535
.0195	6.2866
.0325	5.5929
.0455	5.0030
.0585	4.3700
.0715	3.7230
.0845	3.3368
.0975	3.1374
.1105	2.8074
.1235	2.3819
.1355	2.0076
.1495	1.6769
.1625	1.2559
.1755	1.0555
.1885	.8837
.2015	.7206
.2145	.5473
.2275	.4389
.2405	.2736
.2535	.2072
.2665	.1385
.2795	.0847
.2925	.0829
.3055	.0641
.3185	.0366
.3315	.0176
.3445	.0083
.3575	.0073
.3705	.0017
.3835	.0020
.3965	.0006
.4095	0.0000
.4225	0.0000
.4355	0.0000
.4485	0.0000
.4615	0.0000
.4745	0.0000
.4875	0.0000
.5005	0.0000
.5135	0.0000
.5265	0.0000
.5395	0.0000
.5525	0.0000

P2814

MASS DEPTH (GM/CM$$2)	NORM DOSE INT=1.0
.0069	7.6711
.0206	7.7800
.0343	6.6813
.0480	5.4751
.0617	4.8792
.0754	4.4885
.0891	4.2892
.1028	3.8884
.1165	3.7075
.1302	3.3146
.1439	2.8489
.1576	2.3458
.1713	2.1578
.1850	1.7480
.1987	1.3835
.2124	1.1828
.2261	.8375
.2398	.7027
.2535	.6578
.2672	.4302
.2809	.2287
.2946	.1444
.3083	.0903
.3220	.0456
.3357	.0170
.3494	.0169
.3631	.0021
.3768	0.0000
.3905	0.0000
.4042	0.0000
.4179	0.0000
.4316	0.0000
.4453	0.0000
.4590	0.0000
.4727	0.0000
.4364	0.0000
.5001	0.0000
.5138	0.0000
.5275	0.0000
.5412	0.0000
.5549	0.0000
.5686	0.0000

82820

MASS DEPTH (GM/CM$$2)	NORM DOSE INT=1.0
.0069	3.6577
.0206	3.8566
.0343	3.9832
.0480	3.8814
.0617	3.6591
.0754	3.4884
.0891	3.3753
.1028	3.3104
.1165	3.1808
.1302	3.1427
.1439	2.9607
.1576	2.7988
.1713	2.6398
.1850	2.4897
.1987	2.3867
.2124	2.2004
.2261	2.0161
.2398	1.8912
.2535	1.7537
.2672	1.6271
.2809	1.3267
.2946	1.2624
.3083	1.0816
.3220	1.0134
.3357	.8754
.3494	.7255
.3631	.5948
.3768	.5572
.3905	.4499
.4042	.3327
.4179	.2470
.4316	.1743
.4453	.1104
.4590	.0820
.4727	.0301
.4964	.0317
.5001	.0067

82824

MASS DEPTH (GM/CM$$2)	NORM DOSE INT=1.0
.0055	3.0074
.0165	3.6488
.0275	3.9875
.0385	3.8888
.0495	3.5611
.0605	3.5464
.0715	3.3778
.0825	3.2163
.0935	2.9840
.1045	2.7736
.1155	2.7131
.1265	2.4817
.1375	2.2104
.1485	1.9879
.1595	1.8716
.1705	1.7209
.1815	1.6159
.1925	1.5288
.2035	1.3653
.2145	1.1991
.2255	1.1675
.2365	1.0120
.2475	.9651
.2585	.9033
.2695	.7805
.2805	.6996
.2915	.6137
.3025	.4823
.3135	.4319
.3245	.4284
.3355	.3746
.3465	.2973
.3575	.2709
.3685	.2405
.3795	.1659
.3905	.1217
.4015	.1000
.4125	.0939
.4235	.0885
.4345	.0839
.4455	.0707
.4565	.0745
.4675	.0482
.4785	.0442
.4895	.0321

B2885

MASS DEPTH (GM/CM$$2)	NORM DOSE INT=1.0
.0065	3.8936
.0195	4.4627
.0325	4.2637
.0455	3.7844
.0585	3.3245
.0715	3.2176
.0845	2.8931
.0975	2.7158
.1105	2.4419
.1235	2.1456
.1365	1.9148
.1495	1.5883
.1625	1.5354
.1755	1.4081
.1885	1.1047
.2015	1.0152
.2145	.9558
.2275	.9152
.2405	.7649
.2535	.6438
.2665	.5847
.2795	.4691
.2925	.3930
.3055	.2917
.3185	.2599
.3315	.2337
.3445	.1745
.3575	.1678
.3705	.1102
.3835	.1128
.3965	.0857
.4095	.0780
.4225	.0525
.4355	.0499
.4485	.0405
.4615	.0278
.4745	.0206
.4875	.0299
.5005	.0150
.5135	.0131
.5265	.0048
.5395	.0087

B2888

MASS DEPTH (GM/CM$$2)	NORM DOSE INT=1.0
.0065	4.2332
.0195	5.1601
.0325	4.8024
.0455	4.3322
.0585	4.0104
.0715	3.5568
.0845	3.1972
.0975	2.8495
.1105	2.4036
.1235	2.1206
.1365	1.9345
.1495	1.7633
.1625	1.5143
.1755	1.2728
.1885	1.0439
.2015	.8593
.2145	.6833
.2275	.5079
.2405	.3742
.2535	.3257
.2665	.2418
.2795	.1860
.2925	.1666
.3055	.1058
.3185	.1037
.3315	.0709
.3445	.0305
.3575	.0304
.3705	.0268
.3835	.0081
.3965	.0128
.4095	.0093
.4225	.0093
.4355	.0043
.4485	0.0000
.4615	0.0000
.4745	0.0000
.4875	0.0000
.5005	0.0000
.5135	0.0000
.5265	0.0000
.5395	0.0000
.5525	0.0000
.5655	0.0000
.5785	0.0000
.5915	0.0000

B2889

MASS DEPTH (GM/CM**2)	NORM DOSE INT=1.0
.0069	5.0045
.0206	5.7031
.0343	5.5272
.0480	5.3807
.0617	4.9006
.0754	4.4977
.0891	4.2193
.1028	3.8889
.1165	3.7667
.1302	3.4073
.1439	3.1393
.1576	2.7080
.1713	2.6109
.1850	2.3556
.1987	1.9733
.2124	1.7357
.2261	1.4306
.2398	1.1931
.2535	.9012
.2672	.7808
.2809	.6278
.2946	.5744
.3083	.4067
.3220	.1880
.3357	.1093
.3494	.0765
.3631	.0438
.3768	.0236
.3905	.0059
.4042	.0013
.4179	0.0000
.4316	0.0000
.4453	0.0000
.4590	0.0000
.4727	0.0000
.4864	0.0000
.5001	0.0000
.5138	0.0000
.5275	0.0000
.5412	0.0000
.5549	0.0000

B2890

MASS DEPTH (GM/CM**2)	NORM DOSE INT=1.0
.0069	2.7836
.0206	3.0956
.0343	3.4039
.0480	3.4310
.0617	3.5040
.0754	3.5398
.0891	3.3440
.1028	3.3259
.1165	3.2805
.1302	3.1549
.1439	2.8782
.1576	2.7850
.1713	2.7070
.1850	2.4545
.1987	2.4111
.2124	2.1839
.2261	2.1250
.2398	1.9147
.2535	1.8043
.2672	1.5908
.2809	1.4313
.2946	1.3378
.3083	1.1957
.3220	1.0143
.3357	.9408
.3494	.8024
.3631	.6779
.3768	.6664
.3905	.5794
.4042	.4914
.4179	.3898
.4316	.3708
.4453	.2726
.4590	.2731
.4727	.2638
.4864	.2144
.5001	.2083
.5138	.1533
.5275	.1429
.5412	.1212
.5549	.1074
.5686	.0548
.5823	.0627
.5960	.0464
.6097	.0281

B2893

MASS DEPTH (GM/CM$$2)	NORM DOSE INT=1.0
.0065	3.6572
.0195	3.9462
.0325	4.0830
.0455	3.9443
.0585	3.6903
.0715	3.4526
.0845	3.1012
.0975	2.8620
.1105	2.6003
.1235	2.3937
.1365	2.1306
.1495	1.9061
.1625	1.7602
.1755	1.6187
.1885	1.4731
.2015	1.3766
.2145	1.1563
.2275	.9817
.2405	.9024
.2535	.7923
.2665	.6426
.2795	.5448
.2925	.4672
.3055	.3439
.3185	.3226
.3315	.2555
.3445	.2522
.3575	.2268
.3705	.1948
.3835	.1384
.3965	.1111
.4095	.0851
.4225	.0684
.4355	.0516
.4485	.0482
.4615	.0266
.4745	.0243
.4875	.0097
.5005	.0203
.5135	.0101
.5265	.0100
.5395	.0083
.5525	.0050
.5655	.0047
.5785	.0002
.5915	0.0000

B2894

MASS DEPTH (GM/CM$$2)	NORM DOSE INT=1.0
.0069	4.0700
.0206	4.5324
.0343	4.7399
.0480	4.6202
.0617	4.6481
.0754	4.4637
.0891	4.3162
.1028	4.0894
.1165	3.7998
.1302	3.5211
.1439	3.3738
.1576	3.0226
.1713	2.6326
.1850	2.4031
.1987	2.1677
.2124	1.8028
.2261	1.6191
.2398	1.3717
.2535	1.1637
.2672	.9550
.2809	.8173
.2946	.7794
.3083	.6206
.3220	.4901
.3357	.3830
.3494	.2595
.3631	.1296
.3768	.0974
.3905	.0621
.4042	.0282
.4179	.0250
.4316	.0203
.4453	.0016
.4590	0.0000
.4727	0.0000
.4864	0.0000
.5001	0.0000
.5138	0.0000
.5275	0.0000
.5412	0.0000
.5549	0.0000
.5686	0.0000
.5823	0.0000

B2895

MASS DEPTH (GM/CM$$2$	NORM DOSE INT=1.0
.0065	2.8946
.0195	3.3210
.0325	3.6845
.0455	3.6230
.0585	3.6726
.0715	3.3896
.0845	3.1081
.0975	2.8839
.1105	2.7085
.1235	2.5527
.1365	2.3409
.1495	2.2050
.1625	1.9866
.1755	1.8025
.1885	1.5937
.2015	1.3640
.2145	1.2157
.2275	1.0408
.2405	.9192
.2535	.7945
.2665	.6699
.2795	.5221
.2925	.5110
.3055	.4122
.3185	.4172
.3315	.3114
.3445	.2892
.3575	.2397
.3705	.2176
.3835	.2388
.3965	.1759
.4095	.1107
.4225	.1171
.4355	.1135
.4485	.0885
.4615	.0692
.4745	.0634
.4875	.0522
.5005	.0459
.5135	.0382
.5265	.0333
.5395	.0111
.5525	.0076

B2896

MASS DEPTH (GM/CM$$2)	NORM DOSE INT=1.0
.0065	5.5384
.0195	6.2774
.0325	5.8432
.0455	5.2143
.0585	4.6116
.0715	3.9748
.0845	3.5742
.0975	2.9649
.1105	2.4535
.1235	1.9723
.1365	1.7357
.1495	1.4841
.1625	1.1962
.1755	.9294
.1885	.7259
.2015	.6422
.2145	.5303
.2275	.3882
.2405	.3371
.2535	.2525
.2665	.2460
.2795	.2009
.2925	.1573
.3055	.1119
.3185	.0947
.3315	.0549
.3445	.0573
.3575	.0356
.3705	.0209
.3835	.0220
.3965	.0085
.4095	.0021
.4225	.0045
.4355	.0027
.4485	0.0000
.4615	0.0000
.4745	0.0000
.4875	0.0000
.5005	0.0000
.5135	0.0000
.5265	0.0000
.5395	0.0000
.5525	0.0000
.5655	0.0000
.5785	0.0000
.5915	0.0000

B2897

MASS DEPTH (GM/CM**2)	NORM DOSE INT=1.0
.0069	3.9038
.0206	4.0311
.0343	4.0656
.0480	4.0227
.0617	3.8238
.0754	3.7310
.0891	3.4558
.1028	3.2820
.1165	3.1894
.1362	2.8956
.1439	2.6361
.1576	2.4606
.1713	2.2769
.1850	2.2267
.1987	2.0574
.2124	1.8978
.2261	1.8630
.2398	1.6619
.2535	1.4724
.2672	1.3542
.2809	1.2389
.2946	1.1375
.3083	.9382
.3220	.8089
.3357	.7498
.3494	.6415
.3631	.5487
.3768	.4513
.3905	.3926
.4042	.3352
.4179	.3082
.4316	.2561
.4453	.1823
.4590	.1262
.4727	.1055
.4864	.0980
.5001	.0878
.5138	.0549
.5275	.0400
.5412	.0361
.5549	.0262

B2898

MASS DEPTH (GM/CM**2)	NORM DOSE INT=1.0
.0069	2.8833
.0206	3.1965
.0343	3.3572
.0480	3.3730
.0617	3.6000
.0754	3.6221
.0891	3.6049
.1028	3.3906
.1165	3.2076
.1302	3.0720
.1439	2.8734
.1576	2.8238
.1713	2.6967
.1850	2.5673
.1987	2.3608
.2124	2.1647
.2261	2.0581
.2398	2.0379
.2535	1.8023
.2672	1.6824
.2809	1.5155
.2946	1.3155
.3083	1.1885
.3220	1.0453
.3357	.8896
.3494	.8349
.3631	.7532
.3768	.6162
.3905	.4977
.4042	.4544
.4179	.3650
.4316	.2933
.4453	.2320
.4590	.2105
.4727	.1615
.4864	.1405
.5001	.1113
.5138	.0761
.5275	.0473
.5412	.0283
.5549	.0197
.5686	.0192
.5823	.0133
.5960	.0082
.6097	.0153
.6234	.0120
.6371	.0017

B2904

MASS DEPTH (GM/CM**2)	NORM DOSE INT=1.0
.0069	3.2309
.0206	3.4930
.0343	3.7298
.0480	3.7590
.0617	3.8283
.0754	3.6188
.0891	3.5305
.1028	3.4033
.1165	3.3762
.1302	3.1657
.1439	3.0287
.1576	2.8357
.1713	2.5461
.1850	2.3622
.1987	2.1586
.2124	1.9977
.2261	1.8451
.2398	1.7174
.2535	1.5339
.2672	1.4771
.2809	1.3049
.2946	1.1858
.3083	1.1281
.3220	.9636
.3357	.9176
.3494	.7995
.3631	.6819
.3768	.5498
.3905	.4806
.4042	.4028
.4179	.3230
.4316	.2410
.4453	.1955
.4590	.1863
.4727	.1517
.4864	.1279
.5001	.0763
.5138	.0644
.5275	.0453
.5412	.0336
.5549	.0124
.5686	0.0000
.5823	0.0000
.5960	0.0000

B2905

MASS DEPTH (GM/CM**2)	NORM DOSE INT=1.0
.0069	2.9024
.0206	3.4251
.0343	3.5892
.0480	3.6097
.0617	3.4979
.0754	3.5183
.0891	3.4865
.1028	3.1749
.1165	3.0031
.1302	2.9242
.1439	2.7544
.1576	2.5429
.1713	2.4624
.1850	2.3437
.1987	2.2092
.2124	1.9788
.2261	1.9417
.2398	1.8172
.2535	1.7664
.2672	1.6460
.2809	1.4239
.2946	1.3630
.3083	1.1852
.3220	1.0591
.3357	.9606
.3494	.8432
.3631	.7744
.3768	.7213
.3905	.6613
.4042	.5475
.4179	.4861
.4316	.4568
.4453	.4656
.4590	.3420
.4727	.2767
.4864	.2163
.5001	.1394
.5138	.1178
.5275	.0798
.5412	.0508
.5549	.0640
.5686	.0505

B2906

MASS DEPTH (GM/CM$$2)	NORM DOSE INT=1.0
.0069	3.2269
.0206	3.5464
.0343	3.9312
.0480	3.8424
.0617	3.6708
.0754	3.6371
.0991	3.7271
.1028	3.5364
.1165	3.3848
.1302	3.1360
.1439	2.9391
.1576	2.7889
.1713	2.5845
.1850	2.4209
.1987	2.3504
.2124	2.1405
.2261	1.9311
.2398	1.7401
.2535	1.7852
.2672	1.5760
.2809	1.3388
.2946	1.2674
.3083	1.0430
.3220	.9316
.3357	.9222
.3494	.7320
.3631	.6637
.3768	.5902
.3905	.4848
.4042	.4140
.4179	.3363
.4316	.2741
.4453	.1877
.4590	.1472
.4727	.1214
.4864	.0655
.5001	.0572
.5138	.0484

B2907

MASS DEPTH (GM/CM$$2)	NORM DOSE INT=1.0
.0069	3.0836
.0206	3.4472
.0343	3.7832
.0480	3.8828
.0617	4.1003
.0754	4.0295
.0991	3.7480
.1028	3.6419
.1165	3.4128
.1302	3.2689
.1439	3.1359
.1576	2.9547
.1713	2.8251
.1850	2.4872
.1987	2.2766
.2124	2.2852
.2261	2.0160
.2398	1.8350
.2535	1.6896
.2672	1.5443
.2809	1.3805
.2946	1.2378
.3083	1.0229
.3220	.8861
.3357	.6648
.3494	.6389
.3631	.5166
.3768	.4481
.3905	.3434
.4042	.2552
.4179	.2014
.4316	.1546
.4453	.1105
.4590	.0721
.4727	.0367
.4864	.0345
.5001	.0220
.5138	.0094
.5275	.0018
.5412	0.0000
.5549	0.0000
.5686	0.0000
.5823	0.0000

B2908

MASS DEPTH (GM/CM**2)	NORM DOSE INT=1.0
.0055	3.2262
.0165	3.7575
.0275	4.1712
.0385	4.2427
.0495	3.8952
.0605	3.8204
.0715	3.5978
.0825	3.1779
.0935	3.0020
.1045	2.6873
.1155	2.5273
.1265	2.3254
.1375	2.0807
.1485	1.9335
.1595	1.7769
.1705	1.5700
.1815	1.4392
.1925	1.3073
.2035	1.2162
.2145	1.0782
.2255	.9965
.2365	.9348
.2475	.7915
.2585	.6792
.2695	.6305
.2805	.5895
.2915	.5755
.3025	.4270
.3135	.4072
.3245	.3703
.3355	.3048
.3465	.2013
.3575	.1946
.3685	.1582
.3795	.1339
.3905	.1058
.4015	.0774
.4125	.0704
.4235	.0378
.4345	.0291
.4455	.0342
.4565	.0279
.4675	.0244
.4785	.0205
.4895	.0175
.5005	.0044

B2919

MASS DEPTH (GM/CM**2)	NORM DOSE INT=1.0
.0069	3.3957
.0206	3.7872
.0343	4.0361
.0480	3.9821
.0617	4.0508
.0754	4.0132
.0891	3.8171
.1028	3.5711
.1165	3.4214
.1302	3.2906
.1439	3.1044
.1576	2.9676
.1713	2.7507
.1850	2.5701
.1987	2.2872
.2124	2.1051
.2261	1.9767
.2398	1.7644
.2535	1.6561
.2672	1.4564
.2809	1.2843
.2946	1.0543
.3083	.9671
.3220	.8513
.3357	.7334
.3494	.5831
.3631	.4584
.3768	.2931
.3905	.1986
.4042	.1466
.4179	.1144
.4316	.0955
.4453	.0519
.4590	.0277

B2920

MASS DEPTH (GM/CM$$2)	NORM DOSE INT=1.0
.0069	3.3211
.0206	3.7044
.0343	3.8514
.0480	3.8708
.0617	3.9441
.0754	3.8115
.0891	3.6587
.1028	3.5141
.1165	3.2061
.1302	3.1096
.1439	3.0000
.1576	2.7512
.1713	2.6616
.1850	2.4162
.1987	2.2864
.2124	2.1423
.2261	1.9378
.2398	1.7113
.2535	1.6054
.2672	1.4838
.2809	1.2991
.2946	1.1216
.3083	1.0222
.3220	1.0073
.3357	.8459
.3494	.7489
.3631	.6057
.3768	.5227
.3905	.4238
.4042	.3441
.4179	.2919
.4316	.2438
.4453	.1696
.4590	.1630
.4727	.1213
.4864	.1243
.5001	.0614
.5138	.0230
.5275	.0177
.5412	.0199
.5549	.0086
.5686	.0020
.5823	.0026

B2922

MASS DEPTH (GM/CM$$2)	NORM DOSE INT=1.0
.0069	3.7584
.0206	4.4330
.0343	4.7535
.0480	4.6871
.0617	4.4386
.0754	4.1191
.0891	3.9050
.1028	3.6040
.1165	3.5096
.1302	3.2742
.1439	2.9992
.1576	2.7713
.1713	2.6357
.1850	2.3910
.1987	2.2087
.2124	2.0143
.2261	1.7998
.2398	1.6544
.2535	1.4486
.2672	1.2789
.2809	1.0612
.2946	.9009
.3083	.8182
.3220	.7576
.3357	.5207
.3494	.3914
.3631	.3359
.3768	.2586
.3905	.2016
.4042	.1440
.4179	.0821
.4316	.0966
.4453	.0853

B2935

MASS DEPTH (GM/CM$$2)	NORM DOSE INT=1.0
.0065	6.0075
.0195	6.1658
.0325	5.5370
.0455	4.9764
.0585	4.4282
.0715	3.7204
.0845	3.4597
.0975	2.9388
.1105	2.5235
.1235	2.1354
.1365	1.9250
.1495	1.6374
.1625	1.3837
.1755	1.1347
.1885	.8900
.2015	.7097
.2145	.5716
.2275	.5022
.2405	.4250
.2535	.2973
.2665	.1660
.2795	.1197
.2925	.0699
.3055	.0772
.3185	.0444
.3315	.0212
.3445	.0247
.3575	.0270
.3705	.0140
.3835	.0064
.3965	.0039
.4095	0.0000
.4225	0.0000
.4355	0.0000
.4485	0.0000
.4615	0.0000
.4745	0.0000
.4875	0.0000
.5005	0.0000
.5135	0.0000
.5265	0.0000
.5395	0.0000
.5525	0.0000
.5655	0.0000
.5785	0.0000
.5915	0.0000

B2936

MASS DEPTH (GM/CM$$2)	NORM DOSE INT=1.0
.0059	4.9368
.0206	5.3533
.0343	5.6195
.0481	5.7511
.0617	5.6193
.0754	5.2756
.0891	4.9020
.1028	4.6085
.1165	4.2535
.1302	3.7924
.1439	3.2992
.1576	2.9632
.1713	2.6874
.1850	2.1301
.1987	1.7668
.2124	1.2719
.2261	.9733
.2398	.7532
.2535	.5546
.2672	.3634
.2809	.1719
.2946	.1272
.3083	.0372
.3220	.0184
.3357	.0070
.3494	.0044
.3631	0.0000
.3768	0.0000
.3905	0.0000
.4042	0.0000
.4179	0.0000
.4316	0.0000
.4453	0.0000
.4590	0.0000
.4727	0.0000
.4864	0.0000
.5001	0.0000
.5138	0.0000
.5275	0.0000
.5412	0.0000
.5549	0.0000
.5686	0.0000
.5823	0.0000
.5960	0.0000
.6097	0.0000
.6234	0.0000

B2937

MASS DEPTH (GM/CM**2)	NORM DOSE INT=1.0
.0169	10.6630
.0206	9.2816
.0343	7.7275
.0480	6.4721
.0617	5.5875
.0754	4.7945
.0891	3.8281
.1028	3.3958
.1165	3.0158
.1302	2.4909
.1439	2.0676
.1576	1.7087
.1713	1.5161
.1850	1.2465
.1987	.9744
.2124	.7013
.2261	.4724
.2398	.3316
.2535	.2103
.2672	.1742
.2809	.1166
.2946	.0622
.3083	.0621
.3220	.0362
.3357	.0099
.3494	0.0000
.3631	0.0000
.3768	0.0000
.3905	0.0000
.4042	0.0000
.4179	0.0000
.4316	0.0000
.4453	0.0000
.4590	0.0000
.4727	0.0000
.4864	0.0000
.5001	0.0000
.5138	0.0000
.5275	0.0000
.5412	0.0000
.5549	0.0000
.5686	0.0000
.5823	0.0000
.5960	0.0000

B2938

MASS DEPTH (GM/CM**2)	NORM DOSE INT=1.0
.0165	5.5047
.0135	5.1035
.0325	5.3302
.0455	4.4920
.0585	4.0013
.0715	3.6028
.0845	3.2282
.0975	2.7472
.1105	2.3788
.1235	2.0532
.1365	1.8312
.1495	1.5510
.1625	1.2249
.1755	.9020
.1885	.7412
.2015	.7002
.2145	.4422
.2275	.3942
.2405	.3115
.2535	.1985
.2665	.1447
.2795	.0741
.2925	.0513
.3055	.0527
.3185	.0135
.3315	.0039
.3445	.0022
.3575	.0047
.3705	.0080
.3835	.0077
.3965	.0057
.4095	0.0000
.4225	0.0000
.4355	0.0000
.4485	0.0000
.4615	0.0000
.4745	0.0000
.4875	0.0000
.5005	0.0000
.5135	0.0000
.5265	0.0000
.5395	0.0000
.5525	0.0000
.5655	0.0000

82939

MASS DEPTH (GM/CM**2)	NORM DOSE INT=1.0
.0055	5.4552
.0195	6.2613
.0325	5.8704
.0455	5.6513
.0585	4.7806
.0715	4.2631
.0845	3.8275
.0975	3.2842
.1105	2.8619
.1235	2.3723
.1365	1.8181
.1495	1.4625
.1625	1.0881
.1755	.8050
.1885	.5829
.2015	.4108
.2145	.2986
.2275	.2244
.2405	.1936
.2535	.1411
.2665	.0696
.2795	.0641
.2925	.0244
.3055	.0109
.3185	.0021
.3315	.0096
.3445	.0002
.3575	0.0000
.3705	0.0000
.3835	0.0000
.3965	0.0000
.4095	0.0000
.4225	0.0000
.4355	0.0000
.4485	0.0000
.4615	0.0000
.4745	0.0000
.4875	0.0000
.5005	0.0000
.5135	0.0000
.5265	0.0000
.5395	0.0000
.5525	0.0000
.5655	0.0000
.5785	0.0000

82940

MASS DEPTH (GM/CM**2)	NORM DOSE INT=1.0
.0069	4.0618
.0206	4.5256
.0343	4.7023
.0480	4.7383
.0617	4.6264
.0754	4.4812
.0891	4.2447
.1028	3.9836
.1165	3.7891
.1302	3.5033
.1439	3.4043
.1576	3.0663
.1713	2.8267
.1850	2.6973
.1987	2.3368
.2124	2.0862
.2261	1.7288
.2398	1.3130
.2535	1.1675
.2672	.8496
.2809	.6427
.2946	.5693
.3083	.4030
.3220	.3511
.3357	.2847
.3494	.2108
.3631	.1211
.3768	.0987
.3905	.0496
.4042	.0390
.4179	.0258
.4316	.0162
.4453	.0029
.4590	0.0000
.4727	0.0000
.4864	0.0000
.5001	0.0000
.5138	0.0000
.5275	0.0000

82943

MASS DEPTH (GM/CM$$2)	NORM DOSE INT=1.0
.0055	3.9602
.0195	4.2556
.0325	4.3277
.0455	3.9915
.0585	3.8411
.0715	3.5483
.0845	3.3191
.0975	3.0505
.1105	2.7882
.1235	2.4876
.1365	2.2606
.1495	2.0251
.1625	1.7461
.1755	1.4546
.1885	1.2722
.2015	1.1540
.2145	1.0113
.2275	.8030
.2405	.7637
.2535	.6669
.2665	.5105
.2795	.4179
.2925	.3192
.3055	.2220
.3185	.1775
.3315	.1940
.3445	.1623
.3575	.1177
.3705	.0638
.3835	.0646
.3965	.0433
.4095	.0348
.4225	.0159
.4355	.0179
.4485	.0211
.4615	.0059
.4745	.0095
.4875	.0036
.5005	.0047
.5135	.0071
.5265	.0058
.5395	.0041
.5525	0.0000
.5655	0.0000

DISTRIBUTION LIST

DEPARTMENT OF DEFENSE

Assistant to the Secretary of Defense
Atomic Energy
ATTN: Executive Assistant

Defense Advanced Rsch. Proj. Agency
ATTN: TIO

Defense Intelligence Agency
ATTN: DT-2

Defense Nuclear Agency
ATTN: SPAS
ATTN: SPSS, T. Deevy
ATTN: SPTD
ATTN: STSP
4 cy ATTN: TITL

Defense Technical Information Center
12 cy ATTN: DD

Field Command
Defense Nuclear Agency
ATTN: FCPR
ATTN: FCTMD

Field Command
Defense Nuclear Agency
Livermore Division
ATTN: FCPRL

Joint Chiefs of Staff
ATTN: J-5, Nuclear Division
ATTN: J-5, Force Planning & Program Div.
ATTN: SAGA/SSD
ATTN: SAGA/SFD

Joint Strat. Tgt. Planning Staff
ATTN: JPTM
ATTN: JLTW-2
ATTN: JLA

Undersecretary of Def. for Rsch. & Engrg.
ATTN: Strategic & Space Systems (OS)

DEPARTMENT OF THE ARMY

BMD Advanced Technology Center
Department of the Army
ATTN: ATC-T, M. Capps

BMD Program Office
Department of the Army
ATTN: Technology Division

BMD Systems Command
Department of the Army
ATTN: BMDSC-H, N. Hurst

Deputy Chief of Staff for Ops. & Plans
Department of the Army
ATTN: DAMO-NCZ

Deputy Chief of Staff for Rsch. Dev. & Acq.
Department of the Army
ATTN: DAMA-CSS-N

DEPARTMENT OF THE ARMY (Continued)

Harry Diamond Laboratories
Department of the Army
ATTN: DELHD-N-RBC, D. Schallhorn
ATTN: DELHD-N-P
ATTN: DELHD-N-P, J. Gwaltney

U.S. Army Ballistic Research Labs.
ATTN: DRDAR-BLE, J. Keefer
ATTN: DRDAR-BLV, W. Schuman, Jr.
ATTN: DRDAR-BLV

U.S. Army Material & Mechanics Rsch. Ctr.
ATTN: DRXMR-HH, J. Dignam

U.S. Army Materiel Dev. & Readiness Cmd.
ATTN: DRCDE-D, L. Flynn

U.S. Army Missile Command
ATTN: DRSMI-RKP, W. Thomas

U.S. Army Nuclear & Chemical Agency
ATTN: Library

U.S. Army Research Office
ATTN: Technical Library

DEPARTMENT OF THE NAVY

Naval Research Laboratory
ATTN: Code 6770, G. Cooperstein
ATTN: Code 2627
ATTN: Code 7908, A. Williams

Naval Sea Systems Command
ATTN: SEA-0352, M. Kinna
ATTN: SEA-0351

Naval Surface Weapons Center
ATTN: Code K06, C. Lyons
ATTN: Code F31
ATTN: Code R15, J. Petes
ATTN: Code K06

Naval Weapons Evaluation Facility
ATTN: L. Oliver

Office of the Chief of Naval Operations
ATTN: OP 65
ATTN: OP 604E14, R. Blaise
ATTN: OP 981

Strategic Systems Project Office
Department of the Navy
ATTN: NSP-272
ATTN: NSP-273

DEPARTMENT OF THE AIR FORCE

Aeronautical Systems Division
Air Force Systems Command
ATTN: ASD/ENFTV

DEPARTMENT OF THE AIR FORCE (Continued)

Air Force Materials Laboratory
ATTN: MBE, G. Schmitt
ATTN: MBC, D. Schmidt
ATTN: LLM, T. Nicholas

Air Force Rocket Propulsion Laboratory
ATTN: LKCP, G. Beale

Air Force Systems Command
ATTN: SOSS
ATTN: XRTO

Air Force Weapons Laboratory
Air Force Systems Command
ATTN: DYT
ATTN: SUL
ATTN: DYV
ATTN: DYS
ATTN: NT

Ballistic Missile Office
Air Force Systems Command
ATTN: MNRTE
ATTN: MNNH
ATTN: MNNR

Deputy Chief of Staff
Research, Development, & Acq.
Department of the Air Force
ATTN: AFRD
ATTN: AFRDQSM

Foreign Technology Division
Air Force Systems Command
ATTN: SDBG
ATTN: SDBS, J. Pumphrey
ATTN: TQTD

Strategic Air Command
Department of the Air Force
ATTN: XPFS
ATTN: XPQM
ATTN: XOBM
ATTN: DOXT

DEPARTMENT OF ENERGY

Department of Energy
ATTN: OMA/RD&T

DEPARTMENT OF ENERGY CONTRACTORS

Lawrence Livermore National Laboratory
ATTN: L-92, C. Taylor
ATTN: L-125, J. Keller
ATTN: L-96, L. Woodruff
ATTN: D. Hanner

Sandia National Laboratories
Livermore Laboratory
ATTN: H. Norris, Jr.
ATTN: T. Gold

Sandia National Laboratories
ATTN: C. Mehl
ATTN: C. Broyles
ATTN: M. Cowan

DEPARTMENT OF ENERGY CONTRACTORS (Continued)

Los Alamos National Scientific Laboratory
ATTN: R. Dingus
ATTN: MS 670, J. Hopkins
ATTN: R. Skaggs
ATTN: D. Shover
ATTN: J. McQueen/J. Taylor

DEPARTMENT OF DEFENSE CONTRACTORS

Aerospace Corp.
ATTN: R. Strickler
ATTN: H. Blaes
ATTN: R. Crolius

APTEK
ATTN: T. Meagher

AVCO Research & Systems Group
ATTN: J. Gilmore
ATTN: J. Stevens
ATTN: Document Control
ATTN: P. Grady
ATTN: G. Weber
ATTN: W. Broding

Battelle Memorial Institute
ATTN: M. Vanderlind

Boeing Co.
ATTN: B. Lempriere

California Research & Technology, Inc.
ATTN: K. Kreyenhagen

Effects Technology, Inc.
ATTN: R. Parrise/M. Rosen
ATTN: R. Wengler/R. Bick

Ford Aerospace & Communications Corp.
ATTN: P. Spangler

General Electric Co.
ATTN: P. Cline
ATTN: N. Dispenzierre

General Electric Company-TEMPO
ATTN: DASIAC

General Research Corp.
ATTN: R. Rosenthal

Institute for Defense Analyses
ATTN: Classified Library
ATTN: J. Bengston

Kaman AviDyne
ATTN: R. Ruetenik

Kaman Sciences Corp.
ATTN: F. Shelton
ATTN: R. Sachs/R. O'Keefe

Lockheed Missiles & Space Co., Inc.
ATTN: F. Borgardt

Lockheed Missiles & Space Co., Inc.
ATTN: T. Fortune

DEPARTMENT OF DEFENSE CONTRACTORS (Continued)

Lockheed Missiles & Space Co., Inc.
ATTN: O. Burford
ATTN: R. Walls

Martin Marietta Corp.
ATTN: L. Kinnaird

McDonnell Douglas Corp.
ATTN: J. Peck
ATTN: L. Cohen
ATTN: H. Berkowitz
ATTN: E. Fitzgerald

Pacific-Sierra Research Corp.
ATTN: G. Lang

Physics International Co.
ATTN: J. Shea

Prototype Development Associates, Inc.
ATTN: J. McDonald
ATTN: N. Harington

R & D Associates
ATTN: P. Rausch
ATTN: C. MacDonald
ATTN: W. Graham, Jr.
ATTN: F. Field
ATTN: P. Haas

Science Applications, Inc.
ATTN: W. Yengst

DEPARTMENT OF DEFENSE CONTRACTORS (Continued)

Science Applications, Inc.
ATTN: W. Layson
ATTN: W. Seebaugh

Southern Research Institute
ATTN: C. Pears

SRI International
ATTN: D. Curran
ATTN: G. Abrahamson
ATTN: H. Lindberg

Systems, Science & Software, Inc.
ATTN: T. McKinley
ATTN: G. Gurtman
ATTN: R. Duff

Terra Tek, Inc.
ATTN: S. Green

TRW Defense & Space Sys. Group
ATTN: L. Donahue
ATTN: W. Wood
2 cy ATTN: D. Jortner

TRW Defense & Space Sys. Group
ATTN: W. Polich
ATTN: V. Blankenship
ATTN: R. Mortensen
ATTN: J. Farrell